University of Southampton

Faculty of Environmental and Life Sciences

Geography and Environment Science

Regime Shifts in Shallow Lakes: palaeoecological and agent-based model approaches

by

Yanjie Zhao

ORCID ID 0000-0001-9307-8138

Thesis for the degree of Doctor of Philosophy

February 2022

Acknowledgements

I would like to thank my supervisory team: John, Patrick, and Pete, for always being patient and supportive in guiding me to complete my doctoral thesis. They gave me space and freedom to independently explore interesting aspects of the PhD topic. As my primary supervisor, John was helpful with project and time management and always helped me out when I fell into rabbit holes. Patrick helped me overcome the anxiety of learning Ecology as an interdisciplinary researcher from Geography and offered tips and resources on quantitative methods, modelling and academic writing. Pete gave many useful feedbacks in palaeolimnology and identified the predominant issues for me. He also drove the Paleo team from Southampton to Dublin (and back) when I attended the INQUA2019, which was an impressive journey. Thanks also to Simon Willcock, who led me in the world of agent-based modelling and the Netlogo environment.

I am grateful for the sports facilities and societies that the University of Southampton offers, which made it easier for me to keep physically and mentally healthy. I was lucky to have supportive colleagues and postgraduate fellows in the Department of Geography and Environment, including Ying Wang, Greg Cooper, Robert Cooke, Seb Dunnett, Andrea Gasparotto, Peipei Chen, Chengxiu Li, Francesco D'Adamo, Sarchill Bagg, Alvaro Castilla, Marjorie Fis, Roseanna Mayfield, Angharad Butler-Rees, Charlotte Hipkiss, Rebecca Collins, Victoria Price, Emma Yusuf, Imi Barnsley and Martin Watts. During the time I spent together, they showed me the dedication to research, the diversity of the world and the possibilities of a life I could barely imagine before I met them. Their teaching assistance experience in GEOG1001, ENVS1006, BIOL6052, GEOG3047 was enjoyable and inspiring.

Finally, I would like to thank Rong Wang, Xiangdong Yang, and Min Xu, without whom I would not have had such a supportive environment to finish my thesis in the last months. Huge thanks to my family and funders, the Chinese Scholarships Council and the University of Southampton. They made my PhD trip possible and have substantially supported my life in these four years.

Abstract

Environmental problems caused by lake eutrophication have become more widespread at a global level, threatening the safety of water, food and other daily needs of people living in the vicinity of lakes. Although lake types, physical conditions and causes of degradation vary from region to region, all threatened lake ecosystems face the same problem of identifying the mechanisms that underlie the deterioration of water quality or cause algal blooms in lakes, and discovering pathways to recovery is becoming an increasingly urgent matter. Theoretical and mathematical models based on Alternative Stable States (ASS) can be used to model and explain the deterioration and restoration of shallow lakes, while multiple patterns of ecosystem state response to external drivers have been validated by a large number of observations in European and North American lakes. In eastern China, eutrophic lakes account for 86.7% and heavily eutrophic lakes for 12.2% of more than 100 lakes in the Middle and Lower Reaches of the Yangtze River plain. Large lakes, such as Chaohu and Taihu, have experienced large cyanobacterial outbreaks in the early twenty-first century, and these disasters will probably be replicated in other lakes under similar conditions. I therefore need to understand the mechanism underlying such catastrophic shifts in lake ecosystems. Natural and anthropogenic influences on the ecological trajectories of lake ecosystems, response mechanisms, and how to avoid subsequent catastrophes are the main questions addressed by this thesis.

To discover the external conditions that predominantly affect lake ecosystems in the lower Yangtse River, I used palaeolimnological tools and selected a typical lake in the middle and lower reaches of the Yangtze River, Lake Taibai, for a case study. The study used information relating to the species composition of subfossil diatom genera as indicators of the reconstructed ecosystem state as well as lake area, depth, chlorophyll content, transparency, ion concentration and nitrogen and phosphorus content as environmental factors to analyse the correlation between environmental changes. In terms of anthropogenic impacts, historical data on lake hydrodynamics, fish farming

intensity and nutrient loading in the basin over past decades were recovered using historical records, literature research and proxy reconstruction to calculate the magnitude of the correlation between ecosystem state driven by human and natural factors and to analyse possible responses by examining feedback mechanisms.

Since it is difficult to use palaeoecological data alone to reveal the dynamic ecosystem changes and emergent mechanisms under the influence of various external factors, I developed an agent-based model (ABM) to simulate the influence of environmental and human activities on lake ecosystems to help analyse how past patterns of shifts in state occurred, the influence of external conditions on these changes and how to avoid the development of catastrophic ecosystem failures. The ABM was constructed on the basis of the predation-prey relationship and other interactions like competition and providing refuge and on known ecological theories to simulate population dynamics in aquatic food webs in response to external drivers. The developed ABM – LAKEOBS_MIX achieves a reasonable balance between generality and realism, providing insights of how ecosystems were affected by various drivers in MLYB-like lakes. The effects of the external environment are implemented as sub-models to the biotic interactions, and the currently available factor models are lake nutrient levels, temperature, water depth, area and changes in the number of fishes in the lake. In-silico experiments were designed with multiple factors to simulate different conditions and measure ecosystem response patterns. The simulations show that the patterns of equilibria developed from the same initial state can be very different due to stochasticity of spatial distribution and decision making of individuals in functional groups. Decades are needed for the modelled ecosystem to form a dynamic equilibrium without external disturbance, which can be altered by any sudden extinction of a functional group. In experiments where nutrient loading constantly impacts on the formed equilibrium, results show regime shifts that occurred in different time and patterns due to changes in the amount, adding pace and timing of nutrient load, the presence of other influencing factors. Besides, recovery pathways are simulated in hyper-eutrophic system state, confirming moderate natural fishing and nutrient removing are efficient approaches to lower the total nutrient level in lake ecosystems.

Combining these two approaches provided us with an improved understanding of the development trajectory of lake ecosystems in the MLYB over the last 100 years. I discovered links between changes in conditions and their corresponding response mechanisms, and according to the results of simulations I was able to develop possible regulatory approaches to avoid abrupt system degradation

Contents

List of Tables

List of Figures

List of Accompanying Materials

The Netlogo source code for the agent-based model LAKEOBS_MIX I built in the Chapter 4 has been uploaded on the computational model library CoMSES. It has been peer-reviewed and is licensed under a GPL-3.0 license. The private link of the model is as follows.

> Yanjie Zhao (2022, January 25). “Agent-based model to simulate equilibria and regime shifts emerged in lake ecosystems” (Version 1.0.0). CoMSES Computational Model Library. Retrieved from: https://www.comses.net/codebase-release/117684ec-2138-4966-86a8-c2b8c369b151/

Research Thesis: Declaration of Authorship

Print name: **Yanjie Zhao**

Title of thesis:

Regime Shifts in Shallow Lakes: palaeoecological and agent-based model approaches

I declare that this thesis and the work presented in it are my own and have been generated by me as the result of my own original research.

I confirm that:

The work was done wholly or mainly while in candidature for a research degree at this university
Where any part of this thesis has previously been submitted for a degree or any other qualification at this university or any other institution, this has been clearly stated.
Where I have consulted the published work of others, this is always clearly attributed.
Where I have quoted from the work of others, the source is always given. With the exception of such quotations, this thesis is entirely my own work.
I have acknowledged all main sources of help.
Where the thesis is based on work done by myself jointly with others, I have made clear exactly what was done by others and what I have contributed myself.
None of this work has been published before submission

Signature: Date:

Definitions and Abbreviations

Abbreviation	Definition
ABC	Approximate Bayesian Computation
ABMs	Agent-Based Models
BMR	Basic Metabolism Rate
Chl-a	Chlorophyll-a
COD	Chemical Oxygen Demand
DIP	Dissolved Inorganic Phosphorus
GEM	General Ecosystem Model
MLYB	Middle-and-Lower Yangtze River Basin
ODD	Overview, Design concepts, Details
PCA	Principal Component Analysis
RS	Regime shift
SD	Secchi depth
SDMs	System Dynamic Models
SESs	Socio-Ecological Systems
Tfe	Total iron
TN	Total nitrogen
TP	Total phosphorus

Chapter 1: Introduction

1.1 Background and rationale

Over the last century, cultural eutrophication has been one of the primary ecological issues for most of the world's freshwater ecosystems (Smith & Schindler, 2009). Such eutrophication results from excessive plant growth owing to nutrient enrichment by human activities and causes undesirable consequences including the degradation of water quality, loss of biodiversity, increased waterborne disease transmission, excess sedimentation and major trophic cascades from altered biological food webs. These factors are major concerns at a time in which the global fresh water supply is facing rapidly increasing demand (Ansari et al, 2011). In subtropical and tropical regions characterised by intense human activities, waters are exposed to a growing probability of accelerated cultural eutrophication and water quality degradation because of fast nutrient enrichment, rapid urbanization and the application of large-scale hydroelectric projects and other disturbances that have taken place over the last century (Gao & Zhang, 2010).

Lakes with high water quality can provide clean drinking water, healthy aquatic habitats for wildlife and wellbeing for surrounding residents, including food security, aesthetic and cultural attributes and the maintenance of catchment-wide biodiversity (Reynaud & Lanzanova, 2017; Schallenberg et al, 2013). Under the adverse pressure caused by human activities, lake ecosystems may deteriorate to undesirable states by shifting from one stable regime to another, causing the loss of ecological and economic resources as well as heavy restoration costs (Scheffer et al, 2001; Schindler, 2012). An example of a regime shift in shallow lakes is an ecosystem abruptly shifting to a eutrophic state induced by excessive exogenous nutrient loading, causing persistent turbid-water conditions and algal blooms (Scheffer et al, 1993). The freshwater shallow lakes in the middle and lower reaches of the Yangtze River Basin (hereafter referred to as 'MLYB') now face unprecedented human-induced eutrophication (Qin et al, 2013) in a region where roughly one-third of all Chinese lakes are situated. Although the history of human modification on lakes is long, more recent industrialization and urbanization have resulted in an exponential rise in use of lake resources and widespread lake deterioration in this region (Zhang; Yang et al, 2018). Significant efforts and billions of dollars have been spent on lake ecosystem restoration, including the establishment of wastewater treatment plants, the closing of heavily polluting factories and the prohibition of aquaculture and fisheries (Wang et al, 2015). It is therefore extremely valuable to study and understand the nature of such critical transitions in order to facilitate optimal management strategies and to avoid the repetition of inappropriate conditions that may continue pushing lakes across catastrophic thresholds.

Many studies have employed the Alternative Stable States (ASS) hypothesis to test and explain complex changes in nature and society, especially as far as changes showing characteristics of abruptness, irreversibility and unpredictability are concerned (Scheffer, 2009). Methodologies and statistical tools have emerged for detecting regime shifts (deYoung et al, 2008; Gal & Anderson, 2010), analysing correlations between system states and drivers, investigating dynamic processes in transitions and even predicting critical transitions by establishing early warning signals (Kéfi et al, 2014). However, there is still a great deal that has yet to be understood concerning patterns of regime shifts and drivers, as well as the interactions that occur between drivers and ecosystem states in many geographic regions that possess characteristic conditions and are subject to anthropogenic disturbance. Motivated by the severe degradation of lakes in the MLYB region, this thesis aimed to investigate the general regime shifts and potential drivers in this area during the last century and test mechanisms of ecosystem change under various pressures using computational modelling to assess the cross-factor effects of drivers on ecosystem state changes.

In more specific terms I firstly mined data relating to ecological and environmental changes at the study site using different methods of literature search and palaeolimnological reconstruction to detect empirical regime shifts and relations between potential drivers and responses using various statistical models and methods. After evaluating the elements and relationships involved, agent-based models were developed to simulate the empirical patterns of regime shifts and to conduct in-silico experiments in multiple conditions.

1.2 Aims and objectives

Issue	Aim	Objectives	Results	Methods
Processes and mechanism of regime shifts are poorly understood in eutrophicated lakes	Investigate evidence of regime shifts, drivers and mechanisms of nonlinear changes in lake ecosystems	Investigate regime shifts and potential drivers in the MLYB	1. Evidence of human activities and ecological impacts	literature review/ paleoenvironmental reconstruction of environmental conditions
			2. Detection of regime shifts	Paleoecological reconstruction of ecosystem state in Taibai Lake
				Breakpoint analyses on ecosystem states' indicators
			3. Putative feedback loops between drivers and ecosystem states	Correlations and regression analysis of factors and ecosystem states
		Build an agent-based model of lake ecosystem changes based on the evidence	4. Modelling relationships of functional groups	Developing an agent-based model based on putative relationships and biological knowledge
			5. Simulating regime-shift scenarios by imposing changes of nutrient load and fish population	Simulating equilibria as an undisturbed stable ecosystem state
				In-silico experiments simulating external drivers on ecosystem
			6. Better understand the mechanism of regime shifts in lake ecosystems	Combining findings in empirical evidence and simulations of the agent-based model

Figure 1-1: Logical framework of the thesis, summarizing the main issues and aims, objectives, main outputs and methods that were used.

As mentioned in the last section, one of the urgent issues facing human wellbeing in lake environments is our poor understanding of various ecological transitions that are under pressure and the mechanisms involved in their interactions. Figure 1-1 summarises the logical sequences in the thesis, which aims to investigate the drivers, responses and mechanisms that underlie the ecological shifts in the lakes of the MLYB.

To achieve our goal, tasks were sub-divided into two main objectives: Firstly, to investigate regime shifts and potential drivers in the MLYB, secondly to test mechanisms behind these ecosystem changes under multiple pressures, using an agent-based model developed on the empirical evidence. To achieve the first objective, I obtain evidence regarding human activities and the ecological impacts of these activities on lakes, analyse the results of abrupt ecological shifts, and understand the relationships between dominant anthropogenic drivers and ecosystem states. The process required a literature review, palaeoenvironmental and palaeoecological reconstruction and multiple forms of statistical analysis. To achieve the objective of modelling the nonlinear ecological changes, an agent-based model was developed and verified based on the empirical data and putative relationships obtained in the previous part. Then the ABM was used to simulate ecosystem changes under different pressures and anthropogenic manipulation as observed in MLYB to provide insights for mechanism of critical transitions and lake management.

1.3 Thesis structure

The thesis consists of seven chapters, including an introduction and a conclusion, and follows a logical framework to serve the above objectives. This chapter introduces the thesis, and Chapter 2 comprises a literature review and evidence syntheses, contributing to the Results in Figure 1-1 and setting up a knowledge background based on currently available information in the scientific community. The first two chapters discuss the wide range of current knowledge in regime shifts in lake ecosystems and prepare me to explore dynamic changes of specific patterns.

Chapter 3 describes a case study in a MLYB lake (Taibai) that investigated regime shifts and their drivers, using palaeoecological and monitoring data to infer ecosystem responses to drivers, and potential feedback loops.

From Chapter 4 onwards, modelling the patterns of nonlinear changes occurring under pressure become the main focus of the thesis (Objective 2). Chapter 4 addresses the rationale and overview, design, and details (ODD) protocol of the LAKEOBS_MIX ABM model and the results of simulated steady states. The model performs as an appropriate system at the individual, population, and ecosystem levels based on verification, sensitivity tests and calibration. In Chapter 5, I re-parameterise the model, setting the results against realistic data from MLYB lakes and simulating the emergent patterns that resemble realistic lake ecosystems in the eutrophication and recovery process. The synergistic effects of nutrient addition and other external forces, such as temperature and changes in depth, are analysed in the in-silico experiments.

Chapter 2: Literature Review.

Theories and evidence of regime shifts in lake ecosystems

2.1 Theory background

The term “ecosystem” was first proposed by Tansley (1935), and was developed further after the 1950s when Odum (1953) incorporated von Bertalanffy’s General System Theory to define ecosystems as conceptual units with spatial and/or temporal demarcation depending on the goal of the study (Marín, 1997). Lake ecosystems are commonly recognised as consisting of the lake and its drainage basin (Wetzel, 2001, p. 131) as the inputs from the catchment areas of any lake are important in regulating biogeochemical processes in the lake itself.

Lakes were recognised very early in System Theory as microcosms within which the dynamics and interactions of food webs could be observed (Forbes, 1887). Holling (1973) stated that freshwater lakes could be evaluated as reasonably self-contained systems. He reviewed anthropogenic nutrient enrichment from sewage, man-made fertilizers and intense fish harvesting as factors that could result in the unexpected collapse of the ecosystem state, citing the progressive reduction of resilience in the Great Lakes in the USA after 1930. Many studies confirmed this pattern, and the consensus was that regime shifts in lakes are influenced by a combination of external forces and the internal resilience of lake ecosystems (Rockström et al, 2009; Scheffer & Carpenter, 2003). Loss of resilience renders ecosystems more vulnerable, allowing them to respond to smaller perturbations (Folke et al, 2004).

The process of ecological transition in eutrophicated lakes has been visualized in conceptual models based on the ASS theory (Figure 2-1). From a clear-water state to a turbid-water state, Folke (2004a) drew a “ball in a cup” diagram to explain mechanisms of regime shifts caused by the accumulation of phosphorus in surrounding agricultural soil and lake mud. These mechanisms and triggered by disturbance by flooding, warming and the overexploitation of predators. Folke assumed that the pristine clear-water state and the turbid-water state are two alternative equilibria (the cup), and the ecosystem state (the ball) moves dynamically between these two basins of attraction. Scheffer (2001) saw the conceptual dimension of resilience as something that could be projected onto the ecosystem state-condition relationship to demonstrate the dynamic process of regime shifts. The stability landscapes in panel c of Figure 2-1 are modified by the lake’s internal structure, and if the resilience is weak enough, a small perturbation can cause the system state to fall into the other basin of attraction. The reason for stability changes could be nutrient loading or changing the quantities of submerged macrophytes in the lake ecosystem, a process that is supported by field investigations (Scheffer et al, 1993; Scheffer & Jeppesen, 2007). When the clear-water basin is small and the ecosystem state responds quickly, switching to anther basin (F2 to F1), the small basin acts as a threshold and the unstable phase (the hill) to cross represents the tipping point to this ecosystem. The general patterns of critical transition share similar features to ecosystem states and causes in many other lakes, and this is what inspired us to study and test the hypotheses in the MLYB.

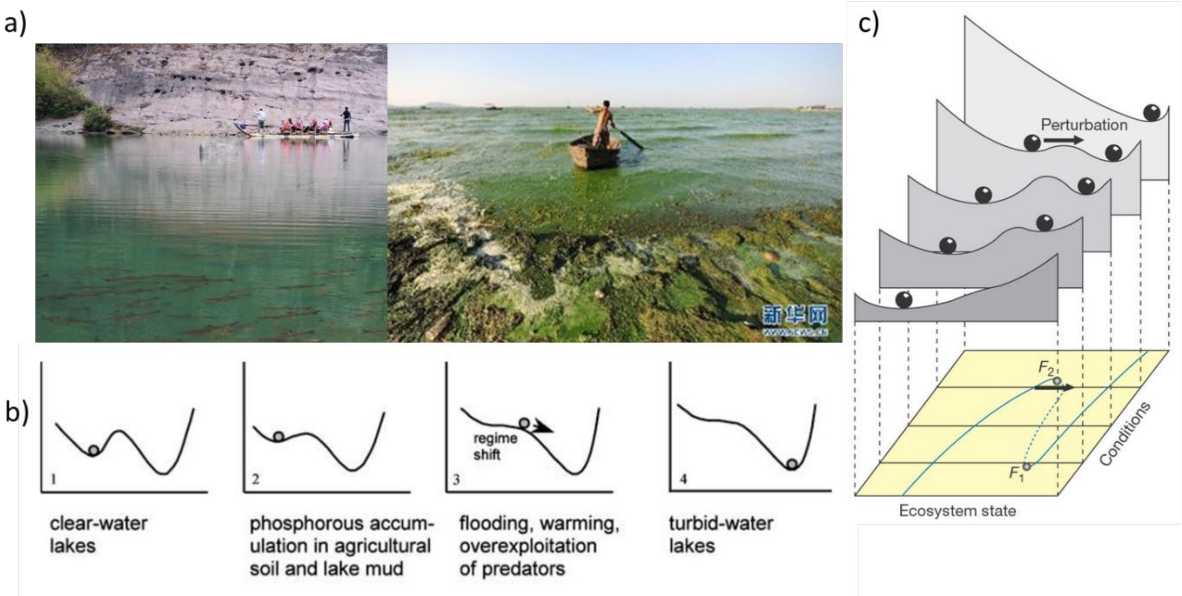

Figure 2-1: Photographs of lakes in clear-water state and turbid-water state with algal blooms (a) and “ball-and-cup” conceptual model illustrating the possible regime shifts between the two states (b & c). Panel b is from Folke (2004) and c is from Scheffer (2001).

2.1.1 Concepts

As part of the premise of regime shift, the concepts of “alternative equilibria” and “multiple/alternative stable states” must be introduced before describing nonlinear ecosystem behaviour (Scheffer and Jeppesen, 1998; Beisner, Haydon and Cuddington, 2003). The ball and cup metaphor is usually used to explain the concepts of ASS, in which the system state (the ball) normally rests in a stable basin of attraction (the cup), but can tip over into another cup following an external disturbance (Carpenter et al, 2001). The transition observed could be a regime shift or a smooth change. The depth of the cup shows resilience, which refers to the capacity of the system state to maintain itself in its current state against pressure, although some disagree with this definition, referring to it as resistance rather than resilience (Capon et al, 2015; Scheffer, 1990).

A shortlist of terms and definitions in the framework covering ASS and regime shifts is summarised in **Table 2-1**. Since these concepts are closely linked with each other and often used together in depicting the transitions in natural systems, the reviewing of concepts familiarised us with key terms and publications.

Table 2-1: Main concepts of multiple stable states, regime shifts, thresholds and other supporting terms

Term	**Definition**	**References**
Ecosystem	A biotic community interacting with its physical environment as a conceptual unit demarcated by the scope of the study	(Marín, 1997; A. G. Tansley, 1935)
Ecosystem state	A numerical description of an ecosystem that includes one or more ecological responses	(Capon et al, 2015)
	The characteristics used to describe the status of an ecosystem at a particular domain in space and time	(Ratajczak et al, 2018)
Ecological response	A time series of values representing an individual component of ecosystem state	(Capon et al, 2015)
Driver/ stressor	External factors that influence the dynamics of a system without themselves being affected by the system	(Ratajczak et al., 2018)

Disturbance/ perturbation	Any process that effects the ecosystem via changes to the biophysical conditions	(Standish et al, 2014)
	A relatively discrete event in time that alters the biotic and/or abiotic components of an ecosystem	(Ratajczak et al, 2018)
Multiple/ Alternative Stable States	Multiple (alternative) basins of attraction within a system	(Suding & Hobbs, 2009)
	Two or more states in which an ecosystem can persist within the same range of driver variables	(Ratajczak et al, 2018)
Hysteresis	The situation in ASS in which the pathway of degradation (or change in one direction) differs from recovery (or change in the opposite direction)	(Suding & Hobbs, 2009)
	A system property that can follow different paths when increasing or decreasing a perturbation.	(Andersen et al., 2009)
Abrupt change	Substantial changes in the mean or variability of a system that occur over a short period of time relative to typical rates of change	(Ratajczak et al, 2018)
Regime shift	The process whereby an ecosystem changes from one ASS to another	(Capon et al, 2015)
	A sudden shift in ecosystem status caused by passing a threshold at which core ecosystem functions, structures and processes are fundamentally changed	(Andersen et al., 2009)
	A significant observed change in an ecosystem. All abrupt ecological changes are regime shifts, but not all regime shifts are abrupt; they can be synonymous with state transitions and phase shifts.	(Ratajczak et al, 2018)
Ecological threshold	Points at which even small changes in environmental conditions (underlying controlling variables) will lead to large changes in system state variables	(Suding & Hobbs, 2009
	The critical value of an environmental driver for which small changes can produce an ecological regime shift	(Andersen et al., 2009)

Tipping point	An ecological threshold beyond which a former ecosystem state cannot be regained even when the pressure is released; synonymous with irreversible change	(Capon et al, 2015)
Critical transitions	Transitions that occur when a threshold is passed, causing the appearance or disappearance of alternative states; synonymous with bifurcations	(Ratajczak et al, 2018)
Resilience	The capacity of a system to absorb disturbance and re-organize itself while undergoing change so as to still retain essentially the same function, structure, identity and feedbacks	(Holling, 1973)
Feedback	A closed-loop process in which the results affect the inputs, influencing future negative and positive results	(DeAngelis et al, 1986)

Setting the regime shift as the focus, related terms can be visualised as a tree diagram according to topical correlations in the literature (Figure 2-2). Mathematical terms describing the attributes of nonlinear changes include bifurcation, threshold, tipping points, critical transition, critical slowing down and early warning signals. Ecological terms based on population dynamics include stability and resilience, which are linked to biodiversity, stable limit cycles and equilibrium states. In terms of mechanisms, feedback loops are frequently used, and these relate to concepts of adaptive food webs and models. Lastly, restoration is of great concern to lake management and hysteresis could be a problem in the recovery process. With this diagram of terms in mind, I find literatures studying specific aspects and pick suitable methodologies to investigate the indicators that I need to examine further.

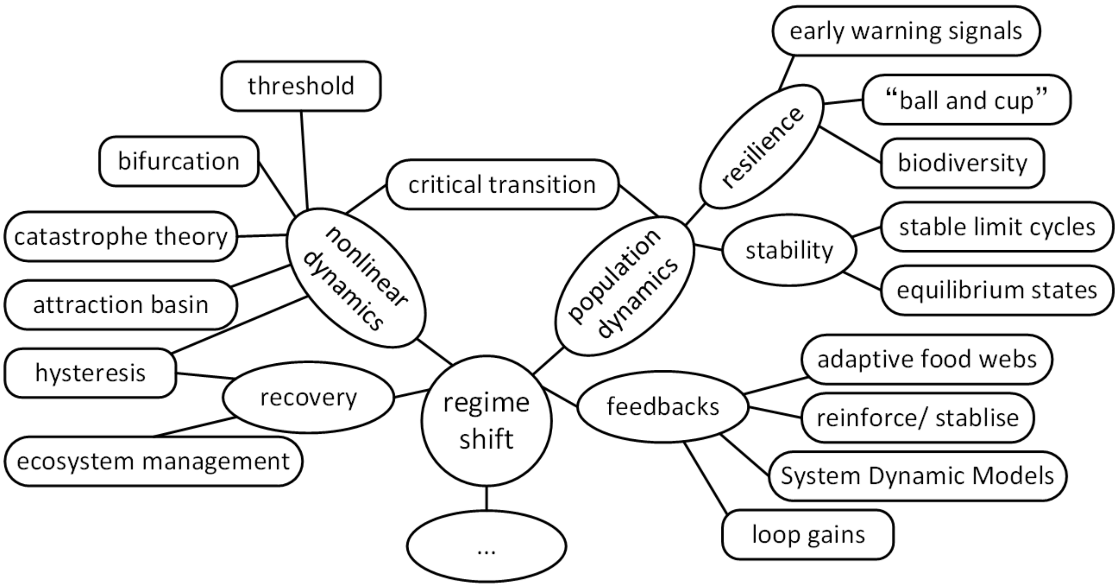

Figure 2-2: Tree diagram of regime shift and related terms according to topical correlations. The diagram aims to reflect the relations of topics and is inevitably subjective.

2.1.2 Theories in a historical perspective

Over the last century, catastrophes have been modelled mathematically in topological terms by René Thom, and the catastrophe theory gained popularity due its ability to successfully account for the behaviour of the catastrophes(Saunders, 1980; Thom, 1975; Zeeman, 1976). However, according to May (1977), catastrophe theory is a localised theory that cannot be used to represent a global description of dynamics. He reviewed mathematical models of ASS in single- and two-species systems and confirmed that it is possible to link ASS theory to observations in real-world cases (ibid). From then on, the two theories and terminologies came to coexist and can be chosen depending on the focus of the studies and citation sources. A mixture of the two produced simple specific models that could be used to represent alternative equilibrium states in freshwater systems (Scheffer, 1990) and the socalled cusp catastrophe model and the ball-in-cup metaphor were thereafter a shared part of the new ecological theory. The cusp model is a simple form of mathematical catastrophe models that exhibit varying transitions in equilibrium states with control parameters. The analogy between a ball swaying in a cup and the system state oscillating around its equilibrium position visualises basins of attraction as the cups and resilience as the depth of each cup. When the ball receives strong horizontal perturbations or the cup turns shallower, the ball (system state) is easy to shift from the previous basin to a neighbouring basin (Marten Scheffer, 1990). The term “regime shift”, originally describing abrupt changes in time based on the abundance of a particular component in marine ecosystems, was extended to describe the changes in ecosystems as a whole (i.e. from one ecosystem state to another). The mix of theories was henceforth considered as a property of ecosystem change (Collie et al, 2004; Scheffer & Carpenter, 2003). Indicators of stability in ecological systems, such as resilience and the domain of attraction and feedback, are also included in the theoretical framework to depict the mechanisms involved in catastrophic shifts between multiple stable states (Folke et al, 2004; Kinzig et al, 2006; Scheffer et al, 2001).

In the context of ecosystem change, three types of regime shifts may exist along a continuum of internal ecosystem structure in the cusp catastrophe model (Figure 2-3). This is determined by the solutions of equilibrium points of the cusp model function (Grasman et al., 2009)

$$\alpha + \beta y - y^3 = 0$$

where y means the system state and α and β are the control parameters. Regime shifts can be smooth, they can be abrupt in reflection of external forces, or they can be discontinuous with hysteresis in terms of recovery. In Danish shallow lakes, Scheffer (2009) found that catastrophe graphs could be used to describe the relationships between in-lake submerged vegetation coverage, lake depth and nutrient loading. Lake depth governs the role of internal ecosystem structure and modifies the driver-response relationship between vegetation coverage and nutrient loading. In shallow lakes, or in shallower parts of lakes, it is easy for nutrient loading to tip the ecosystem balance represented by vegetation cover, whereas in deeper lakes or deeper parts of lakes, the state changes more gradually.

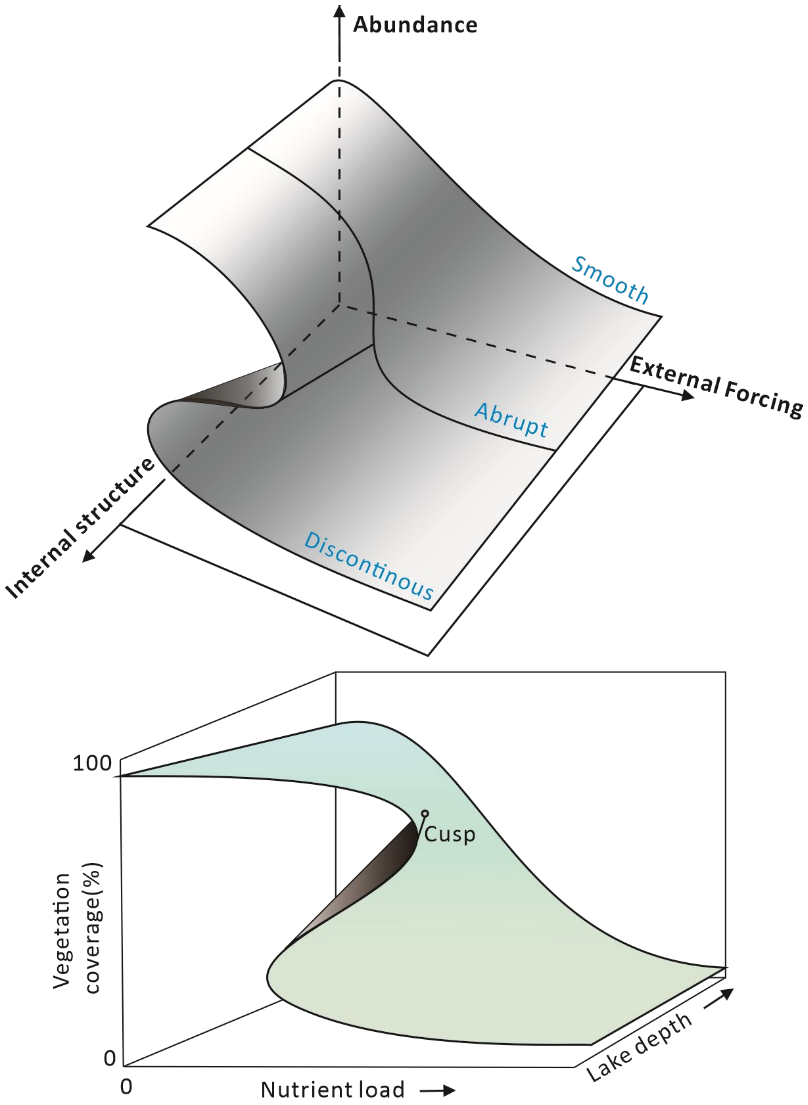

Figure 2-3: Cusp catastrophe models illustrating three types of regime shifts along a continuum of internal ecosystem structure (adapted from Collie et al, 2004) and the application in aquatic ecosystem (adapted from Scheffer, 2009)

The amount of research based on this framework has been increasing rapidly in theoretical, modelling, experimental and empirical observations and reviews are published every few years. As anthropogenic activities begin to cause even more significant impacts to the environment, it is recognised that “planetary boundaries for humanity” should not to be exceeded in order to avoid disastrous consequences, as human activity has pushed the Earth’s systems to the brink of their stable environmental state since the beginning of the Holocene era (Rockström et al, 2009). Despite being relatively new, this concept has opened debates in sustainability awareness and changed our attitudes towards catastrophes, assumptions, approaches, methodology and indicators of change (Nature, 2009), inspiring different views on the relationships between drivers and responses in the Earth’s systems (Montoya et al, 2018).

Long-term manipulation and restoration experiments have been conducted in a range of Dutch and Danish lakes, providing continuous monitoring data and field observations (Meijer, 2000; Sondergaard et al, 2008). Models have been used to clarify specific problems relating to system processes, such as how thresholds cascade through scales (Kinzig et al, 2006), how mutualistic communities collapse in sequence (Dakos & Bascompte, 2014) and what indicators can be used as early warning signals before tipping points are reached (Wang et al, 2012; Wilkinson et al, 2018). Overall, research based on regime shifts and resilience frameworks is expanding, with high-quality reviews and appraisals from all viewpoints published in theory development (Andersen et al, 2009; Peterson et al, 2015), experiment proceedings (Schroder et al, 2005), methodologies (Contamin et al, 2009) and empirical studies.

In order to obtain an objective view of current scientific work and opinions, a literature review was conducted by searching “regime shift” and “lake” in the Scopus and

Web of Sciences citation databases. A total of 347 articles were examined either by looking at their abstracts or by reading the full texts, and the main parameters of empirical observation and data, methodology and conclusion were recorded. The analysis of these articles and papers confirmed a growth in the number of ecological studies on regime shifts and the diversity of geographical distribution, methodology, temporal range of detection windows and drivers. Most studies looked for transitions between clear-water state to turbid-water state in multi-decadal range as a part of eutrophication.

2.2 Preliminary findings

Three terms of interest were searched for as topics in the literature database of the Web of Sciences (WoS) Core Collection, namely “regime shift”, “Alternative Stable States” and “critical transition”. Although overall numbers of publications have grown in the past 40 years, publications on the topic of “regime shift” have increase more rapidly and have become the most popular subject since 2005. Analysing publications according to disciplinary categories, the fields that contribute most to the “critical transition” topic are largely when compared to the fields that contribute most to the “regime shift” topic (Figure 2-4). Among the records containing the term “critical transition”, the vast majority are studies in physics and chemistry, while studies in ecology (92 out of 1900) and environmental sciences (48 out of 1900) constitute a small minority. In contrast, among the records on the topic of “regime shift”, most studies come from the disciplines of ecology, oceanography, marine freshwater biology and environmental sciences (1562 out of a total of 2036), with a small portion coming from the field of economics. These findings are consistent with our knowledge of terminology development in studies on nonlinear ecological changes, and confirm that more research surrounds the “regime shift” topic, and this research addresses and explains nonlinear changes in natural ecosystems following the newer theory frameworks. A subset of “regime shift” based on a combination of “regime shift” and “lake”, was subsequently searched on WoS to discover more detailed information relating to finished or ongoing empirical studies and their results.

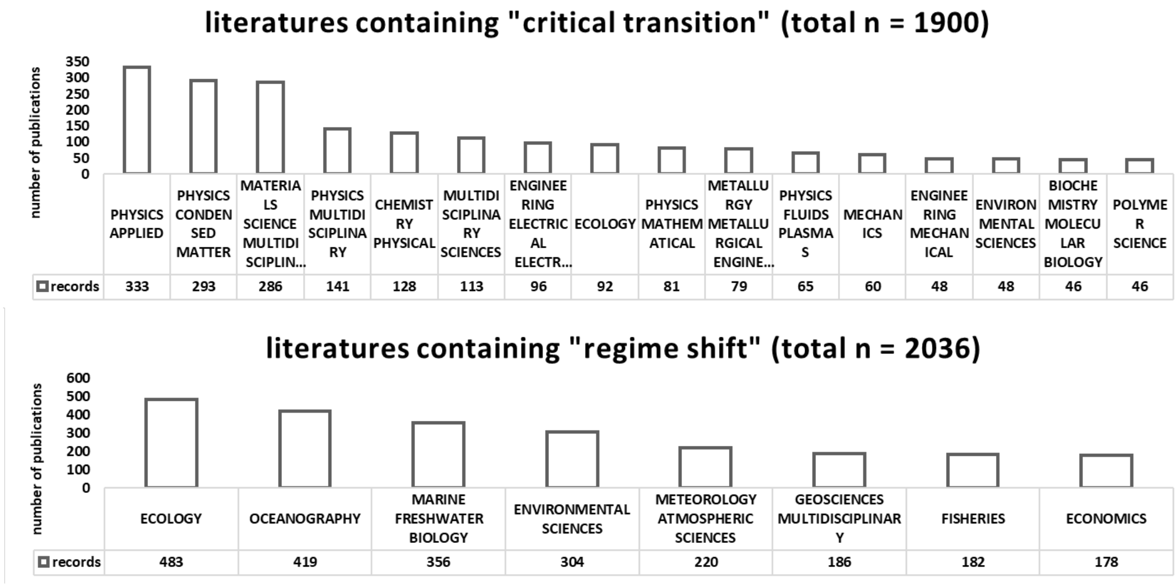

Figure 2-4: Number of publications by categories analysed in WoS Core Collection. Categories with less than 5% are not included. Categories may overlap with each other.

2.3 Exploratory literature search

From the publications searched in the last subsection, literature containing “regime shift” seems more related to the ecosystem-level phenomenon this thesis aims aim to explore. Thus, as a further exploratory step, a combination of the term “regime shift” and the site type “lake” was searched on Elsevier’s citation database Scopus and Clarivate’s The Web of Science (WoS) Core Collection in fields of article titles, abstracts and keywords at the same time. The time ranges of publications in both databases were set at between 1970 and 2020. A total of 648 articles were found in the databases, although the results included 207 duplicates, leaving 441 individual articles and papers. A list of information was exported into an Excel spreadsheet showing authors, title, year, source title, citation count, abstract, author keyword, index keyword, language and the type of publication. Abstracts of the 441 articles were scanned in order to examine the main methodologies used and results related to regime shifts and study sites. Ninety-one articles that used “regime shift” without testing a hypothesis or providing evidence in lakes were eliminated. Meanwhile, three articles that were inaccessible in terms of their full text were removed due to the lack of any detail confirming thein methodology used. If the article contained empirical data, the locations of the lakes, the time scale of the study and the span of detected regime shifts were further identified and recorded (see the figure below).

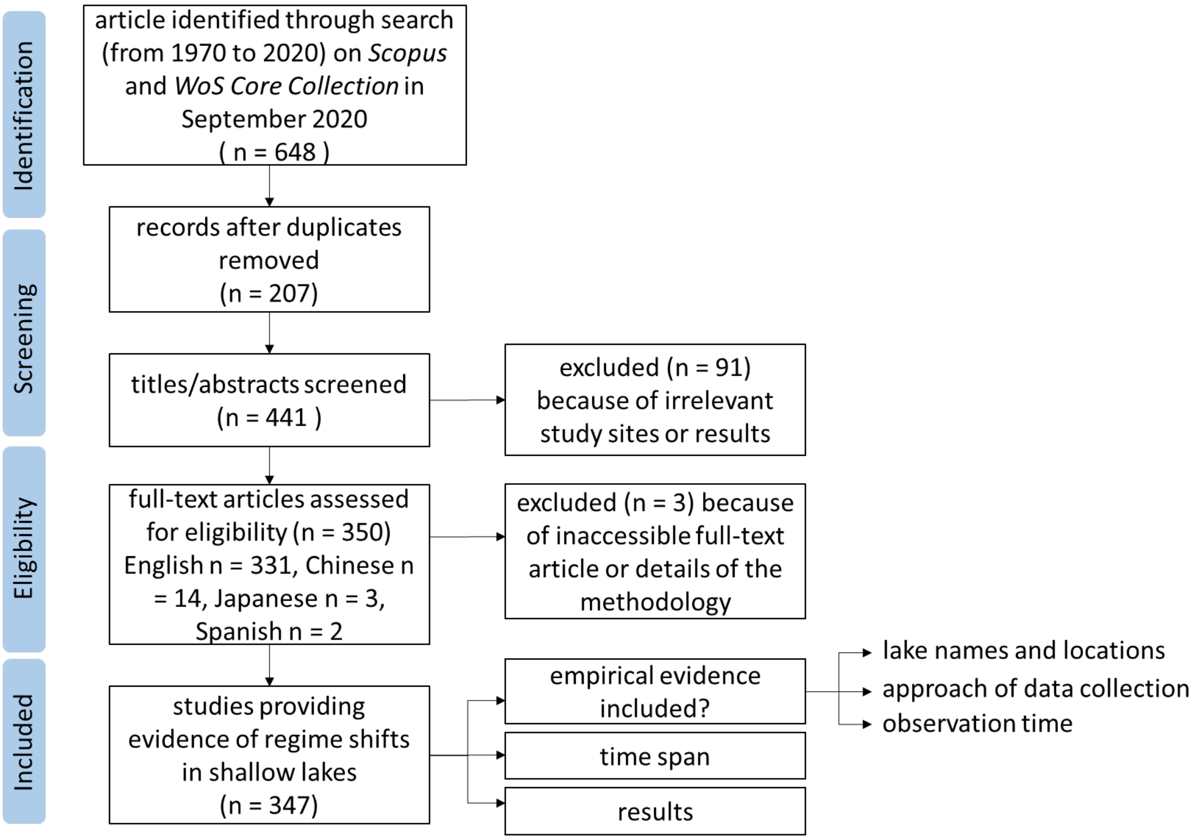

Figure 2-5: Processes used for searching and selecting literature

Searches that explored the trend of publications on different topics were also conducted in the WoS Core Collection so that the results would be comparable.

2.3.1 Empirical evidence

Among the collected literature that used “regime shift” and “lake” in their keywords, titles or abstract, 74% included empirical evidence and/or work based on empirical data, and the remaining 26% were based mostly on mathematics, computational modelling, review and opinions. The case studies of regime shifts were globally distributed and aggregated in

Europe, China, North America, south Oceania, and the Arctic regions (Figure 2-6). Case studies and reports discussed hundreds of shallow lakes that were reported to be abruptly and persistently deteriorating to a phytoplankton-dominant turbid state. These lake environments were finding it difficult to recover from such abrupt changes and included lakes in Scandinavia (Jeppesen et al, 2007), middle-and-lower Yangtze River basin in China (Qin et al, 2013), the southern part of the Laurentian Great Lakes (Carpenter, 2005) and wetlands in Murray-Darling basin in Australia (Kattel et al, 2015). In terms of climatic zones, tropical, subtropical, temperate and polar lakes were included. In terms of continents, Asia, Europe and America shared a similar proportion (around 30%) in the number of publications and study sites (Figure 2-7). Some lakes were studied more intensely than others. In the collection, Lake Taihu appears in seven articles as having been monitored from the 1960s to the 2000s, while Lake Poyang appears in eight articles, having been analysed using remote sensing, monitoring, meteorological data and comprehensive historical data.

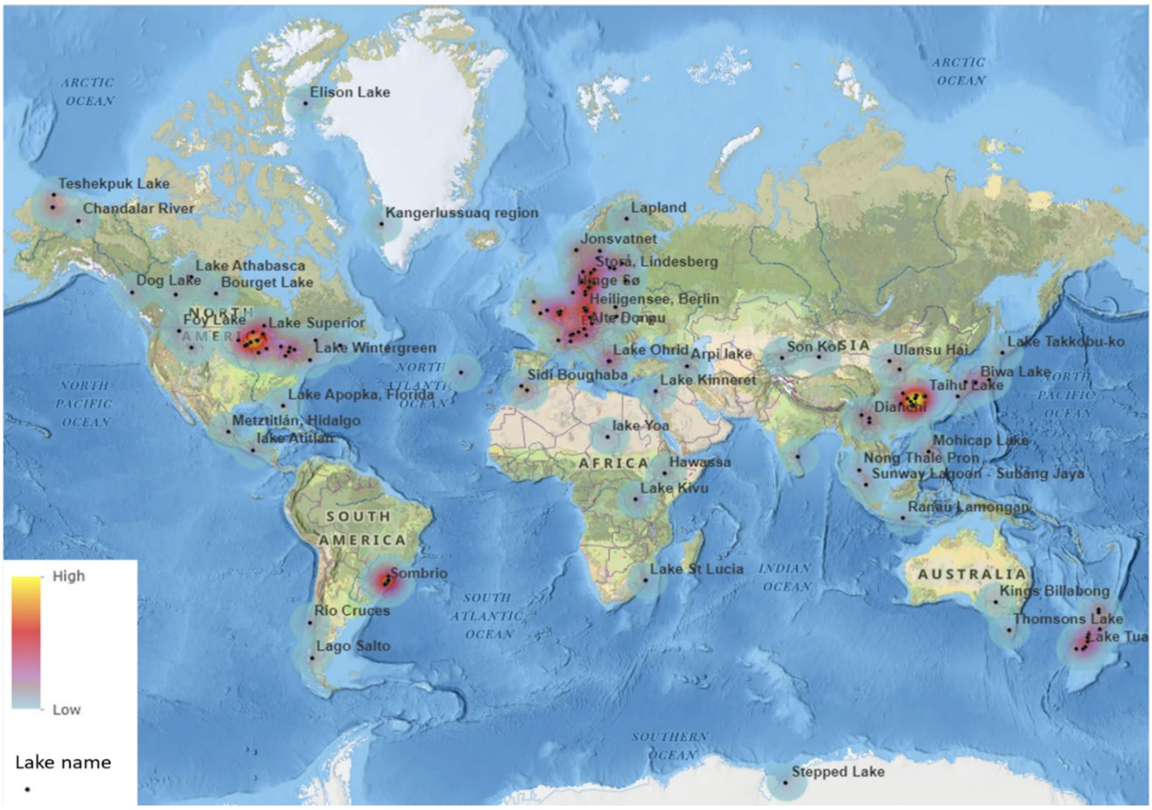

Figure 2-6: Locations of global lakes with publications of regime shifts and a heat map of the study-site density

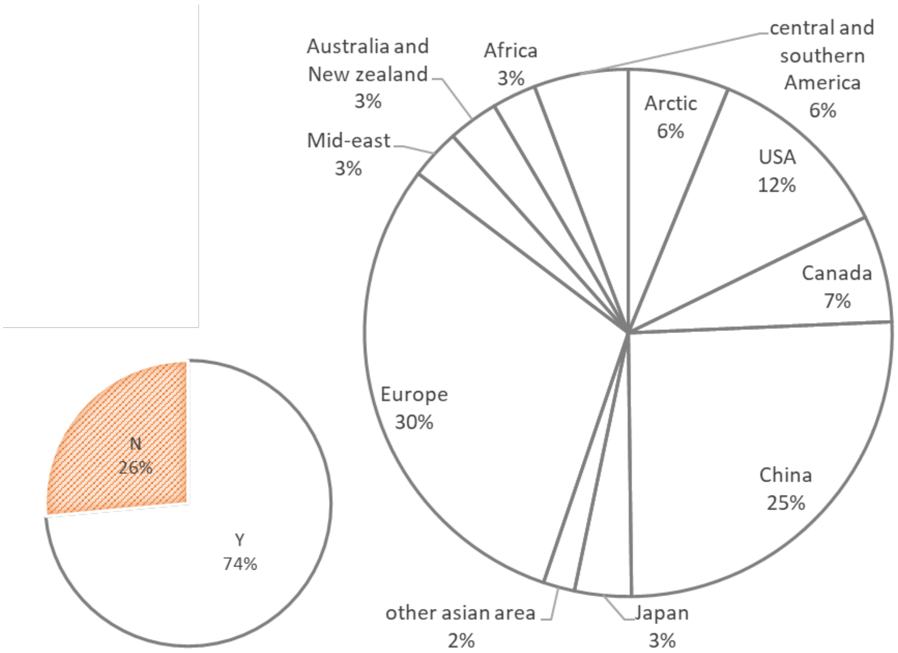

Figure 2-7: Number of publications on regime shifts and geographical distribution of case studies in the literature searched (Y indicates case studies in the article and N indicates no empirical evidence. The total number in the left circle is 348 and the right circle 259).

The 259 empirical studies include a huge diversity in terms of assumptions and results, methodologies and observation scales. Most studies use regime shifts as a basis for examining ecological data to look for plausible mechanisms. As well as studies testing hypotheses against their data, the impact of regime shifts is also assessed in ecosystems globally, and a database of regime shifts has been established to help review the mounting cases (Biggs et al, 2018). Drivers that triggered regime shifts described in the studies share many similarities in lake environments, most commonly nutrients (121 out of 347) and climate (91 out of 347).

2.3.2 Environmental factors and interactions

Lake eutrophication is a complex ecological process influenced by factors from multiple sources. The main control factors can be summarised based on explicit global scientific evidence based on four aspects that are determined by the geographic locations of lakes (Figure 2-8). Nutrient loading derived from human activities and geological substrates directly impacts on the lake sediment attributes and trophic level of lakes. It is also impacted by inflow of external matters, depth of the lake basin, light penetration, heat diffusion and thermal stratification, oxygen supply and depletion, lake shores, seasonal variation and water flows.

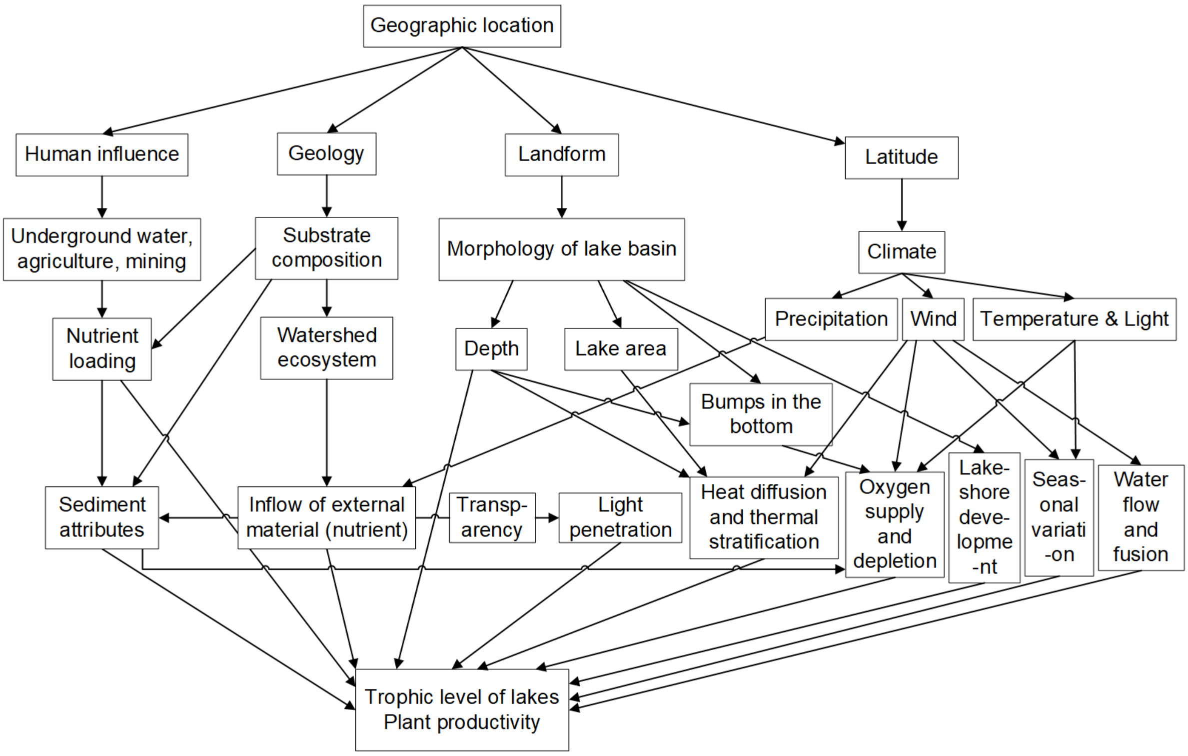

Figure 2-8: A conceptual framework of main control factors of lake eutrophication (adapted from Jin & Tu, 1990, p. 13)

From the literature collected, stresses on lakes from the natural and human sources include climate change, changes in food web structure (changes in predators, macrophytes, fish and other creatures), excessive phosphorus input and total phosphorus concentration. In the Regime Shift Database (https://www.regimeshifts.org/), when searching for freshwater eutrophication, drivers that could cause lakes shifting from an oligotrophic to a eutrophic state include nutrient input, vegetation conversion, habitat fragmentation and species introduction or removal as the main external direct drivers. Population growth, demand for food, changes in agricultural processes or intensity, urban growth, deforestation, rainfall variability and global warming often work as indirect drivers. Floods are also listed as an important type of shocks, since they bring unusual amounts of sediments and make lakes more turbid, which can reinforce phosphorous recycling feedback and maintain the turbid state (Rocha et al, 2017). The interactions between these environmental factors and ecosystem state are key to understanding mechanisms of regime shifts.

2.3.2.1 Nutrient input

Excess nutrients in water often cause algal blooms. The formation processes and maintenance of algal blooms are dependent upon feedback loops, where increasing nutrient input can overwhelm the capacity of vegetation to control phosphorus levels in water and encourage algae to grow, and the algal blooms can prevent sunlight from penetrating to the bottom of lakes. The decay of algal blooms can lead to the depletion of oxygen levels in water and cause anoxia and more decayed matter, emphasising the depletion of oxygen. Mechanism are well established and common to many areas around the world.

2.3.2.2 Climate patterns

Climate variations around the globe affect changes in the Earth’s system and regional ecological patterns. Using a Köppen-Geiger climate classification map derived from high-resolution climatic datasets of temperature and precipitation from 1980 to 2016 at a 1-km resolution (Beck et al, 2018) , the MLYB is in the area of “Cfa” and “Cwa”, meaning it is a warm temperate climate with hot summer climate zones (Figure 2-9), which shares a similar climatic pattern with the southeast coast of the United States, inland locations in South America and some areas in south Africa and eastern Australia. The climatic conditions form the basic background that determines patterns of ecological change and should be noted in comparative case studies.

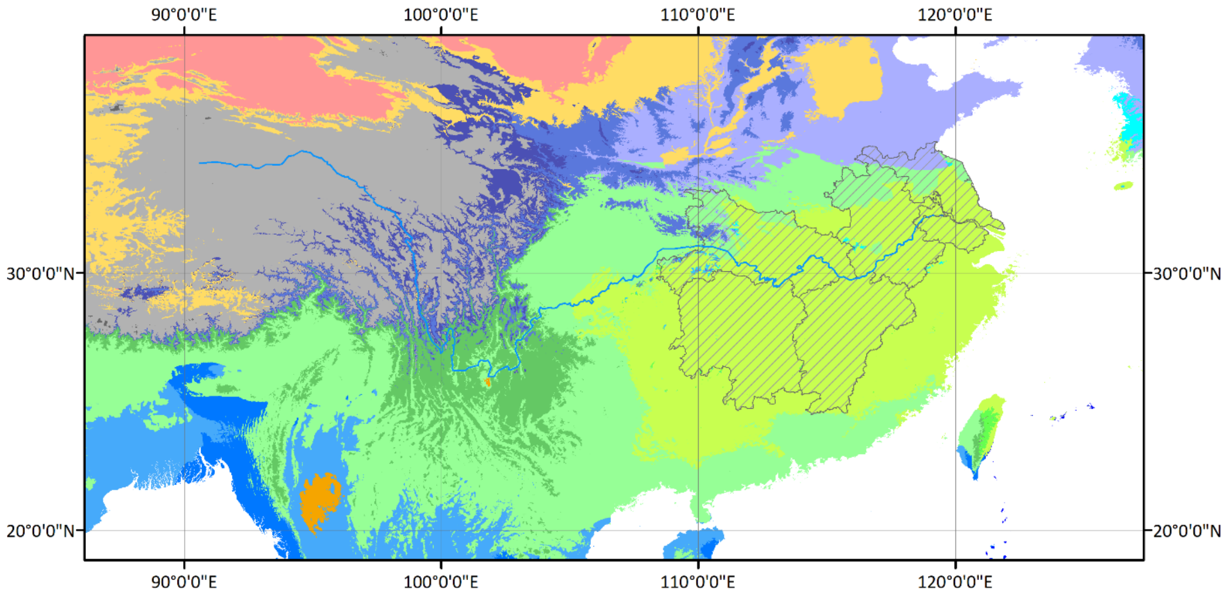

Figure 2-9: Middle and Lower Yangtze River Basin (the river is shown as a blue line and the provinces it passes through are shaded in grey lines) against the background of the Köppen-Geiger climate classification map (1980-2016)(Beck et al, 2018)

Anqing station (30.6167°N, 116.9667°E) is situated in the center of MLYB region, providing a representative case of local temperature monsoon climate. I obtained Integrated Surface Data of Anqing station from 1956 to 2021 for the temperature of the air and liquid precipitation depth dimension in six-hour duration from National Climatic Data Center, National Oceanic and Atmospheric Administration, USA. The resolution of the data is three hours. The annual temperature, ranging from 15.92 to 19.00℃ , is 17.17℃ in average (Figure 2-10). The annual precipitation, ranging from 655.9 to 4273.6 mm, is 1459.71mm in average (Figure 2-11). Seasonal variability is significant, showing simultaneous trends of peaks in temperature and precipitation as a characteristic of monsoon climate. July is the warmest month (29.15℃) with the most precipitation

(235.40mm) and January is the coldest month (4.18℃) with a small amount of precipitation (52.80mm).

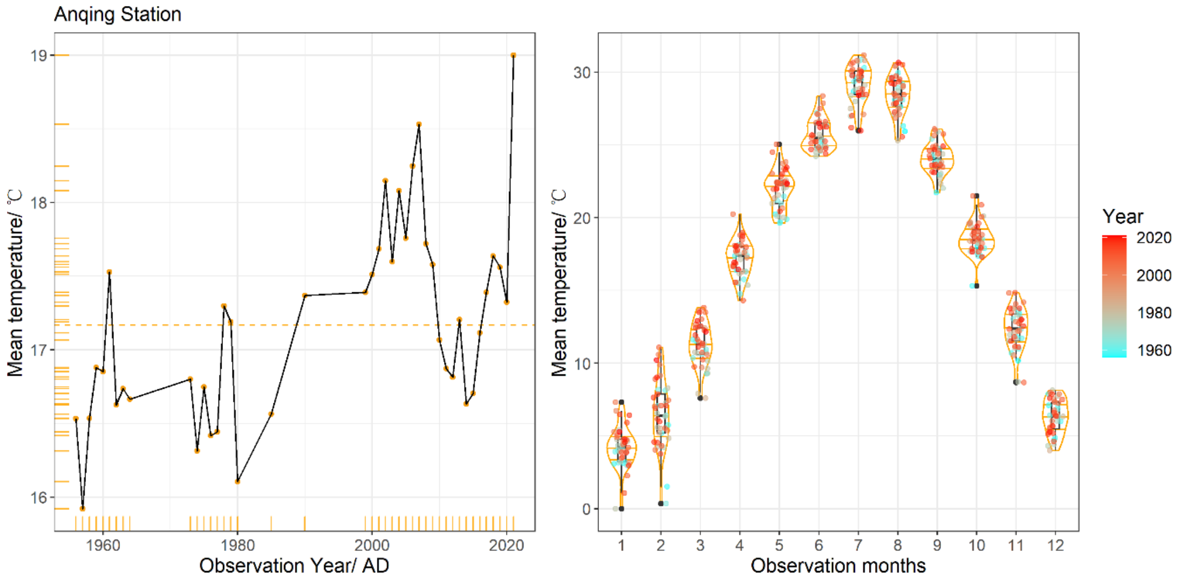

Data from National Climatic Data Center, NOAA

Figure 2-10: Annual(left) and monthly(right) mean temperature monitored in Anqing station between 1956 and 2021. The unit is Celsius degree. In the left plot, the average temperature of all recorded observations is plotted in an orange dash line. In the right plot, points are coloured in a gradient from cyan to red showing the years of observation.

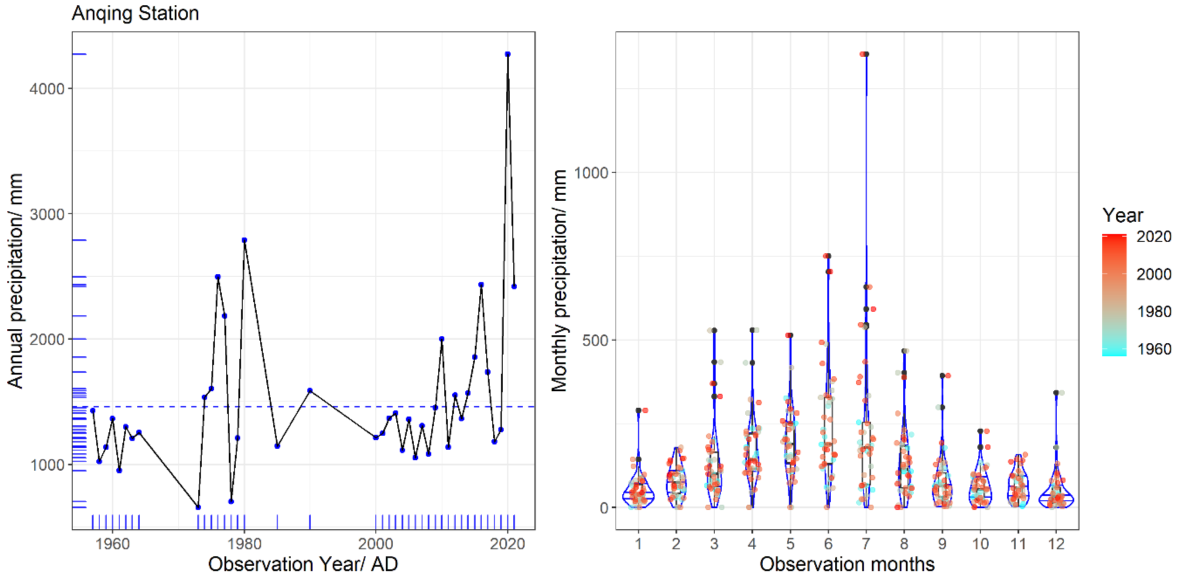

Data from National Climatic Data Center, NOAA

Figure 2-11: Annual(left) and monthly(right) mean precipitation depth monitored in Anqing station between 1956 and 2021. The unit is millimeter. In the left plot, the average precipitation of all recorded observations is plotted in a blue dash line. In the right plot, points are coloured in a gradient from cyan to red showing the years of observation.

2.3.2.3 Climate change

Climate change, including changes of temperature, precipitation and other environment condition (e.g. drought and wetness), is a slow yet important driver influencing aquatic ecosystems on physiological processes and population dynamics. In East China where MLYB is situated, surface air temperature and precipitation have experienced quasi-20-year oscillations from 1880 to 1998 (Qian & Zhu, 2001). Relatively high temperature occurred between 1920s to 1940s and in 1990s. Precipitation over the 1900s to 1910s and after the 1980s has been above the average level of 1350 mm. Due to the strong influence of the East Asian monsoon, drought and flood are the major climate disasters in the MLYB region. The increasing precipitation has caused frequent floods along the Yangtze River since mid-1980s. The IPCC Sixth Assessment Report predicts global warming of at least 1.5℃ during the 21st century unless deep reductions in CO_2 and other greenhouse gas emissions occur in the coming decades (IPCC, 2021), which implied a warmer climate in future MLYB.

As the response of global warming, the extent and duration of ice cover, and dissolved oxygen concentration would decline, and primary productivity would increase in freshwater ecosystems. Though temperate shallow lakes are considered not as vulnerable as alpine lakes under global warming, the influence is physically fundamental. For example, winter temperature can influence zooplankton grazing on algae(Scheffer, 2001), and temperature and DO influence algae dormancy, recruitment and growth(Kong & Gao, 2005), consequently modifying the emergence of algal blooms.

2.3.2.4 Food web structure

Changes in food web structure represent another dominant causative force for regime shifts, including species introduction or removal, population changes in predators, macrophytes or planktivorous fish. Alterations in the food chain directly affects the interactions, strengths or links within food webs and can often cause the loss of resilience in the structural equilibrium of lake ecosystems. For example, Kuiper et al (2015) used an ecosystem model of non-stratifying shallow lakes to simulate a catastrophic regime shift in ecosystem state and found impending shifts in shallow lakes are preceded by a destabilizing reorganization of interaction strength in food webs.

2.3.3 Methodologies for exploring regime shifts

Studies on regime shifts are diverse in methodology, and can include modelling using conceptual, mathematical and computational approaches (Kong et al, 2017; Kuehn, 2011), laboratory simulation experiments (Veraart et al, 2012), whole-lake case studies or experiments including biomanipulation (Carpenter et al, 2011; Seekell et al, 2013; Sondergaard et al, 2017) and the historical and palaeolimnological analysis and reconstruction of sediment cores (Doncaster et al, 2016; Wang et al, 2012).

The methodologies used in empirical studies vary between the disciplines of ecology and physical geography. Ecological approaches usually involve whole-lake experiments, laboratory experiments, lake surveys and monitoring. Geographical methods, on the other hand, are more likely to be based on sediment cores, analysis of a lake's history and comparisons between different lakes in geographical gradients. These methodologies (palaeolimnology, monitoring, sampling, experimentation, remote sensing images, meteorological data and comprehensive historical data) govern the lengths of observational data and resolutions used to detect regime shifts (Figure 2-12). The temporal range of regime shift detection windows is large, varying from a few years to ten millennia and more. Multi-decade studies on regime shifts provide the most productive temporal range, followed by multi-annual and multi-centennial cases. This may be due to that the time ranges of both monitoring data and sediment cores in current successful cases are mainly multi-decadal. The resolutions of some regime shifts can be at a higher magnitude than the lengths of detection windows in other areas of research. Palaeolimnological studies, for example can trace and identify distinct shifts in diatom assemblage composition responding to Dansgaard-Oeschger (DO) climate variability from ca 36.2 to 31.7 kyr BP (Ampel et al, 2010). Ecological experiments that last for two or three years and use high-resolution data can show regime shifts as seasonal or annual changes (Bégin et al, 2020; Seekell et al, 2013; Zhang et al, 2010). For spatial regime shifts, the temporal range is zero, and in terms of regime shifts and thresholds, the target in ecology is a homeostasis-type equilibrium that emphasizes internal (biotic) regulation feedback mechanisms (Briske et al, 2010; May, 1977; Scheffer, 1990). Meanwhile, in palaeolimnology, the conventional theory is based on systems being largely abiotically driven, usually due to long time scales (Jeppesen et al, 2001). Many ecologists believe that empirical data are not sufficient in themselves to test hypotheses rigorously enough (Hillebrand et al, 2020) or a conjunction fallacy happens when regime shift assumptions are made in empirical studies (Spears et al, 2017). In palaeolimnological studies, consistent definitions, practical detection methods (Andersen et al, 2009) and solid examples of scenarios (Biggs et al, 2018; Rocha et al, 2015) are generally used to help assess the ecosystem driver-response relationship and improve the visualisation of possible internal dynamics in lake ecosystems across centuries and even millennia (Ampel et al, 2010; Jeppesen et al, 2018; Randsalu-Wendrup et al, 2016).

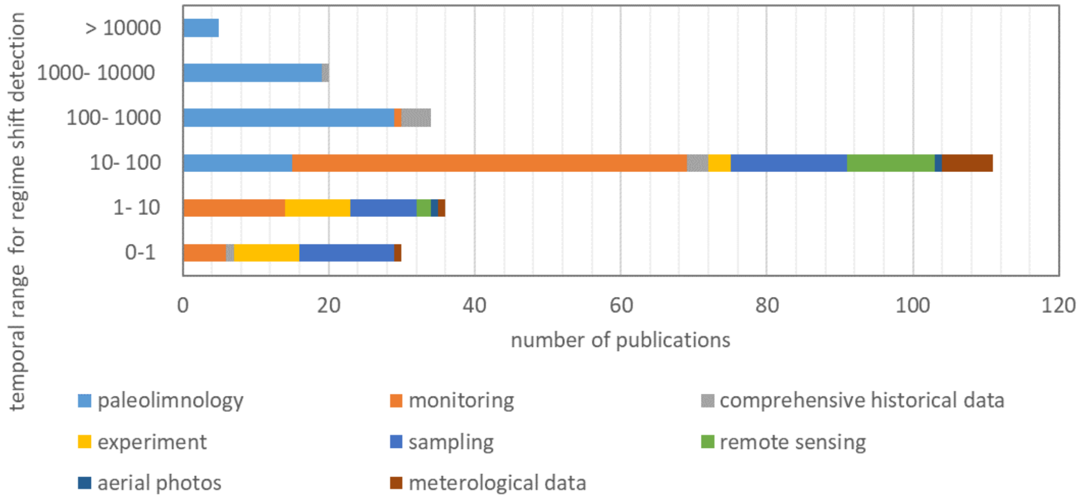

Figure 2-12: Temporal ranges of regime shifts in the literature studied

Whole-lake experiments are conducted to test early warning signals and understand the mechanisms involved through the manipulation of ecosystem changes (Carpenter et al, 2011). There are nine papers in the literature collected for this thesis, covering four sets of whole-lake experiments, two in the USA between 2008 and 2011 (Carpenter et al, 2011; Pace et al, 2013; Seekell et al, 2013) and 2013 to 2015 (Wilkinson et al, 2018), one in Lake Alinen Mustajärvi and Lake Valkea-Kotinen in Finland over two years (Kankaala et al, 2019) and one in Lake Major in Hungary between 1999 and 2009 (Tátrai et al, 2011).

In terms of methodology, conceptual and mathematical modelling was used in 64 out of the 348 papers and articles on regime shifts in lake ecosystems. As many of the papers combined empirical data analysis with theoretical modelling, the roles of modelling in these studies could be to enhance conceptual understanding, predict future scenarios, test hypotheses against data and extrapolate data from empirical evidence. A shortlist of categories of models was summarised according to the frequency in which they turned up in methodology. Computational models include PCLake, Ecopath and Ecosim, as well as agent-based models, mathematical equation-based models, system dynamic models and minimal models. They sometimes overlap in individual studies, such as situations in which an agent-based model was used together with a system dynamic model (Martin et al, 2020; Martin & Thomas, 2016; Han Su et al, 2016) and each category scores half a point in studies such as these. There are many kinds of models in the remaining shortlist (Figure 2-13). In the thesis, I finally chose an agent-based model and a system dynamic model to facilitate the simulation of ecological transition in lake ecosystem, the reason for this is justified in the subsection 4.1. Related models using other modelling methods are described and appraised in the Appendix B.

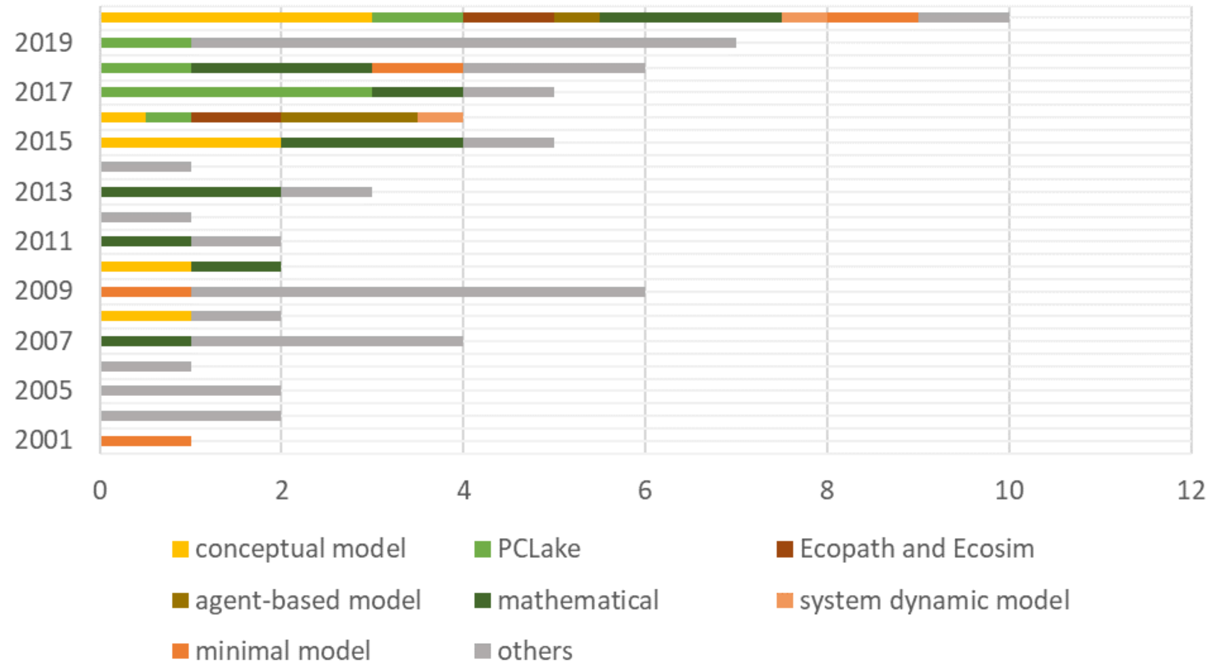

Figure 2-13: Number of publications in the literature collection using modelling methodologies and proportions for each category. The total values of the bars show the number of publications in each year that used modelling.

2.3.3.1 Palaeolimnology

Palaeolimnologists use the regime shift theory to analyse their time series data and to address the long-term dynamic interactions between biotic and abiotic compartments (Jeppesen et al, 2018; Randsalu-Wendrup et al, 2012; Sayer et al, 2006; Smol et al, 2005; Wang et al, 2012).

Since Holling (1973) discussed the impact of human activities on lake systems, such activities can be successfully traced back through history over surprisingly long periods of time using palaeolimnological records. By 2020, palaeolimnology has become one of the main methodologies used to study regime shifts in lakes. However, few reviews have specifically focused on work in this field. I obtained 73 papers (out of 348) that used palaeolimnological data as one of the main methodologies when focusing on ecological changes. In most papers, regime shifts are discovered through break-point detection (Andersen et al, 2009). Among all the proxies for ecosystem response, diatoms are used most often, followed by other subfossils of pollen, chironomids and macrofossils of plants and invertebrates.

2.3.3.2 Statistical analysis

The statistical analysis of regime shifts began when studying marine ecosystems using massive time series monitoring datasets, and include 100 environmental time series analyses, 31 climatic and 69 biological records in the period between 1965 and 1997 in the North Pacific (Hare & Mantua, 2000). The methodology used to detect and explain marine regime shifts was borrowed and applied to lake ecosystems, including the setting up of typical alternative attractors summarised in field studies, such as submerged plants versus phytoplankton dominance, anoxic P-recycling in deep waters, floating-plant dominance, sediment stability, cyanobacterial dominance, breakpoints in the trophic cascade and alternative attractors in multi-species communities (Scheffer & Van Nes, 2004).

2.3.3.3 Modelling

The motivation to develop models after empirical studies is mainly due to gaps found in three areas of the preliminary palaeoecological work. The first gap is between the time scales of palaeoecological data and modern ecological theories. One of the strengths of palaeolimnology is that it provides a long-term perspective from which to observe changes in lake environments based primarily on the knowledge of modern ecology and human-environment interactions. However, the extent to which conventional hypothesis-driven ecological frameworks can be applied to the past is still under debate (Perry et al, 2016), which means that modelling can offer us a virtual space in which the rule base is more abstract and less dependent upon time. The second gap lies between the coarse resolutions and sometimes uneven intervals of palaeoecological reconstruction and the high demand of time series resolution in conceptual hypotheses. The third gap is between the demand of a greater understanding of cause-and-effect relationships and the framework of descriptive reconstruction. In disciplines concerning interactions between people and the environment, including geography and archaeology, generative simulation models are increasingly being used for in-silico experiments and to help practitioners move beyond simplistic pattern matching (Perry et al, 2016).

2.3.3.4 Feedback loop diagrams

The interactions I address here are adapted from the hypothetical interactions involving ASS in shallow lakes with empirical evidence (Figure 2-14).

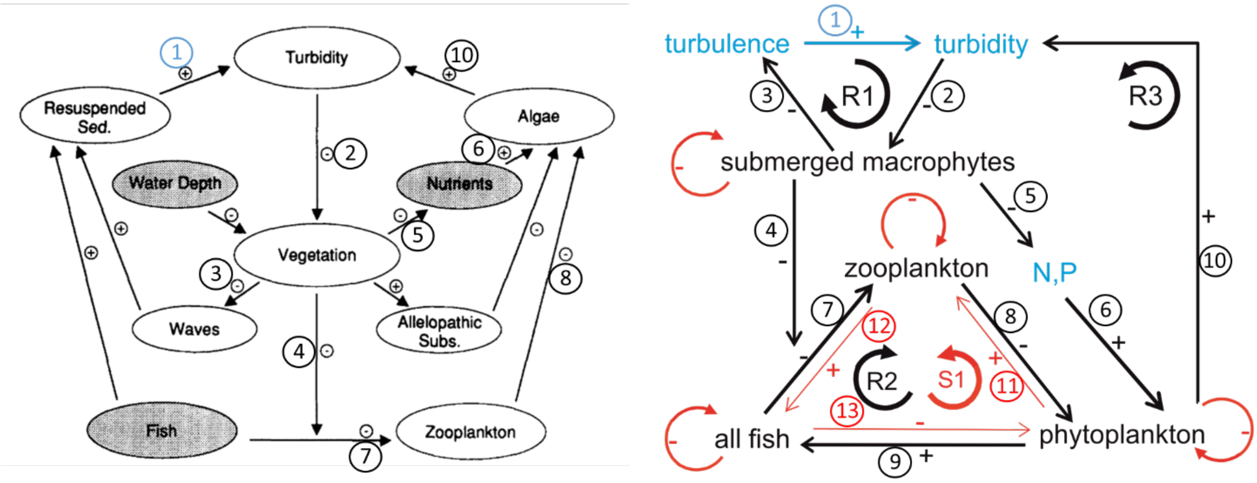

Figure 2-14: Sources of functional relationships in feedback loops. Left is from Scheffer et al (1993) and right is conceptual model of feedback in Taibai Lake. Arrows with the same numbers show the same process.

R1 (arrows 1,2 and 3) is discussed in the literature as an important reinforcing loop by which submerged macrophytes keep water in clear state (Scheffer, 1998). Increases in water transparency make better growing conditions for submerged macrophytes, which in turn stabilise sediments and enhance transparency, shaping an effective positive feedback loop (Jeppesen, 1998). R2 (arrows 7, 8 and 9) and S1 (arrows 11,12 and 13) are also extracted from the aquatic food web and planktivorous and omnivorous fish are involved in this loop. R3 (arrows 2, 5, 6, and 10) are based on widely accepted functional relationships that lead to regime shifts. The function group of fish includes herbivores, omnivores and planktivores as a majority, because according to the Taibai investigation report the piscine community is composed of fish from the Yangtze River, grass carp (*Ctenopharyngodon idella*), silverhead carp (*Hypophthalmichthys molitrix*) and bighead carp (*Aristichthys nobilis*). The following table lists the arrows (effects) and supporting evidence.

Table 2-2: Arrows of interaction in the causal loop diagram of lake ecosystems

Arrow No.	**Linkage (starting - ending)**	**Effect**	**Evidence**
1	Turbulence - turbidity	+	More turbulence leads to more vertical mixing and sediment suspension in shallow lakes (Meiburg et al 2012)
2	Turbidity - submerged macrophytes	-	Turbulence can uproot and reduce vegetation. Turbidity decreases light penetration for photosynthesis (Scheffer, 1998)
3	Submerged macrophytes - turbulence	-	Plants prevent turbulence mechanically. Negative correlation is found between vegetation and turbidity in the field
4	Submerged macrophytes - predation efficiency of fish on zooplankton	-	Vegetation stands as an important refuge for pelagic copepods against fish predation
5	Submerged macrophytes - N, P	-	Nutrient uptake by cells transfers N and P to internal pools of stored nutrients (Valiela, 1991).
6	N, P - phytoplankton	+	Nutrient uptake by cells (Valiela, 1991).
7	Fish - zooplankton	-	Food web
8	Zooplankton - phytoplankton	-	Food web
9	Phytoplankton - fish	+	Food web
10	phytoplankton - turbidity	+	Phytoplankton suspends in water and increases turbidity.
11	Phytoplankton- zooplankton	+	Food web
12	Zooplankton - fish	+	Food web
13	Fish - phytoplankton	-	Food web

2.4 Evidence syntheses in Chinese lakes

2.4.1 Background

Inspired by the theory of multiple stable states in lake ecosystems that was being developed in Europe (May, 1977; Scheffer, 1990), Li (1997) developed a conceptual model based on ecological observations in some of China's shallow lakes, including Taihu Lake, Gehu Lake, Wulihu Lake and Donghu Lake. In practice, he found that regime shifts often occurred after sudden changes in nutrient levels rather than gradual changes, and even in the same stable state the lake ecosystem often showed significantly distinct properties in different nutrient levels. Li's model includes three dimensions: external nutrient loading, nutrient level and the relative dominance of submerged macrophyte and planktonic algae. The upper level represents the clear-water state in which submerged macrophytes dominate, while the lower level represents the turbid-water state, in which planktonic algae dominate. Divided according to nutrient levels, Figure 2-15 shows three situations (a, b and c) in lake water. S1, S2, S5 and S6 are stable states while S3 is a transitional phase and S4 is a metastable equilibrium. This conceptual model can be used to explain the main ecological trajectories of regime shifts that occur in shallow Chinese lakes, providing a standard framework against which to understand the relationships between the detected regime shifts and the ecological thresholds with similar human-intervention history.

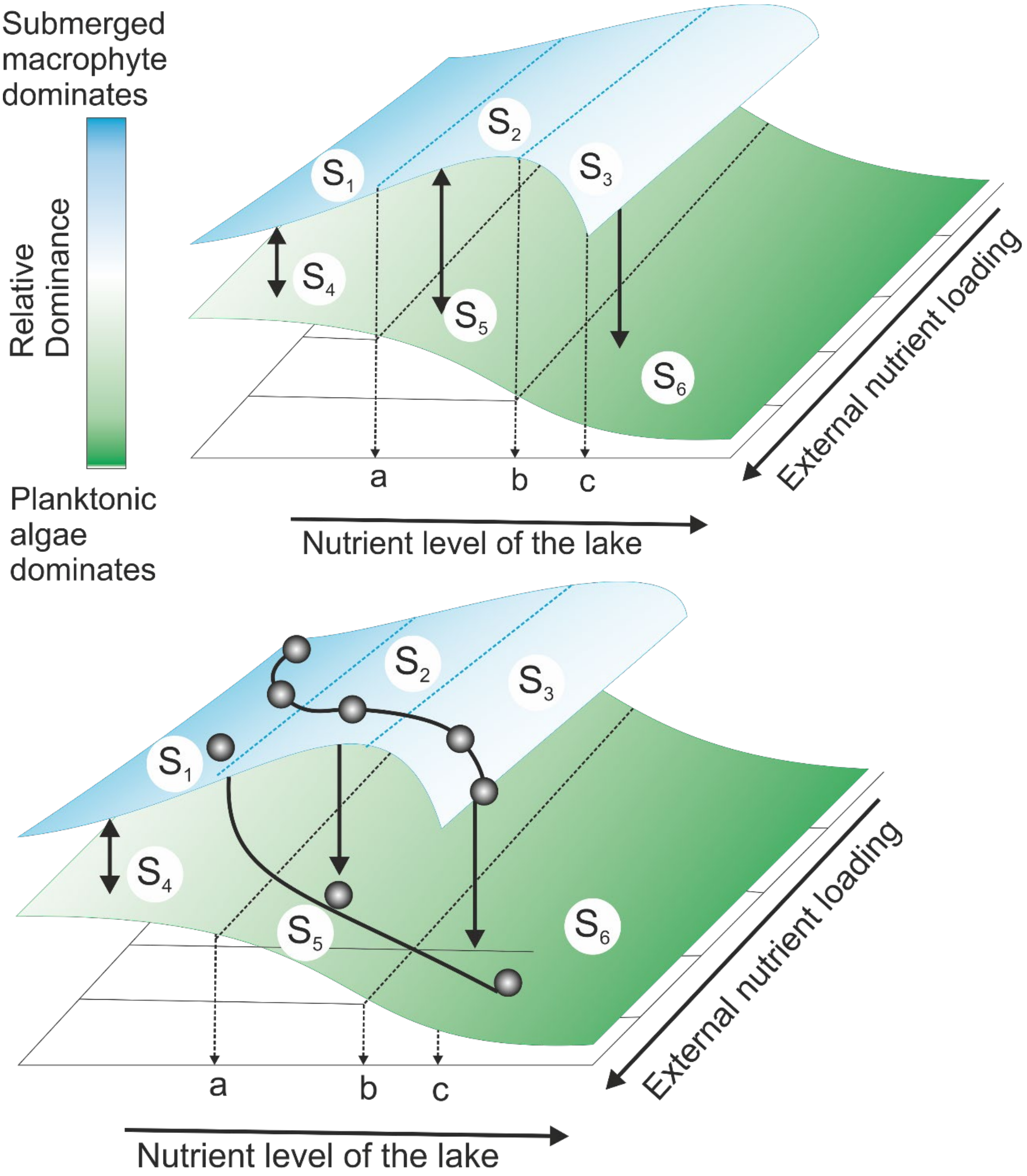

Figure 2-15: Conceptual model of multiple stable states and possible approaches of eutrophication in shallow lakes (Li, 1997)

Li (1997) offered examples of three possible scenarios that could lead to eutrophication: In the first (S1→S2→S3→S6), natural eutrophication is caused by external nutrient loading and accumulation, and accelerated by aquaculture pollution in Gehu lake. The second (S4→S5→S6), in lakes with large pelagic areas such as Taihu, Chaohu and Hongze, strong winds and turbulence prevent the dominance of submerged macrophytes, and in northern bays of Taihu lake, mechanized snail harvesting by suction, trawl fishing and the high population of grass carp prevent the growth of submerged macrophytes. In Li's third example S1→S2→S5→S6 represents the removal of submerged macrophytes and the large-scale input of grass carp triggered the phase shift and accelerated eutrophication in Donghu and Wulihu lakes. This framework has been widely used as a reference in studies of ecological trajectories in eutrophicated Chinese lakes.

In the last two decades, ASS and regime shifts have been studied in more Chinese lakes on different temporal and spatial scales. Among 502 samples taken from 108 lakes with an area greater than 10 km^2 in eastern China, 283 turbid-state samples were collected with a transparency of less than 0.5m, including 56% in the flood season and a further 12% of the total number of lakes with a transparency greater than 1m (Nanjing Institute of Geographical and Limnological science, CAS, 2019). It is worrying that over half of the lakes in this area are in a turbid-water state, and recent investigation concerning lake trophic status in the middle and lower reaches of the Yangtze River showed that most lakes could be categorized as possessing mesotrophic or eutrophic status (Qin et al, 2013). Regime shifts were detected in eleven lakes in China (Lugu, Erhai, Xingyun, Yangzong, Zhangdu, Liangzi, Wushan, Taibai, Longgan, Chaohu and Taihu) from palaeoecological evidence (Zhang et al, 2018). Dong et al (2021) reviewed lake ecosystem regime shifts in China by studying 73 sediment cores. Of the 55 lakes studied in different regions of China, tipping points were detected in 34 of them, 63% of the total. These tipping points were earlier in the lakes of eastern China, dating back to the 1970s, especially in the MLYB. Tipping points for lakes in western China dated back to the 1990s, with urban lakes shifting earlier than the rural lakes. Few regime shifts were detected in lakes in the Inner Mongolia and Xinjiang regions.

According to a 2020 report published by China's Ministry of Ecology and the Environment, the baseline of TP in the middle and eastern lakes of China is 0.029 mg/L, which falls in the third category of water quality (TP > 0.025 mg/L) before extra loading. With huge efforts based on the government's legislative guidelines and policies to mitigate lake eutrophication and control water pollution, external nutrient loading has been reduced (Huang et al, 2019). However, global warming may change the balance of phosphorus recycling and cause fluctuations in the nutrient levels of the water. Despite controls in nutrient loadings, TP increased in Taihu Lake water in 2017, and in Longgan, Huangda and Po Lakes in 2019. Given that ecosystem restoration and environmental protection remain a central priority in China's 14th Five-Year Plan (2021-2025), there may come a time when regime shifts occur as many Chinese lakes recovering to a clear-water state. To achieve effective ecosystem management, a synthesis of the present studies of Chinese shallow lake ecosystems is needed to assess local regime shift patterns and potential mechanisms of transition. The synthesis should aim to reveal the actual situation by answering the following questions. Firstly, what are the ecological patterns of regime shifts in Chinese shallow lakes? Secondly, what are the nominated drivers on these regime shifts? and thirdly where do the tipping points of the lake ecosystems respond to those drivers?

2.4.2 Methodology

2.4.2.1 Literature search strategy

Following the ROSES (RepOrting standards for Systematic Evidence Syntheses) protocol (Haddaway et al, 2018), relevant scientific literature were examined to assess the current studies of regime shifts, multiple stable states, critical transitions, thresholds and tipping points as well as the effect of major drivers on ecosystem changes in Chinese shallow lakes. I searched for relevant phrases by topic, using titles, keywords and abstracts in the WoS core collection in English and in the Wanfang database in Chinese from the earliest available dates to November 2020. For literature in English, the Boolean search string used was TOPIC: ("regime shift" AND "lake" AND "ecosystem" AND "China" OR "stable states" AND "lake" AND "ecosystem" AND "China" OR "multiple states" AND "lake" AND "ecosystem" AND "China" OR "critical transition" AND "lake" AND "ecosystem" AND

“China” OR “tipping point” AND “lake” AND “ecosystem” AND “China” OR “threshold” AND “lake” AND “ecosystem” AND “China”). For the Chinese literature, the Boolean search string used was 主题: (“稳态” AND “湖” AND “生态系统”) OR (“临界转换” AND ”湖” AND “生态系统”) OR (“阈值” AND “湖” AND “生态系统”) OR (“临界点” AND “湖” AND “生态系统”)), and the document types included journal articles, degree dissertations, conference papers, legislation, scientific reports and local chronicles. Refining search results to categories of environment, ecology, limnology, geography, and biodiversity conservation, and document types of articles, reviews and book chapters, I obtained 47 articles from the WoS, and 169 journal articles, 206 degree dissertations, ten conference papers and six scientific reports in the Wanfang Database.

2.4.2.2 Selection criteria and critical appraisal

When scanning titles and abstracts, the inclusion criteria was that the article contained empirical data relating to at least one Chinese freshwater lake, and that detecting regime shifts should be a main part of the results. Literature without detailed information of occurrence, drivers and regime shift thresholds, or results that included time scales that are either less than a year or more than a millennium were excluded, as were laboratory tank experiments so that the time series would be longer than the generation time of target populations in order to show informative natural variability. Meanwhile, for studies of the same sites and studies of regime shifts updated by the same authors, the articles with most elaborate description of the regime shifts and mechanisms were included, while others that included repetitive information were excluded. As a result, I was able to select fifteen articles from WoS and six articles and five PhD dissertations from the Wanfang Database. I included seven further papers in English from our reference list that were not picked up by the search results because of the lack of the keyword “China” in their titles, keywords or abstracts, or because the sources were outside the WoS Core collection.

The quality of the detection process was appraised according to aspects of data measurement validity, appropriate detection methodology for regime shifts and the explanatory power of drivers as the causes of effects under the guidance of well-recognised appraisals on regime shifts and multiple stable states (Capon et al, 2015; Peterson, 1984). The quality of the appraisal determines how convincing the results of regime shifts are in these studies, and therefore also governs the weight of conclusions taken in the synthesis insofar as answering the three above questions was concerned.

Table 2-3: Criteria for quality appraisal in literature studying regime shifts in Chinese lakes

	Appraisal aspect	**Rating rule**
Data validity	Data collection	Direct measured data: 1; reconstructed time-series data or space for time substitution - 0
Detection methods	Statistical significance in time-series detection	Statistically significant: 3; not very significant - 2/1; not significant or no results shown on significance: 0.
Response-driver relationship	Significance of correlation	Statistically significant: 3; not very significant – 2/1; not significant or no results shown on significance -0.

2.4.2.3 Data extraction

The attributes of regime shifts (occurrence time, ecosystem state, thresholds, response-driver relationship, and major drivers), properties of study sites (lake area, water depth, temperature, retention time, catchment land use type) and the main processes that contribute to regime shifts are identified in the literature. Data were archived in an Excel spreadsheet together with the results of the critical appraisals.

2.4.3 Evidence and interactions

2.4.3.1 Detected regime shifts

Regime shifts were found to have occurred in at least fifteen Chinese shallow lakes (between 1 and 4m average depth) over recent centuries. The ecological change trajectories consisted of clear-water state to turbid-water state, clear-water state to grass-algae hybrid state, and grass-algae hybrid state moving back to clear-water state and then shifting to turbid-water state.

Table 2-4: Studies examining regime shifts in Chinese shallow lakes. Regime shift type: ‘d’ for driver-threshold shifts, ‘s’ for state-threshold shifts and ‘r’ for restorative shifts

Occurrence year	**Drivers**	**Lake site**	**Examining object**	**Reference**
1996, 2009, 2014	fish stocking, nutrient loading, drought	Yilong lake	planktonic algae	(Zhao, 2013; L. Zhao et al, 2020)
1950s, 1990s	hydrodynamics, nutrient level, aquaculture	Taibai lake	subfossil diatom	(Y. Zhao et al, 2016)
1963, 1980	hydrological regulation, nutrient loading	Chaohu lake	Fatty acid and n-alkanes	(Kong et al, 2017)
1960s	dam regulation, warming	Baiyangdian lake	subfossil pollen	(Y. Yang et al, 2018)
1950s	hydrological modification, nutrient loading from aquaculture, warming, wind	Taibai, Wushan, and Zhangdu lakes	subfossil diatom	(K. Zhang, Yang et al, 2018)
1970s		Chaohu; Taihu Lake	subfossil diatom	
the late 1960s		Zhangdu; Liangzi Lake	subfossil cladocera	
the late 1980s		Changdang Lake	subfossil pollen	
1978, 1980s	nutrient loading	Chaohu lake	subfossil diatom	(Min Xu et al, 2019)
1950	hydrological conditions, dams	Zhangdu lake		
1963	annual temperature, grain size, P	Shahu lake	subfossil chironomid	(Cao et al, 2020)
1975	P, Zn, Cu	Yanxi lake		
1980	dam, silt, Cu	Futou lake		
1985	fish stocking, warming, nutrient level	Donghu lake	phytoplankton, zooplankton, fish	(Haojie Su et al, 2020)
1990	nutrient level (TP, TN)	Xijiu lake	subfossil chironomid	(C. Zhang et al, 2020)
1997 ~2004	nutrient level, pollution, aquaculture	Gehu lake	submerged macrophyte	(Xu et al, 2020)

The occurrence time of regime shifts in these lakes are in close proximity with each other and share a similar background of drivers, including nutrient loading, fish stocking and hydrological regulation as anthropogenic forces, with warming, droughts and flooding as natural forces. Detection methods are mostly based on the Sequential T-test Analysis of Regime-Shifts algorithm (hereafter STARS) and change-point analysis using F-statistics. One study used the heuristic segmentation algorithm.

Table 2-5: data collection, data types and detection techniques of regime shifts in the studies. Data type: o=observed, e=experimental, r= reconstructed from sediments

Timespan	Data type	Detection methodology	Mechanism explained?	References
1989-2019	o	STARS	Y	(Zhao, 2013;Zhao et al, 2020)
1900-2006	r	STARS, F-statistics	Y	(Zhao et al, 2016)
1860-2010	r	STARS, F-statistics	N	(Kong et al, 2017)
1906-2012	r	the heuristic segmentation algorithm (sliding t test)	N	(Yang et al, 2018)
1850s- 2010s	r	STARS	N	(Zhang, Yang, et al, 2018)
1900-2000	r	STARS, F-statistics	N	(Xu et al, 2019)
1900-2020	r	STARS, ARIMA	N	(Cao et al, 2020)
1956-2019	o, r	change-point analysis (F-statistics)	Y	(Su et al, 2020)
1989-2018	r	STARS	Y	(Zhang et al, 2020)
1984-2018	o	change-point analysis (F-statistics)	Y	(Xu et al, 2020)

2.4.3.2 Effects of environmental factors on regime shifts

According to the review of regime shifts that occurred in MLYB, a dataset of environmental factors and the times of regime shifts was gathered to explore the effects of the environment on biological transformation. The lakes were chosen according to the presence of regime shifts, the availability of survey data and the completeness of knowledge of the lake, including factors such as water level and drainage ratio. The final list includes nine lakes, namely Taihu, Changdang, Chaohu, Shitang, Wushan, Taibai, Longgan, Futou and Liangzi. The data consist of 29 lake variables, including geographic attributes (latitude and longitude), physical attributes (water level, water depth, lake area and drainage ratio), chemical attributes (pH, Cond, Tfe, SiO_2, NO_2-N, NO_3-N, NH_4-N and DIP), transparency (SD), nutrient attributes (TP, TN, COD and Chla), biogeochemical elements (K, Na, Ca, Mg, Cl, SO_4, CO_3 and HCO_3), and the RS time detected by diatom subfossils. The geographical and physical attributes were collected and calculated from investigation reports, and other environmental attributes were gathered from a field survey of these lakes in the summer of 2008. The drainage ratios of Changdang and Shitang Lake are not available, partly because the two lakes are fluvial in character.

Table 2-6: Lake variables and RS time reconstructed by diatom subfossils

Name	**water level**	**depth**	**lake area**	**drainage ratio**	**SiO2**	**SD**	**TP**	**Chla**	**RStime diatom**
Unit	**m**	**m**	**km2**		**mg/L**	**mg/L**	**mg/L**	**mg/L**	**AD**
Taihu	3.5	2.8	2325.73	15.87	4.67	0.58	0.11	7.89	1974
Changdang	4.6	1.3	84.28	NA	6.68	0.54	0.12	25.77	1976
Chaohu	10.5	3.5	784.91	17.18	5.72	0.36	0.19	15.67	1978
Shitang	11	2.1	11	NA	6.8	0.47	0.07	10.4	1981
Longgan	15.6	3.2	256.25	8.55	4.36	0.84	0.05	3.71	1944
Taibai	15.8	2.5	27.42	9.92	8.86	0.53	0.09	7.63	1957
Wushan	16.5	2.1	15.77	29.81	9.41	0.41	0.21	35.8	1961
Liangzi	20.5	4	338.83	10.73	3.11	1.36	0.04	5.53	1948
Futou	22.8	2.2	141.22	9.82	3.49	0.97	0.04	4.27	1995

To summarise the relationships between each of the environmental factors and RS time in the diverse conditions of different lakes, Multiple Factor Analysis (MFA) was used with the *Factoextra* and *FactoMiner* packages in R (Pagès, 2002; Salgado et al, 2020). In the analysis, the 29 variables were divided into the eight group categories shown in Table 2-7 so that the individual and combined contributions of their effects could be calculated. All quantitative variables were normalised to a zero mean and unit variance before MFA, and the RS time by diatom was listed as supplementary information and was thus not involved in the correlation matrix. Information was standardised by dividing the maximum eigenvalue using the *decostand()* function in the *Vegan* package in R before superimposing the results onto the MFA dimensions.

The MFA on the RS lake data showed that the first two dimensions explained 75.8% of the total variance (Figure 2-16). The first dimension was linked to variations in all groups of more than 10%, while the second dimension was mainly associated with physical attribute groups and geochemical elements (>25%). More specifically, the variables that contributed results that exceed the average rate to dimension 1 were SD, water level, longitude, drainage ratio, TN, COD and NO3-N. The variables that contributed results that exceeded the average rate to dimension 2 are the geographical latitude of the lake, its surface area, drainage ratio, pH, Tfe, longitude, water level, DIP, CO_3 and SiO_2 (Figure 2-17). Visually, dimension 1 separates SD, water level and depth from other factors, and dimension 2 comprises a spectrum of diverse biogeochemical factors.

RS time, as a variable, lies in the middle of the environmental variables in the multivariate space at 0.264 and 0.179 in this plot. The lakes are situated in difference climatic zones and show diversity in terms of environmental characteristics. They can be roughly categorised into four groups: Firstly, large, turbid-water lakes with low water levels and a shallow depth (Taihu, Chaohu, and Changdang Lakes); secondly medium-sized clear-water lakes with high water levels and small drainage ratios (Liangzi, Futou and Longgan Lakes); thirdly small and highly turbid lakes with large drainage ratios (Wushan Lake), and fourthly other lakes that have no special characteristics (Shitang and Taibai Lakes. According to the RS time detected by diatom, the tipping points occurred in the 1970s in the large, turbid-water lakes, in the 1940s and 1990s in the medium clear-water lakes, and in the 1960s in the small, very turbid Wushan Lake.

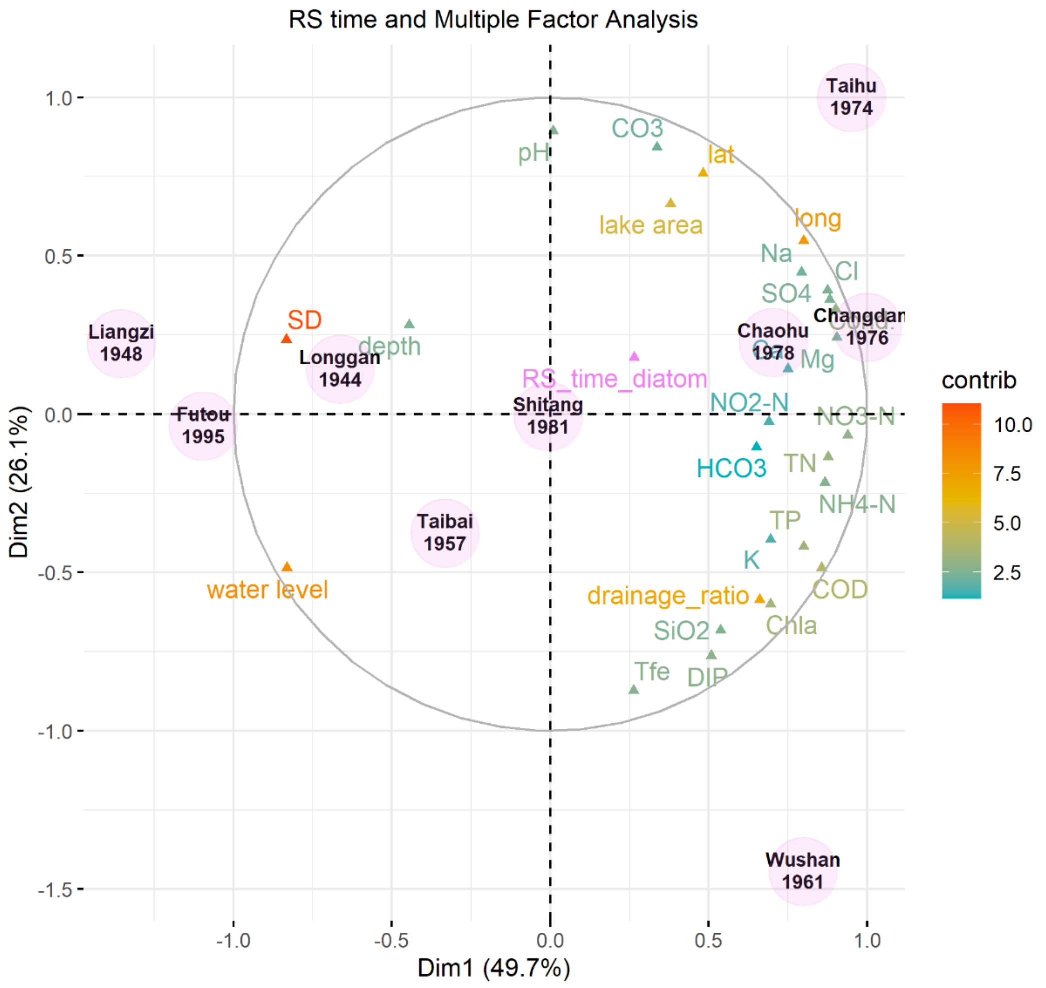
RS time and Multiple Factor Analysis
Dim1 (49.7%)
Dim2 (26.1%)
1.0
0.5
0.0
-0.5
-1.0
-1.5
-1.0
-0.5
0.0
0.5
1.0
Taihu 1974
Liangzi 1948
Longgan 1944
Futou 1995
Shitang 1981
Taibai 1957
Chaohu 1978
Changdan 1976
Wushan 1961
pH
CO3
lat
lake area
long
Na
Cl
SO4
Mg
SD
depth
RS_time_diatom
NO2-N
NO3-N
HCO3
TN
NH4-N
TP
K
COD
drainage_ratio
Chla
SiO2
Tfe
DIP
water level
contrib
10.0
7.5
5.0
2.5

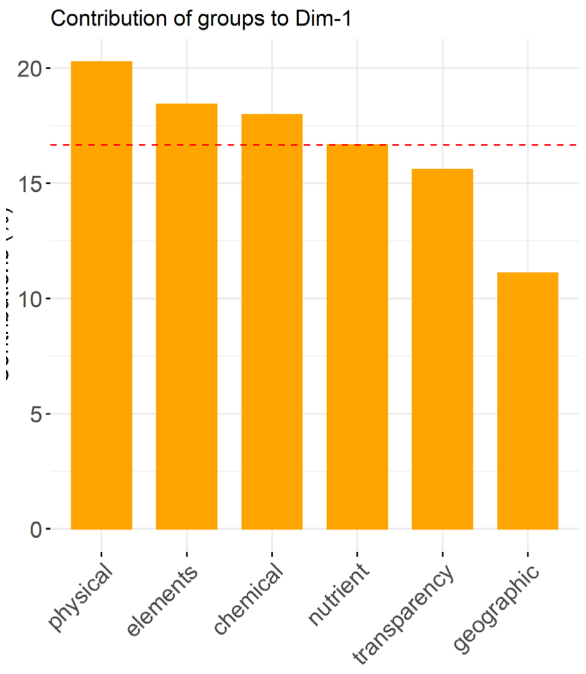
Contribution of groups to Dim-1
20
15
10
5
0
physical
elements
chemical
nutrient
transparency
geographic

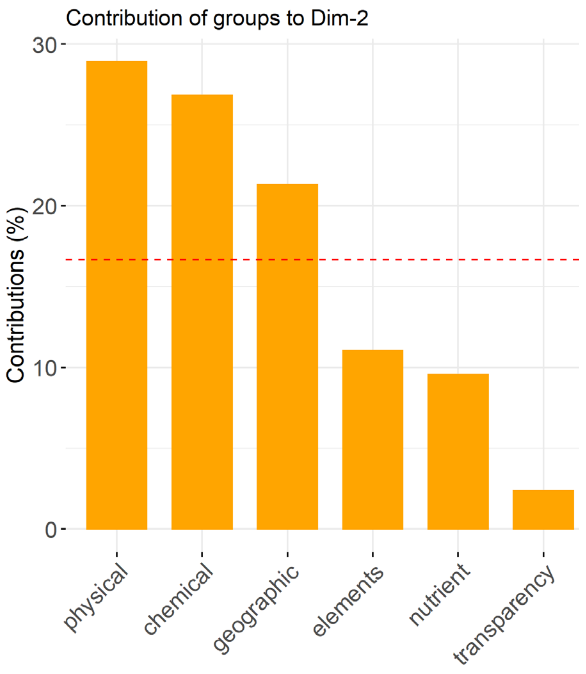
Contribution of groups to Dim-2
Contributions (%)
30
20
10
0
physical
chemical
geographic
elements
nutrient
transparency

Figure 2-16: Multiple Factor Analysis (MFA) of RS times in nine lakes and the contributions of groups to these dimensions

The exploratory analysis shows that the occurrence times of RS in MLYB are distributed in clusters and the main factors that are strongly related to the clusters' directions are lake area, SD, water level, depth, drainage ratio, SiO2, Tfe and DIP. The correlation matrix shows the RV coefficients between variables (Figure 2-18). The largest RV coefficient is 0.84, showing a great similarity between variables in the nutrient group and the chemical group.

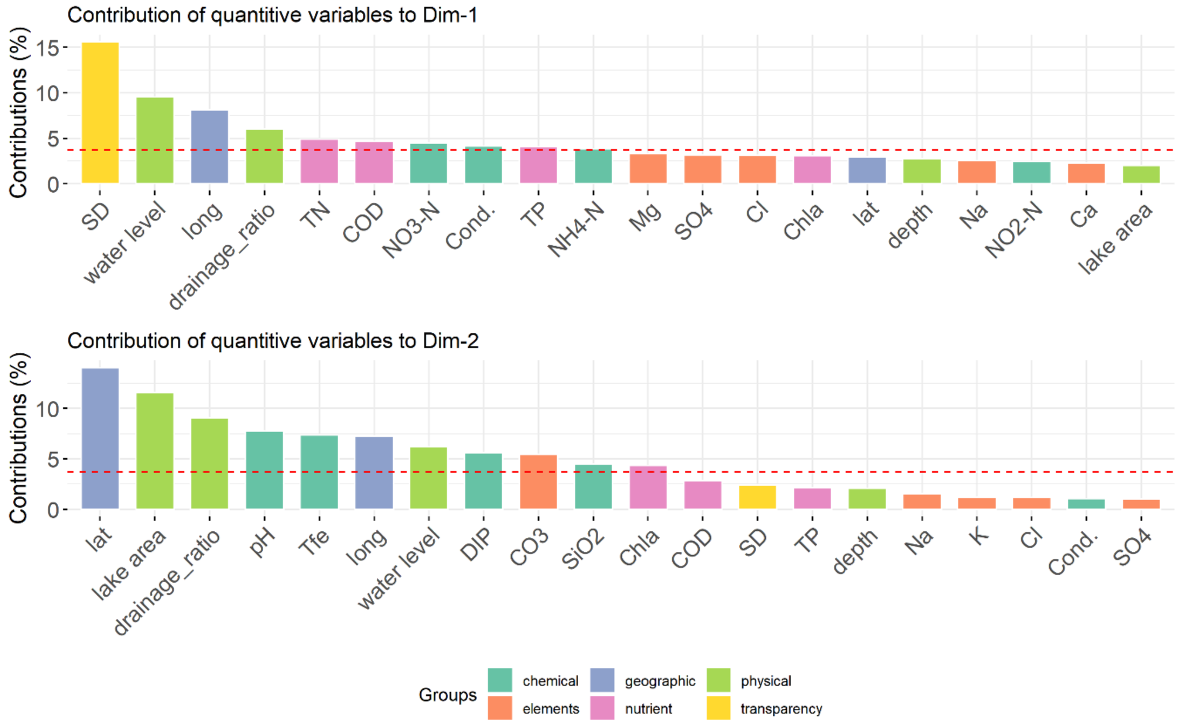

Figure 2-17: Contributions of environmental variables to dimensions 1 and 2 of MFA analysis for MLYB lakes.

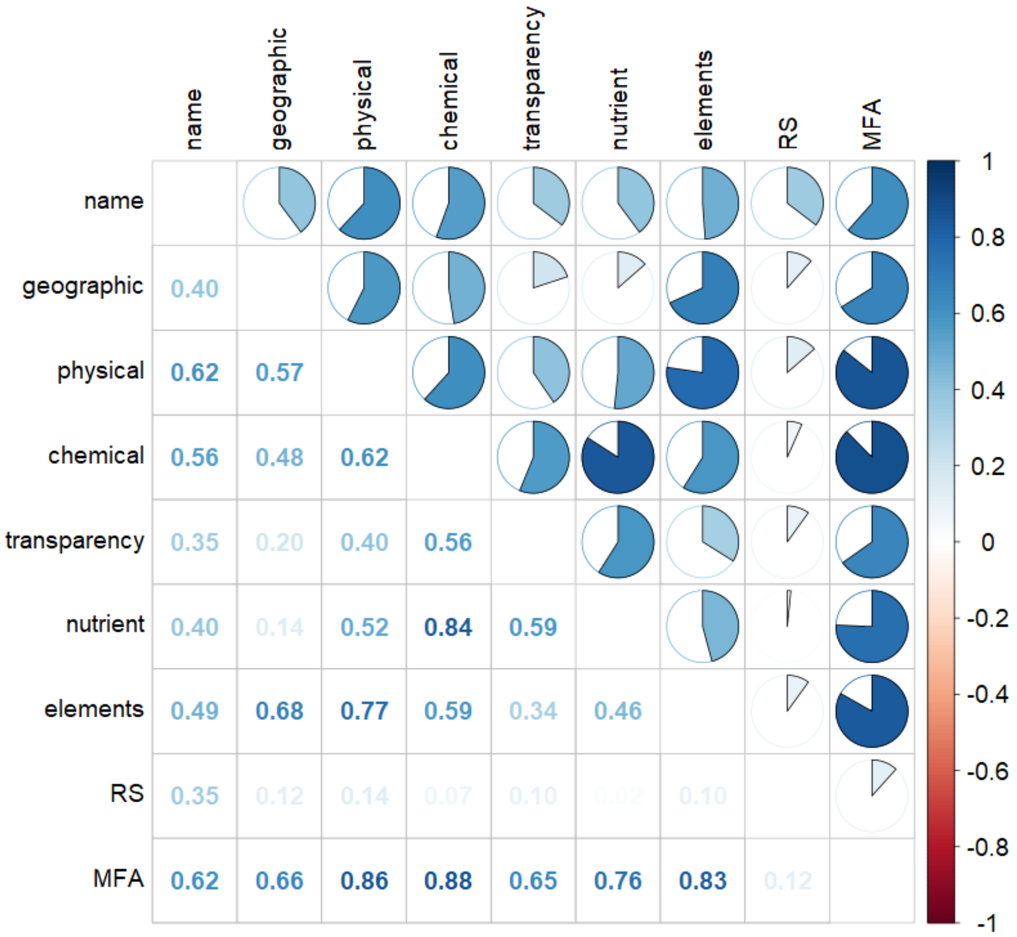

	name	geographic	physical	chemical	transparency	nutrient	elements	RS	MFA
name									
geographic	0.40								
physical	0.62	0.57							
chemical	0.56	0.48	0.62						
transparency	0.35	0.20	0.40	0.56					
nutrient	0.40	0.14	0.52	0.84	0.59				
elements	0.49	0.68	0.77	0.59	0.34	0.46			
RS	0.35	0.12	0.14	0.07	0.10	0.02	0.10		
MFA	0.62	0.66	0.86	0.88	0.65	0.76	0.83	0.12	

Figure 2-18: Correlation matrix of variable categories using MFA analysis. The colour represents the correlation. The red end represents the most negative correlation (-1) while the blue end represents the most positive correlation (1).

In the above section 2.4.3.1 and section 2.4.3.2 reviewing the detected regime shifts, main drivers were proposed and tested against the response of the ecosystem state at community level, and the correlations were found to be statistically significant. Although the nutrient levels of phosphorus and nitrogen are seen to be the most influential factor, there could be many other dimensions of environmental factors that drove ecological changes in the lake ecosystem in the past. Related results of experiments on response-driver relationships must therefore inevitably be reviewed against the background of Chinese shallow lakes. Based on the results of different regime shift scenarios, these lakes can be further categorised by external conditions, such as climate, temperature, nutrient level, geological background, human activity type and ASS before and after regime shifts.

In terms of climate and temperature, the photosynthesis rate of blooming algae in Taihu lake increases between 10 and 28℃, and the most suitable temperature for the growth of blue-green algae is between 28 and 33℃. In other subtropical shallow lakes such as Poyang and Hongze, the most suitable temperatures for the blue-green algae are also above 30℃ (Guo et al, 2015). A water temperature ranging from 24℃ to 30℃ was a necessary condition for algal blooms, although a temperature higher than 30℃ significantly inhibits the growth of blue-green algae (Wang et al, 2008). The in-situ experiments may be influenced by the combined effects of nutrient recycling and warming.

When considering light, comparative light intensities of less than 5% means that shoots of annual submerged macrophytes, including *Vallisneria natans*, *Hydrilla verticillata Royle*, *Ceratophyllum demersum L*. and *Potamogeton crispus L.* become whitened and lose the ability to grow (Li & Lian, 1996).

When water levels were persistently higher than 3.5m and 3.0m, *Potamogeton maackianus* and *P. wrightii* respectively died in great numbers in the East Taihu lake (Li et al, 2020). When wind speeds are higher than a threshold of 6.5 m/s, sediment resuspension is caused, releasing internal phosphorus in Taihu lake (Boqiang Qin et al, 2006). Meanwhile, when the biomass of *Hypophthalmichthys molitrix* and *H. nobilis* exceeded 40~50 g/m^3, algal blooms decreased in Donghu lake, Wuhan (Xie & Liu, 2001).

2.4.3.3 Effects of drainage ratios on nutrient loading

External effects such as nutrient loading and hydrological modifications were observed to be essential factors. With larger catchment/lake area ratios, nutrient loadings from chemical fertilizer from farmland, sewage from residents and industrial pollution should increase proportionally in the same period. I collected the data for many Chinese shallow lakes that had undergone eutrophic regime shifts and calculated the catchment/lake area ratios and the approximate nutrient-loading time before transition. Ideally, this process will enable us to see the role of the catchment/lake area ratio in eutrophication.

Assumptions:

1) As farmland is the primary land-use type in Chinese lake catchments, the bigger the catchment area, the higher the level of nutrient loading in the lake.

2) Lake volumes are proportionate to lake areas (a flat-bottom model).

Hypotheses:

1) In lakes where the catchment/lake (C/L) ratio has remained constant in the last century, larger C/L ratios should lead to more rapid eutrophication rates and less nutrient-loading time before thresholds.

2) In lakes with modified catchment areas (through hydrological engineering or urbanization) or lake areas (reclamation, climatic), increasing the C/L ratio will always accelerate eutrophication or trigger a regime shift instantly.

3) Plotting C/L ratio as the x-axis and nutrient-loading time before regime shifts as the y-axis, a negative correlation should be found in Chinese shallow lakes with similar nutrient backgrounds. Outliers may be influenced by biomanipulation, aquaculture, and nutrient baselines.

4) Factors that control the correlation include number of upstream flows, population density, land use and urbanization level in the catchment.

5) In the future, when the general nutrient level in the Yangtze River is lower, the C/L ratio will still be an essential morphological parameter influencing nutrient-loading or pollution accumulation time before regime shifts.

Results:

Most lakes in the Yangtze river basin have C/L ratios of between 0-20, although Wushan is an outlier (29.81). Baiyangdian has a huge C/L ratio as it has nine upstream rivers, and the climate is colder and drier than the Yangtze river basin.

Table 2-7: Sizes of lakes and their catchments and the ratios of catchment/lake area

Lake name	Lake size (km^2)	Catchment size (km^2)	C/L ratio	Land-use type	Time of the abrupt shifts
Taihu	2325.7	36900	15.87	Urban land	1975
Chaohu	784.9	13486	17.18	Urban land	1978
Longgan	420.0	3591	8.55	Cropland, aquaculture	1944
Taibai	25.2	250	9.92	Cropland, aquaculture	1958
Wushan	16.1	480	29.81	Cropland, aquaculture	1963
Liangzi	304.3	3265	10.73	Cropland	1948
Zhangdu	42.3	524	12.39	Cropland, aquaculture	1950/1962
Futou	126	1238	9.82	Cropland, aquaculture	1980/1995
Baiyangdian	366.0	31200	85.25	Cropland, forest	1963
Yanxi	14.2	67	4.72	Cropland, aquaculture, urban land	1975

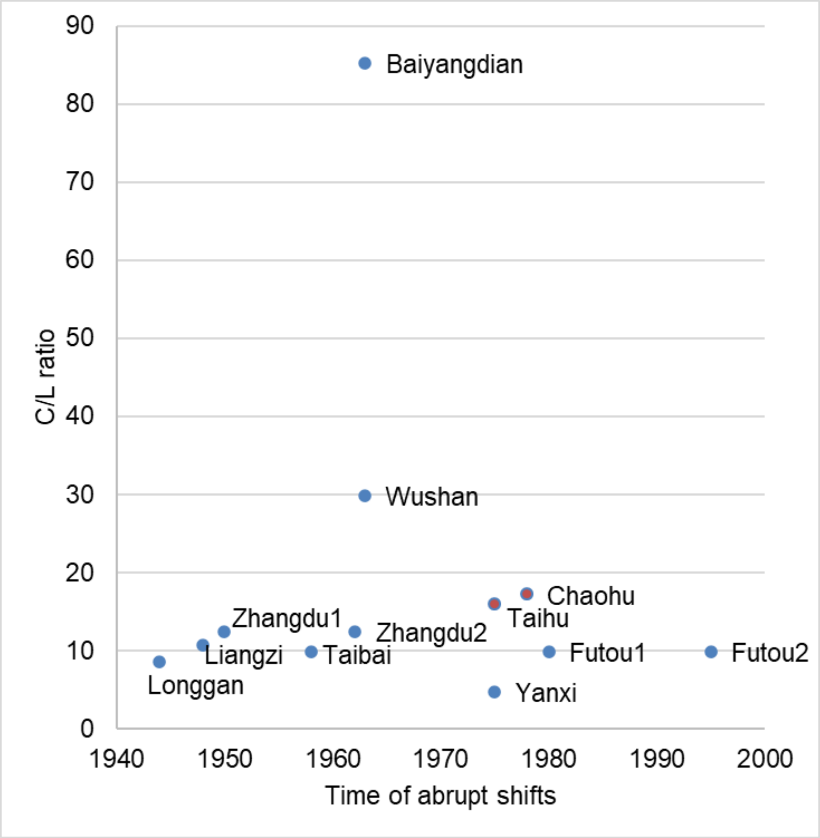

Figure 2-19: C/L ratio level and timing of regime shifts

Hypothesis 1 is not accepted according to the data, either because of substantial instant disturbance (damming/reclamation or nutrient concentration/retention time) and lake area change. All of the lakes in the Yangtze river basin are connected to the Yangtze river at some point, so the lakes' relationships are hierarchical. For example, the nutrient loading in Wushan lake flows into and thus influences Taibai lake and consequently influences Longgan lake in the lower reaches of Taibai. This kind of relationship could have triggered cascading regime shifts by sharing nutrients, algae, zooplankton or fish, or a combination of all these factors, adding another unclear layer of external factors.

Most of the lakes have undergone land reclamation since 1950 and the return of farmland to the lake after 2006. Areas of reclamation can be as high as 50%, so the surface areas of the lakes have significantly changed. Building dams and cutting down the connections between lakes and the

Yangtze River has also significantly impacted the whole catchment area. Each point in Figure 2-19 should be considered as a snapshot of the dynamic trajectory in each specific lake.

2.4.3.4 Trajectories and thresholds of regime shifts

In terms of lake management, identifying regime shifts and their main drivers is only the first step, and understanding the mechanisms of ecological change in lakes is the key to future scientific planning. An assessment of local ecological thresholds is therefore always valuable.

According to this framework, the results of ecological thresholds and related changes are reviewed in Chinese shallow-lake case studies. From clear-water state to turbid-water state, the threshold in concentration of total phosphorus (TP) is around 100- 120 mg/m^3 and the concentration of Chlorophyll is 30 mg/m^3. When the TP level exceeds 50-60 mg/m^3, a grass-algae hybrid state comes into being before turning phytoplankton-dominant. However, there is little available information on restoration thresholds, suggesting that less than 50 mg/m^3 of TP can help recovery to a clear-water state in subtropical shallow lakes. The TP thresholds were found to be roughly equal in shallow lakes (1-2 m <mean depth <3-4 m; c. 0.1 km^2 <area <at least 350 km^2) from temperate to subtropical zones (Wang et al, 2014). Data suggests that there are no reversible case studies at present, and all case studies show hysteresis or no recovery.

Table 2-8: Forward and backward ecological trajectories in Chinese lakes, partly adapted from Wang et al. (2014)

TP Thresholds (mg/m^3)		**Lakes (area, mean water depth)**	**Location**	**Method**	**Reference**
Forward $S_3 \rightarrow S_6$ (threshold c)	Backward $S_4 \rightarrow S_1$ (threshold a)				
120	50	50 lake-years (0.5-355km^2, 0.6-3.6m)	28- 32°N	Multi-lake survey	(Wang et al, 2014)

70-110	N/A	Taibai lake (25km^2, 3.2m)	29°N	Sediment fossil diatom-TP transfer function (1796 - 2003)	(Xiangdong ; D Yang et al, 2006)
100	30	Erhai lake (248km^2, 10.2m)	25- 26°N	Monitoring data (1985-2010)	(Zhen et al, 2011)
90	45	Yilong lake (28km^2, 3.9m)	23°N	Monitoring data (1989-2009)	(Zhao, 2013)
Forward $S_3 \rightarrow S_6$	Backward $S_6 \rightarrow S_2$				
30	N/A	20 lakes	Yangtze floodplain (28- 32°N)	Sampling in 2004	(Pan et al, 2015)
N/A	20	Taihu lake (2250km^2, 2.0m)	31°N	Seasonal monitoring (2009-2012)	(Xu et al, 2015)
$S_? \rightarrow S_?$					
5.21~ 10.57	N/A	138 shallow lakes	Eastern China (26-40°N)	Monitoring data of water quality and phytoplankton community (1986-2014)	(Zhang et al, 2018)

Table 2-9: Deterioration trajectories and thresholds in Chinese lakes

TP Thresholds (mg/m^3)		Lakes (area, mean water depth)	Location	Method	Reference
$S_2 \rightarrow S_3$ (threshold b)	Deterioration $S_3 \rightarrow S_6$ (threshold c)				
61	115	Dahong Habour of Gehu lake (0.32km^2, 1.24m)	31°N	Sampling and investigation (2009-2010)	(Tao et al., 2012)
50	N/A	Taihu lake (2250km^2, 2.0m)	31°N	Seasonal monitoring (2009-2012)	(H. Xu et al., 2015)
60	N/A	97 lakes	28-34°N	Sampling and investigation in 2014	(Haojie Su et al., 2019)

2.5 Discussion

2.5.1 Arguments on regime shift

As well as the increasing popularity of ASS, thresholds and regime shifts, contrasting arguments have been presented along with feedback to help the development of theory. Since it is important for users to be aware of any controversies concerning this theory and how to avoid or narrow the gap between theories, this section looks at publications relating to debates and criticisms concerning regime-shift topics in order to synthesise the arguments and the associated evidence. In general, the problems generally centre around of doubts about the theoretical framework, gaps between theory and empirical observations and the effectiveness of empirical detection. Details of the arguments are introduced in separate sections.

2.5.1.1 Doubts on the theoretical framework

Inconsistent terminology

Inconsistencies in terminology relate to concepts such as ‘state’, ‘transition’ and ‘regime shifts’, which have been broadened to include multiple stable states. However, systems that display regime shifts or models that use states and transitions do not always have multiple stable states (Capon et al, 2015). Meanwhile, phrases such as ‘phase shifts’, ‘regime shifts’, and ‘thresholds’ are used almost interchangeably and applied to both smooth continuous changes and discontinuous leaps in state, which does not help us to develop a clear theory (Petraitis, 2013). The idea that multiple stable states underlie the observation of sudden and nearly irreversible shifts in natural communities has been elaborated in several different areas of ecology, and each subdiscipline uses different terms for the same phenomena – or worse, the same term for different phenomena (Petraitis, 2013).

Oversimplification

The ASS hypothesis represents an oversimplification of real-world ecosystems and the physical forcing in systems is underestimated (Dent et al, 2002).

A rare phenomenon

The frequency of non-linear change relative to that of linear change is questionable, as evidence of pressure-induced non-linear changes is found to be rarer than gradual, monotonic changes in freshwater ecosystems (Capon et al, 2015). Empirical data on ecological changes in estuaries and near-shore marine ecosystems show that changes in these systems are not often starkly relative to historical variability (Mac Nally et al, 2014).

Untestable hypotheses

Given that threshold transgressions will not increase over time, threshold-related concepts would be untestable in ecology, as their absence could always be ascribed to insufficiently long observation periods (Hillebrand et al, 2020).

Publication bias

Publications are generally biased towards positive results in hypothesis testing (Capon et al, 2015). Failure to test for evidence is usually presented in less commercially exposed forms, such as grey literature (Hillebrand et al, 2020).

2.5.1.2 Gaps between theory and application

Vague meanings

The phrase “multiple stable states” has a very precise meaning in mathematical models, but not in practice. Similar problems exist in defining how big a shift must be to be considered dramatic, or how fast it should occur to be deemed sudden (Petraitis, 2013).

How close is close enough?

It is challenging to determine whether an observed pattern in nature actually matches the model. The comment from May (1977) that "empirical observations remain largely anecdotal, and…theory remains metaphorical" on multiple stable states theory is still appropriate, and making links between anecdotes and metaphors remains one of the biggest challenges facing ecologists (Petraitis, 2013).

Opposing findings

An analysis of response pattern of re-oligotrophication in 22 Danish lakes showed that resistance to change with decreasing TP concentrations is weaker than the rate predicted by the alternative state hypothesis, and the two alternative states are less stable than originally anticipated (Jeppesen et al, 2007). This can result from weak feedback loops in the system that can easily be broken and replaced, thereby leading to a comparatively smooth change.

In 24 naturally eutrophic shallow lakes (12.4-670.4 µg TP L^{-1}) with variable submerged aquatic vegetation cover (0-100%) on the western Boreal Plain in Canada, 71% of lakes were unstable, with 14% switching more than once in 6 years and more than 73% lakes switching 2- 9 times over a 20-year period (Bayley et al, 2007). Although the frequency of system switching doesn't necessarily mean that they don't have a tipping point, the lake systems in the above examples are more strongly abiotically regulated than internally stabilised according to theory. Evidence of tipping points in these ecosystems is not convincing, almost always because the nominal pressures have not been reached (i.e. pressures were of a press trajectory) in the study scope, meaning that the stability of putative alternative states could not be evaluated (Mac Nally et al, 2014).

Cause and effect

Apart from typical examples (Scheffer & Jeppesen, 2007), the causal relationship between drivers and response systems in specific case studies remains unclear (Sayer et al, 2006). Insufficient demonstration of mechanistic links between pressures and consequent ecological change therefore become one of the main hindrances to making valid evidence of regime shifts (Capon et al, 2015; Mac Nally et al, 2014; Peterson, 1984).

Questionable practical value

The usefulness of thresholds is questioned if the occurrences rely on the complex interaction of multiple pressures and their detection is only possible under very high signal-to-noise ratios (Hillebrand et al, 2020). Although regime shifts may be a useful theoretical concept that can help us to address the ways in which ecosystems function or cease to function, the difficulty in application reduces practical values in problem solving and environmental management (Groffman et al, 2006).

2.5.1.3 Effectiveness of empirical detection

Confusion about criteria

There is a lack of agreement on practical and operational criteria for identifying and analysing regime shifts across different system types and disciplines. In fields such as oceanography, large and statistically significant step changes in ecosystems are considered as regime shifts, while in ecosystem ecology much more emphasis is placed on whether feedback processes have been reorganized in a way that moves the system toward a different attractor (Biggs et al, 2018).

Reinvention of methods

Andersen (2009) pointed out that the rapid growth of literature on the detection of abrupt changes makes it hard to maintain a logical overview and increases the risk of unnecessary reinvention and rediscovery.

Proxies

In some cases, a single species is used as an example to explain an entire assemblage, despite the fact that differences in life history of the sentinel species lead to different rates of response to drivers (Petraitis, 2013). However, systems theory relates to whole system behaviour and not to individual components of that system. Community composition is used as the proxy for ecosystem state, which may respond to the environment more sensitively than the abundance or extinction of a single species.

Temporal and spatial scales

In regime shift databases, the scales of empirically detected regime shifts vary from weeks to centuries in time and from local to global in scale (Biggs et al, 2018). Choosing the right scale and sample size depends upon prior knowledge of natural variations (Petraitis, 2013), while the timescales of transitions and the choices of variables may exclude other forms of transition.

2.5.1.4 Constructive suggestions to narrow gaps

Along with the gaps discussed above, constructive suggestions have been provided to help narrow the gaps in our understanding of catastrophic changes in ecosystems. In theoretical terms it has been suggested that more definite alternative conjectures based on observations could improve our understanding of ecological changes as well as opening debates upon the dominant hypothesis (Petraitis, 2013). In terms of application, each particular system should be experimentally analysed again for its potential for bi-stability, and I should not expect all ecological systems to exhibit ASS (Schroder et al, 2005). Meanwhile, more research is needed to determine whether there are general principles or inherent differences in applying threshold concepts to different types of ecosystems, ecosystem attributes or the provisioning of ecosystem services (Groffman et al, 2006).

2.5.1.5 An example of debate on empirical data

In a study conducted in 71 shallow eutrophic lakes in Holland, seasonal patterns of chlorophyll-a concentrations were sampled monthly between 1975 and 1991 and analysed to check for relationships between the occurrence of clear water phases (CWP) and climatic conditions. The study concluded that the probability of clear water phases increased with the temperature of the lake water and was also highly correlated with oscillations in the North Atlantic climate system

(NAO) (Scheffer et al, 2001). The evidence in the reasoning consisted firstly of the pronounced correlation between average lake temperature (ALT) of lake Veluwe and the NAO winter index and secondly a regression analysis showing incidences when CWP comes on an earlier day (d) in years with a high NAO index (d = 155.5 - 2.9 × NAO + 0.03 × ALT; slopes $p < 0.001$; adjusted R2 = 0.26). Thirdly, the reasoning showed a linear regression of the appearance day of CWP and the first quarter lake temperature ($d = 184 - 8.4 \times T_1$; slopes $p < 0.01$; adjusted $R^2 = 0.20$), and fourthly a multiple logistic regression between the probability of CWP and NAO index (r = 0.335, $p < 0.005$). Fifthly, a multiple logistic regression between the probability of CWP and the average chlorophyll *a* concentration (r = -0.067, $p < 0.001$), and sixthly a simulation model derived from a simple periodically forced algae-zooplankton model predicted that lake warming resulted in more and earlier CWP. Overall, the reasoning claimed that the time shift effect of CWP meant that the dynamics of entire food webs were profoundly affected by climate change and lake warming. The underlying mechanism of the simulation model was that the grazing pressure from zooplankton directly affected algal biomass and water clarity, which was under top-down control from the population of planktivorous fish. According to his minimal plankton model, the possible limit cycle and stable equilibrium of a system comprising only zooplankton and algae would be destroyed by pressure from fish predation (Scheffer, 1998, pp. 156-165). I know that lake warming has an effect on the life cycles of individual species and consequently entire food webs, but how the impacts combine to affect water transparency is unclear.

The reasoning and conclusion of this study were strongly criticised by van Donk et al (2003) and Jeppesen et al (2003). One of the main reasons for this criticism is that Scheffer et al (2001) neglected to account for the restoration efforts to enhance water transparency, such as biomanipulation through fish removal and nutrient reduction in many shallow Dutch lakes since the late 1980s in his study. The same empirical data and the same model were reassessed with the additional knowledge that the period when lake restoration enhanced CWP coincided with the period of high NAO index values and high temperatures (Van Donk et al, 2003). In the new analysis, the correlations between the probability of CWPs and NAO in individual lakes were found to be less convincing (with only 4 of 26 lakes showing significant positive correlations) while the overall regression model remained significant ($\chi^2_{26} = 236.9$, $p = 6 \times 10^{-36}$). Two lakes showed significant negative correlations. Combining the criticism that the simple model should not make detailed quantitative prediction without sensitivity and uncertainty analysis, the hypothesis that climatic warming has caused an increase in the probability of CWPs over the past 40 years is rejected.

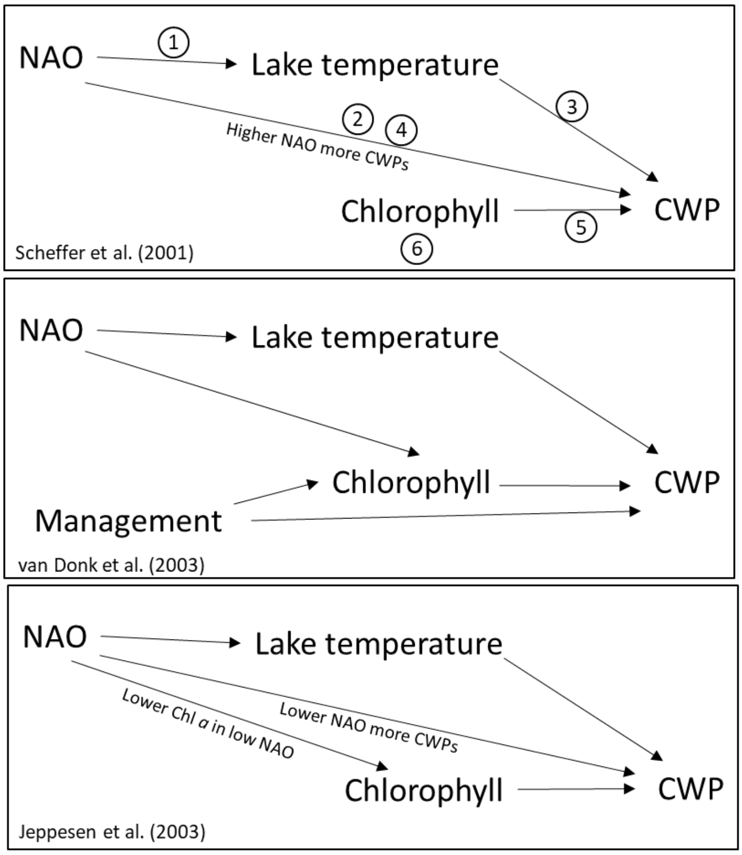

Figure 2-20: Conceptual model of the effects of climate and management on chlorophyll concentration and CWP probability in these three papers, inspired by van Donk et al. (2003). The numbers in the circles represent the evidence provided by Scheffer et al (2001b) discussed in the text

Motivated by different opinions on the role of temperature on lake water clarity, Jeppesen et al (2003) analysed data from 29 shallow Danish lakes over the past 8-12 years. The correlation between winter NAO and annual temperatures and between the probability of CWP and annual mean chl *a* (circle number 1 and 5 in Figure 2-20) confirmed similar results, but the probability of CWP is not significantly related to NAO, and Chl *a* tended to be lower in the years with the lowest NAO. In response, Scheffer et al argued that the management effect should be considered as the average annual Chl *a* and used as an independent variable for nutrient loading. Meanwhile, the statistical test by van Donk et al (2003) removed 64% of clear-water phases from the data, leaving little data to analyse. Removing the same group of suspicious lakes, Scheffer et al still found similar significance in correlation between NAO and Chl *a,* and the slope of the NAO effect was remarkably stable despite biomanipulations to improve water transparency. However, the inflation in statistical significance is admitted by using different lake-years as independent.

Finally, a solution to the debate was proposed. It was suggested that a large-scale experiment should be conducted in low-NAO years, and the behaviours of manipulated and non-manipulated lakes when the NAO changes should be studied. The debate would be clearer if the effect of temperature on water transparency in a algae-zooplankton-fish system could be better understood. The studies exemplify the challenges many empirical studies face today in terms of knowledge of ecosystem history, validity of statistical analysis and opposite inferences that can be deduced from similar evidence (Capon et al, 2015; Hillebrand et al, 2020).

2.5.2 Research plan in the MLYR

There have been some regional and individual case studies investigating regime shifts in Chinese lakes, but there are still many lakes in the MLYB that lack information relating to changes in system states and driving forces. Based on the results of the literature review, I found that as well as similarities in environmental contexts and transition windows in lakes in MLYB, much heterogeneity exists between lake ecosystems due to different physical conditions and human disturbance. To understand the states as well as the driving forces and mechanisms of state change in response to these driving forces, it is essential to select a specific case study for analysis. The data investigating lake surface water quality in 2008 show that the MLYB lakes have a scattered distribution in water quality, lake depth and size. Most attributes of Lake Taibai are close to the mean values except conductivity and the concentration of SiO_2 (Figure 2-22). I therefore chose Lake Taibai as the study site for analysing empirical data indicating ecosystem state and drivers on a centennial scale.

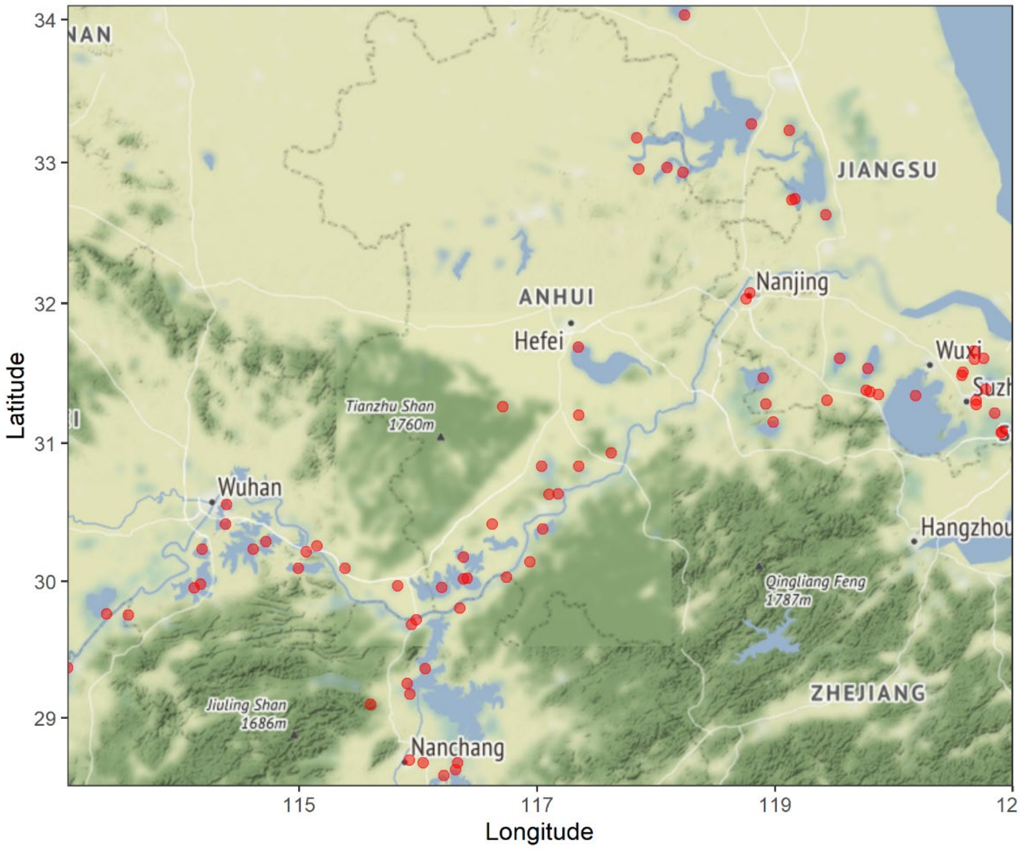

Figure 2-21: Locations of lakes used in the MLYB lake investigation, Summer 2008

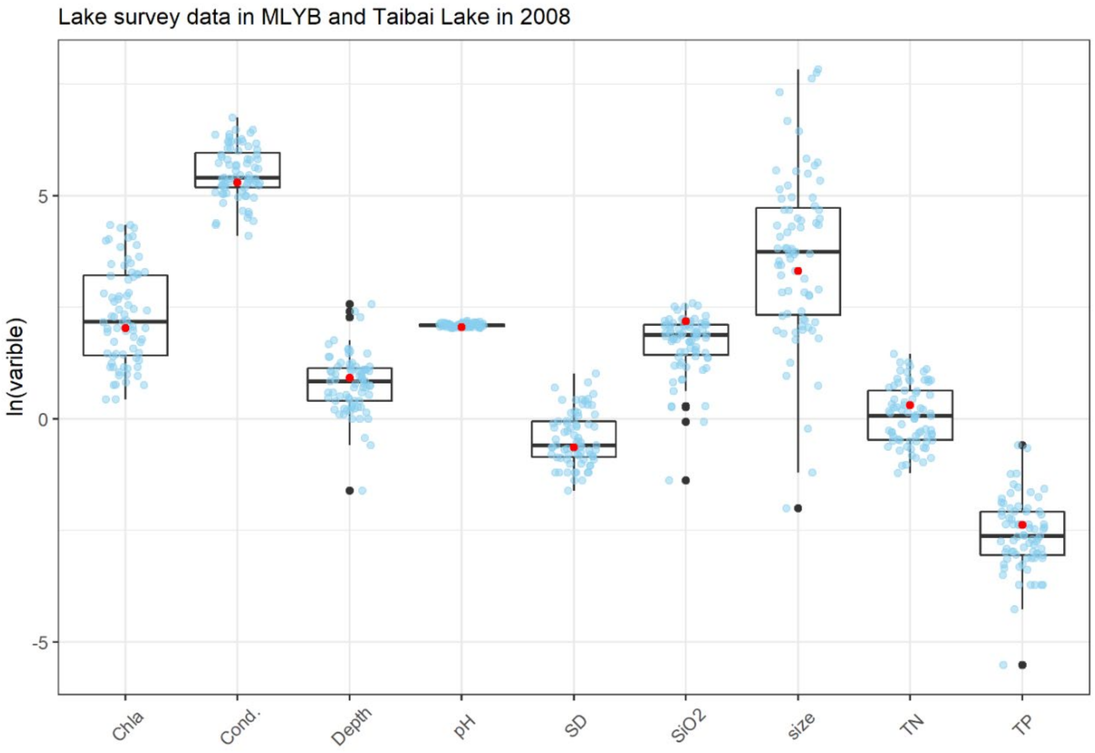

Figure 2-22: Surface water quality of the MLYB lakes including Taibai Lake in 2008. Dots are water quality data of each lake. The specific attributes including the concentration of Chla, conductivity, water depth, lake size, pH, Secchi Disk, the concentration of SiO_2, Total Nitrogen(TN) and Total Phosphorus(TP) are set as the horizontal axis while the log values of variables are set as the vertical axis. Colours are used to distinguish Taibai(red) and other MLYB lakes(blue).

Lake Taibai has no dedicated ecosystem observatory, and available data on the lake’s ecosystem are very sparse. I therefore needed to consult various data sources to fulfil our collection needs. Palaeoecological data from sediment cores in the centre of the lake can be recovered using a palaeolimnological approach and combined with surrounding meteorological stations, survey reports and historical documents. Changes in the area of Lake Taibai and changes in land use of the lake catchment over recent decades can be categorised using remote sensing images to analyse environmental change. Statistical methods for detecting transitions in the ecosystem were selected from the literature to detect tipping points and combined with multivariate statistical analysis methods on the biome. These regression analysis methods should reveal whether there has been a regime shift in the lake, and the date and causes of its occurrence.

Chapter 3: Revealing regime shifts using fossil diatom assemblages in Taibai Lake

Note: This chapter contains a published paper and its citation information is: Zhao Y, Wang R, Yang X, Dearing JA, Doncaster CP, Langdon P, Dong X. Reconstruction of Ecological Transitions in a Temperate Shallow Lake of the Middle Yangtze River Basin in the Last Century. Water. 2022; 14(7):1136. https://doi.org/10.3390/w14071136

Abstract

Exogenous drivers may cause a gradual and reversible change in the equilibrium of a lake, or they may force it over a threshold and into a persistent alternative stable state, described as a regime shift in the ecosystem. In the mid-and-lower Yangtze River Basin (MLYB), major environmental problems in shallow lakes have been eutrophication and abrupt algal blooms due to anthropogenic disturbances over the last century. Much value should therefore be placed on understanding the changes in shallow-lake ecosystems that characteristically precede changes in the state of the lake. Here I describe a case study based on the palaeolimnological signature in diatom assemblages of various types of regime shifts caused by historically documented anthropogenic drivers in Taibai Lake, a temperate shallow lake. I evaluate the effectiveness of palaeolimnological data as a surrogate for long-term monitoring. Algorithms using sequential *t* and *F* statistics detected breakpoints in the time series of diatom assemblages in 1994-1996, 1974-1977, 1952-1956, and 1931-1934. The

regression analysis suggests that the hydrodynamic ecosystem and aquacultural ecosystem relationships fit better in the breakpoint regression model and the relationship between nutrient loading and ecosystem state is more suited to the linear model. Feedback loops help us to reconstruct the dynamic changes in Taibai that have been influenced by major stressors, and our study exemplifies the value of using systemic approaches to identify regime shifts and their possible causes in shallow lakes from palaeolimnological records. The case study of Taibai can be seen as an example of reconstructing ecological regime shifts in shallow lakes in the MLYB in order to understand state changes in lake ecosystems, which will benefit effective lake management.

3.1 Introduction

Shallow-lake ecosystems provide a broad range of indispensable services encompassing water and food security, aesthetic and cultural values and the maintenance of catchment-wide biodiversity. There are wide variations between different lakes and lake systems (Reynaud & Lanzanova, 2017). Lakes with high water quality can provide clean drinking water, healthy aquatic habitats for wildlife and can also contribute to the wellbeing of surrounding residents (Schallenberg et al, 2013). Through their connections with river systems, engineered lakes may also contribute to flood regulation and hydroelectricity. Under the pressure of human activities, however, lake ecosystems may deteriorate to undesirable states by shifting irreversibly from one stable regime to another, causing losses in ecological and economic resources and leading to heavy restoration costs (Scheffer et al, 2001; Schindler, 2012). An example of a regime shift in a shallow lake is an ecosystem abruptly shifting to a eutrophic state induced by excessive exogenous nutrient loading, resulting in a persistent turbid-water state and algal blooms (Scheffer et al, 1993). Such regime shifts are well known in China, a country with numerous lakes. Roughly a third of all Chinese lakes are situated in the middle and lower reaches of the Yangtze River (hereafter referred to as 'MLYB'), and these freshwater shallow lakes now face unprecedented anthropogenically-induced eutrophication (Qin et al, 2013). Understanding the nature and scenarios of such regime shifts in order to facilitate optimal management strategies is crucial, as inappropriate actions could push lakes that are already at risk of shifting across catastrophic threshold changes.

Regime shifts in lakes are caused by a combination of the external forces and the internal resilience of the lake ecosystems (Rockström et al, 2009; Scheffer & Carpenter, 2003). The ecosystem becomes vulnerable and will respond to smaller perturbations after losing resilience (Folke et al, 2004). Studies on regime shifts are diverse in terms of methodology, but include conceptual, mathematical and computational approaches (Kong et al, 2017; Kuehn, 2011), laboratory simulation experiments (Veraart et al, 2012), whole-lake experiments including biomanipulation (Carpenter et al, 2011; Seekell et al, 2013; Sondergaard et al, 2017) and historical environment reconstruction using sediment cores (Doncaster et al, 2016; Wang et al, 2012).

As a guide to making ecological data tests operational, Andersen et al (2009) summarised hypothetical regime shift scenarios in terms of three principal alternative relationships between drivers and state responses (Figure 3-1, a-c). These scenarios were constructed from a review of regime shifts inferred from the statistical analysis of time series based on monitoring data. Jeppesen et al (2018) have since added two further scenarios of driver recovery based on their empirical findings in the North Water area between Canada and Greenland (Figure 3-1, d and e). They identified recoveries in some periods of ecosystem reconstruction that could be traced back to ca. 4500 years ago based on lake sediment data, archaeological findings and historical records of climate change. Despite dissimilar data sources between regime shift and recovery, the five patterns shown in in Figure below indicate possible relationships between driver and ecosystem state changes in time-series in a regime-shift-centred view. These provide us with a simple operational framework on which to categorize real regime shifts and their mechanisms.

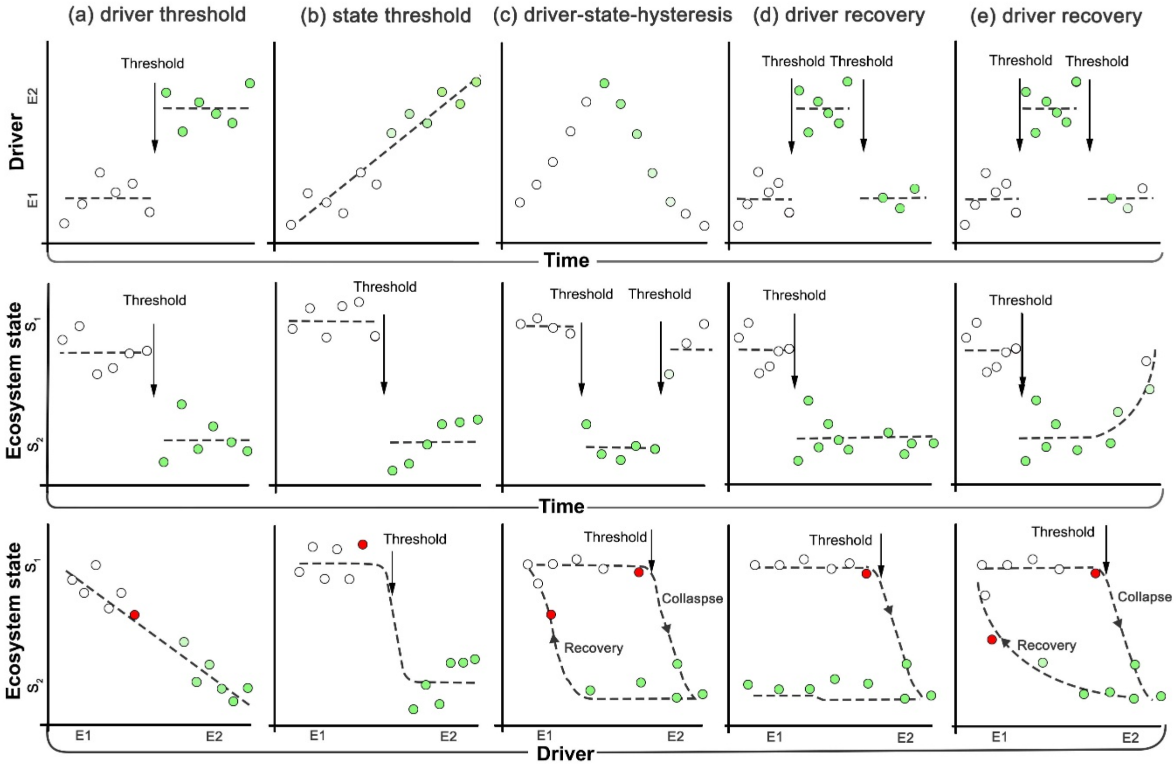

Figure 3-1: Conceptual models of alternative types of regime shift and threshold transitions (a-c after Andersen et al, 2009; d and e after Jeppesen et al (2018)). White and green dots distinguish ecosystem states S1 and S2 respectively. Red dots identify threshold points of abrupt and persistent change in driver or ecosystem state, and arrows identify the direction of change. The three rows show the driver (top row) and ecosystem (middle row) state developing through time, and the ecosystem response to the driver (bottom row) along with consequences for ecosystem structure.

The first two scenarios (Figure 3-1, a and b) depict a single transition under the influence of different types of drivers. The Driver Threshold scenario shows an abrupt change in the driver over time which is mirrored by an abrupt change in the ecosystem state, as well as a linear state response to the driver. The State Threshold scenario shows a linear driver causing the same abrupt change in ecosystem state and response pattern. The other three scenarios simulate possible combinations of single transitions with drivers reversing after state thresholds are exceeded. The Driver-State Hysteresis scenario (c) shows an abrupt transition in state caused by a gradually strengthening driver followed by a time-lag, or hysteresis, during the gradual weakening of the driver. The Driver Recovery scenarios (d and e) show abrupt switches in a driver, such as total phosphorus in a shallow lake, with the switch back to a weak driver resulting in no recovery or hysteretic recovery.

To understand the mechanisms of transition, feedbacks can reveal the causality of the ecological transitions. Complex systems that include multiple components comprise feedback loops of various lengths, effects and strengths. Negative feedback must prevail to keep the system stable (Neutel & Thorne, 2014), while positive feedback destabilises the system and encourages change toward an alternative state (Kefi et al, 2016; Scheffer et al, 2012). In a case study of eutrophication, the time series of diatom assemblages and water quality appeared to identify a critical transition in 2001, which was concurrent with observed algal blooms in Erhai lake (Wang et al, 2012). In Taibai Lake in the MLYB, Liu et al (2012) inferred that the turbid algae-macrophyte mixed state shifted to a macrophyte-dominated state in approximately 1950. The ecosystem state further shifted to a hyper-eutrophic algae-dominated state after 1990. The dynamics of ecosystem services in MLYB lakes (Xu et al, 2017) and the ecological network parameters relating to critical transition (Wang et al, 2019) have also been assessed more recently, and these assessments make Taibai a potentially excellent case study in which to investigate scenarios relating to regime shifts in MLYB shallow lakes. Empirical data for Taibai and its catchment are available, including monitoring data, palaeolimnological data, investigation reports and historical records. I can therefore evaluate the utility of the conceptual framework by comparing the fit of alternative hypothetical scenarios to the observed driver-response relationships, and by constructing system dynamic diagrams from empirical evidence. Specifically, I can use the evidence to address the following research questions:

1) What changes in ecosystem states do subfossil diatoms show

2) Can I detect the existence of thresholds in the relationship between stressors and ecosystem states

3) Can I reveal driver-response interactions through the analysis of historical data and feedback loops?

3.2 Materials and methods

3.2.1 Lake and catchment history

Taibai Lake (29°56′ to 30°01′N, 115°46′ to 115°51′E, 16.0 m above sea level) covers an area of 25.1 km^2 and lies within a 960.0 km^2 catchment. It is a shallow lake, with a maximum depth of 3.9 m and an average depth of 3.2 m, and has been eutrophic approximately since 2000 (Yang et al, 2006). Human activities and environmental changes were retrieved from historical and palaeolimnological records (Table 3-1). Nutrient loading from chemical fertilizer application of catchment farmland, intensive aquaculture, and untreated sewage has changed slowly. Anthropogenic activities within the Taibai catchment (damming, sluices, hydroelectricity, land reclamation, and restoration) influenced the hydrology and ecology. The change in the function of the lake to intensive fishing and aquaculture resulted from the adoption of modifications to the social system.

Table 3-1: Human activity in Taibai during the last decades

Periods	**Human activity and palaeolimnological evidence**
1970s-present	2000-present: Reducing vegetation coverage [4]
	2000-present: Widespread adoption of flush toilets that are not connected to local piped sewage systems and a lack of new treatment plants have added to the increased nutrient loading[5]
	1987-present: Fish farm owners introduced economic domestic fish into the lake, upgrading the intensity of aquaculture to a high level, resulting in exponential growth in aquaculture products [1]
	1983-1993: High sedimentation flux correlated to soil loss due to intensive cultivation development [5,6]
	1978-2013: The population in the lake catchment increased and human settlements expanded, while farmland and lake area shrank [2,3]
	1976-present: Tongsipai Floodgate cut the dispersal route for younger fish[1]
The 1950s-1980s	1950s-1978: Rapidly developing local industrialization, mainly chemical fertilizer factories,[2] after which the lake received more nutrient loading from increasing domestic sewage, poorly treated industrial waste, and flushed chemical fertilizer[4]
	1958-1970: High sedimentation flux correlated with land reclamation around Taibai[5]
	1955-1962: Dam construction: Jingzhu, Kaotian, and Xianrenba reservoirs were built in the upper reaches of Taibai. The lake outflow passes through lake Longgan to the east of Taibai and drains to the Yangtze River[5]
Before 1950s	The lake had periodic direct inflow connections with the Yangtze River during floods[1, 5]

[1] Taibai investigation report 1987; [2] Huanggang Yearbooks 2010; [3] Land Use and Cover Change (LUCC) analyses of satellite images of Taibai catchment (Figure 3-2); [4] (Jian, 2001); [5] (Liu et al, 2007); [6](Gui et al, 2018).

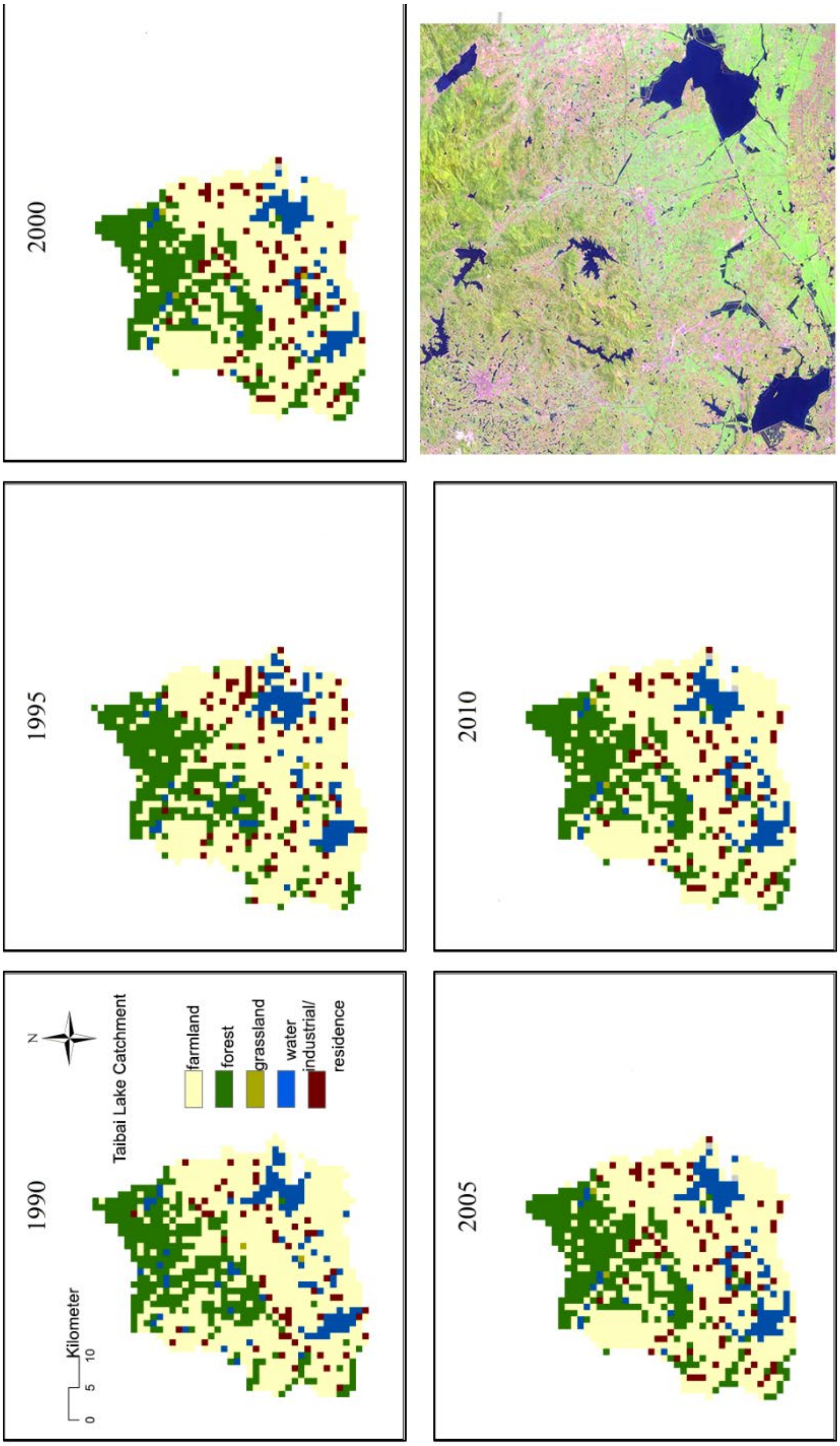

Figure 3-2: Land use/land cover change (LUCC) from 1990 to 2010 in the Taibai basin

3.2.2 Palaeolimnological reconstruction

An 83.5-cm long preliminary core TN2007 (Taibai North) was recovered using a Kajak gravity corer in 2007 at a water depth of 1.5 m from the northern section of Taibai Lake (29°59′44.3″N, 15°48′26.5″E). The TN2007 core was sampled at 0.5-cm intervals from a 0 to 20-cm depth, and at 1.0-cm intervals from 20 to 83.5 cm depth for diatom analysis. The samples were dated using Pb^{210} and Cs^{137} radionuclide techniques with a High Purity Germanium (HPGe) Gamma Spectrometer and a constant rate of supply (CRS) model (Appleby, 2008). In the laboratory, sediments were washed in a water bath with 30% H_2O_2 and 10% HCl (Battarbee et al, 2001), and cleaned subsamples were dried onto coverslips and mounted onto microscope slides. At least 300 diatom valves were counted in each subsample under a light microscope using an oil immersion objective (magnification ×1,000) and phase-contrast optics. Diatom taxonomy followed Krammer and Lange-Bertalot (2008). All diatom data were calculated as relative percent abundances, and taxa with an abundance of less than 2% of the total were excluded from the statistical analysis. The diatom diagram was drawn using the *tidypaleo* package in R, and the zones were identified using the constrained incremental sum of squares (CONISS) and the broken-stick model (Bennett, 1996) in R.

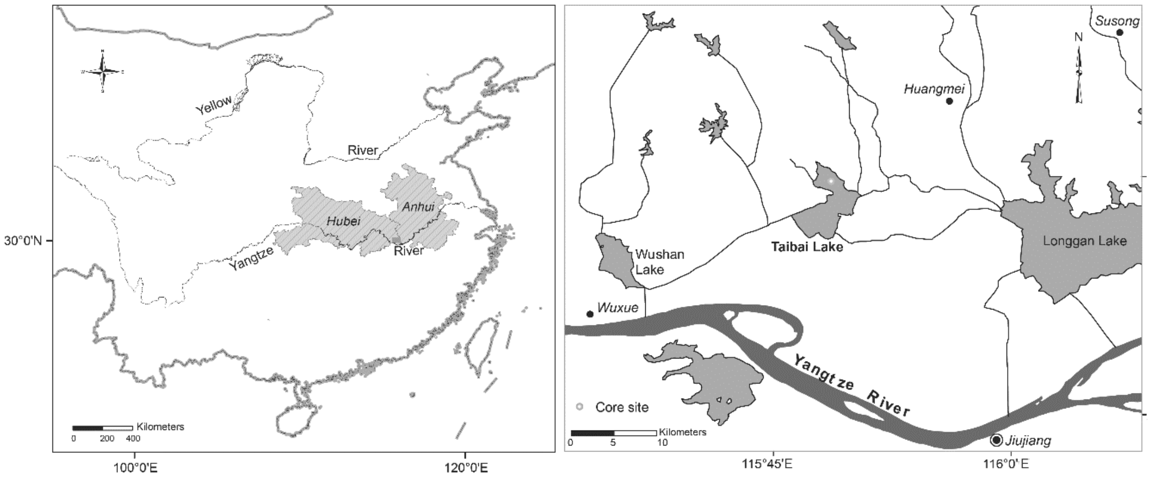

Figure 3-3: Map of Taibai Lake catchment in MLYB. Left-hand map shows the middle-lower reach of Yangtze River in China, between Hubei and Anhui province (shadowed area), and the location of Taibai Lake catchment. The right-hand map shows the northern central coring site in Taibai, the northern reservoirs draining into the lake and connecting rivers and canals to other lakes and the Yangtze River.

I used diatom species as sensitive indicators of environmental change due to the diverse variety of freshwater diatom biotopes (Seckbach & Kociolek, 2011; Smol et al, 2002). For example, the abundance of planktonic *Aulacoseira granulata* is closely correlated with the connection between a water body and the main stream, as it has a relatively high rate of sinking and requires significant levels of turbulence to maintain its position in the water (Reid & Ogden, 2009). Changes in diatom composition have been shown to represent structural changes of lake primary producers well (Doncaster et al, 2016; Wang et al, 2019).

Grain size in the core was measured using a Malvern automated laser-optical particle-size analyser (Mastersizer-2000; Malvern Instruments Ltd, Worcestershire, UK) after removing organic matter by treatment with 30% H_2O_2. Total organic carbon (TOC) content was testing using a CE-440 elemental analyser (EAI Exerter Analytical INC., North Chelmsford, MA, USA) after treating 0.5g dry samples with 5% Hydrochloric (HCl) acid. The relationship between the grain size of lake sediments and critical shear stress (Dearing, 1997) was used as an indicator of river discharge to a lake (Chiverrell et al, 2019; Dearing et al, 2008), meaning that grain size can identify hydrological changes in lakes in the MLYB (Xue et al, 2017).

The catchment is known to have had excessive fertilizer applications to agricultural land (Ju et al, 2009), suggesting that records showing the increased use of agricultural fertilizers might be used to represent surplus nutrient loading in a semi-quantitative way. Fish production biomass in Taibai between 1964 and 2013 was taken as an indicator of aquaculture intensity.

3.2.3 Statistical analysis

To reduce the complexity of data, Principal Component Analysis (PCA) was applied to the relative abundance of diatom species, and the first principal component (PC1) were calculated to evaluate the variation in the diatom assemblages. Statistical methods for detecting breakpoints included sequential *t* test and the *F* test (the Chow test) in PC1 scores. Firstly I used the sequential *t* test algorithm provided as an Excel add-in by Rodionov (2004) to monitor regime shifts. The algorithm required input thresholds of regime length *l* and probability level *p*, and provided us with the lengths of stable periods, the Regime Shift Index

(RSI), and the mean values of stable states. In this study I set *l* at 5 samples and *p* at 0.05. Then the PC1 scores were tested for major discontinuities in a Chow test for 15% of the whole 86 observations (with 23 interpolated data points). Structural changes were detected using the R package *Strucchange* (Zeileis et al, 2003). The potential tipping points of the diatom community composition indicated by PC1 were summarised from the results of the above detections.

In order to explore the discontinuity in the relationships between ecological responses and their main stressors, I also applied linear and breakpoint regression analyses to a combination of diatom assemblage composition, grain size, fertilizer application and fish production to compare magnitudes of the coefficient of determination r^2 between linear fitting and step-change alternatives. Due to constraints in available data, I used proxies to calculate the strengths of the stressors involved. The hydrodynamic state was estimated using the palaeo-record of grain size. Nutrient loading and aquaculture intensity were approximated by historical records showing N-P-K fertilizer application within the Hubei province and fish production. Informed by the previous tests and the characteristics of data, the number of breaks was set as 1 in the step-change model. The r^2 values allowed us to compare the robustness of two alternative patterns of response, namely gradual change, and abrupt transition. The *p* values were also listed for comparison.

3.2.4 Diagrams of interactions and feedback

Based on these data and processes, I built up a model of the dynamic interactions in Taibai's ecosystem that created functioning positive feedback loops. Three abiotic elements, namely turbulence, turbidity, and nutrients, and five biotic elements including phytoplankton, zooplankton, submerged macrophytes, decapods, and fish were selected as they have played important roles in ecological processes according to our available records. I also identified the most important external drivers as damming, fertilizer applications in the catchment and the use of artificial fish food. Functional positive feedback and its effects were assessed for several periods. Following the conceptual model of feedback loops, I created a sequence of causal loop diagrams to help visualize the destabilizing processes that occur before regime shifts in Taibai Lake.

3.3 Results

3.3.1 Changes in diatom assemblage composition

Taibai lake has undergone major changes in diatom assemblages, with a general shift towards a higher relative abundance of both the periphytic *Fragilaria ulna* varieties *acus* and *Nitzschia subacicularis* and the benthic varieties *Nitzschia palea* and *Navicula menisculus* and a decrease in the relative abundance of planktonic *Aulacoseira* taxa (*A. alpigena*, *A. ambigua* and *A. granulata*). In this case study I presented the more common diatom taxa according to biotope groups, and three diatom assemblage zones were identified according to the relative abundance of the taxa and cluster analysis (Figure 3-4). The depth data of samples were used as the vertical axis.

The bottom zone (42.5-20cm) was dominated by the heavily silicified planktonic *A. granulata* and benthic *Gyrosigma acuminatum*. In this area, *A. granulata* gradually declined (75%-45%) and benthic species increased (mainly *G. acuminatum*). In the middle zone (19.5-10cm), the diatom flora was dominated by benthic taxa *G. acuminatum* (30%-38%) while *A. granulata* declined dramatically at 19.5cm from 45% to ~20%. At the same time, the relative abundance of periphytic *N. subacicularis* and small planktonic *A. alpigena* and *A. ambigua* increased. The top zone (9.5- 0 cm) was characterized by the dominance of benthic *N. palea* and periphytic taxa (*F. ulna* varieties *acus* and *N. subacicularis*). In this section, both *A. granulata* and *G. acuminatum* decreased to under 10% in terms of relative percentage of abundance. The boundaries of the zones are dated at 1956 (19.5cm) and 1991 (9.5cm) according to the depth-age data using the ^{210}Pb-CRS model corrected by the ^{137}Cs 1963 peak (Liu et al, 2012).

The first and second principal components explain 35.6% and 12.7% of the total variance respectively. This means that the PCA axis 1 sample scores can be used as an indicator of major variations in the diatom assemblage composition. The trend of PC1 declined gradually along the core and PC2 changed in a similar way to the variation of the relative abundance of *G. acuminatum*, which can be explained by the contributions of the diatom species (Figure 3-5c). In the biplot of the first two components, samples fell into three clusters: 2006-1996, 1996-1948 and 1947-1850.

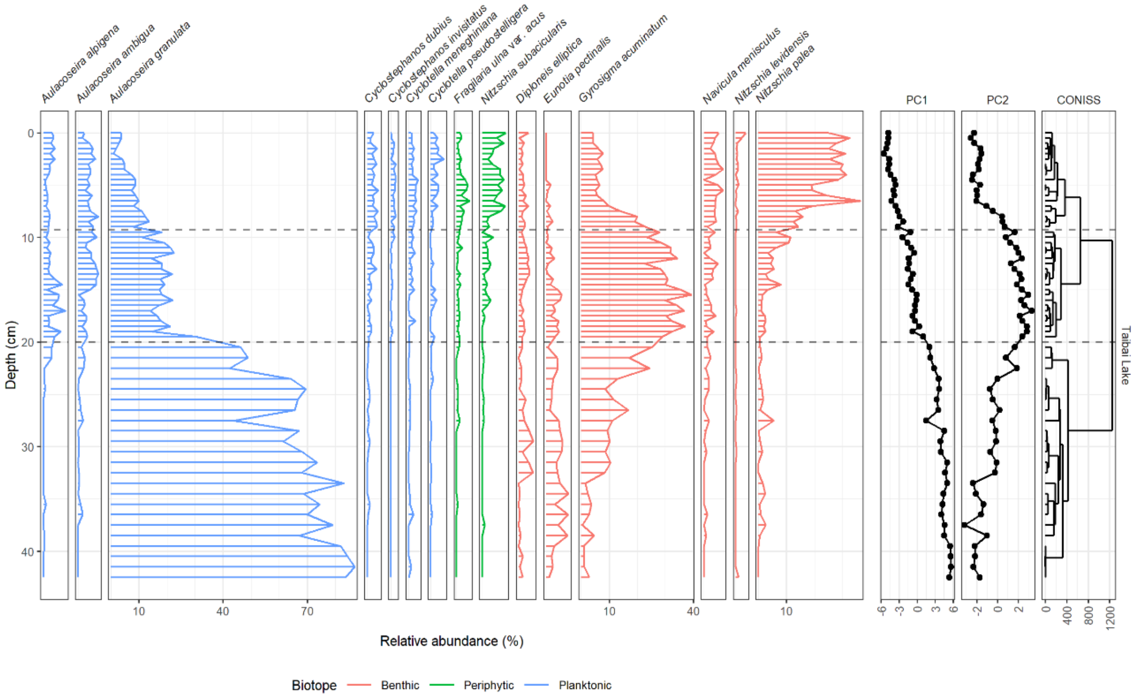

Figure 3-4: *Stratigraphic diagram of diatom assemblages for TN2007 with the first two axis of PCA and broken-stick model zones*

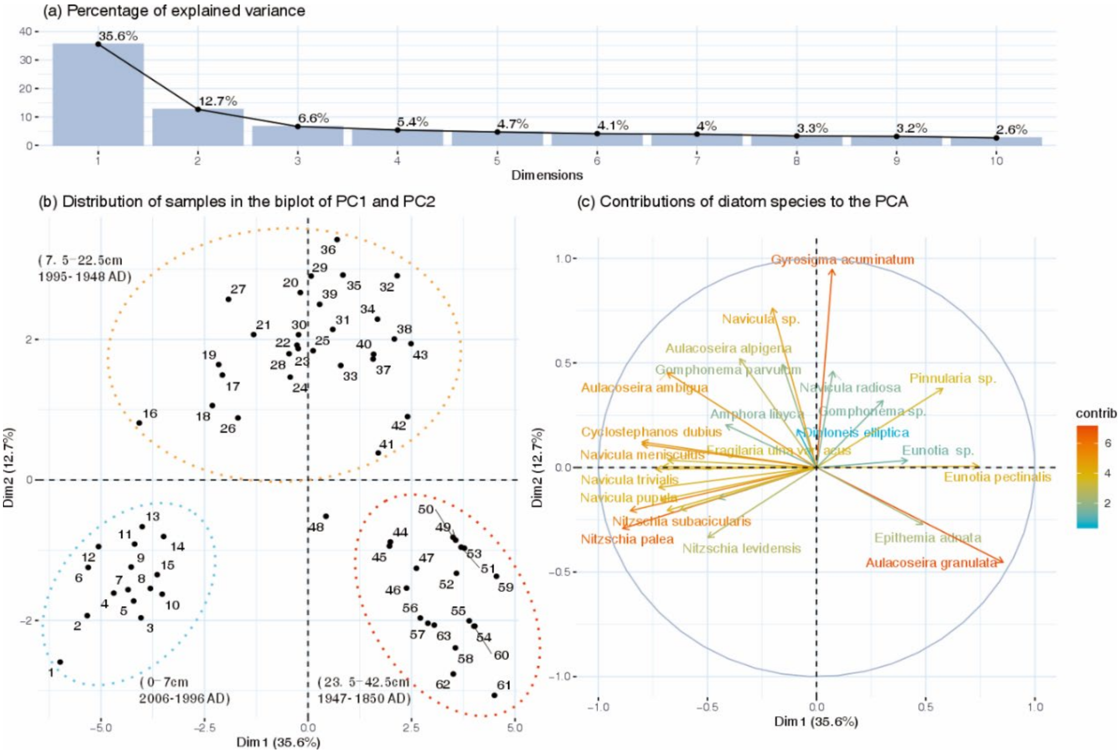

Figure 3-5: Explained variance of principal components, PC-scores along the first two axes of the PCAs and contributions of diatom species. (a) percentage of explained variance; (b) distribution of sediment samples in the PCA biplot; (c) contributions of diatom species to the total variation.

3.3.2 Tests for ecological thresholds

Statistical tests to find the tipping points on PC1 of diatom assemblages were conducted in terms of depth for the convenience of even intervals and interpreted in time. In the analysis of the *Breakpoints* function, the linear regression model found four breakpoints at depths of 7.0 cm, 14.0 cm, 20.0 cm, 28.0cm, which can be inferred as 1996, 1974, 1956 and 1934. For the *F* statistics, sup.*F* = 279.97, p-value < 2.2e-16, and ave.*F* = 131.19, p-value < 2.2e-16. The highest confidence of *F* statistics appears at 13.5cm in depth, which relates to 1977. In the STARS *t*-test method, regime shifts were detected at 8.0 cm, 14.0 cm, 21.0 cm, and 28.5cm in depth, which can be inferred as 1994, 1974, 1952 and 1931 respectively. The parameters used in the analysis are sig=0.05, cut-off length=10, and Huber's parameter=1. The regime shift index in 1994 is higher than the other three values, and the RSI in 1952 is the lowest. To summarise, the possible tipping points are 1994-1996, 1974-1977, 1952-1956 and 1931-1934.

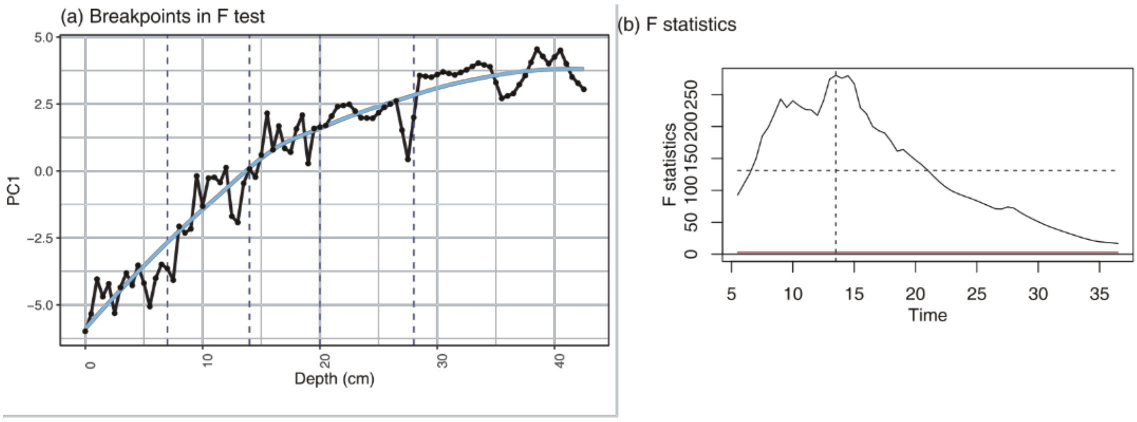

(a) Breakpoints in F test

(b) F statistics

(c) Shifts in STARS detection

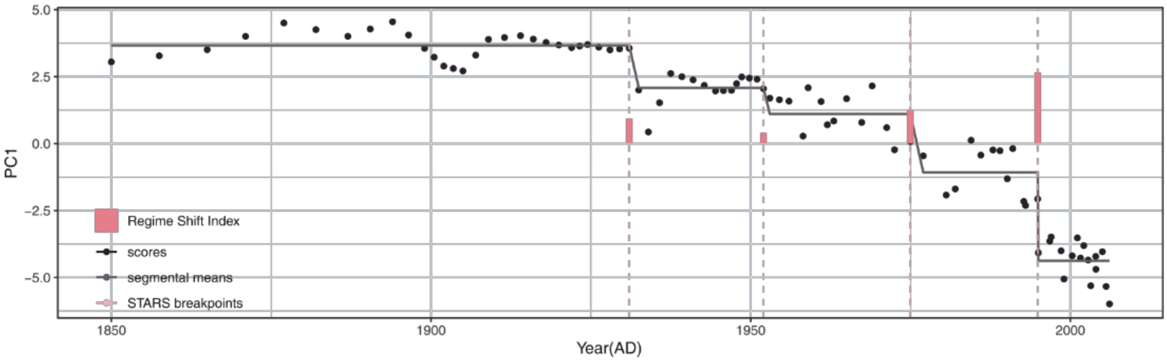

Figure 3-6: Breakpoints detected using multiple approaches of the sequential t-test and F test

The empirical relationships between environmental drivers and ecosystem states were tested and plotted in a linear regression model and a breakpoint regression model in R environment. In each plot, the model with a higher r^2 value is coloured in blue (linear regression) or red (step-change), with the alternative model showed in grey. Comparing the

R-square values, the values of the step functions are greater when considering hydrodynamic and aquacultural factors. Despite these higher explanatory powers, the *p* values of step functions are all greater than 0.1, while linear regression models all show significance with *Pr(>|t|)* <0.001.

Table 3-2: Linear regression models containing no breakpoints between the stressors and ecological responses

	Intercept ±SE	**Slope ±SE**	**R^2**	**Pr(>|t|)**	***F*-test of model fit**
PC1~MD	11.5268± 1.4251	2.1657± 0.2746	0.5308	1.33e-10	*F*(1,55)= 62.22, p < 0.001
PC1~FA	6.7809± 0.5283	-1.5404± 0.1112	0.7771	<2e-16	*F*(1,55)= 191.8, p < 0.001
PC1~FP	-2.43085± 0.20452	0.26146± 0.05417	0.3864	2.41e-05	*F*(1,37)=23.3, P < 0.001

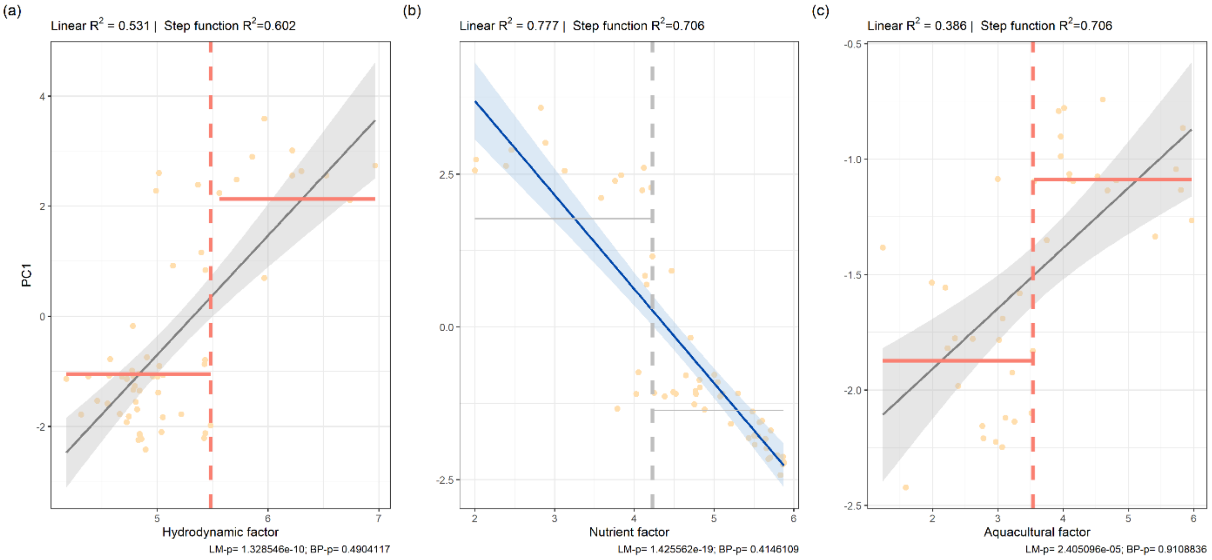

Figure 3-7: Regression models of the state-driver responses in Taibai Lake

3.4 Discussion

3.4.1 Classification of regime shifts and driver-response interactions

Driver-state interactions are envisioned in a straightforward manner with the help of regression models. When the driver-threshold transition is mediated by large and abrupt changes in hydrodynamics, the process is postulated as a driver-threshold scenario. After 1977, the nutrient loading and intensive aquaculture affected the ecosystem of Taibai Lake slowly and progressively, helping to change the state-driver response and the shift in thresholds, which is consistent with the state-threshold scenario. Recovery scenarios in the framework (Figure 3-1, c-e) were not examined in the Taibai data because none of the ecosystem states or nominal drivers showed any reversed trends over the last century. This is a widely occurring situation for disturbed Chinese shallow lakes in the MLYB that have not been engineered or manipulated to improve water quality (Qin & Zhu, 2006; Yang et al, 2006).

There are difficulties in using statistical approaches to test criteria related to the flexible definition of regime shifts, and errors in hypothesis-testing may occur due to random fluctuations induced by intervention events or missing variables due to lack of records (Andersen et al, 2009). Five step-change points were detected using t-tests, but only the most significant two were accepted because they showed comparatively persistent stable states and the shifts were more distinctive than the other three. Statistical tests can therefore be considered suitable for the exploratory examination of empirical data or samples, but a regime shift needs to be confirmed using more ecological reasoning. Overall, the paper combined existing theories and methods, and applied them in detecting regime shifts from palaeolimnological data, offering a new tool to recognise ecological changing patterns on multi-decadal timescale.

3.4.2 Feedback loops illustrating regime shifts

To identify putative mechanisms that underpin regime shifts in Taibai, I need to show how the ecosystem response to hydrological change influenced its subsequent response to developments in agriculture and aquaculture. An ecosystem state-response transition requires a growing positive feedback loop when the existing webs of stabilising feedback are weakened (Scheffer et al, 2001). Taibai shows evidence of a transition of ecosystem state in the 1990s without any sudden corresponding environmental change, which may result from the failure of self-regulating feedback loops. To clarify the presence of feedback mechanisms in different periods, I created causal loop diagrams from aggregated interactions between major functioning system groups (phytoplankton, zooplankton, fish, and submerged macrophytes) and the external drivers (turbulence, turbidity, nutrients, and artificial diets) I inferred from the documented qualitative evidence. The causal loops linked main functional groups such as phytoplankton, zooplankton and submerged macrophytes as well as some environmental variables. Fish are defined as a super-group to reduce any further complexity and maintain coherence with statistical dataset. These functional groups can be used to characterise the major interactions that contribute to progressive ecological changes in Taibai. The ecosystem before 1950s is assumed to be a comparatively natural baseline state. With strong connections to the Yangtze River at that time, the lake had a fast hydraulic retention time, a turbulent flow, and high levels of turbidity due to the presence of suspended sediment. According to an internal investigation report on Taibai, the natural fish community from the Yangtze River dominated the lake.

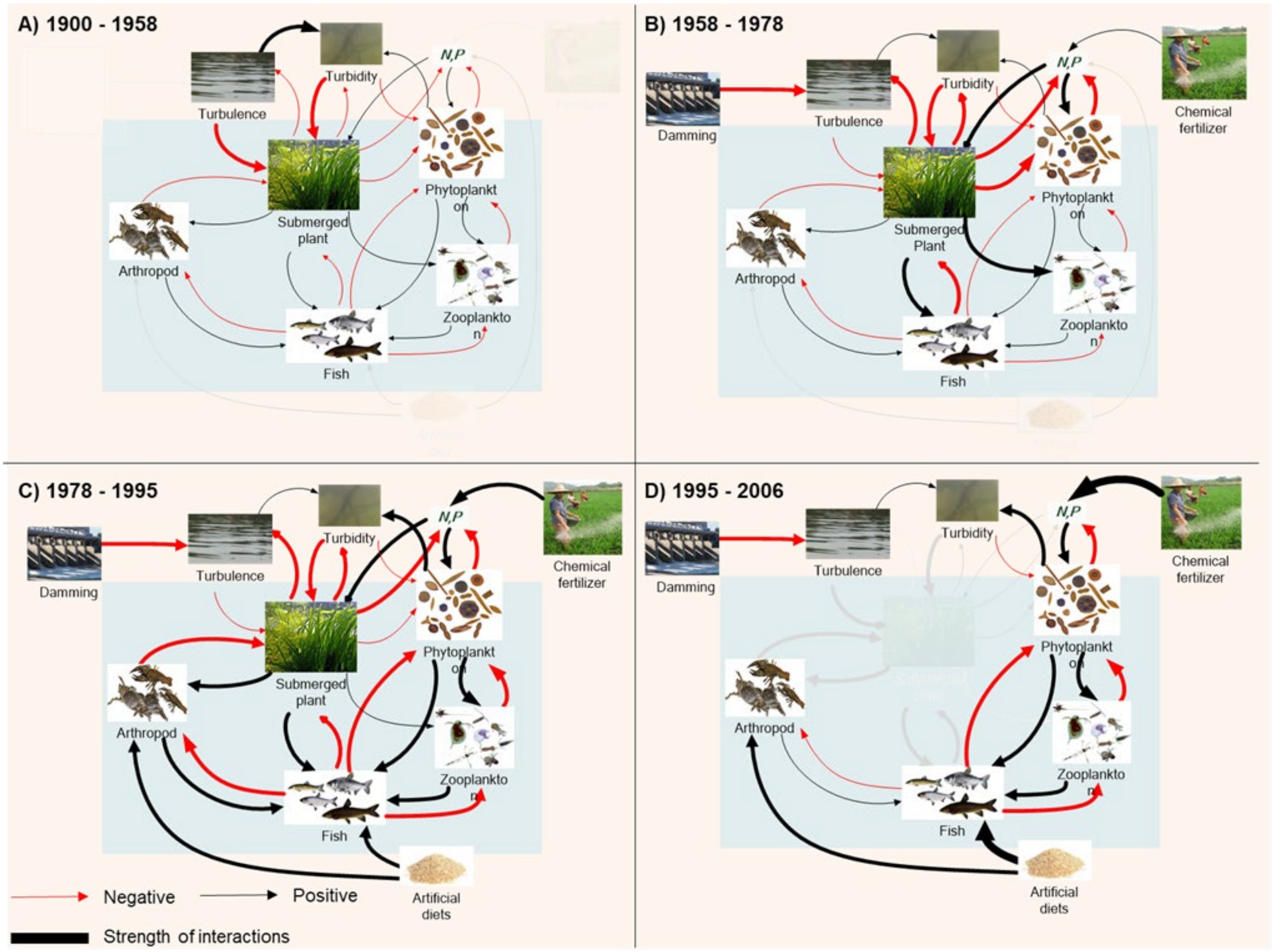

Figure 3-8: Putative development of feedback loops in the Taibai lake ecosystem from 1900 to 2006. The green colour represents a simple positive feedback loop of just two components and red colour represents a multi-component positive feedback loop.

The thickness of the lines represents the comparative strength of the connection. Figure 3-8A shows the lake in a natural state of connection to the river before hydrological control. Figure 3-8B shows large-scale changes in the environment and ecosystem due to hydrological engineering, which had strong positive effects on submerged plants and formed positive feedback circles. Figure 3-8C Shows how after 1978 massive quantities of grass carps, crabs and crayfishes were added to the lake. Artificial diets were also added as a supplement at this stage to increase productivity. Figure 3-8D shows the situation when planktivorous fish became dominant in simpler feedback loops after the disappearance of merged macrophyte. The arrows represent the direction of causation between two elements.

In the first period, from 1958 to 1978, a major change occurred due to hydrological engineering. Damming resulted in longer retention times, a less turbulent aquatic environment and less suspended sediment, helping to increase water transparency and creating ideal conditions for submerged macrophytes. These submerged macrophytes stabilised sediments and enhanced the transparency of the lake, helping plants to thrive, shaping an effective positive feedback loop (Jeppesen, 1998). This scenario concurs with the subfossil evidence of increasing dominance by epiphytic and benthic diatoms and biogeochemical records. In core TN2007, total organic carbon (TOC) increased after 1957, showing a boost in primary production, possibly caused by macrophytes and algae. In the aquaculture preparation period from 1978 to 1995 (Figure 3-8C), large numbers of grass carp and freshwater crabs were introduced to reduce the submerged macrophytes and make space for economic fish species. Grass carp readily consumed the submerged macrophytes, breaking the positive macrophyte-turbidity feedback loop. Phytoplankton became dominant at this point, driving a larger zooplankton community, while villagers added artificial food for grass carp. Another positive feedback loop was then activated, in which phytoplankton increased turbidity and turbidity then inhibited macrophyte growth, allowing the phytoplankton to expand in excessive numbers.

In the third period after 1995 (Figure 3-8D), macrophytes started to disappear under the influence of strong bio-manipulation (Jian, 2001). Against a background of rising nutrient loading, fish species and their numbers were being manipulated through the introduction of specific juvenile fish to rapidly growing number of planktivorous carp. The system appears to have stabilised with no major algal blooms despite increases in nutrient loading from agricultural runoff. The absence of algal blooms in water with a high TP concentration of around 100 mg/L may be due to the grazing of large numbers of planktivorous fish, as was found in other MLYB lakes (Liu & Xie, 1999). Amplified by internal feedback loops, it seems that Taibai Lake became an alternative clear-water state with rising nutrient concentrations and a low abundance of submerged macrophytes similar to Lake Krankesjön (Blindow et al., 1993). These potential feedback mechanisms are plausible and show that all parts of the lake ecosystem in Taibai interact closely in certain ways, forming networks that contain amplifying and stabilising feedback loops in a dynamic state. Influences from one external driver to another, from an external driver to a function group, and from a function group to another group are dependent on the strength of ecological pathways, which leads to cascading effects and changing diversity within the ecosystem structure.

Functional feedback with the potential to actively shape the ecological threshold of regime shifts are integrated into the causal loop diagram. There are self-damping effects within the populations, negative 2-link feedback loops in trophic networks, two sets of positive 3-link feedback loops (R1 and R2) and a positive 4-link feedback loop R3. The other positive 4-link loop between submerged macrophytes, zooplankton, phytoplankton and turbidity is not annotated because macrophytes reduce the negative effect of fish predation on zooplankton and the reliance of the process on predation makes this entire loop weaker than the others. R1 is nonetheless a self-reinforcing process between vegetation, turbulence and turbidity and has a single direction due to the relationship between turbulence and turbidity. R2 describes the basis of aquatic food webs between phytoplankton, zooplankton, and fish, where the combination should produce a negative equilibrium state. R3 circulates among four components, namely nutrients, submerged macrophytes, fish and phytoplankton, making a weak positive feedback loop. All the positive feedback loops in Taibai's ecosystem serve to amplify external disturbances, which are mainly linked to human activities during the last century.

I can also interpret the conceptual model to analyse dynamic changes over time. Pre-1950s, Taibai Lake is recorded as having strong connections to the Yangtze River, as demonstrated by the record of the median diameter of grain size at a markedly higher size. A natural wild fish community associated with the Yangtze River dominated the lake community (Table 3-1).

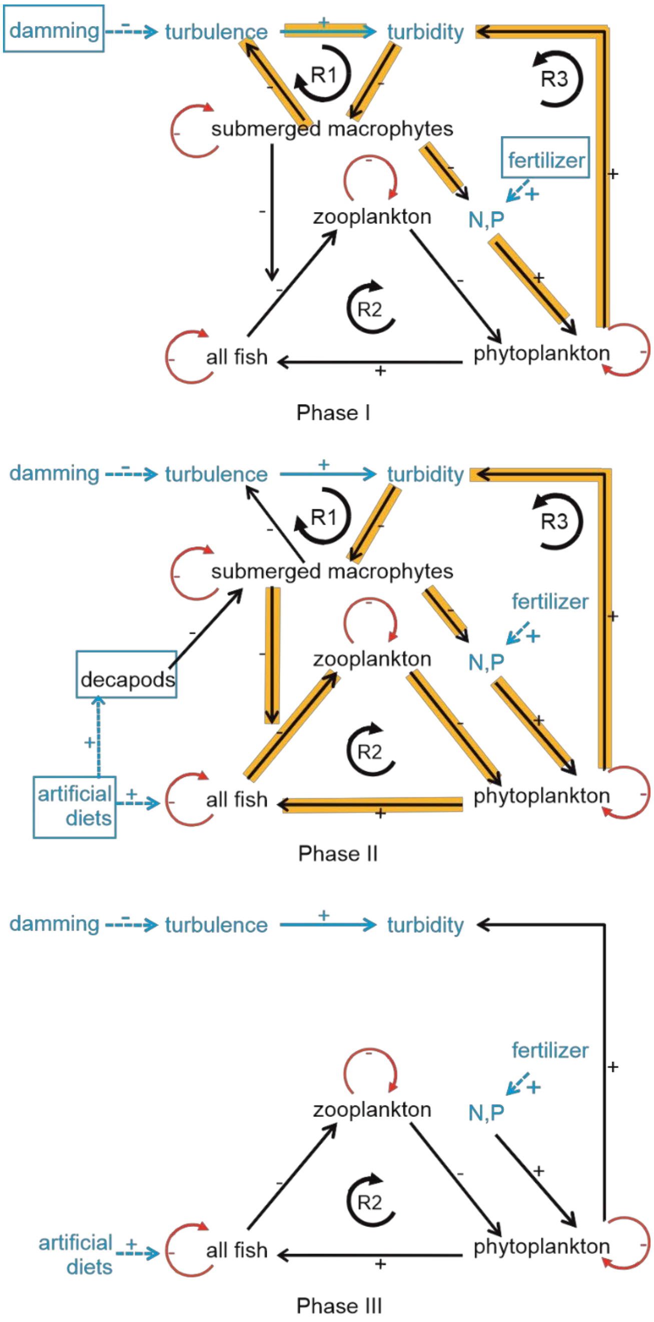

Figure 3-9: Diagrams of reconstructed dynamic changes in Taibai lake in recent decades. Straight arrows show positive ("+") and negative ("-") interactions. New interventions are shown in blue boxes, and yellow highlighted arrows indicate triggering forces that stimulate circular interactions. When one link drops out, the whole feedback loop is gone. In a closed loop, an odd number of negative interactions represents a negative or stabilizing feedback loop (red arrows); an even or zero number of negative interactions represents a positive or reinforcing loop ("R", black arrows).

Phase 1: An initial change occurred in approximately 1956 after damming significantly reduced turbulence. Nutrient runoff from increasing fertilizer usage became linked with the effect of reduced turbidity, leading led to an increase in R3. The increased nutrients benefitted the phytoplankton, while the reduced turbidity led to an increase in submerged macrophytes and a reduction in sediment nutrients. The reconstructed biogeochemical indicator of total organic carbon increased after 1956, showing a rise in biological production.

Phase 2: Additional external drivers such as decapod culture and artificial fish food modified the trophic networks through positive feedback. Herbivorous decapods and grass carp were introduced to reduce the number of submerged macrophytes, and this effect was reinforced through R1 and R3. Villagers added artificial food for carp and decapods, on the premise that the dietary demands of the fish exceeded the primary production of the lake (Table 3-1). Planktivorous fish were introduced, amplifying the initial changes in R2, boosting phytoplankton and reducing zooplankton, as the negative feedbacks constraining R2 were weakened through the dampening effect of fish and zooplankton. As a result, the decrease in zooplankton and increase in phytoplankton were reinforced. The decrease in submerged macrophytes and the increase phytoplankton reinforced each other in R2 and R3 to threaten the key components of the submerged macrophytes.

Phase 3: In the late 1990s, records show that submerged macrophytes had almost disappeared. The feedback links were gone and only R2 remained in terms of positive feedback in the key relationships. The overall reinforcing effect became weaker, but still destabilized the new equilibrium by increasing phytoplankton levels. With human aquaculture interventions, the three-link feedback loops between fish, zooplankton and phytoplankton probably continued as a weak positive loop.

3.4.3 Spatial variations in the lake

Heterogenous community compositions of diatoms were found when a second core was taken in the same area of Taibai Lake, triggering a reflection on spatial variability and ecological variation within the lake ecosystem.

In order to supplement the sediment record between 2007 to 2014, a core sample TBN2014 (Taibai North) was taken using a gravity corer at a depth of 2.5m in the northern centre of Taibai Lake in 2014 (29°59′40″N, 115°48′31″E). Using the World Geodetic System 1984(WGS84) as the reference coordinate system, the distance between core TN2007 and TBN2014 was calculated as roughly 150m. The TBN2014 core was sampled at 0.5 cm intervals along the whole 73.5 cm of its length for diatom analysis. The core was analysed in the State Key Laboratory of Lake Science and Environment at the Nanjing Institute of Geography and Limnology, Chinese Academy of Sciences. Both cores were dated using ^{210}Pb and ^{137}Cs radionuclide techniques with a High Purity Germanium (HPGe) Gamma Spectrometer, using the constant rate of supply (CRS) model (Appleby, 2008).

I conducted Canonical correlation analysis (CCA) to measure the association between the diatom abundances and environment variables from the modern surface water samples of 76 lakes within MLYB in 2008. The PC1 scores of diatom assemblages in the sediment cores were then superimposed on the CCA biplot of modern data to visualise the ecological trends along time. The implicit assumption is that the relationships between the diatoms and environmental variables should be similar in all lakes in the MLYB during the last century. Field measurements of lakes in MLYB were based on Secchi depth, pH, conductivity, dissolved silica (SiO_2), dissolved iron (TFe) and chlorophyll-a (Chl-a) using water quality measuring probes from the YSI company. Water samples were further analysed in the laboratory for chemical oxygen demand (COD), TP, TN, nitrites (NO2-N and NO3-N), ammonia (NH4-N) and contemporary diatom communities.

TN2007 and TBN2014 core sediments show similar characteristics in the radionuclide records of ^{210}Pb and ^{137}Cs (Figure 3-10).

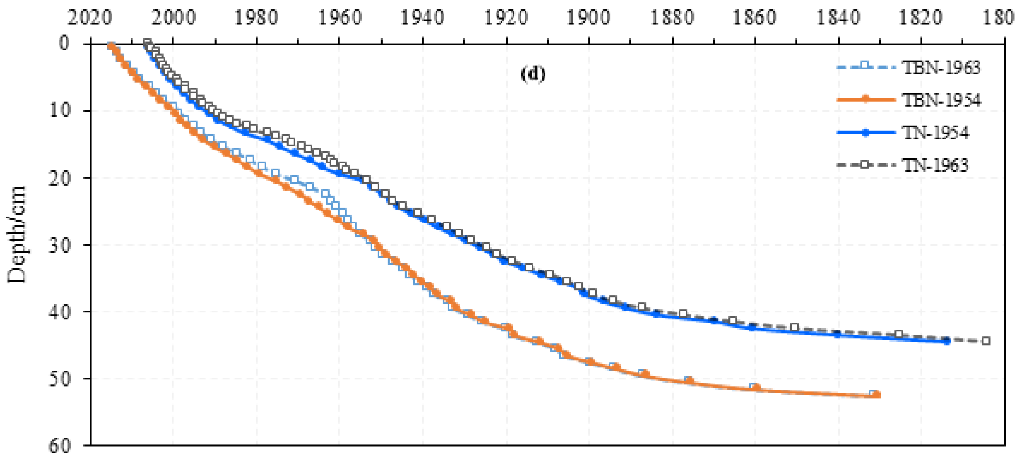

Figure 3-10: Chronology of ^{210}Pb adjusted composite models with alternative ^{137}Cs time markers in 1954 and 1963 in TBN2014 and TN2007 cores

Diatom taxa in TN2007 and 61 other taxa were identified in TBN2014. The diatom assemblages in the two cores had different compositions, with TN2007 more planktonic and TBN2014 more epiphytic (Figure 3-11). The two cores also showed different changes in composition. In TN2007, diatom assemblages changed across three periods: Firstly, from 1850 to 1956, planktonic *Aulacoseira granulata* and benthic *Gyrosigma acuminatum* were dominant; secondly, from 1956 to 1995, epiphytic and benthic species dominated and eutrophic planktonic species including *Aulacoseira alpigena* and *Cyclostephanos dubius* made their first appearances. Thirdly, the percentage of planktonic species characteristic of eutrophic habitats increased between 1995 and 2006. In contrast, TBN2014 reveals a local history of largely planktonic diatoms from 1942 to 1960, followed by a growing predominance of epiphytic and benthic species, including *Eunotia species*, *Gyrosigma acuminatum* and *Navicula* species up to 1991, after which point epiphytic diatoms gradually declined and planktonic diatoms dominated, while nearly 30% of benthic species were still present in the lake. The temporal changes in the diatom community composition from core TN2007 suggest at least two major changes, which first improved the conditions for epiphytic and benthic diatoms, before leading to a strong decline in numbers of epiphytic diatoms. The higher percentage of epiphytic diatoms present in the recent samples from core TN2007 compared to TBN2014 is probably due to growth of macrophytes in shallower water based on light-penetration advantages in TN2007. The results indicated spatial heterogeneity of biological communities in the northern centre of Lake Taibai, which should be a bathymetrically uniform area. This may result from small-scale variations in bottom profiles, aggregated benthic animals, or sediment transport by deep currents (Downing & Rath, 1988). Revisiting the question "How representative of the whole lake are fossil assemblages in a single sediment core?", the findings showed that sediment heterogeneity could be evident within a comparatively flat site even though it could be satisfactorily small in some cases (Heggen et al., 2012). This alerts us to the need for careful design of sediment sampling when ecosystem states and responses are to be studied.

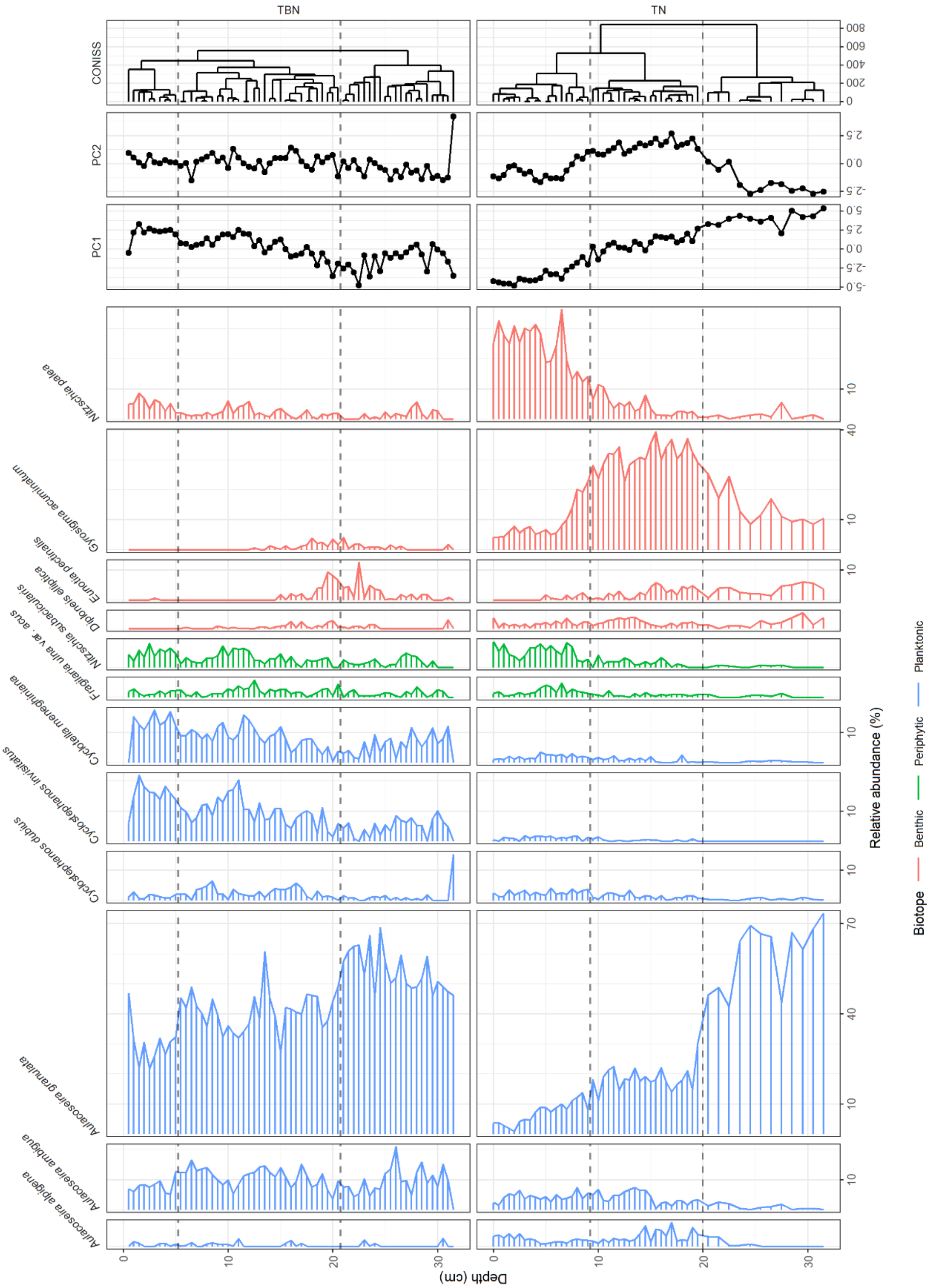

Figure 3-11: Relative abundances of diatom assemblages in TN and TBN cores, and their PC1, PC2 and cluster analysis divided into biotopes

In the results of the CCA and projecting samples in two cores, temporal trends are shown to correlate with available environmental factors (Figure 3-12). Crosses represent 76 investigated lakes in the MLYB and red vectors show the correlation between the constrained environmental variables and the lake diatom community. The directions of vectors show correlations between community composition changes and environmental variables. Environmental changes are positively correlated if they are in a similar direction, and negatively correlated if they are in the opposite direction. Vector length indicates the variable's strength of influence on diatom assemblage change in the training set. Very small levels of correlation have been deleted for convenience, and the remaining vectors help us to interpret temporal changes in the Taibai samples.

Orange diamonds represent the diatom assemblage of the TN2007 core between 1850 and 2007, and blue triangles show diatoms in the TBN2014 core between 1950 and 2014, with both distributed in constrained ordinations among explanatory variables. The grey numbers around the symbols show the dating of samples in TN2007 and TBN2014. The projecting samples are distributed in different areas and share the same general direction between 1970-2004, which correlates positively with TP and SD, showing a deterioration in the water quality. From 1850 to 1970, diatom samples in TN2007 change along CCA axis 2, showing a strong positive correlation with lake area, conductivity and depth. This means that despite the fact that the diatom communities in the two cores represent different microhabitats, both have responded in a similar manner to the main forcing mechanisms since 1950. The pre-1950 influence of the lake area is likely to represent changes in the effective catchment area as much as actual lake surface area, before the major dams were constructed. The analysis shows clear similarities in ecological trajectories in the two cores but indicates different causes for these trajectories. This confirms our conclusions about the time of the regime shift and the external forces in Taibai lake and shows the responding mechanisms underlying spatial patchiness within the lake’s ecosystem.

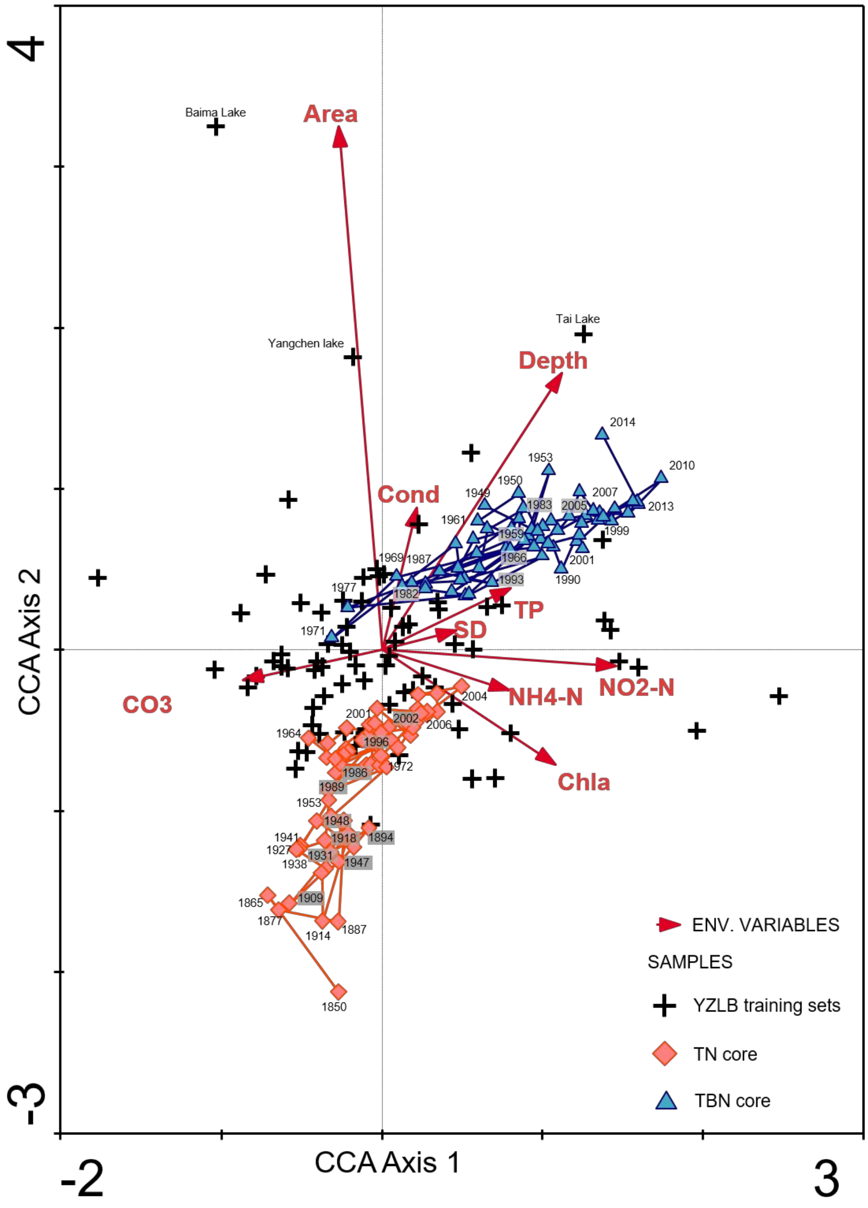

Figure 3-12: CCA analysis of diatom training set in MLYB lakes supplemented with TN2007 and TBN2014 core in time series

3.4.4 Policy implications

Regime shifts in many modern ecosystems are driven by human actions that tend to make them simpler and more homogenized, resulting in lower levels of biodiversity and environmental quality (Folke et al, 2004). Another tendency is the disturbance to negative feedback, allowing positive feedback to take control of the ecosystem. Understanding the role of human activity and how it affects regime shifts is therefore important to ecosystem management and studies. The work in Taibai achieves this goal from two aspects. Firstly, the new case studies add to the growing number of identified regime shifts in centralized databases such as the Regime Shift Database (Biggs et al, 2018; Folke et al, 2004), providing us with a wider knowledge base that can be viewed through the lens of theory to assist policymaking. In our study hydrological change, nutrient loading and aquacultural interference are factors that changed the structure of the ecosystem in Taibai Lake, leading to abrupt transition, and these results should also apply to similar cases in other MLYB lakes. Secondly, providing a historical perspective on local ecological regime shifts in this way focuses attention on the longer-term impacts of specific policies and trade-offs. In historical terms, Taibai Lake was an ecosystem that showed greater natural biodiversity and amenities than exist today. However, local society exploited the lake's functions to provide economic gain through small-scale hydroelectric power, fish farming and nutrient-rich river runoff (Xu et al, 2017). Future efforts to raise the natural capital of the lake will be challenging if these economic gains are to continue.

As an example of riverine shallow lakes in MLYB, Taibai demonstrates the problems of human actions on regional lake ecosystems and highlights the external forces that can push lake ecosystems across regime thresholds. As the Chinese government and local governments move forward with more environmentally aware policies to promote the protection of the Yangtze River and the lakes in its basin (Chen, 2020), the issue of how to restore the ecosystems with the experience and understanding I have learned from their deterioration remains.

Chapter 4: Building an ABM to simulate natural equilibria in MLYB lake ecosystems

4.1 Introduction

The palaeoecological reconstruction of the centennial lake succession histories and contemporary lake observations provide valuable indications of changes in the state of lake ecosystems and changes in aquatic communities under the influence of environmental change. By analysing the contribution made by the main drivers and changes in the feedback loops within the system, general empirical patterns of ecosystem change can be identified and applied in lake management and future scenario prediction (Dearing, 2013). Chapter 3 analysed the relationships between changes in the composition of the diatom community in the sediment cores of Lake Taibai over the past century as well as major environmental changes in the surrounding area, and concluded that the occurrence of a major regime shift is associated with hydrodynamic changes. However, the results of the statistical tests mainly reflected the observations and correlation between driving forces and system state indicators at the macroscopic phenomenological level but did not relate to our wider understanding of processes and structural changes underlying regime shifts and other critical shifts. Understanding the role of the driving forces, especially human disturbance, at the micro-scale in causing non-linear changes in ecosystem state is important in terms of improving ecosystem scenario reconstructions. For lake managers and surrounding residents, the ability to link abrupt changes in the ecosystem and recovery hysteresis to specific causative behaviours will improve the accuracy of system management strategies and save economic costs. In the case of Lake Taibai, I have hypothesised and constructed a theoretical model of the interactions between major functional groups and responses to external drivers based on ecosystem changes as well as environmental change. Can computer models also simulate nonlinear changes in an empirically studied lake ecosystem? To address this question and to understand the patterns that emerged in Taibai and surrounding MLYB lakes, this chapter focuses on model construction based on our existing knowledge and data relating to lake ecosystems and model behaviour analyses, while improving the general understanding of alternative stable states and changing ecosystem responses under pressure is discussed in the following chapter.

There is already a large number of models that simulate ecosystem succession by focusing on specific ecological and environmental problems. These include steady-state models, biogeochemical models, population dynamics models, individual-based models and structural dynamics models (Jørgensen & Fath, 2011). These models differ in their fundamental principles and in the degree to which they simplify real ecosystems. Janssen et al (2015) reviewed 42 operational aquatic ecosystem models and found that roughly 80% of them belonged to dynamic, process-based, biogeochemical, mass balance, partitioning and complex dynamic models. All of these modelling tools can be used to simulate time-varying system dynamics and environmentally driven scenario analyses, but are not all able to explain the formative mechanisms that underlie abrupt system changes and critical transitions. In ecosystem-related modelling, agent-based models (ABMs) have been found to successfully simulate across different scales (Cornell et al, 2019; Grimm, 1999). Not only can they simulate changes in population dynamics on a temporal scale, but they can also be used to provide an explanation of population phenomena from an individual ecological perspective.

ABMs are also known as individual-based models (IBMs), multi-agent modelling or multi-agent-based simulations (MAS). They are ‘bottom-up’ models that simulate a community or system of organisms functioning together through agents that represent individuals or groups of organisms that display specific characteristics and behavioural patterns (DeAngelis & Mooij, 2005). ABMs can simulate hypothetical scenarios based on reconstructed evidence. For example, the HOMINIDS ABM simulates the spatial patterns of early Pleistocene human migration based on empirical field data collected in East African habitats (Griffith et al, 2010). In palaeoecological terms, ABMs are a way of experimenting with theory and synthesising past environment-community interactions, and can therefore be used to help us move beyond simple pattern matching (Perry et al, 2016) by focusing on micro-level interactions between organisms and between organisms and their environment. ABMs can also identify spatial variation in ecosystems and can model the prevalent stochasticity of natural systems which can influence the structure of ecosystems and the outcome of non-linear responses. A major challenge in the study of complex systems is how to understand the way in which seemingly organised collective behaviour emerges from small-scale interactions between individuals (Levin, 1998; Rammel et al, 2007). Because the complex dynamics exhibited by system agents can be identified experimentally, ABMs that can simulate emergent phenomena from the bottom up are well suited to addressing our micro-scale understanding of ecosystem response mechanisms and developmental patterns (Railsback, 2001).

Based on the main feedback loops and individual ecology of the Lake Taibai ecosystem, I developed an ABM model to simulate the dynamics of lake ecosystem changes under pressure. This chapter describes the construction of that model, the model sensitivity analysis and driver impact analysis and the steady state experimental results in the system. From these results it is possible to observe the general process of constructing the ABM model, the behavioural characteristics of the model and the patterns of the lake ecosystem under undisturbed conditions. Simulations of eutrophication and de-eutrophication recovery scenarios for Lake Taibai under the influence of specific drivers will be presented in the next chapter.

4.2 The model

I constructed the ABM model based on the conceptual model of feedback loops inferred from palaeoecological data on ecosystem transitions in Lake Taibai by setting up simple predation or competition relationships, environment dispersal and individual life cycles (my model development process is summarised in Appendix A). The aim of the model was to address the broader understanding of the mechanisms through which eutrophication-induced critical transitions have occurred in MLYB lakes over the past century. Among all the available platforms, NetLogo is by far the most dominant platform to develop ABM in ecology, social sciences and archaeology because it is free, performs well and has rich open sources in its user communities (Abar et al, 2017). The Netlogo environment offers a user-friendly interface for coding and BehaviourSpace function for sensitivity tests and has a combined System Dynamic

Model in its official library to facilitate the efficient construction of a system model. For this study, it provides me with rich accessible examples of codes covering various questions on its official library[1] as well as model databases such as the CoMSES network[2] to learn from. This is why the Netlogo programming environment was selected from many development tools like Swarm, RePast, AnyLogic.

The lake ecosystem model was written from scratch in Netlogo language and designed with the purpose of modelling regime shifts in a MLYB lake as presented in Chapter 3, using algorithms based on well-established open-source models (Appendix B). This section describes how I developed the ABM model, which was named LAKEOBS_MIX and aimed to improve our understanding of nonlinear changes in lake ecosystems using the NetLogo (version 6.2.0) programming environment.

4.2.1 Overview

4.2.1.1 Purpose

The ABM model was constructed primarily to integrate existing ecological observations and changes from longer term palaeoecological reconstructions to increase our understanding of the ecological mechanisms underlying the occurrence of abrupt changes in lake ecosystems, particularly those that appear in the form of critical transitions. Under conditions of known lake ecosystem characteristics and external drivers, the aim was to model the mechanisms of

---

[1] http://ccl.northwestern.edu/netlogo/models/community/index.cgi

[2] (https://www.comses.net/codebases/)

formation, hysteresis and recovery before and after the occurrence of critical transitions in the lake's ecosystem. As mentioned above in the section 4.1, the lack of realistic ecosystem models hinders the application of ecological theories in empirical data. This model was thus motivated to mitigate the shortage and designed as a spatially explicit model. Based on individual ecology theories and feedback mechanisms, I used the emergent power of ABM to demonstrate the role that changes in biological functional groups take in the formation of critical transitions and to test the performance of multiple recovery pathways to inform the management of eutrophic water bodies in which ecological transitions have already occurred.

4.2.1.2 Entities, state variables and scales

Each agent is a basic unit of an ABM, and can be a physical or virtual entity that acts, perceives its environment, communicates with others and possesses the necessary skills to achieve its goals (Ferber, 1999). A patch is a specific agent in the *NetLogo* environment that is often used to represent the spatial environment. Computational ABMs are generally based on agents and their interactions and the ways in which they simulate system patterns at a higher scale, with possible emergent behaviour (Li et al, 2010). In this model, the architecture comprised a grid of 31 × 31 (961) patches, each representing 1m, totalling 9.61 km^2 of lake area. The model was wrapped both horizontally and vertically so that agents can enter through the left side and appear at the right side, resembling the Mercator Projection (cylindrical projection) that is applied in the common world map. Each grid cell had attributes of 'water?' and 'refuge?' to determine its specific usage. Shades of patch colour indicated the state of lake eutrophication as defined by the concentration of nutrients in water.

In the survey of lakes in the MLYB (Nanjing Institute of Geographical and Limnological science CAS, 2019), dominant functional groups in ecosystems consisted of phytoplankton, zooplankton, zoobenthos, macrophytes, planktivorous fish and herbivorous and piscivorous fish. Most of these groups live in the pelagic zone of lakes and contributed to major lake functions including water quality and fishery resources. Most debates over the factors that regulate trophic interactions in lakes have focused on the freshwater pelagic zone, even though many planktivorous fish are also benthivores that rely to a large extent on benthic food sources (Jeppesen et al, 2003). This is partly because pelagic food webs and their effect on nutrient dynamics is comparatively straightforward, and most nutrients contained in the food are soon returned to the water through excretion after being taken up by phytoplankton (Scheffer, 1998). Six dominant functional groups in pelagic ecosystems were modelled as agents, namely phytoplankton, zooplankton, submerged macrophytes, planktivorous fish, herbivorous fish and piscivores (Figure 4-1). Agents were represented as super-individuals of the above groups for the convenience of modelling large populations (Scheffer et al, 1995).

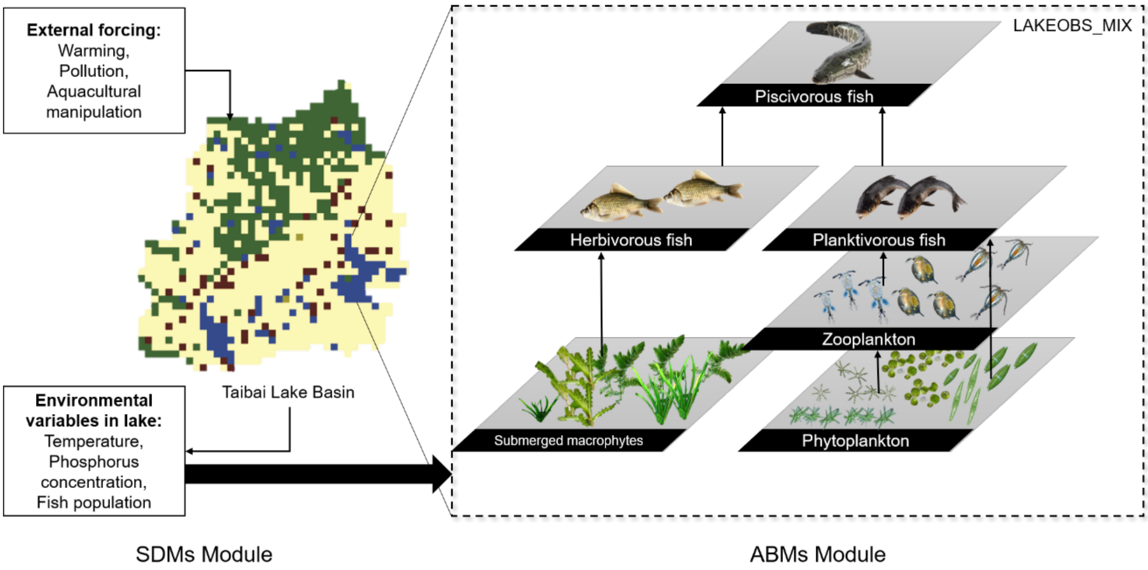

Figure 4-1: Conceptual diagram of the components and interactions in the LAKEOBS_MIX integrated model

All biotic communities live on and interact with the areas closest to them in terms of spatial distance. Each community lives with routines based on rules and the goal of survival. Primary producers, such as phytoplankton and submerged macrophytes, can live alone in suitable conditions, while consumers live with (one of) their prey. Each agent has attributes relating to identity number, colour, heading, position, breed, energy, biomass, age and survival energy. Phytoplankton and submerged macrophytes have extra variables of light-attenuation and growth rate, which are known to facilitate the photosynthesis process. The modulation process for environmental change was implemented with the aid of Netlogo System Dynamics Model (SDM) tool, which reads the driving force of patterns of change and their parameters from the 'Drivers scenarios' section of the ABM. After judgement and calculation, the SDM produces new environmental variables influenced by external drivers that are immediately fed into the Ecosystem ABM module.

The main elements and interactions were modified from the feedback loop diagram in the previous section 3.5.2. The relationships between the communities and drivers in the model can be drawn in the schematic form as follows. Competition and prey-predation relationship are the main interactions influencing the abundance and presence of communities while external drivers push around the biome.

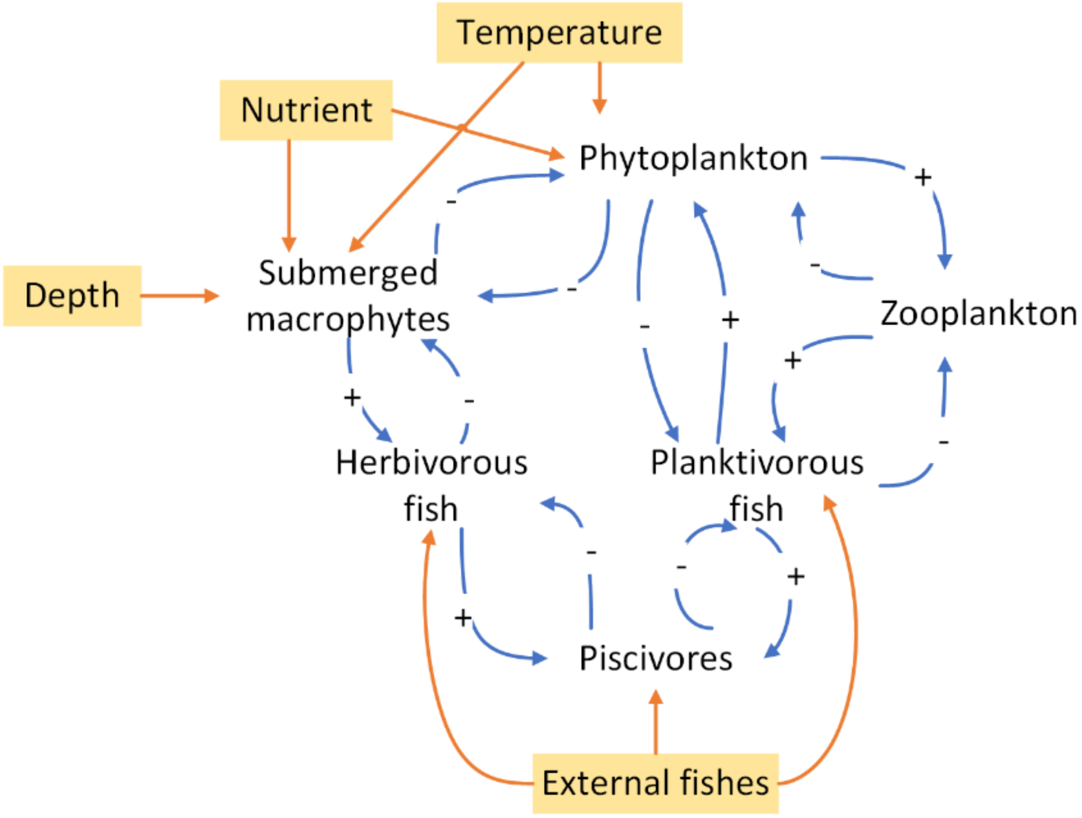

Figure 4-2: A schematic diagram of feedback loops and drivers in the model. The yellow rectangles highlight external drivers which affect the biotic communities in orange arrows. Blue arrows show general positive or negative interactions in the biome with the signal "+" or "-" respectively.

4.2.1.3 State variables and parameters

State variables consist of environmental, agent-level and aggregation-level variables. Most environmental variables are assigned as 'global' variables, which means the diffusion between patches is zero in terms of time lag and the physical environment is overall homogenous. Individual variables describe the states of each individual aspect, while the aggregation variables show higher aggregation-level performance by individuals, including population, biomass and reproduction. Environmental and aggregation-level variables are listed in Table 4-1 and agent-level variables are presented in the 'Submodel' section.

Table 4-1: State variables on aggregation level in LAKEOBS_MIX

Code	**Abbr.**	**Description**	**Unit**
tick	t	time step in model	D
water-temperature	T_w	average temperature of lake water	℃
water-depth	D	average depth of lake water	M
max-pxcor	W	lake width	100m
max-pycor	H	lake height	100m
phytoplankton-amount	N_{phyp}	phytoplankton population	ind.
submerged-macrophyte-amount	N_{sm}	Submerged macrophyte population	ind.
zooplankton-amount	N_z	zooplankton population	ind.
planktivore-fish-amount	N_{pf}	planktivorous fish population	ind.
herbivore-fish-amount	N_{hf}	herbivorous fish population	ind.
Piscivore-amount	N_{pisc}	piscivores population	ind.
phytoplankton-concentration	C_{phyp}	phytoplankton biomass, measured as organism mass in volume	mg/m^3
zooplankton-concentration	C_Z	zooplankton biomass, measured as organism mass in volume	mg/m^3
sm-concentration	C_{sm}	submerged macrophyte biomass, measured as organism mass in volume	mg/m^3
fish-concentration	C_{fish}	all fish biomass, measured as organism mass in volume	mg/m^3
pf-concentration	C_{pf}	planktivorous fish biomass, measured as organism mass in volume	mg/m^3
hf-concentration	C_{hf}	herbivorous fish biomass, measured as organism mass in volume	mg/m^4

pisci-concentration	C_{pisci}	piscivore biomass, measured as organism mass in volume	mg/m^5
total-nutrient-concentration	NC_{tot}	total concentration of nutrient in the system	µg/L
global-free-nutrient-concentration	NC_{free}	concentration of nutrient available in water	µg/L
phytoplankton-being-eaten	NBE_{phyp}	Sum of phytoplankton being grazed	ind.
zooplankton-being-eaten	NBE_{z}	Sum of zooplankton being eaten	ind.
macrophyte-being-eaten	NBE_{sm}	Sum of macrophyte agents being eaten	ind.
planktivore-being-eaten	NBE_{pf}	Sum of planktivorous fish being predated	ind.
herbivore-being-eaten	NBE_{hf}	Sum of herbivorous fish being predated	ind.
piscivore-being-eaten	NBE_{piscl}	Sum of piscivorous fish being predated	ind.
this-tick-being-eaten	NBE	Sum of agents being eaten	ind.
phytoplankton-natural-die	ND_{phyp}	Sum of phytoplankton out of energy	ind.
zooplankton-natural-die	ND_{z}	Sum of zooplankton out of energy	ind.
macrophyte-natural-die	ND_{sm}	Sum of macrophyte out of energy	ind.
planktivore-natural-die	ND_{pf}	Sum of planktivorous fish out of energy	ind.
herbivore-natural-die	ND_{hf}	Sum of herbivorous fish out of energy	ind.
piscivore-natural-die	ND_{piscl}	Sum of piscivores out of energy	ind.
this-tick-natural-die	ND	Sum of agents dying out of energy	ind.
this-tick-reproduction	RP	Sum of new-born agents	ind.

In the model, major parameters are listed in Table 4-2. Some parameter values refer to value ranges in the investigation report of lakes in the Eastern region of China, including MLYB lakes (Ministry of Ecology and Environment of PRC, 2020). The 2019 mean water temperature in Taibai Lake was 15.47℃ in March and 31.31℃ in July. Mean Total Phosphorous (TP) was 69 µg/L in spring and 228 µg/L in summer (Nanjing Institute of Geographical and Limnological science CAS, 2019). The mean depth of Taibai was 3.16 m and the lake area where the depth was greater than 3.4m was roughly 11 km^2.

To facilitate model verification and experimentation, the shortcut “system-composition” was designed to determine the initial composition of biological communities in the model, which is basically a character selector. The selection includes “OFF“, “only algae“, “only macrophyte”, “algae + zoopk”, “algae + zoopk + planktivores”, “algae + zoopk + planktivores + piscivores”, “algae + macrophytes “, “algae + zoopk + macrophytes”, “macrophytes + herbivores”, “algae + macrophytes + herbivores”, “algae + macrophytes + zoopk + planktivores”, “algae + macrophytes + zoopk + planktivores + herbivores”, “algae + macrophytes + zoopk + planktivores + piscivores”, and “algae + macrophytes + zoopk + planktivores + herbivores + piscivores”.

Table 4-2: Main functional parameters, abbreviations, descriptions and units in the model

Code	**Abbrev.**	**Description**	**Unit**
system-composition	SYSC	functional groups that exist in system	chr[3]
ini-water-temperature	T_{ini}	the initial lake water temperature	℃
ini-water-depth	D	the initial water depth	m
Initial-nutrient	NC_{ini}	the initial nutrient concentration	µg/L
photoperiod	PP	portion of daytime	d^{-1}
phytoplankton-start-amount	$N_{p,0}$	the initial number of phytoplankton	ind.
macrophyte-start-amount	$N_{sm,0}$	the initial number of macrophyte	ind.
zooplankton-start-amount	$N_{z,0}$	the initial number of zooplankton	ind.
planktivore-fish-start-amount	$N_{pf,0}$	the initial number of planktivorous fish	ind.
herbivore-fish-start-amount	$N_{hf,0}$	the initial number of herbivorous fish	ind.
piscivore-start-amount	$N_{pis,0}$	the initial number of piscivores	ind.
zoopk-hunt-rate	HR_z	possibility of zooplankton eating algae	%

---

[3] ‘chr’ is an abbreviation of characters, ‘num’ of numbers and ‘ind.’ of individuals in the expressions of units

pf-hunt-rate	HR_{pf}	possibility of planktivorous fish eating food	%
hf-hunt-rate	HR_{hf}	possibility of herbivorous fish eating macrophytes	%
pisci-hunt-rate	HR_{pisci}	possibility of piscivores eating other fish	%
phytoplankton-reproduce-rate	RR_{p}	possibility of phytoplankton reproducing when energy is sufficient	%
macrophyte-reproduce-rate	RR_{sm}	possibility of macrophyte reproducing when energy is sufficient	%
zooplankton-reproduce-rate	RR_{z}	possibility of zooplankton reproducing when energy is sufficient	%
planktivore-reproduce-rate	RR_{pf}	possibility of planktivores reproducing when energy is sufficient	%
herbivore-reproduce-rate	RR_{hf}	possibility of herbivores reproducing when energy is sufficient	%
piscivore-reproduce-rate	RR_{pis}	possibility of piscivores reproducing when energy is sufficient	%
zooplankton-reproduce-energy	Er_{z}	threshold energy of zooplankton being matured to reproduce	J
planktivore-reproduce-energy	Er_{pf}	threshold energy of planktivorous fish being matured to reproduce	J
herbivore-reproduce-energy	Er_{hf}	threshold energy of herbivorous fish being matured to reproduce	J
piscivore-reproduce-energy	Er_{pis}	threshold energy of piscivores being matured to reproduce	J
nutrient-concentration-in-phytoplankton	NC_{phyp}	hypothetical proportion of nutrients absorbed by phytoplankton in weight	g/g
nutrient-concentration-in-zooplankton	NC_{z}	hypothetical proportion of nutrients absorbed by zooplankton	g/g
nutrient-concentration-in-sm	NC_{sm}	hypothetical proportion of nutrients absorbed by submerged macrophytes	g/g
nutrient-concentration-in-fish	NC_{f}	hypothetical proportion of nutrients absorbed by fish	g/g

Besides the main body of the model, there is also a set of environmental parameters that influence the changing variables and patterns of the external conditions of the ecosystem in the following table.

Table 4-3: Parameters defining external forces, including units and value ranges

Parameter	**Unit**	**Range**
driving-scenario	chr	[“Equ”,”Manual”,”TBNutADD”,”TBNutADD_TempADD”,”TBComprehens”]
drivers-pattern	chr	[“OFF”,”temperature”,”depth”,”nutrient loading”,”nutrient loading + temperature “,”reclamation”,”refuge-on”,”Adding herbivores”,”Adding planktivores”,”adding piscivores”,”nutrient loading + reclamation + depth + temperature”,”nutrient loading + reclamation + depth + temperature + planktivores”]
temperature-variation-rate	% per year	[-50,50]
depth-variation-rate	% per year	[-50,50]
reclamation-length	% (max-pxcor)	[0,100]
reclamation-width	% (max-pycor)	[0,100]
refuge-length	% (max-pxcor)	[0,100]
refuge-width	% (max-pycor)	[0,100]
nutrient-variation-rate	% per interval	[-50,50]
nutri-adding-interval	num	(input numerical)
herbivore-adding	Ind. per interval	[0,100]
hf-adding-interval	Ind. per interval	[0,100]
planktivore-adding	Ind. per interval	[0,100]
pf-adding-interval	num	(input)
piscivores-adding	num	(input)
pisci-adding-interval	num	(input)

To observe the changing environment as a result of the system dynamic model (SDM) module in ABM, a list of variables was set up.

Table 4-4: Environmental variables directly modified by parameters of external forces, with units

Variable	**Unit**
water-area	hectare
water-depth	m
water-temperature	℃
reclamation area	m^2
refuge area	m^2
herbivoresADD	ind./day
planktivoresADD	ind./day
piscivoresADD	ind./day

4.2.1.4 Process overview and scheduling

The main process sequences in this model are initialisation, individual life cycles, environmental change and cycles of individual birth and death with the degree of environmental change. The initialisation process includes the initialisation of the environmental conditions as well as the initialisation of the biota and some data cleaning and data logging algorithms to prepare for multiple model runs. In coding order, initialisation runs sequentially through the functions of initialising parameters, setting drivers, creating functional groups, linking the system dynamics model and preparing to record exported data. Each function is synthesised according to a series of instructions that complete the determination of input parameters and the assignment of values to individual variables. The initialisation process can be completed by clicking the 'setup' button on the Netlogo interactive interface. The initialisation process is followed by the main loop, which consists of updating all of the environmental variables within the system, receiving input on environmental changes, biome life cycles, and data logging. The main loop process can be executed by clicking the 'go' button on the Netlogo interactive interface. In the default mode the programme will automatically cycle through the process, with each cycle marked as a logging time. The environmental change input function is performed by both the ABM and the SDM, which means that the parameters are entered into the SDM from the ABM interface, processed by the SDM and returned to the ABM to update the variable assignments from the last cycle. The biome life cycle is the core aspect of the model and consists of six groups of biomes that are arranged to execute instructions. Finally, the values of all variables at the end of the cycle are recorded and derived, after which the variable ‘age’ is added to all individuals by one day. When the model is composed of all six components and the initial condition is parameterised as the nominal clear state (details in appendix D), 1000 ticks in a model run took 254 seconds, which is equal to 4 minutes 14 seconds. The running time could increase. The specific algorithms for each procedure are described in the submodels section.

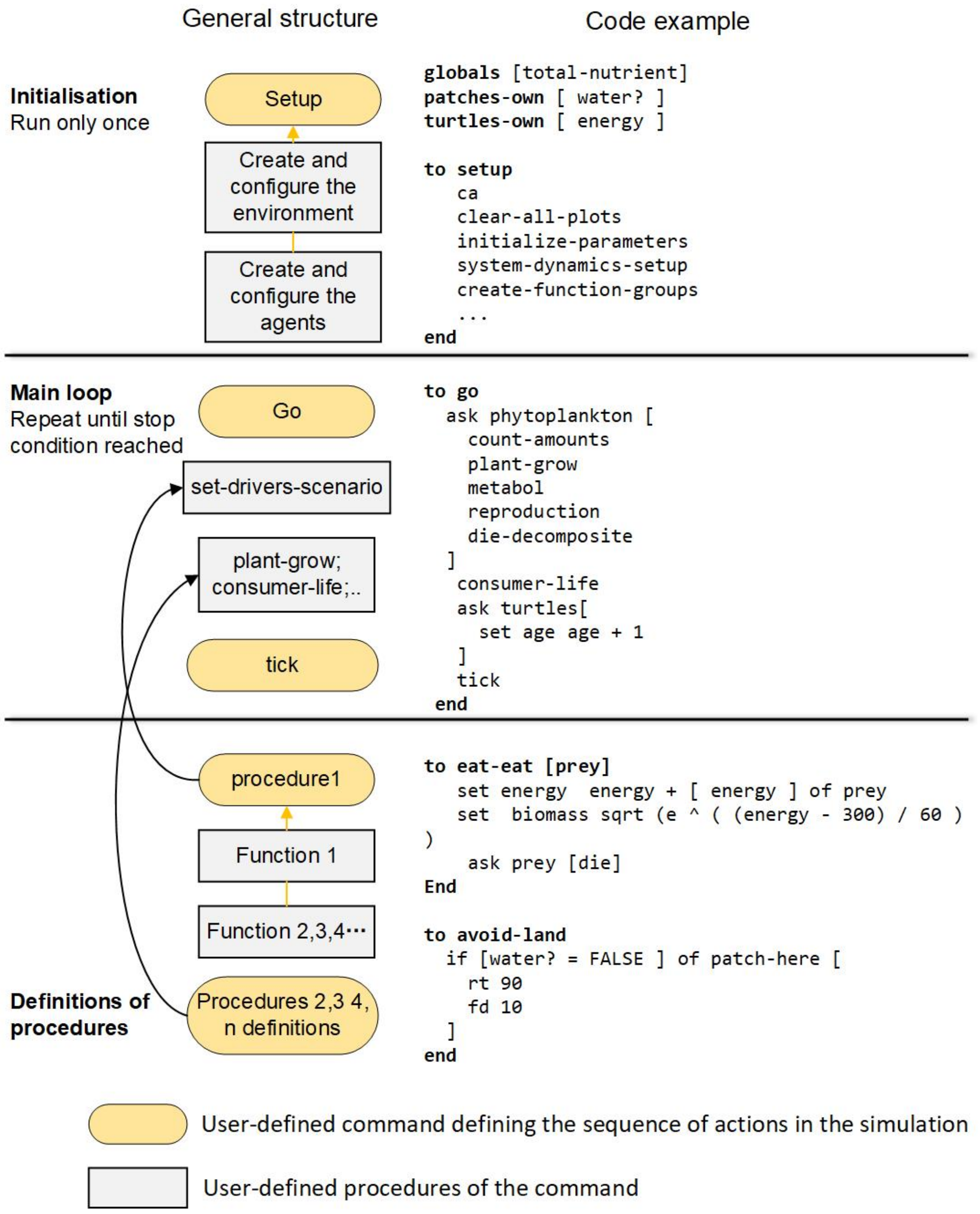

```
globals [total-nutrient]
patches-own [ water? ]
turtles-own [ energy ]

to setup
   ca
   clear-all-plots
   initialize-parameters
   system-dynamics-setup
   create-function-groups
   ...
end
```

```
to go
  ask phytoplankton [
    count-amounts
    plant-grow
    metabol
    reproduction
    die-decomposite
  ]
   consumer-life
   ask turtles[
     set age age + 1
   ]
   tick
 end
```

```
to eat-eat [prey]
   set energy  energy + [ energy ] of prey
   set  biomass sqrt (e ^ ( (energy - 300) / 60 )
)
    ask prey [die]
End

to avoid-land
  if [water? = FALSE ] of patch-here [
    rt 90
    fd 10
  ]
end
```

Figure 4-3: Conceptual diagram of the general structure and code examples in compartments of initialisation, main loops and functions in the model. A typical Netlogo model starts the overall initialisation with the command "Setup" and repeats rules with the continuously executed command "Go". The main execution commands consist of many small procedures nested within the main execution procedures like "Setup" and "Go". In the code example, the main procedure "Go" includes a procedure "consumer-life" for defining life cycles of animals, which is further composed of detailed behaviours like "eat prey" and "keep swimming in water".

4.2.2 Design concepts

4.2.2.1 Basic principles

As the aim of the model is to observe ecosystems as they undergo abrupt changes and critical transitions, it was designed with the expectation that it could be used to help develop a state of system equilibrium, as well as emergent population behaviour driven by external forces. The model is based on individual biology like photosynthesis and metabolism processes (details in the following section 4.2.4.2 to 4.2.4.4), but it can also be used to calculate the behaviour of natural systems under conditions of uncertainty. The design principles of the ecosystem are therefore as simple and basic as possible. The model has five primary assumptions: Firstly, that total nutrient quality is conserved within individual organisms and within the water column in the absence of external disturbances in the ABM simulation; secondly, that energy and matter are conserved within living individuals and are imported via sunlight and food; thirdly that increasing nutrient concentrations within the appropriate range can promote photosynthetic rates in producers; fourthly that predators search for the nearest food on a spatial basis, and fifthly that the modelled lake is characterised as a well-mixed and shallow lake with an average lake depth between 1 to 4 meters, resembling most MLYB lakes.

Once the assumptions of the model have been established, individuals are given basic rules about the life cycle that are mainly derived from simplified biological experience and knowledge. After referring to individual levels of ecological knowledge, multiple ecological models and homeostatic models, I established rules of biological under four main categories: nutrient cycling, photosynthesis, metabolism and mass-energy conversion.

Nutrient cycling

As long as there is no external disturbance, the total nutrient concentration is fixed and exists either as an inorganic form in water or as an organic form incorporated in the agents. Parameters that define the ability of agents to absorb nutrients are listed as "*nutrient-concentration-in-phytoplankton*", "*nutrient-concentration-in-zooplankton*", "*nutrient-concentration-in-fish*" and "*nutrient-concentration-in-sm*". The observation variables are *total-nutrient* ($\mathrm{NC_{tot}}$), *initial-nutrient* and *global-free-nutrient* ($\mathrm{NC_{free}}$), which are related to each other as shown in the following Equation 4-1 and Figure 4-4.

$$\begin{aligned}\mathrm{NC_{free}} = \mathrm{NC_{tot}} - \mathrm{C_{phyp}} \times \mathrm{NC_p} - \mathrm{C_z} \times \mathrm{NC}_z - \mathrm{C_{sm}} \times \mathrm{NC_{sm}} \\ - \mathrm{C_{fish}} \times \mathrm{NC_{fish}}\end{aligned}$$

Equation 4-1

where $\mathrm{NC_{p,}}$ $\mathrm{NC}_{z,}$ $\mathrm{NC_{sm,}}$ and $\mathrm{NC_{fish}}$ are nutrient concentration in organisms, and the units are dimensionless.

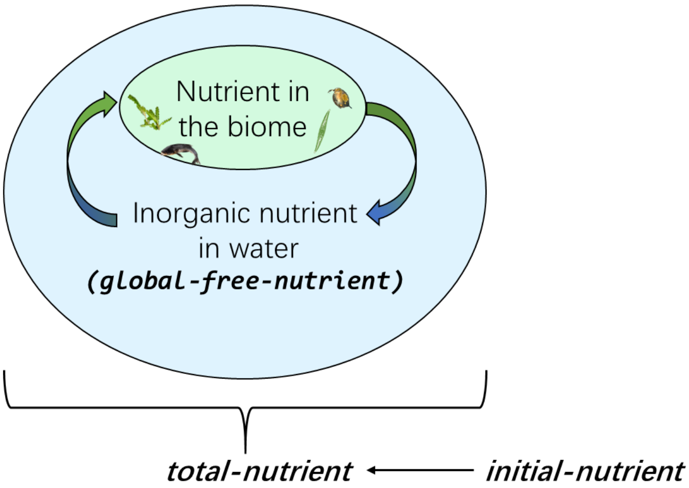

Figure 4-4: A simplified diagram showing nutrient cycling and related model variables

Figure 4-4 shows in simplified form the nutrient cycles between the biotic bodies of organisms in the ecosystem and water. The green ovals represent the nutrients in the organisms, which can used for storing energy and participating in vital chemosynthesis. Each functional group of organisms has a distinct and fixed nutrient occupancy (C), so the nutrient content of an individual's body is proportional to its own biomass. In the absence of any external inputs, the total nutrient content of the system is fixed, so that any unabsorbed nutrients left in the water are considered to be inorganic nutrients for use ($\mathrm{NC}_{\mathrm{free}}$), represented in the light blue area in the diagram. The nutrients in these two areas change dynamically as organisms grow, reproduce and die, but the total amount remains constant. The total nutrient content only increases or decreases when there is a nutrient load or reduction in the surrounding environment.

Photosynthesis and plant growth

Growth rates of an agent for phytoplankton and submerged macrophytes are influenced by local light attenuation (*I*), global temperature variations (*T*) and available nutrient concentration (*N*).

$$growth\_rate = f(T) * f(I) * f(N) \qquad \text{equation 4-2}$$

The dependence of algal growth on temperature applies the Arrhenius function, which can be used to describe the maximal growth rate as a function of temperature (Goldman & Carpenter, 1974).

$$f(T) = Ae^{-\frac{E_a}{RT}} \qquad \text{equation 4-3}$$

In equation 4-3, A is the pre-exponential factor, E_a is the activation energy for the reaction, T is the absolute temperature of the lake water (in Kelvin scale,$°K$) and R, which is the universal gas constant, takes 8.31 J/mol·K. The parameters A and E_a were determined by the empirical data of growth rates of freshwater algae (Dauta et al, 1990). As a result, an empirical set of parameters for the maximum growth rate of plants can be described as:

$$\boldsymbol{f(T) = 5.35 \times 10^9 \times e^{-6473\,/\,(T\,+\,273.15)}} \qquad \text{equation 4-4}$$

When plants overcrowd each other they form self-shading, and the epiphytic community may to a large extent also shade submerged macrophytes (Sand-Jensen & Søndergaard, 1981). In the model without epiphytes, the sum of phytoplankton and vegetation biomass describes the rough distribution and adjusts the light attenuation available to the growing agent.

$$f(I) = lightAttenuation = \ e^{-(\sum B_{phy_3} + \sum B_{sm_3})} \qquad \text{equation 4-5}$$

where $\sum B_{phy_3}$ represents the sum of the biomass of the phytoplankton within a radius of 3 m from this agent, and $\sum B_{sm_3}$ refers to the sum of the biomass of the submerged macrophytes biomass within radius of 300 m.

The effect of nutrient limitation on the growth rate of algae and plants is described according to the Monod model (Goldman & Carpenter, 1974). The general Monod function, or the Michaelis-Menten equation (equation 4-6), simulates the growth rate of microbes that are dependent on limiting factors.

$$\frac{1}{X}\frac{dX}{dt} = \mu = \mu_{max}\frac{S}{K_S + S} \qquad \text{equation 4-6}$$

where S is the activator, K_S is the activation coefficient, and μ_{max} is the maximal production rate. In the LAKEOBS_MIX model, global-free-nutrient $\mathrm{NC_{free}}$ shows the availability of limited nutrients in the water, and K_S takes 60.

$$f(N) = 6 * \ \mathrm{NC_{free}}/(\mathrm{NC_{free}} + 60) \qquad \text{equation 4-7}$$

To prevent any overflow of growth rate, a max-growth-rate $1 \times f(N)$ is set for individuals under optimal conditions.

Maintenance and survival

Individual energy for maintenance is roughly equal to the BMR (Basic Metabolism Rate), and can be approximated as

$$BMR = B_0 M^{\alpha} e^{-E/kT} \qquad \text{equation 4-8}$$

where B_0 is a constant, $M$is body mass, α is a scaling coefficient of around 3/4, E is activation energy in eV of around 0.65 (Sibly et al, 2013), T is body temperature in Kelvins scale and k is Boltzmann's Constant (der Vaart et al, 2016). For modelling purposes, the body temperature of agents was not considered as having any effect, so the logarithm of equation 4-8 to the base of the mathematical constant e is

$$\ln(BMR) = \ln(B_0) + \alpha \ln(M) - E/kT \qquad \text{equation 4-9}$$

As the term $\ln(B_0) - E/kT$ is seen as a constant here, I use a instead to simplify the equation

$$BMR = e^{a} \times M^{\alpha} \qquad \text{equation 4-10}$$

The BMR in the model is calculated in exponential terms, where α is an individual variable that changes between function groups. The range of α is set at around the empirical value of 0.75, and body mass takes in an empirical range of between 0.1 to 100 g.

Grazing and predation

For consumers, eating food energy. In the run of consumer life cycles, each zooplankton agent first searches for a phytoplankton agent on the same square of one hectare ($100\text{m} \times 100\text{m}$), and grazes all phytoplankton in this area if the random result of 'rolling dice' between 1 to 100 is smaller than the $zoopk - hunt - rate$. The way zooplankton eats food uses the *graze-eat* function:

$$\Delta energy_{food} = \sum energy_{prey} \qquad \text{equation 4-11}$$

Herbivorous fish and piscivores eat one prey at a time, using the *fish-eat-eat* function:

$$\Delta energy_{food} = \frac{energy_{prey}}{2} \qquad \text{equation 4-12}$$

Predating strategies and moving speed allows predatory fish, namely piscivores, to search for fish prey in a 16-hectare range and to move faster to catch other animals. The energy intake by predation is half the energy of prey as the assimilation rate of predation is lower. For planktivorous fish, each agent can eat two phytoplankton agents and one zooplankton agent in the surrounding hectare.

$$\Delta energy_{food} = energy_{prey} \qquad \text{equation 4-13}$$

The parameters in grazing and predation indicate the consumers' ability to take in energy and survive. If the energy input from food exceeds the requirements of maintenance and reproduction, then any excess is stored in the animal's energy reserves without the cost of storing for modelling purposes. Surplus energy from food has no appetite limit, f but is constrained by the parameters of food-intake probability.

Energy reserve

Energy reserves are stored as carbohydrates and fat in the tissues of plants and animals, allowing them to maintain their functions during periods of cold or starvation (Sibly et al, 2013). At the end of the modelling day, leftover energy reserves are calculated and examined against the criteria for survival. Agents with a remaining energy level lower than the least energy required (“survival-energy”) are considered to die from exhaustion.

The net energy reserved in the day of a phytoplankton or a submerged macrophyte is represented by a subtraction of BMR from the energy gained in photosynthesis:

$$\Delta\, plantenergy = energy \, * \, growthrate * \, photoperiod - \, BMR \qquad \text{equation 4-14}$$

where the photoperiod is the proportion of light exposure in a day. For zooplankton and fish, the net energy gained in a run is:

$$\Delta\, zooenergy = E_{foodgain} - \, BMR \qquad \text{equation 4-15}$$

In consequence, the biomass changes:

$$M = \sqrt{e^{(energy-300)/60}} \qquad \text{equation 4-16}$$

4.2.2.2 Emergence

The emergence is expected as an ecosystem-level transition in this model and can be indicated by population, biomass, . community composition, time spent reaching a state of equilibrium, and numbers of coexisting communities. Their variation results from agents’ attributes.

4.2.2.3 Objectives

The objective of the model is to create a lake ecosystem that tends to be stable on its own and tips to an alternative stable state after being disturbed. The objective of the phytoplankton and submerged macrophyte agents according to the model is to maximize the energy available from sunlight as well as their reproductive success. The objective of the consumer agents is to maximize their intake of digestible food during the swimming process.

4.2.2.4 Prediction

In natural ecosystems, fish may make decisions working on the principle of reward value maximization, as has been found in training experiments (Torigoe et al, 2021). However, for simplification, agents in this experiment are considered to have no ability to learn from previous experiences or predict the results of their behaviour in this model.

4.2.2.5 Sensing

Environment sensing

In each run, environmental changes driven by the SDM are sensed firstly by phytoplankton and submerged macrophytes, followed by zooplankton and fish. The agents of the primary producers sense nutrient availability, temperature and the density of surrounding algae and plants, and change their growth rate accordingly. Animal agents in the model do not sense any environmental variable directly, although they do sense the presence of food and shelter formed by the submerged macrophytes that surround them.

Food detection

Animals can sense their prey nearby and then move to the closer position to catch that prey. Different communities have different spatial ranges in which they can detect available food.

Zooplankton, planktivorous fish and herbivorous fish can only detect food within 1m^2, while piscivorous fish can sense food within up to sixteen hectares.

Obstacle detection

With a macrophyte agent living within a 4-hectare neighbourhood, planktivorous and piscivorous fish slow down their swimming speeds. When meeting land unexpectedly due to reclamation or the construction of a refuge area the fish at the front are prevented from predation, and turn 90° right to move away from the position.

4.2.2.6 Interaction

Submerged macrophyte agents cannot move once they have sprouted on a patch, and phytoplankton agents can only spread in conditions of overcrowding. They have no direct interactions with each other. Animals interact with their prey and avoid obstacles in the process.

4.2.2.7 Stochasticity

Stochasticity play a key role in shaping scenarios in the model, which may not be emphasised in other types of models. Stochasticity exists in the spatial distribution of agents, the directions of movement, The chances of encountering another agent to interact with, decisions to eat or not during a particular day, decisions to reproduce or not, the selection of positions for offspring, the availability of food in the surrounding area and any obstacles in that area. At the beginning of each run, a certain number of agents were created and randomly distributed in the water area. When animals find their food, a fixed probability for them to eat and obtain energy exists using a dice-rolling algorithm. The stochastic distribution of agents in the setup stage may decide the final pattern that emerges, as this pattern is influenced by stochasticity in movement, reproduction and eating processes.

4.2.2.8 Observation

Since the emergence of shifts or critical transitions in ecosystem state are of interest, the data produced by the model are mainly based on a community or ecosystem level. Spatially explicit patch data and agents' attributes of age, energy, mass and growth rate can also be aggregated daily and tested for model verification. In the model setup stage, if "logData" is selected as 'On', a list of environmental conditions and community descriptions will be collected for each day studied. The list includes "*drivers-pattern*", "*total-nutrient*", "*global-free-nutrient*", "*water-temperature*" and "*water depth*", as well as reclamation area, lake area, refuge area, population of six groups, biomass of six functional groups with fish aggregated, number of phytoplankton being eaten, number of zooplankton being eaten, number of submerged macrophyte being eaten and the added number of herbivorous fish, planktivorous fish and piscivores.

The areas used for parameter setting and variable observation were arranged in categories on the model interface (Figure 4-5). The green scale, the green input window, the selector and the switches on the left side of the figure can be used to adjust the values and options of the parameters. The parameters are divided into three blocks which belong to the "initial condition", "Biological communities" and "Drivers scenarios" categories. The purple button is the command execute button, which can be used for a single or continuous execution of the function.

The observation area includes three kinds of data: text boxes, displays of individual variable values, time series plots and an option to enable the "logData" function to export pre-defined variable of a single simulation values for each day directly into an external directory. The text box (top left of Figure 4-5) contains a description of the initial basic physical conditions of the lake system and the random seed used in the current simulation (such as 1496922334). Single variable values are displayed for relatively important and low-change variables such as the total-nutrient level of the system, the components of the system and the population of each functional group. Individual variables provide an accurate sense of the quantity. When dynamic changes in the time series were significant, I created three main blocks of graphs. The purpose of designing and classifying these graphs is to facilitate a rapid examination of the current state of various dimensions of the ecosystem.

At the top are the macroscopic graphs showing the environment and trophic levels, and these include a graph of nutrient changes over time, a graph of total energy changes in the trophic levels, as well as the current water depth, water temperature, reclamation area, refuge area and total nutrient concentration. In the middle are observations of population size and biomass, including current population size and population and biomass trends over time for each of the six functional groups. There is also a graph window in the middle to allow visual observation of the spatial position of individuals in real time in the model system. Light green dots represent phytoplankton, green plant shapes represent submerged plants, blue worm shapes represent zooplankton, grey fish represent planktivorous fish, blue fish represent herbivorous fish and black fish represent piscivorous fish. The graph window sits within a chronological display (which needs to be pre-set according to starting age), the surface area of the lake (the default is 961 hectares) and the number of components in the whole ecosystem (between 0 and 6). The bottom section examines individual properties and interaction changes. The graphs comprise statistics on the number of mortalities (the number of mortalities due to predation and the number of natural mortalities due to energy depletion are counted separately), statistics on the total number of births and statistics on the number of external additions (currently there are only three additions: planktivorous, herbivorous and piscivorous fish species). These observations help the model user to understand the dynamics of the simulated lake ecosystem and the way it responds to environmental change from the community level to the individual level.

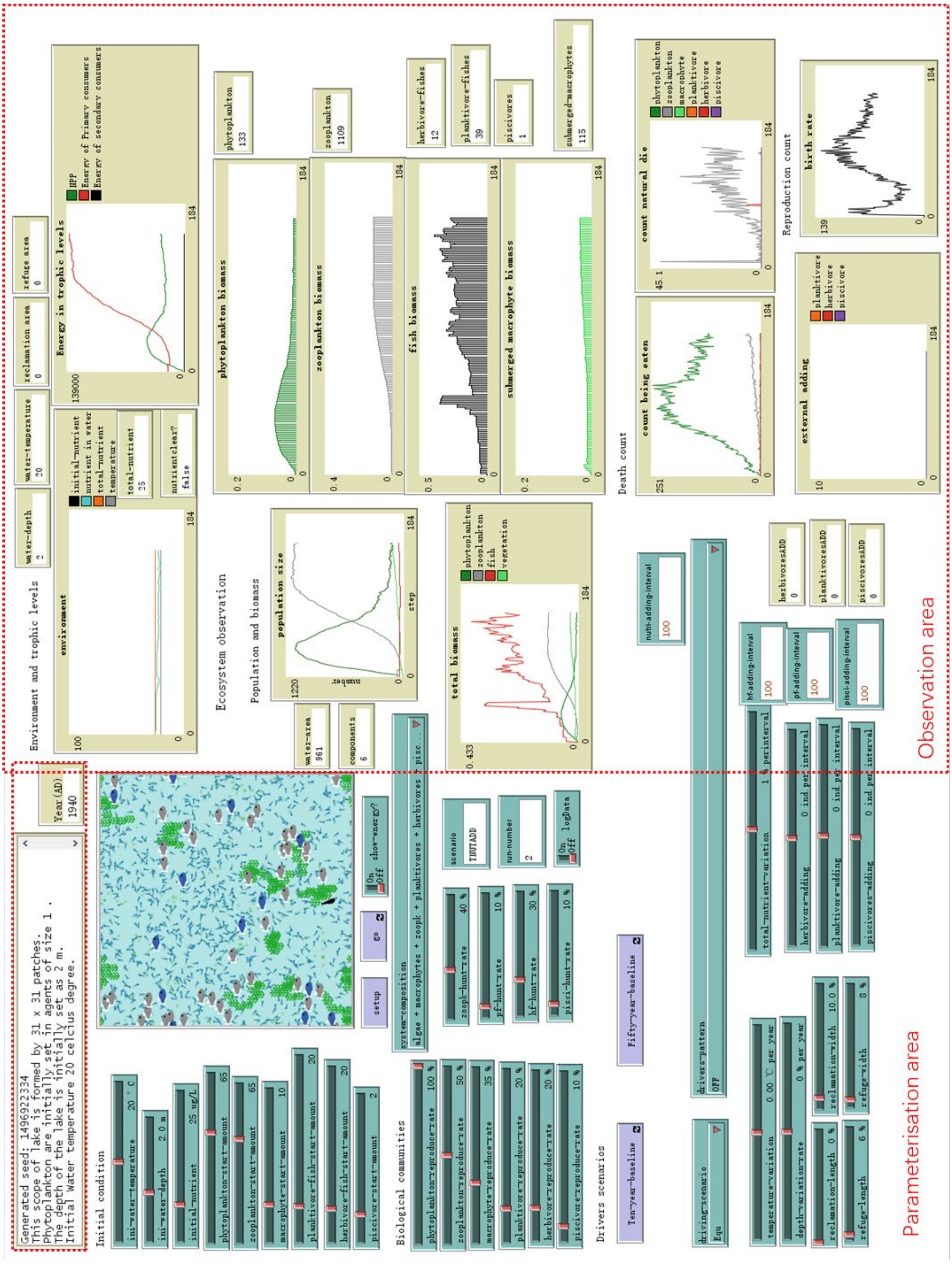

```
Generated seed: 1496922334
This scope of lake is formed by 31 x 31 patches.
Phytoplankton are initially set in agents of size 1 .
The depth of the lake is initially set as 2 m.
Initial Water temperature 20 celcius degree.
```

Year (AD) 1940

water-depth 2
water-temperature 20
reclamation area 0
refuge area 0
total-nutrient 25
nutrientclear? false
phytoplankton 133
zooplankton 1109
herbivore-fishes 12
planktivore-fishes 39
piscivores 1
submerged-macrophytes 115
water-area 961
components 6
herbivoresADD 0
planktivoresADD 0
piscivoresADD 0

ini-water-temperature 20 °C
ini-water-depth 2.0 m
initial-nutrient 25 ug/L
phytoplankton-start-amount 65
zooplankton-start-amount 65
macrophyte-start-amount 10
planktivore-fish-start-amount 20
herbivore-fish-start-amount 20
piscivore-start-amount 2

phytoplankton-reproduce-rate 100 %
zooplankton-reproduce-rate 50 %
macrophyte-reproduce-rate 35 %
planktivore-reproduce-rate 20 %
herbivore-reproduce-rate 20 %
piscivore-reproduce-rate 10 %

system-composition algae + macrophytes + zoopk + planktivores + herbivores + pisc...
zoopl-hunt-rate 40 %
pf-hunt-rate 10 %
hf-hunt-rate 30 %
pisci-hunt-rate 10 %
show-energy? Off
scenario THUTADD
run-number 2
logData Off

driving-scenario Equ
drivers-pattern OFF
temperature-variation 0.00 °C per year
depth-variation-rate 0 % per year
reclamation-length 0 %
refuge-length 6 %
reclamation-width 10.0 %
refuge-width 8 %
total-nutrient-variation 1 % perinterval
herbivore-adding 0 ind per interval
planktivore-adding 0 ind per interval
piscivores-adding 0 ind per interval
nutri-adding-interval 100
hf-adding-interval 100
pf-adding-interval 100
pisci-adding-interval 100

Figure 4-5: The main interface of my ABM model spin-up in the Netlogo environment in Windows 10. The red dashed boxes represent entities for observation, including generated random seed, current time (Year), and biological and environmental variables.

4.2.3 Initialisation

All parameters need to be set up before each simulation begins, and on the first day in the model, all agents live together (as they would in a new aquarium) with certain numbers of functional groups under set environmental conditions. In the first 1000 days, the groups cope with the new environment and each other, and spin up till reaching a balanced ecosystem with a comparatively stable composition and with no external disturbance.

The model does not use any input from external sources such as data files. Empirical and theoretical parameters take approximate ranges from literature if possible. After evaluating a suite of initial values as parameters (details in Appendix D), no more input is needed, but to manipulate external conditions, parameters related to drivers can be set as a follow-up input.

4.2.4 Submodels

4.2.4.1 The Environment-change submodel

The environment is the background against which all the biological activity in the model takes place, and is updated first each day. Once the initialisation parameters for the environment have been set, the simulation does not require any further input unless new scenarios for environmental change are set. The input variables for the Environmental-change submodel mainly consist of two selective variables which determine the names of the parameters to be manipulated, and 14 quantitative variables which describe the magnitude of each of these variables. As summarised from empirical studies in the MLYB, causes for abrupt ecological shifts between the 1950s and the 1980s may include climate change (as a moderating factor), land reclamation, agricultural intensification and industrialization (Guo et al, 2019; Zhang et al, 2018). Meanwhile, the aquacultural manipulation, such as the introduction of a large amount of juvenile planktivorous fish, is evaluated as a significant factor. The overall relationships between these external factors are shown as coloured blocks in Figure 4-6 which represents a simplified network used to model realistic environmental impacts.

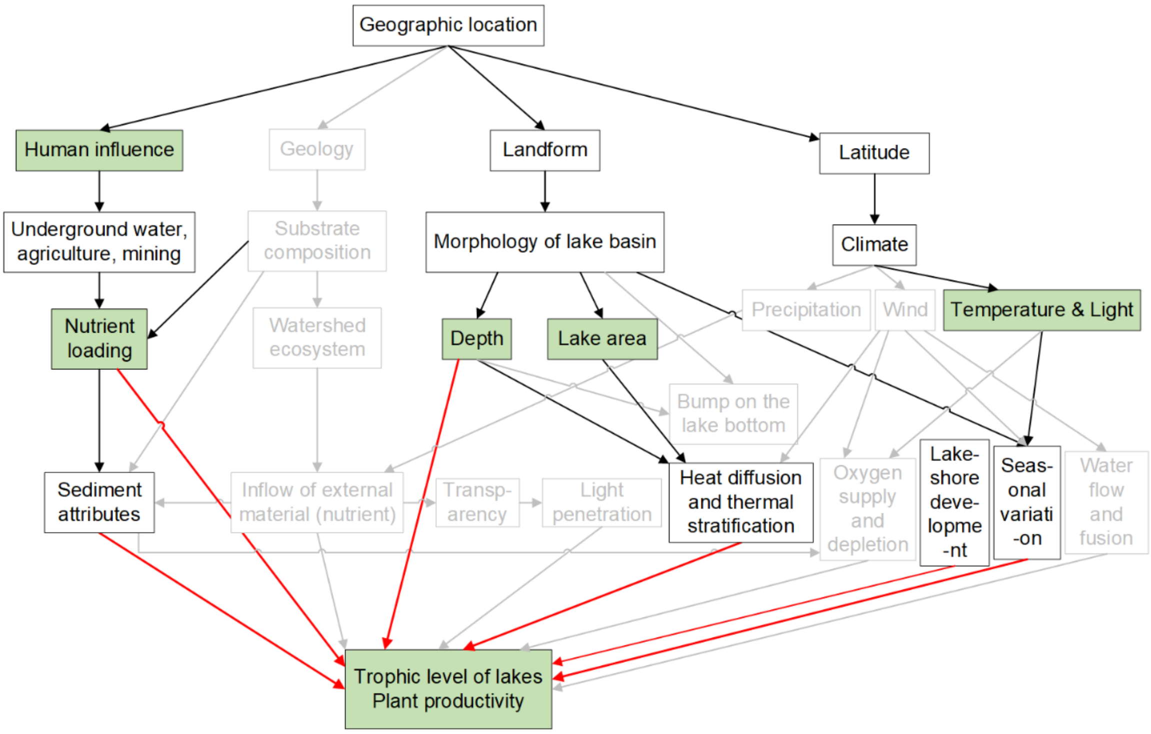

Figure 4-6: External factors as external variables in the model. The text boxes in grey were neglected and those in black were included in the model as environmental variables affecting the lake ecosystem by red arrows.

The parameters that control the pattern of environmental change in the model are shown in Table 4-5. The “drivers-pattern” sub-section contains items that can be manipulated in the environmental submodel and which can be modified according to the various characteristics of the experiments involved. After defining what the drivers are, the model user can modify the changing rate of drivers quantitatively.

Table 4-5: Variables, value ranges and units in the environmental submodel

Variable	Values/ Ranges	Unit
driving-scenario	“Equ” “Manual” “TBNutADD” “TBNutADD_TempADD” “TBComprehens” “restoration-1” …	*<chr>*
drivers-pattern	“modifying piscivores” “nutrient loading + temperature + planktivores + herbivores” “nutrient loading + reclamation + depth + temperature” “nutrient loading + reclamation + depth + temperature + planktivores” “nutrient loading + reclamation + depth + temperature + planktivores + herbivores” …	*<chr>*
Temperature-variation	[0, 10]	°C per year
Depth-variation-rate	[-50, 50]	% per year
Reclamation-length	[0, 100]	% max-pxcor
Reclamation-width	[0, 100]	% max-pycor
Refuge-length	[0, 100]	% max-pxcor
Refuge-width	[0, 100]	% max-pycor
Total-nutrient-variation	[-50, 50]	% initial-nutrient per interval
Nutri-adding-interval	[1, ∞]	day
Herbivore-adding	[-∞, ∞]	ind. per interval
Hf-adding-interval	[1, ∞]	day
Planktivore-adding	[-∞, ∞]	ind. per interval
Pf-adding-interval	[1, ∞]	day
Piscovores-adding	[-∞, ∞]	ind. per interval
Pisci-adding-interval	[1, ∞]	day

In the SDM, each variable changes separately according to the parameter to which it is relevant. After Δd (one day), the increment of water temperature is calculated as:

$$\Delta temp = \text{temperature\_variation} \ * \ \alpha_{\text{t}} * \ \text{temp} \ / \ 3650$$

where $\alpha_t = \begin{cases} 1, \ \text{member? "temperature" drivers\_pattern} \\ 0, ! \, \text{member? "temperature" drivers\_pattern} \end{cases}$ and temp is the water temperature before the day. The increment of water depth is:

$$\Delta depth = \text{depth\_variation\_rate} * \ \alpha_d \ * \ \text{depth} \ / \ 36500$$

where $\alpha_d = \begin{cases} 1, \ \text{member? "depth" drivers\_pattern} \\ 0, ! \, \text{member? "depth" drivers\_pattern} \end{cases}$ and depth is the water depth before the change. For nutrient load into the lake, the increment of nutrient load is:

$$\Delta nutri = \text{total\_nutrient\_variation} \ * \ \alpha_n * \beta_n * \ \text{initial\_nutrient} \ / \ 1000$$

where $\alpha_n = \begin{cases} 1, \ \text{member? "nutrient" drivers\_pattern} \\ 0, ! \, \text{member? "nutrient" drivers\_pattern} \end{cases}$, $\beta_n = \begin{cases} 1, \ \text{Day} \ mod \ \text{nutri\_adding\_interval} \ = \ 0 \\ 0, \ \text{Day} \ mod \ \text{nutri\_adding\_interval} \ \neq \ 0 \end{cases}$, and Day represents the simulation date ("*ticks*") in the model.

The changes in temperature noted above, as well as depth and nutrient, can be calculated by adjusting the "temperature_variation","depth_variation_rate", and "total_nutrient_variation" to positive (or negative) values. Fish placement and removal are implemented in a similar way, using different statements. In the case of "planktivores" (or "herbivores" or "piscivores") in the drivers-pattern, to add a specific number of fish to the system, the number of additions should be set to a positive number, and to reduce the number of specific fish from the system, the number of additions should be set to a negative number. By performing a “pf-adding-interval” (or “hf-adding-interval” or “pisci-adding-interval “) in the system based on the number of “planktivore-adding” attributes I can set the model for that species of fish. This combination allows flexible customisation that reflects the pattern of changes in the environment, for example to simulate a gradual pattern of addition, set the adding interval to very small to represent a small number of young fish being added at a time, or to simulate a large number of fish being added, adding set the adding interval to larger to reflect a larger input of fish. To reduce a fish from the system to simulate a fishing scenario, set the number of additions to negative. For planktivorous fish, when the procedure identifies negative planktivore addition, a planktivorous fish with an abs (planktivore-adding) number of existing fish is randomly selected to end its life cycle, and at the same time its nutrient concentration is subtracted from the system.

To facilitate the simulation of specific scenarios, the driving-scenario parameter selector sets up scenarios based on environmental change using different parameter settings, including no change (“Equ”), eutrophic changes (“TBNutADD”, “TBNutADD_ “TempADD”, and “TBComprehens”) and de-eutrophic changes (“restoration-*n*”). The ‘Equ’scenario is used to test the steady-state equilibrium of a lake ecosystem in the absence of any disturbance, while the ‘Manual’ scenario can also be selected for manual parameter adjustment.

4.2.4.2 The Primary Producer submodel

The primary producers in the model, such as submerged plants and phytoplankton, have essentially similar life processes. In the case of phytoplankton (Figure 4-7), each individual undergoes several processes each day, namely growth, reproduction, dispersal and death. The process of growth involves photosynthesis and respiration, and the accumulated energy is the remaining of the solar energy assimilated in photosynthesis process minus respiration (see Section 4.3.2.1 for basic principles). Due to differences in reproductive rates in real terms, the reproduction rate of submerged plants is generally set to less than the reproduction rate of phytoplankton (usually 30%). The reproduction rate determines the probability of an agent to split into two agents when the energy criterion is met. For example, when the reproduction rate of algae reaches 100%, in each day its population will increase by the number of all algae with energy reserves beyond the fertility criterion. In the process of reproduction it is calculated that the energy of the parent is halved and the energy of the offspring will be half of the energy of the parent before reproduction, which is basically the same as the initial energy value of the individual. At the end of the process, the remaining energy of all individuals is checked. If an individual entity falls below the minimum threshold required for survival, then that individual is considered to have died of natural causes as it cannot sustain itself. After death its energy disappears and the nutrients are returned to the water.

Submerged plants differ from phytoplankton in that phytoplankton can disperse their pores to the neighbouring areas with lower densities of surrounding phytoplankton when the individual's perceived light attenuation is low. Submerged plants are limited by their root systems to disperse via reproductive organisms like pores, bulbils and fragments in the vicinity of the parental plant.

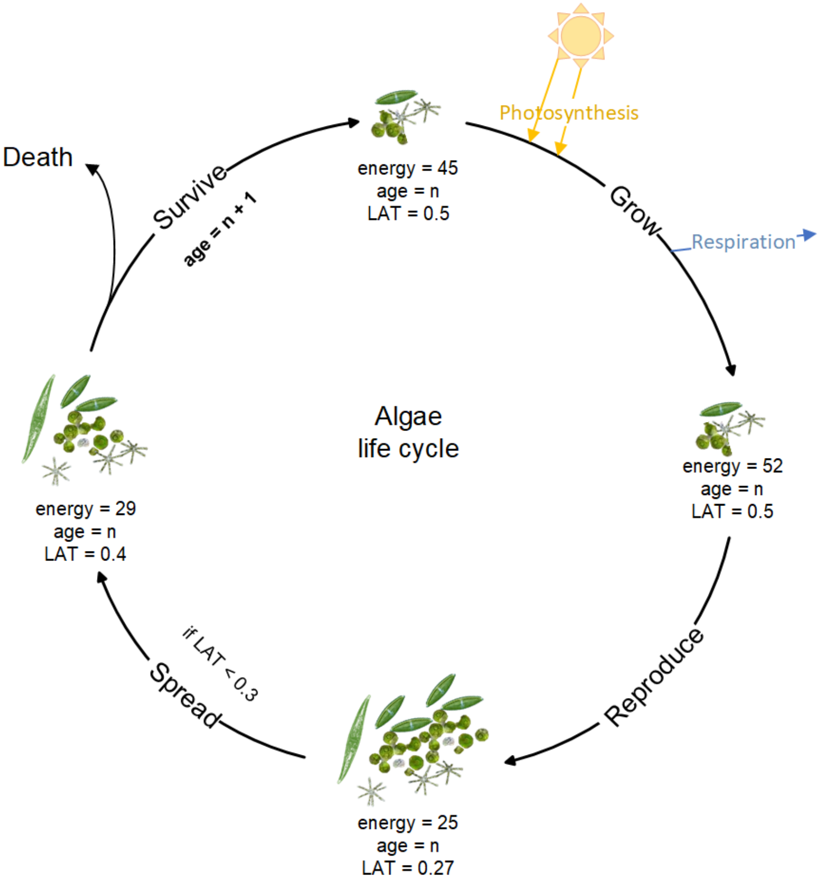

Figure 4-7: Daily life cycle of phytoplankton submodel, developed and adapted from Bronmark & Hansson (2005).

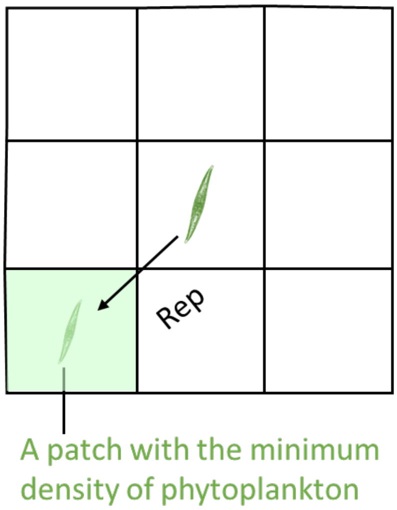

Figure 4-8: Spatial selection of a phytoplankton offspring in the reproduction procedure. When the original phytoplankton in the centre square has to choose one neighbouring patch for its offspring, it checks the surrounding eight patches and chooses a patch with the least amount of phytoplankton on it to lower competition intensity.

4.2.4.3 Zooplankton agents submodel

As primary consumers, the main source of food for zooplankton is phytoplankton and the main method of energy dissipation is metabolic, with the added risk of being grazed upon by planktivorous fish. Zooplankton have a certain probability of grazing individual phytoplankton from within one hectare of their location per day, as determined by the zoopk-hunt-rate parameter. Zooplankton move at a speed of 20m/day, with the direction of movement randomly adjusted within 45° of their current direction. When the energy threshold required for reproduction is reached and offspring can be hatched, the rate of reproductive behaviour is determined by the zooplankton-reproduce-rate.

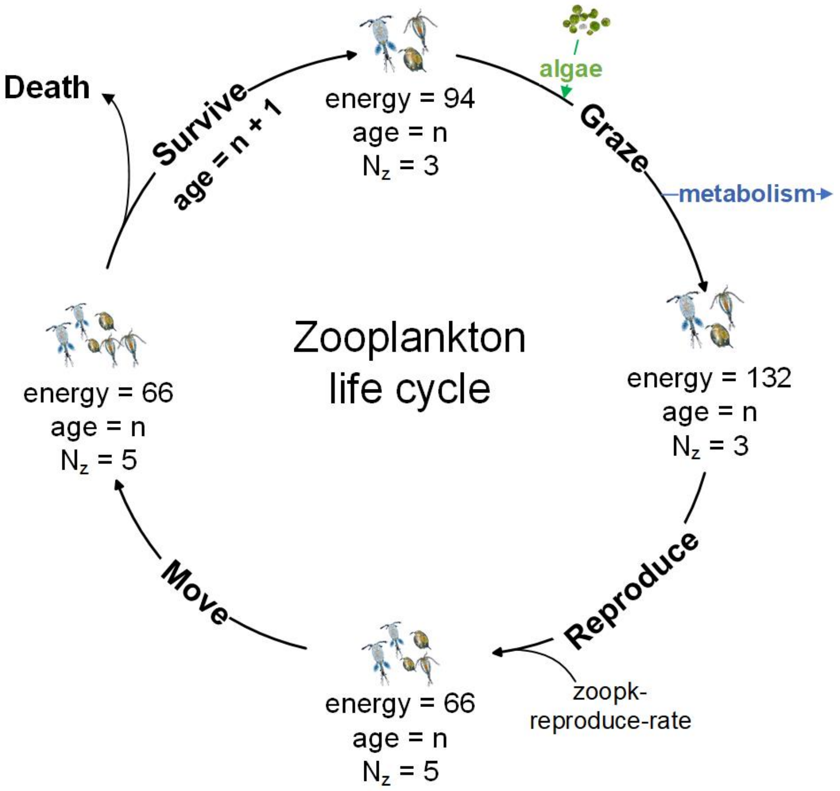

Figure 4-9: The life cycle of zooplankton agents. The diagram shows three agents aged n as the initial state, with an average individual energy reserve of 94 J. After reproduction the number of zooplankton increased to 5, and the average energy per individual is decreased while the total energy remains the same. The age of each zooplankton increases by a factor of 1 after a full day of life cycle. Diagram developed and adapted from Bronmark & Hansson (2005).

4.2.4.4 Fish submodel

The life cycle of fish is similar to that of zooplankton, insofar as they obtain energy through predation and assimilation, while metabolic processes consume energy and fish may be preyed upon by natural predators. The mass of an individual fish-agent is much greater than that of a phytoplankton-agent and therefore its metabolic rate is higher. In the default initial settings the mass of a phytoplankton-agent is 1g, the mass of a zooplankton agent is 1.5g, the mass of a submerged plant-agent is 3g. However, the mass of a planktivorous and herbivorous fish-agent is 20g and the mass of a piscivorous fish agent is 40g. Based on these initial mass settings, the daily metabolic energy of a zooplankton-agent is 0.387 J, while the daily metabolic energy of a piscivorous fish-agent is 1.148 J. The metabolic energy of a planktivorous fish-agent is also 1.148 J per day, but the metabolic energy of a piscivorous fish-agent is 2.828 J per day. The metabolic energy consumption increases as the body weight of the individual increases.

The daily diet of planktivorous fish-agents consists of up to two phytoplankton and one zooplankton within a patch (1 hectare). The daily diet of a herbivorous fish-agent consists of one individual submerged plant within a patch. Piscivorous fish-agents feed daily on other fish-agents present within 200 m of their location, and can only feed on one fish-agent a day, with a limited chance of not feeding within the pisci-hunt-rate parameter. When submerged vegetation is present within the patch, the movement speed of planktivorous and herbivorous fish-agent decreases to 20 m/day and that of piscivorous fish-agent to 50 m/day. Both are limited by energy thresholds and probability parameters.

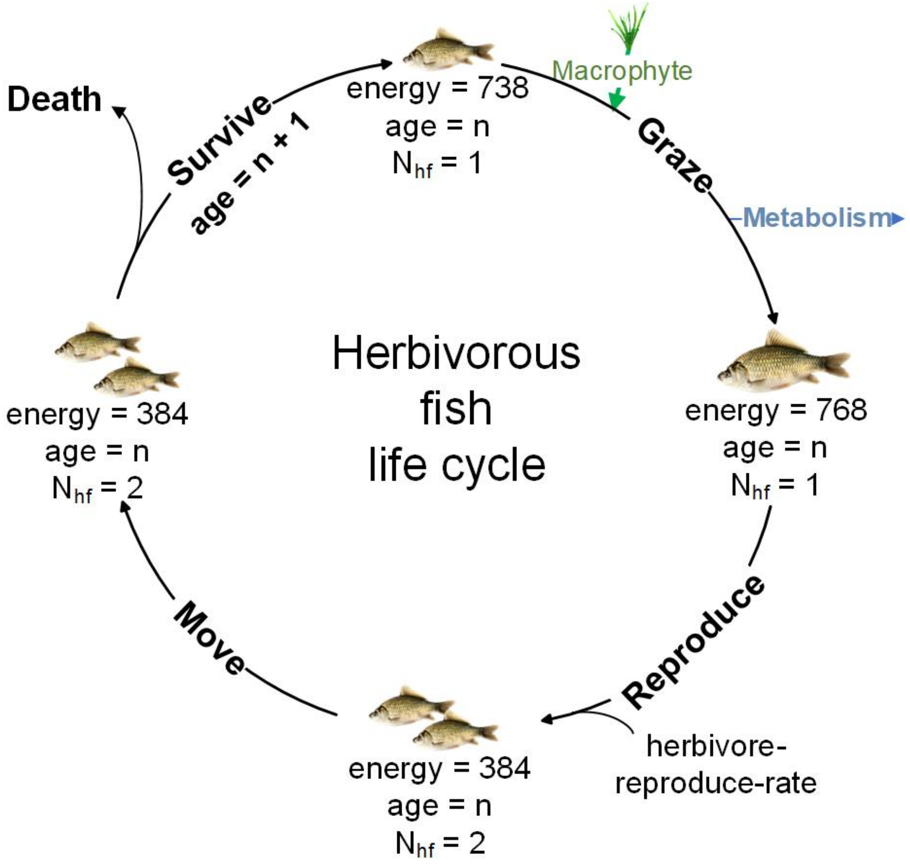

Figure 4-10: The daily life cycle of an herbivorous fish-agent. This herbivorous fish-agent first gains a net increase in energy of 30J by grazing on vegetation, so that its energy reserves exceed the threshold for reproduction (760 J) and a probabilistic decision is made to reproduce, at which point the fish-agent completes its 'split' into two small fish-agents, each with about half the energy of the previous one. This offspring of the herbivorous fish-agent will then move away from the mother, and if it is incapable of reproducing and its energy reserve falls below the basic value, the fish-agent dies. Fish-agents with energy savings above the basic value increase in age by one day and wait for other individuals to interact with. Diagram developed and adapted from Bronmark & Hansson (2005).

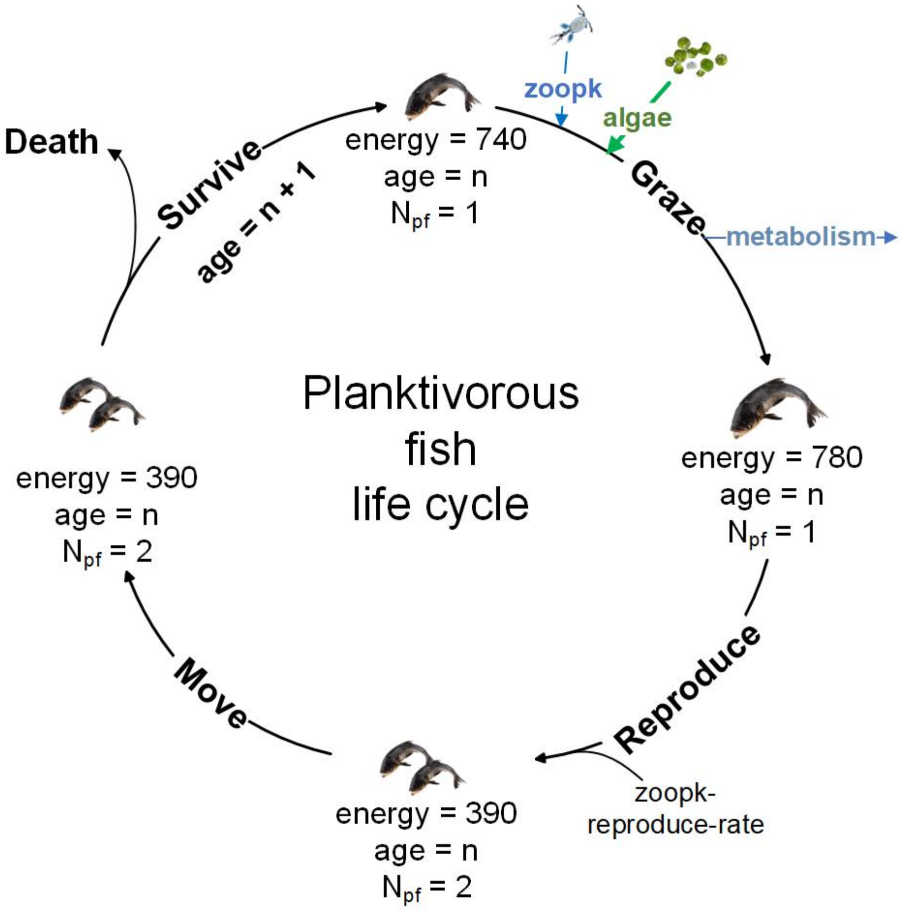

Figure 4-11: The daily life cycle of a planktivorous fish-agent. Each planktivorous fish-agent eats 2 phytoplankton agents and 1 zooplankton at maximum. Diagram developed and adapted from Bronmark & Hansson (2005).

4.3 Calibration and validation

To make the model resemble the actual Lake Taibai ecosystem, relevant parameters in the model were adjusted to field data of Taibai lake. I calibrated the numerical ranges of endogenous parameters using One-Factor-at-A-Time (OFAT) and Approximate Bayesian Computation (ABC) rejection method (Nunes & Prangle, 2015) with a tolerance of 0.3. The OFAT method makes only one element change in each set of experiment. It was used to scan overall trends along the gradients of the parameter's matrix in the model, varying 50% from nominal values or 10% from percentage values. The ABC rejection method gives the 'best guess' of parameters by comparing prior and expected posterior distribution of modelling outputs for model's parameters after 1000 runs with random samples from the prior distribution. The posterior distribution is the range of parameters that produce acceptable model outputs that best fit the empirical data. Finally the accuracy of the estimation processes can be examined using coverage plots (der Vaart et al., 2016). The rejection-ABC algorithm was implemented using the *abc* package in R.

In the summer of 2008 and 2019, field surveys of Lake Taibai measured TP, Chl-a, phytoplankton and zooplankton concentrations. Summer was a high water season for the MLYB lakes, with water depths averaging 2.75 m and surface water temperatures averaging 31°C. Nutrients were expressed in terms of TP, and were generally considered as one of the key limiting factors for primary productivity in the lake (Qin et al, 2013). They were detected at very high concentrations around 0.50 mg/L, compared to 0.092 mg/L in Lake Taibai in the summer of 2008. Phytoplankton and zooplankton biomass were counted under a microscope in the NIGLAS laboratory. In the 2019 survey, the mean phytoplankton biomass in the surface water was 12 mg/L and the mean zooplankton biomass was 0.18 mg/L (but with a high level of heterogeneity as one is 0.32 mg/L and the other 0.03 mg/L). Estimates of phytoplankton to zooplankton ratios ranged from 36 to 422 to 1, which is the reference range for recent phytoplankton-zooplankton biomass ratios in the model.

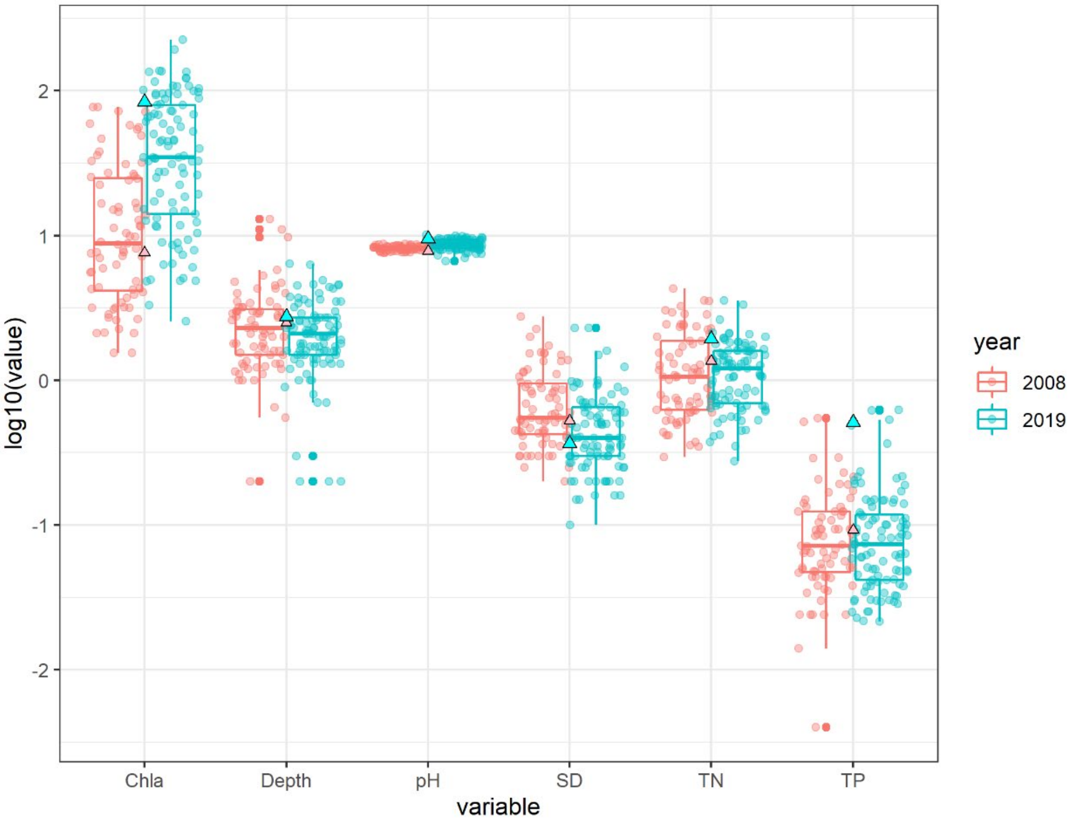

Figure 4-12: Survey data of variables Chl-a, depth, pH, SD, TN and TP in MLYB lakes in 2008 (dots in red) and 2019 (dots in cyan) where the y-axis values are logarithmic. Attributes of Taibai Lake in 2008 (red) and 2019(cyan) are drawn in triangles.

Shown in the graph above, the nutrient indicators (TP, TN) and chlorophyll a concentration in Lake Taibai increased in data between 2008 and 2019, while the clarity (SD) decreased, showing a deteriorating water quality environment (Figure 4-12, Table 4-6). Among the MLYB lakes, Taibai was in the middle of the intervals of these indicators according to the boxplots in the 2008 survey.

Table 4-6: Comparison of water quality measurements in Taibai lake in 2008 and 2019. When there was more than one sampling point, mean values were calculated.

Year	Depth	pH	SD	TP	TN	Chl-a
Unit	m		m	mg/L	mg/L	μg/L
2008	2.50	7.801	0.525	0.092	1.353	7.634
2019	2.75	9.465	0.365	0.511	1.928	83.864
Annual changing rate	0.023	0.151	-0.014	0.038	0.523	6.930

As survey data from Lake Taibai are limited, information from other lakes in the MLYB region was also used as a basis for judging the plausibility of the model. The ratio of algal, aquatic plant and fish biomass in Poyang Lake was estimated to be approximately 100:145:1 based on survey reports from 1987 to 2011 (Yu et al, 2013). The Poyang Lake Authority (2011) reported that an adult herbivorous fish weighing 1.5 kg consumed 0.5 kg of macrophytes in a single day, implying a three-to-one mass ratio of herbivorous fish to grazing macrophytes. Calibrating and validating the model has been difficult because of the spatial and temporal stochasticity. I used the multivariate analysis method CCA to reveal the changing ecosystem states in experiments and proved the mechanism in the model valid through the similarity of ecological patterns between the modelling results and data in the real lake ecosystem.

4.4 Sensitivity analysis

A sensitivity analysis of a model usually provides a quantitative indication of the parameters that have the greatest effects on the output variables and the responses of the output variables to the input variables within a given range. This was carried out by changing the parameters, forcing functions or submodels and observing the corresponding responses in state variables. The sensitivity S of a state variable x responding to a parameter P is defined as:

$$S = [\partial x/x]/[\partial P/P]$$

The sensitivity analyses in the thesis were proposed at several aggregation levels for a better understanding of model behaviours. Firstly, prior submodel analyses were conducted in biological groups, with changing parameters and outputs expected from the interacting submodels. Secondly, larger subsystems composed of three to five agent groups were tested, resembling possible patterns in lakes in which few functional groups dominated. Finally, the full integrated model was analysed based on the above findings of the behaviours of the submodels. A two-step approach based on the scheme by Janse et al (2010) was followed for this sensitivity analysis: a) the Morris Elementary Effects Screening method (Morris, 1991; Thiele, 2014) was used to select the most responsive parameters from all the parameters in the model, and b) the Soboljanse sensitivity analysis (Janse et al, 2010) can evaluate the effect of a factor when multiple factors are varied as well, thus measuring effects from the single factors and interactions between the factors via the Monte Carlo method. Let f be a model with k independent inputs, i.e. $X = \{x_1, x_2, \dots, x_k\}$ and if only X_i ($i \in [1, k]$) varies by a given value Δ while other inputs remain the same, the Elementary Effect EE in the Morris method is

$$EE_i = \frac{f(x_1, \dots, x_{i-1}, x_i + \Delta, \dots, x_k) - f(X)}{\Delta}$$

Then the experiment is repeated with N different values of X randomly sampled in a k-dimensional input space Ω^k, so the absolute mean (i.e., $\mu_i{}^*$) and the standard deviation (i.e., σ_i) of the N EEs are calculated as the screening measures:

$$\mu_i{}^* = \frac{\sum_{r=1}^{N} |EE_{i,r}|}{N}$$

$$\sigma_i = \sqrt{\frac{\sum_{r=1}^{N} (EE_{i,r} - \mu_i)^2}{N - 1}}$$

where $EE_{i,r}$ represents the r-th EE of the parameter x_i. The absolute mean $\mu_i{}^*$ has better ability to detect the influential factors than the normal mean values. Thus, an input parameter x_i is identified as an influential factor with insignificant nonlinear effect if $\mu_i{}^*$ is high but σ_i is low, or as an influential factor with strong interaction if both metrices are high. If the $\mu_i{}^*$ is close to zero, the parameter is identified as a non-influential input.

The Soboljansen method is variance-based, and represents the change in the relationship between input and output as a probability distribution, decomposing the variance of the output into main effects (first-order effects) and variable combination effects (total effects)(Jansen, 1999).The simulation designs and analyses were implemented in the R platform "nlrx" package (Salecker et al, 2019), where methods such as Morris Screening (`simdesign_morris()`) and Sobol variance decomposition (`simdesign_soboljansen()`) could be conducted.

Within a certain range, the combination of parameters was randomly generated using a Latin HyperSquare(LHS) experiment design. The sensitivity analysis included 6 parameters that were critical to the population dynamic processes to analyse the ways in which the population of ecosystem components changed with each parameter and each combination of parameter values. The ranges of parameters were chosen according to realistic values in model design. For each factor, the range testing for sensitivity was ±50% from the nominal value. The time steps lasted for 1825 days, equal to 5 years. Each test had 5 repetitions to identify changes in trends.

Table 4-7: Variables and their values tested in the sensitivity analysis to initialisation

Parameter	**Unit**	**Values**		
		Min	**Max**	**Step**
ini-water-temperature	℃	10	30	2
ini-water-depth	m	1	3	0.2
initial-nutrient	μg/L	12	38	2
macrophyte-start-amount	ind.	4	12	1
piscivore-start-amount	ind.	4	12	1
planktivore-fish-start-amount	ind.	10	30	2

In the sensitivity analysis to endogenous or exogenous parameters, input parameters were selected from a 100 x 12 parameter matrix with random variable parameters the table below using the LHS method. Outputs are the population number of phytoplankton, zooplankton, submerged-macrophytes, planktivorous-fishes, herbivorous-fishes, and piscivores, and number of existing components.

Table 4-8: Parameter settings of the sensitivity test to endogenous drivers

Experiment name	**LHS_ENDO**		
NetLogo repetitions	1	Simulation method	LHS
Generated random seeds	-638843216	Runtime (ticks)	5000
Variable parameters (input)	min	max	step
phytoplankton-reproduce-rate	20%	100%	20%
zooplankton-reproduce-rate	20%	100%	20%
macrophyte-reproduce-rate	20%	100%	20%

planktivore-reproduce-rate	20%	100%	20%
herbivore-reproduce-rate	20%	100%	20%
piscivore-reproduce-rate	20%	100%	20%
zoopk-hunt-rate	20%	100%	20%
pf-hunt-rate	20%	100%	20%
hf-hunt-rate	20%	100%	20%
pisci-hunt-rate	20%	100%	20%

Table 4-9: Parameter settings of the sensitivity test to exogenous drivers

Experiment name	**LHS_EXO**	**Random seeds**	**388365058**
NetLogo repetitions	1	idsetup	“setup”
Simulation method	LHS	idgo	“Ten-year-baseline”
Constants parameters(input)			
reclamation-length	10%	Runtime (ticks)	7300
Variable parameters (input)			
	min	max	step
total-nutrient-variation	-10	10	2
reclamation-width	0	100%	10%
herbivore-adding	0	5	1
planktivore-adding	0	5	1
piscivores-adding	0	5	1
depth-variation-rate	-10%	10%	2%
temperature-variation	-4℃	4℃	1℃

4.5 Evaluating community structure

To observe the effects of changes in ecosystem structure on elastic changes and steady state formation during initial state collapse more clearly, it is necessary to measure properties such as the connectivity and modularity of the ecosystem structure. The ecological network consists of components as vertices and the relationships between them as edges. For predation relationships the weights of edges are represented by the following equation:

$$weight = N_i^{eat} \times HR$$

where N_i^{eat} represents the amount of food foraged during a single day and HR represents the likelihood of successful predation by the predator in this relationship. As well as predation relationships, competitive relationships also exist between phytoplankton and submerged plants, which can be represented in the network relationships by using half the weight value of the weakest predation relationship. The main direct effects of environmental drivers on ecosystem components are temperature and nutrients on primary producers and human activities on fish stocks and harvesting. The effects of changes in lake depth and area on the components of the lake ecosystem are indirect and global in this model, and are therefore not included in the network analysis process, although they are analysed as a part of the multivariate statistical analysis of the model results. The weights for the relationships between environmental drivers and ecosystems are all set as 1, and networks of direct linkages in the LAKEOBS_MIX model are shown in Table 4-10.

Table 4-10: Ecological network of model LAKEOBS_MIX describing endogenous and exogeneous interactions

Source	Target	Weight	Source	Target	Weight
Endogenous			**Exogeneous**		
sm	phypk	0.05	nutri	phypk	1
zoopk	phypk	0.4	nutri	sm	1
pf	zoopk	0.1	pf	phypk	1
pf	phypk	0.2	human	phypk	1
hf	sm	0.3	human	pf	1
pisci	pf	0.1	human	hf	1
pisci	hf	0.1	human	pisci	1
			human	sm	1
			temperature	sm	1
			temperature	phypk	1

Ecosystem networks were analysed on the *R* platform using the *igraph* programme for general network property detection and cluster analysis. In order to find collapse paths that make sense in terms of structural relationships, such as core groups that are more connected, the clustering analysis used the Fast greedy algorithm (Clauset et al, 2004), the random walk algorithm (Pons & Latapy, 2005) and the Girvan-Newman algorithm (Newman & Girvan, 2004) to calculate the results of the modular groupings of ecological networks, which are represented as dendrograms and network relationship schematics. In addition, the modularity (Q) of each grouping outcome (membership) was calculated as:

$$Q = \frac{1}{2m} * \sum_{i,j}((A_{i,j} - \frac{k_i \times k_j}{2m}) \times \Delta(c_i, c_j))$$

where m is the number of edges, $A_{i,j}$ is the element of row i and column j of the adjacency matrix of A, k_i is the degree of *i* and k_j is the degree of *j*. c_i is the component of *i*, c_j is the component of *j*, and $\Delta(c_i, c_j) = \begin{cases} 1, & ci = cj, \\ 0, & ci \neq cj \end{cases}$ (Clauset et al, 2004). In general, modularity calculates how good the division of membership is.

4.6 Homeostasis scenario

Homeostasis scenarios are simulations for observing dynamic stable states without disturbance in the model. The ABM is developed on the basis of individual rules instead of steady-state solutions, with extra efforts of tuning the system state becoming as stable as needed by the iteration of parameters until the right initial conditions are found. The parameters for the homeostasis scenarios were used as the initial settings for sensitivity analyses and the in-silico experiments of external drivers. These are the parameter values that allow the system results to be largely stable and realistic, based on sensitivity tests of the pattern-oriented model and calibration with empirical data.

Table 4-11: Nominal values of initial settings of clear-water states in the model

Variable	Value	Unit	Variable	Value	Unit
System-composition	"algae + macrophytes + zoopk + planktivores + herbivores + piscivores"				
ini-water-temperature	20	℃	planktivore-reproduce-rate	20	%
ini-water-depth	2	m	herbivore-reproduce-rate	20	%
initial-nutrient	25	µg/L	piscivore-reproduce-rate	10	%
phytoplankton-start-amount	65	ind.	zoopk-hunt-rate	40	%
zooplankton-start-amount	65	ind.	pf-hunt-rate	10	%
macrophyte-start-amount	10	ind.	hf-hunt-rate	30	%
planktivore-fish-start-amount	20	ind.	pisci-hunt-rate	10	%
herbivore-fish-start-amount	20	ind.	show-energy?	false	
piscivore-start-amount	2	ind.	driving-scenario	"Equ"	
phytoplankton-reproduce-rate	100	%	drivers-patterns	"OFF"	
zooplankton-reproduce-rate	50	%	max-pxcor	30	100m
macrophyte-reproduce-rate	35	%	max-pycor	30	100m

The model usually reaches a steady state over a period of 10 to 20 years in multiple random runs, so 10 to 20 years have been used for the steady state scenario and "steady state for the first 10 years + unspecific duration of manipulation" for the manipulation experiment. The observation is usually stopped after a new system state is seen to emerge in the results of the manipulation experiment and which persists for at least ten years in the simulation. The parameterisation of the manipulation used in the experiments on external conditions is described in Appendix D.2.

4.7 Results

4.7.1 Sensitivity analyses

4.7.1.1 Sensitivity of equilibria to initial conditions and decision-making

The results of the homeostasis simulations generated using 100 different random seeds lasting for 20 years (Experiment# EQC_100rseed_y20 in Appendix D.1) show that the experiments resulted in several different patterns in ecosystem states. In temporal terms, the results can be divided into three phases according to variation patterns shown in Figure 4-13: the introduction phase (within Day 0-1000, before the grey dashed line), the adjustment phase (roughly Day 1000-3650, between the grey dashed line and the second black dashed line), and the equilibrium phase (after the second black dashed line). The phase divisions of population changes are based on broad population trends, especially for functional groups with more obvious trend changes such as zooplankton, submerged plants and planktivorous fish. In this subsection, the main features and differences in steady states resulting from multiple long-term model simulations are described. The analysis of dynamic changes between the components in typical simulations and the changing relationships before and after extinctions are presented in the following subsection 4.5.2 and 4.5.3.

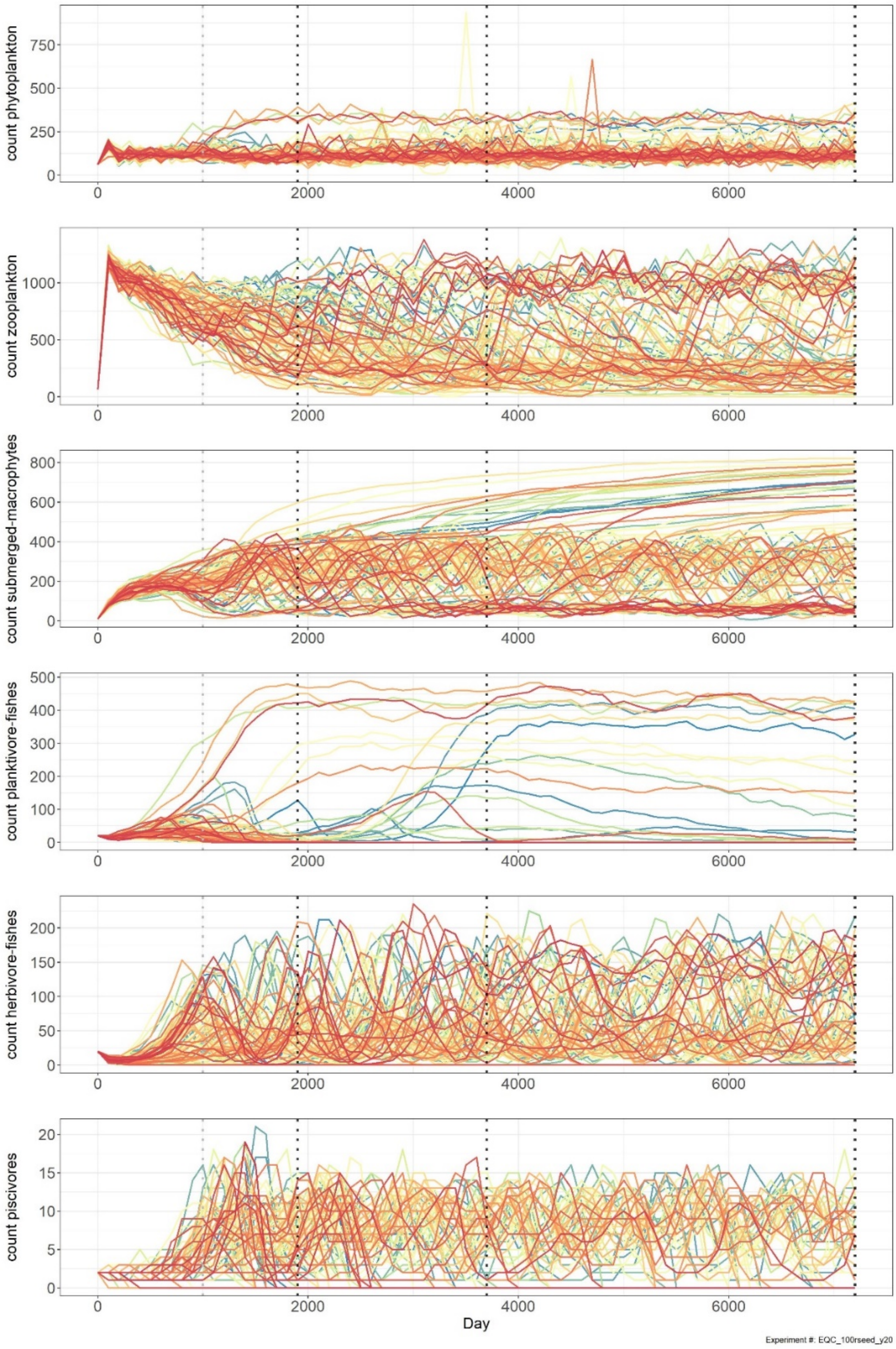

Figure 4-13: Population changes in 100 runs generated with different random seeds in the Experiment# EQC_100rseed_y20. The grey dash at Day 1000 marks the end of the introduction stage. The black dashes on Days 1901, 3701 & 7201 represent the sampling intercepts in 5, 10 and 20 years to be analysed later.

In the introduction phase, significant variations in population represent the fast competition and adaptation of functional groups to each other from the initial state of the new ecosystem. This stage is characterised by drastic changes in population and comparatively homogenous trends in different runs. After the introduction stage, the adjustment stage is characterised by heterogenous compositional changes in different runs. Among all the six components, planktivorous fish, herbivorous fish and piscivores are more vulnerable to extinction due to insufficient reproduction. The extinction of a community in the model represents a significantly low population in realistic lake ecosystem, which makes it important to justify compositional changes. At the end of the 20-year simulation, planktivorous fish went extinct in 80 runs, herbivorous fish in 30 runs and piscivores in 67 runs of the total of 100 runs (Figure 4-14). The timing of the occurrence of fish extinctions provides clues as to the emergence of steady state, as extinctions in the system essentially alter the structure of the system state. There are almost no extinctions of planktivorous fish before Day 1000, and extinctions of herbivorous fish plateau after an initial rise, with a small number of extinctions of piscivorous fish. Between Days 1000 and 2000, in the adaptation stage, the number of planktivorous fish extinction events begins to rise steadily, with a slow rise in herbivorous fish and a rise in the number of piscivorous fish extinctions. After Day 3650, more extinctions occurred in herbivorous and piscivorous fish, but the general trends of the six components are more stable and periodic than they were before Day 3650. Some exceptions to the general rules can be seen, such as the yellow and orange lines with acute peaks on Days 3501, 4501 and 4701 in the phytoplankton population generated from random seeds 116382348, 18432310 and 1545070373.

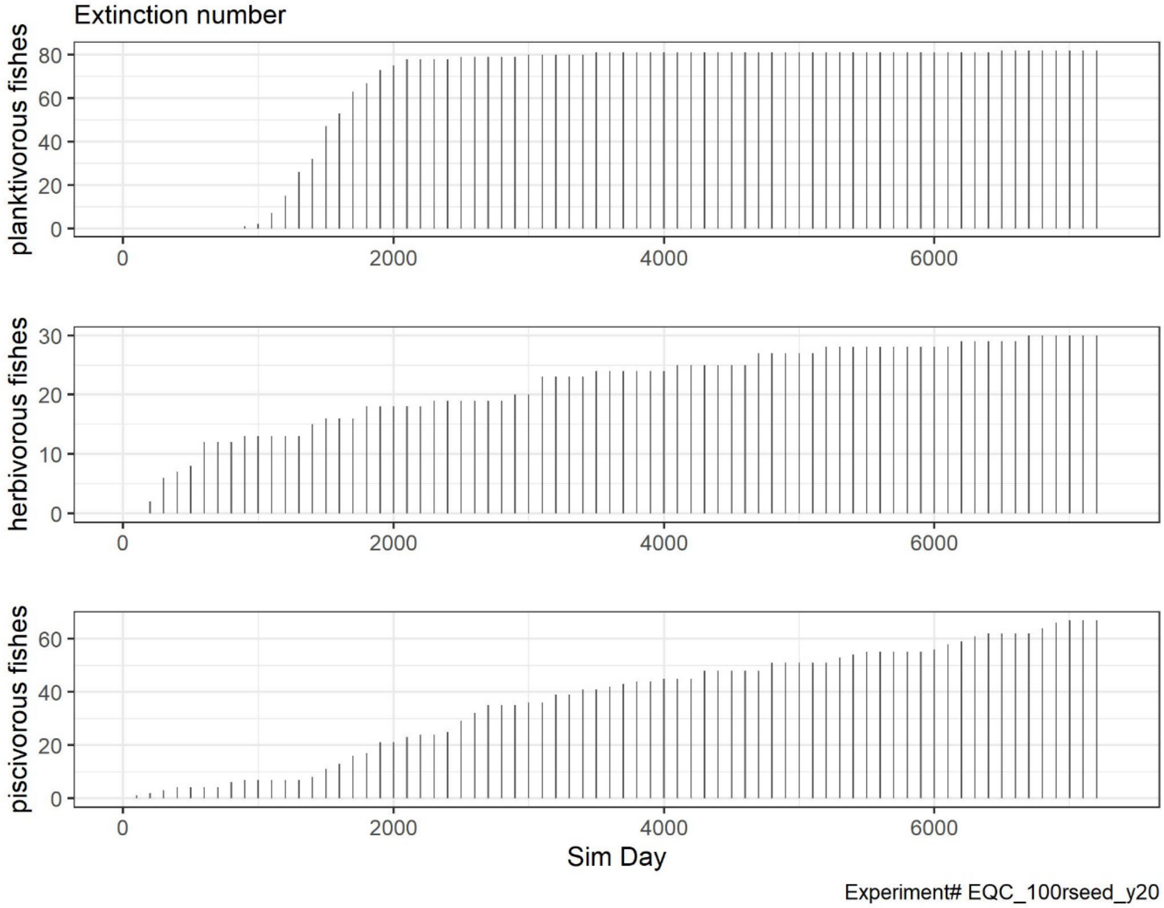

Figure 4-14: Numbers of runs in which fish become extinct in the system at different simulated days (Sim Day). The sampling resolution is 100 days.

The system compositions of steady states show seven patterns in these steady states after 20 years (on Day 7201) (Table 4-12). The most frequent functional group combinations at the end of year 20 were “p+z+sm+hf” and “p+z+sm+hf+pisci” (both 33%), followed by “p+z+sm “ (15%), “p+z+sm+pf” (14%), “p+z+sm+pf+hf” (4%) and “p+ sm “ (1%). This means that the steady states containing phytoplankton, zooplankton and submerged macrophytes accounted for 99% of the 100 experiments. The probability of the survival of herbivorous fish alone was the same as the probability of coexistence of piscivorous and herbivorous fish, and a little more than twice that of the survival of planktivorous fish alone. The coexistence of planktivorous and herbivorous fish and the extinction of piscivorous fish occurred in four of the simulations, and one experiment showed that only the primary producers remained extinct at the end.

Table 4-12: The occurrence of homeostasis compositions and component numbers at 5, 10 and 20 years (on Day 1901, 3701 & 7201) respectively. Data are taken from the Experiment # EQC_100rseed_y20, where 100 simulations were conducted using 100 different random seeds and identical remaining initialisation parameters. The abbreviation 'p' represents phytoplankton, 'z' stands for zooplankton, 'pf' stands for planktivorous fish, 'hf' stands for herbivorous fish, 'sm' represents submerged macrophytes and 'pisci' represents piscivorous fish.

Ecosystem composition	**Components**	**Occurrence**	**Ecosystem composition**	**Components**	**Occurrence**
Day 1901 (~ 5 years)			**Day 7201 (~ 20 years)**		
p+pf+sm	3	**3%**	p+sm	2	**1%**
p+z+sm+hf	4	**7%**	p+z+sm	3	**15%**
p+z+sm+pf	4	**6%**	p+z+sm+pf	4	**14%**
p+z+sm+pf+hf	5	**5%**	p+z+sm+hf	4	**33%**
p+z+sm+hf+pisci	5	**63%**	p+z+sm+pf+hf	5	**4%**
p+z+sm+pf+pisci	5	**9%**	p+z+sm+hf+pisci	5	**33%**
p+z+sm+pf+hf+pisci	6	**7%**			
Day 3701 (~ 10 years)					
p+pf+sm	3	**9%**			
p+z+sm+hf	4	**17%**			
p+z+sm+pf	4	**13%**			
p+z+sm+pf+hf	5	**6%**			
p+z+sm+hf+pisci	5	**55%**			

The number of ecosystem components peaked at four in the steady-state results in probability distribution, meaning that two functional groups became extinct (Figure 4-14). From the perspective of the system components, the main change between the adaptation phase and the equilibrium phase (Years 10 -20) is the "p+z+sm+hf+pisci" ecosystem state in Year 10, which is composed of phytoplankton, zooplankton, submerged plants, herbivorous fish and piscivorous fish. This 'p+z+sm+hf+pisci' state changes to 'p+z+sm+hf' and 'p+z+sm' due to the extinction of piscivorous fish or fish in general. The “p+pf+sm” ecosystem observed at the end of the tenth year may have collapsed to “p+ sm” as a result of the extinction of planktivorous fish.

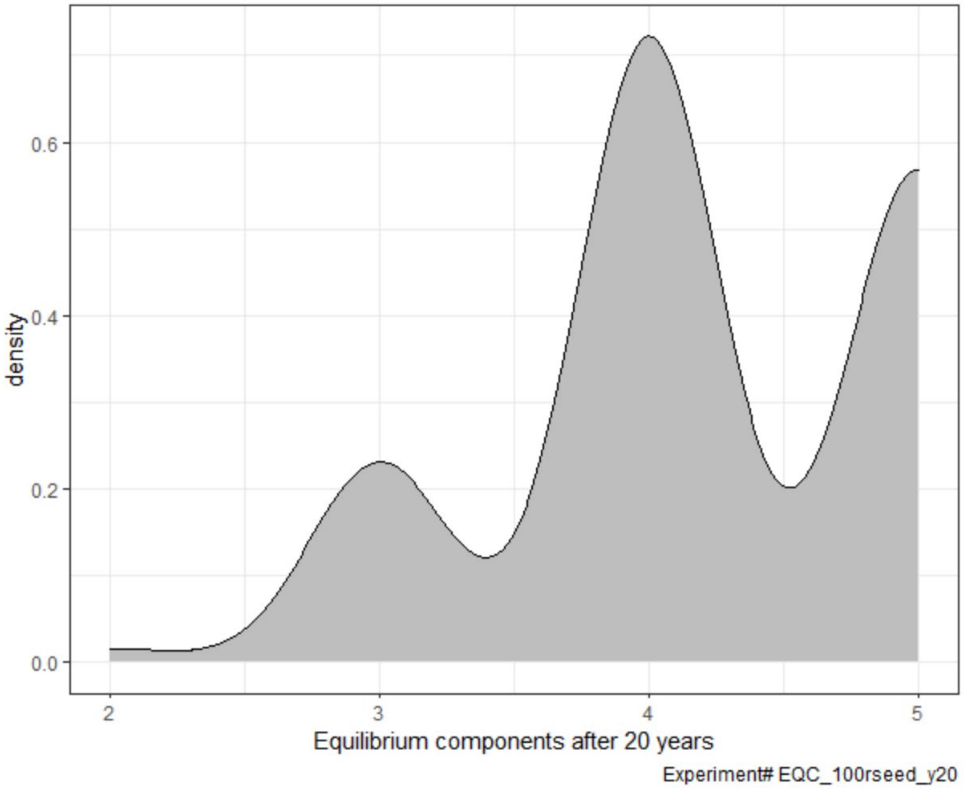

Figure 4-15: Probability density distribution of component numbers in steady states after 20 years of undisturbed simulation

The full matrix of population changing patterns for these ecosystem assemblages, shown in Figure 4-16, provides an intuitive sense of the steady-state behavioural patterns involved in this experiment. The scale of the coordinates is the same for each small window, which means that differences in population and magnitude can be visually compared. Over the 20 year period of this simulation, some systems have established an extremely stable state (e.g. -

2093836078 in the top leftmost corner), with the last remaining functional group of population changes appearing almost flat. Some systems reach dynamic equilibrium eventually, with population changes ending up as oscillations of regular cycles (such as -1157874135 in the third row of the fourth column), while others end up with an equilibrium in which the population of a functional group is overwhelmingly dominant in such a way that it is impossible to tell the extent of population change in other minority groups relative to the total population of their group (such as 2145391771 in the bottom right corner). Some aspects of the simulated system do not look like they have reached equilibrium by the end of year 20, particularly in terms of the way that the population change trends for submerged plants and zooplankton show instabilities (the rightmost three simulations in the third row, for example). In summary, the emergent phenomena produced by this ABM range from equilibrium patterns that were expected at the time of design to patterns of ecosystem state changes that do not appear to have reached equilibrium after 20 years and show some signs of stochasticity. The preliminary examination offers a list of random seeds and their development patterns for use in experiments.

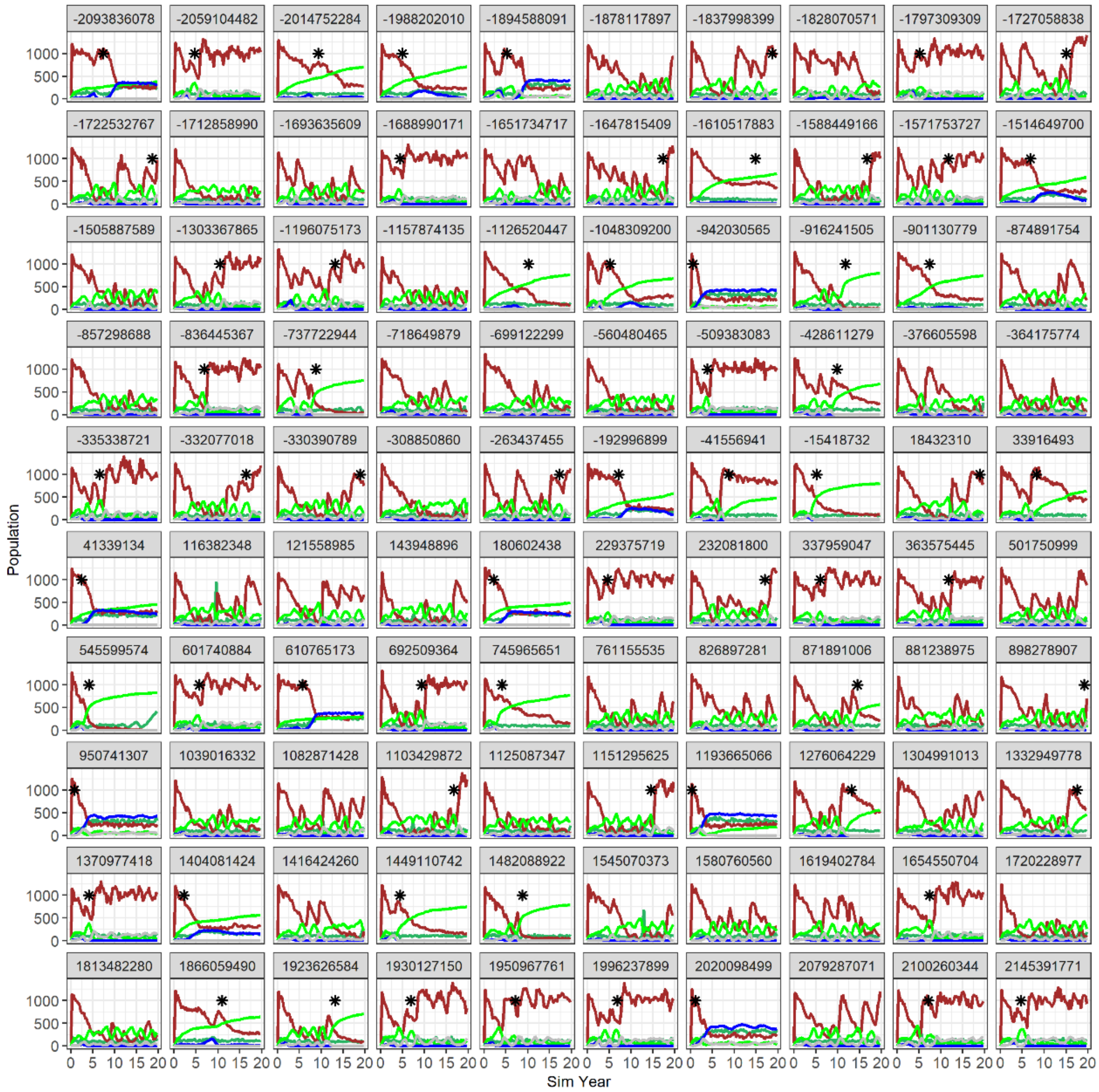

Figure 4-16: Overview of population change patterns in the runs in Experiment# EQC_randomseed_y20. The top of each small panel shows the Netlogo random-seed number, and the horizontal axis represents the year time of the simulation while the vertical axis represents population size. Dark green represents phytoplankton, red-brown represents zooplankton, light green represents submerged plants, blue represents planktivorous fish and grey represents herbivorous fish. Asterisks on the panels show the point when piscivorous-fish disappeared because their numbers are too small to be seen as lines.

4.7.1.2 Sensitivity of population numbers to initialisation

The sensitivity index μ^* in the Morris Elementary Screening method show that the initial condition of temperature, nutrient level, and number of planktivorous fish are the most important controlling factors to phytoplankton, zooplankton and planktivorous fish in the model and these inputs have strong interactions with other inputs due to high σ. Zooplankton population was more affected by the initial amount of planktivorous fish than the nutrient level. The initial amount of submerged macrophytes and piscivorous fish as well as water depth are the least influential inputs for phytoplankton and zooplankton. The μ^*- σ plots for algae, zooplankton and planktivorous fish show strong nonlinear effects because most points fell in the region between function y= x and y= 2x. To submerged macrophytes, the factors were not interactive with each other with small σ values.

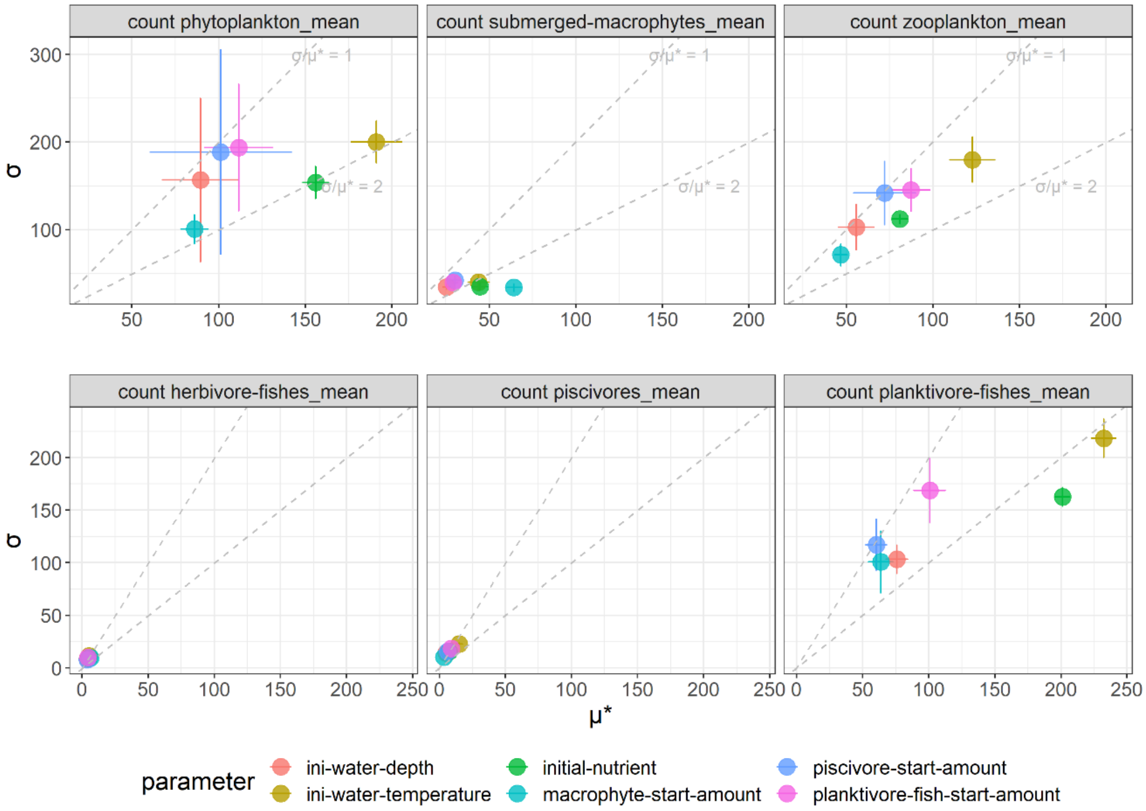

Figure 4-17: Elementary effects of parameters through Morris screening methods (the "μ^*" represents factor importance and "σ" represents interaction)

Table 4-13: Mean elementary effects of parameters on biotic communities

parameter	μ-p	μ-z	μ-pf	μ-sm	μ-hf	μ-pisci
ini-water-temperature	191.064	122.838	232.38	43.968	5.238	15.15
initial-nutrient	156.006	81.018	201.126	44.688	4.908	7.44
planktivore-fish-start-amount	111.57	87.366	100.884	29.304	4.416	9.18
piscivore-start-amount	101.262	72.15	60.402	30.444	3.798	6.372
ini-water-depth	89.52	55.842	75.99	25.422	3.918	5.28
macrophyte-start-amount	86.1	46.86	63.732	64.308	6.498	3.462

The variance decomposition by Soboljansen Method shows the nutrient and temperature contribute the most in total variance, much higher than other parameters like water depth, initial amounts of fishes. In first-order variance, temperature contributes less than nutrient concentration, initial amounts of fishes and water depth.

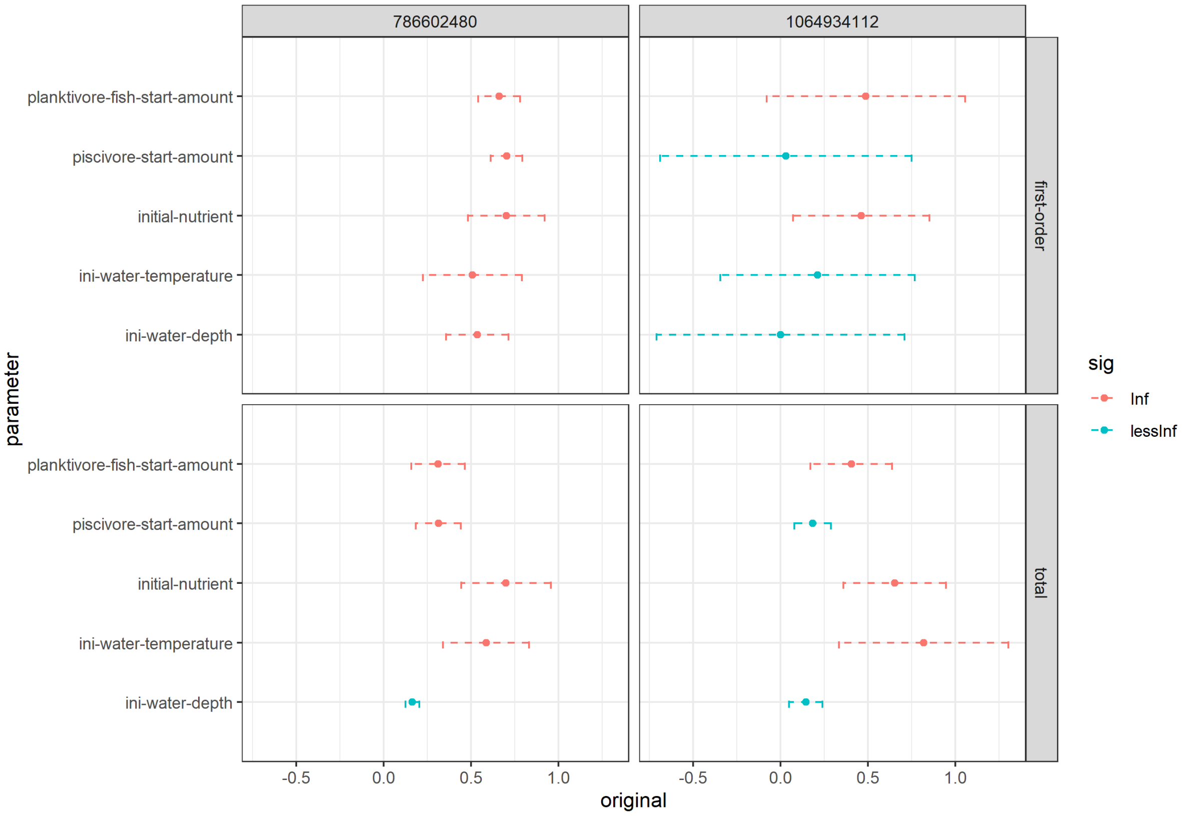

Figure 4-18: First-order and total-order Soboljansen's indices for important parameters. The parameters exhibiting more contribution is drawn in red while the less important parameters in cyan.

Besides the quantitative estimates of sensitivities, scatter plots intuitively show the responses of the model's output $f(X)$ to changing input variables x_i. When the water temperature varies between 10 to 30 Celsius degrees, there was a clear spectrum in population number of phytoplankton, zooplankton, planktivorous fish and submerged macrophyte while herbivorous and piscivorous fish often went extinct in low temperature. Transgressing a certain threshold, the trend of ecological responses to the temperature headed to a different direction.

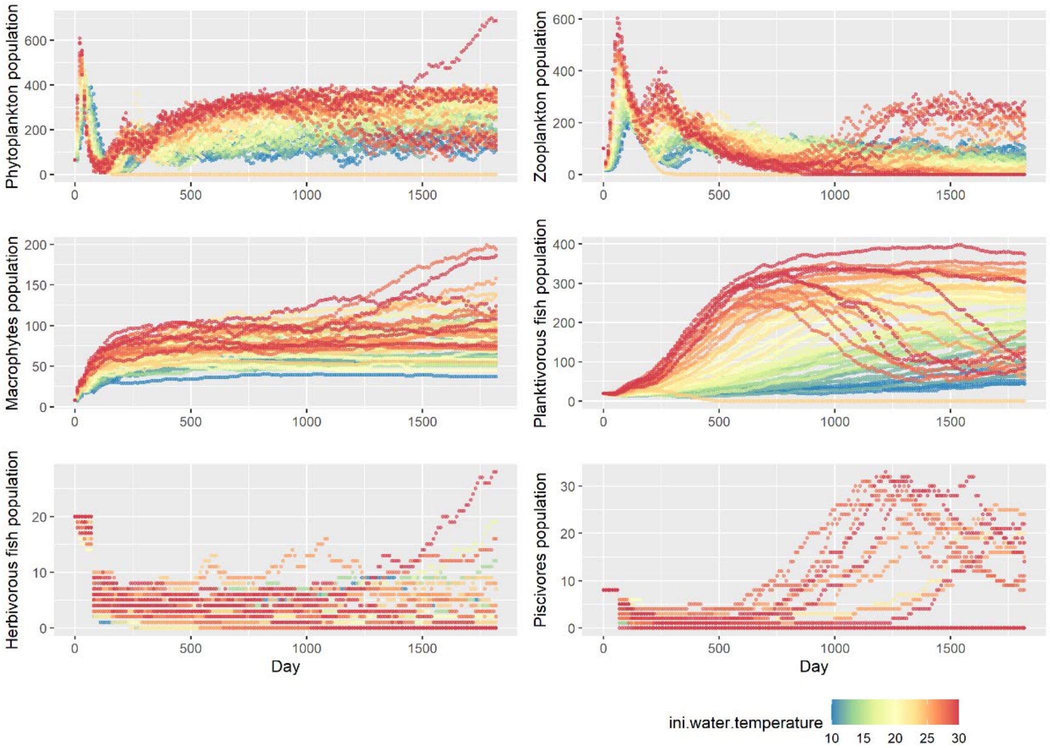

Figure 4-19: Population change in sensitivity tests on temperature (ranging from 10 to 30 ℃)

The population changes with nutrient level, varying from 15 to 35 μg/L show a very similar pattern to the ecological responses to temperature change. The effect of nutrient level on each component seems linear within an observed range.

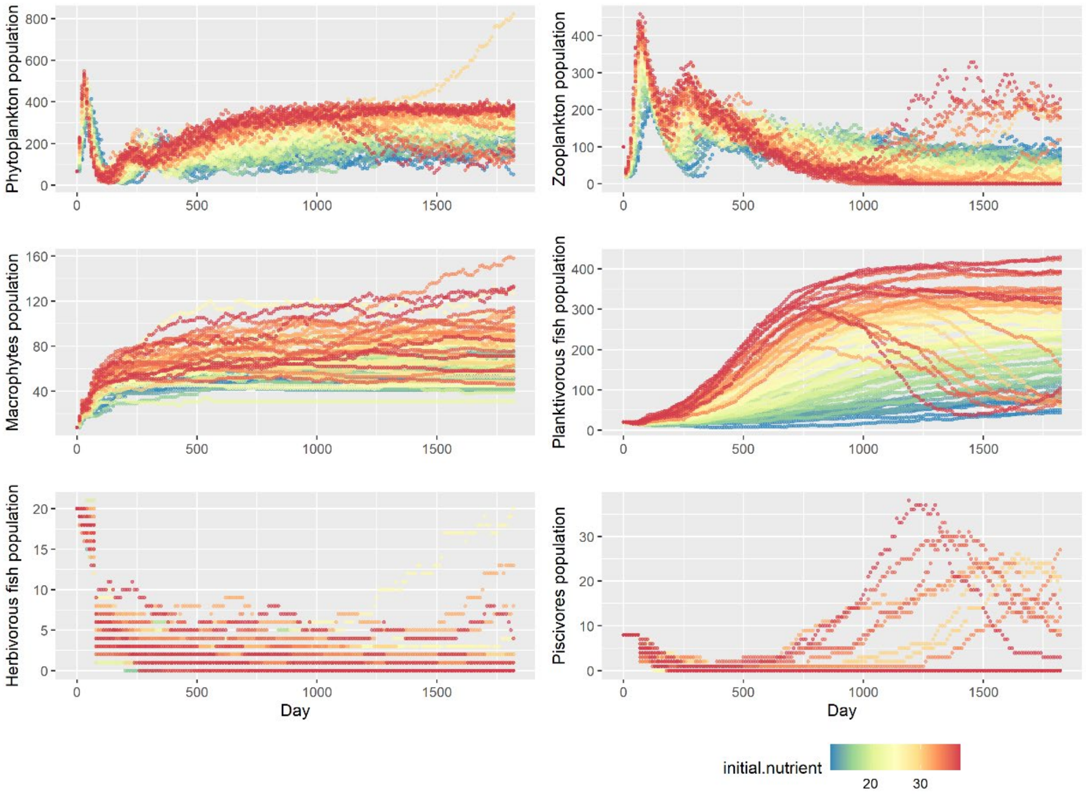

Figure 4-20: Population changes in sensitivity tests on total nutrient level (ranging from 12 to 38 µg/L)

Apart from the dominant factors, the effects of water depth and the initial amount of planktivorous fish on the population numbers of components seem negligible as there are little difference.

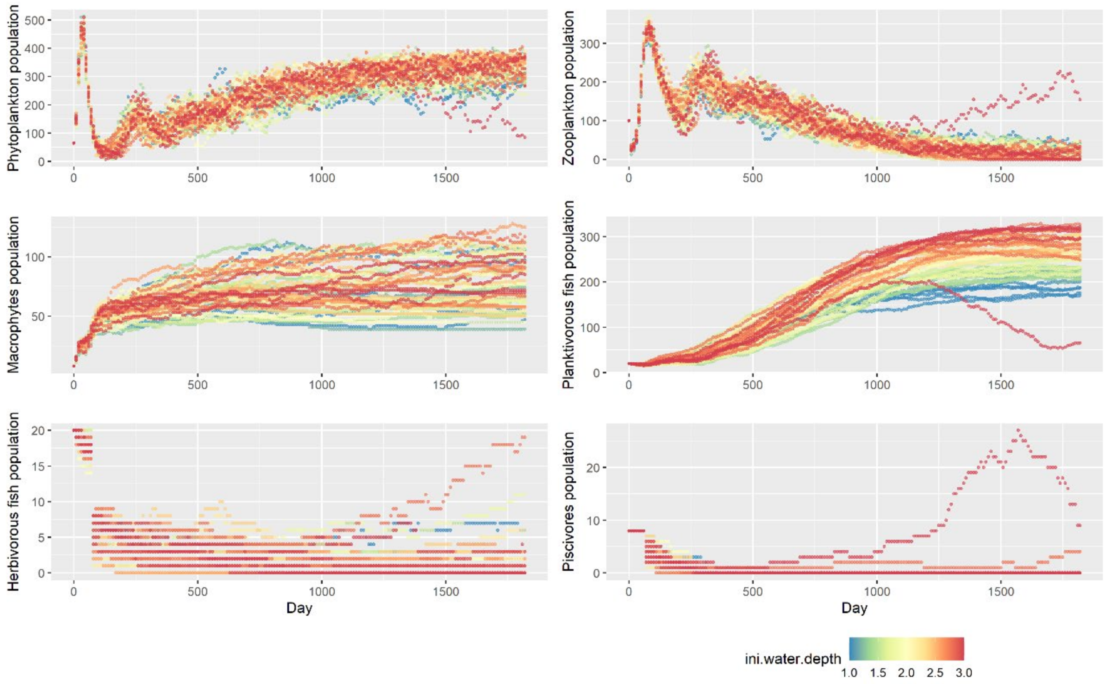

Figure 4-21: Population changes in sensitivity tests on water depth (ranging from 1.0 to 3.0 m)

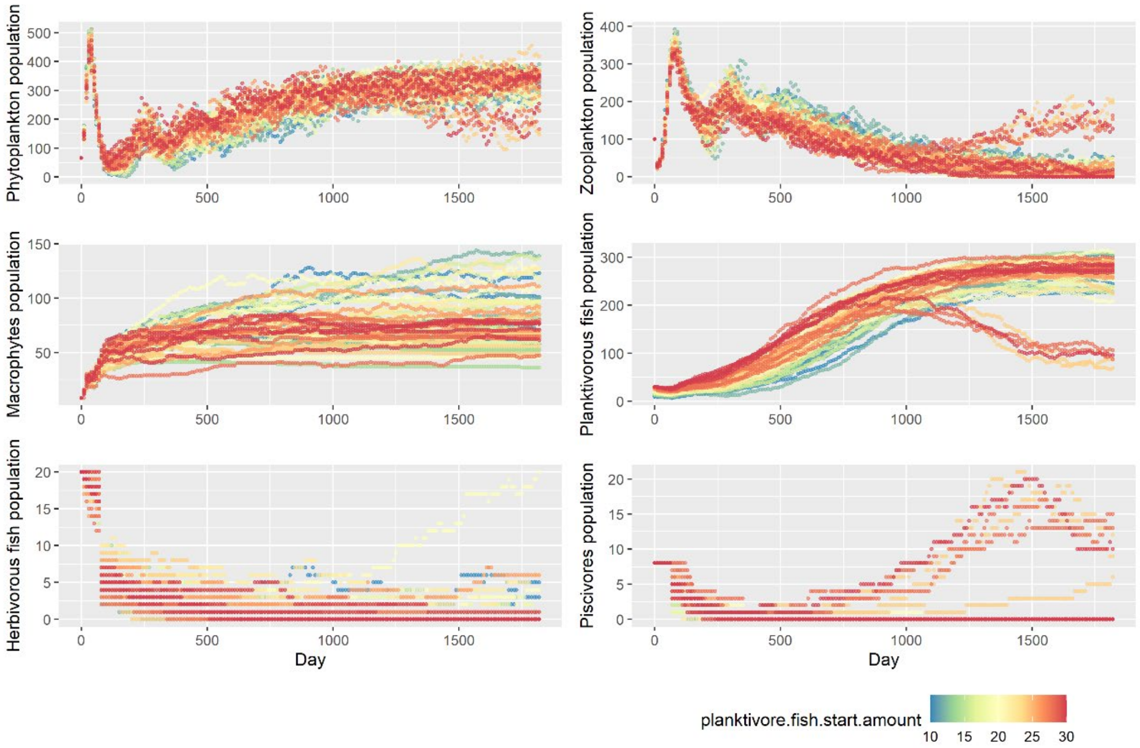

Figure 4-22: Population changes in sensitivity tests on initial planktivorous fish amount (ranging from 10 to 30 ind.)

4.7.1.3 Sensitivity of population numbers to biological parameters

The sensitivity analyses to endogenous parameters show the effects of the predefined attributes on the ecological responses. In the figures below, the Partial Correlation Coefficients of the biological parameters show that planktivorous and herbivorous fish seem less responsive to the endogenous parameters than the other four components. The parameter “phytoplankton_reproduce_rate” is positively related with phytoplankton, zooplankton piscivorous fish while the probability of zooplankton hunting for prey is negatively related to these three components. Phytoplankton was positively correlated with the parameters of “phytoplankton_reproduce_rate”, “herbivore_reproduce_rate”, and “planktivore_reproduce_rate”. Submerged macrophytes were positively correlated with “zoopk_hunt_rate”, “macrophyte_reproduce_rate”, “piscivore_reproduce_rate” and “pisci_hunt_rate”. The reproduction rate of phytoplankton is positively related to the food web involving planktons and planktivorous fish and negatively related to the food web involving macrophytes and herbivorous fish. The effect of “zoopk_hunt_rate” is totally reverse.

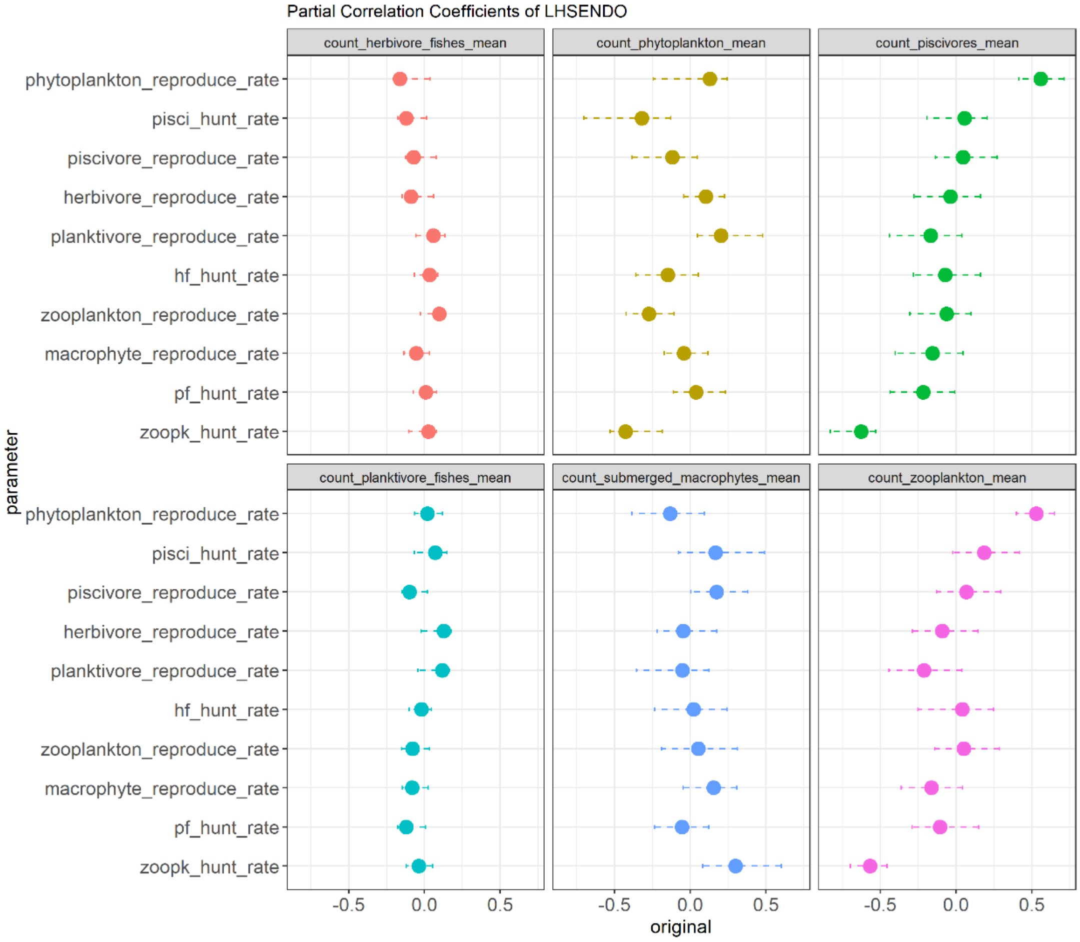

Figure 4-23: Partial Correlation Coefficients of the endogenous parameters in the model

4.7.1.5 Calibration of biological parameters

The ABC rejection calibration was performed following a LHS experiment design. The biological parameters varied in ranges, as shown in the table below. Ten samples of parameter combinations were tested with 100 random seeds. The output metrics are "phytoplankton-concentration", "zooplankton-concentration","sm-concentration" and "fish-concentration" at the 5000th step of simulation.

Table 4-14: Biological parameters and their variations in the LHS experiment design. Parameters were randomly taken from these ranges and used to run experiments.

	Min	Max	Step	Random distribution
phytoplankton-reproduce-rate	20	100	20	qunif
zooplankton-reproduce-rate	20	100	20	qunif
macrophyte-reproduce-rate	20	100	20	qunif
planktivore-reproduce-rate	20	100	20	qunif
herbivore-reproduce-rate	20	100	20	qunif
piscivore-reproduce-rate	20	100	20	qunif
zoopk-hunt-rate	20	100	20	qunif
pf-hunt-rate	20	100	20	qunif
hf-hunt-rate	20	100	20	qunif
pisci-hunt-rate	20	100	20	qunif

The target of the output metrics was set as "phytoplankton-concentration" = 0.009, "zooplankton-concentration" = 0.001, "sm-concentration"= 0.15 and "fish-concentration" = 0 according to the realistic pattern in Taibai Lake described in Subsection 4.3. The tolerance threshold was 0.3, and the resulting rejection distribution of parameters is shown in the following figure.

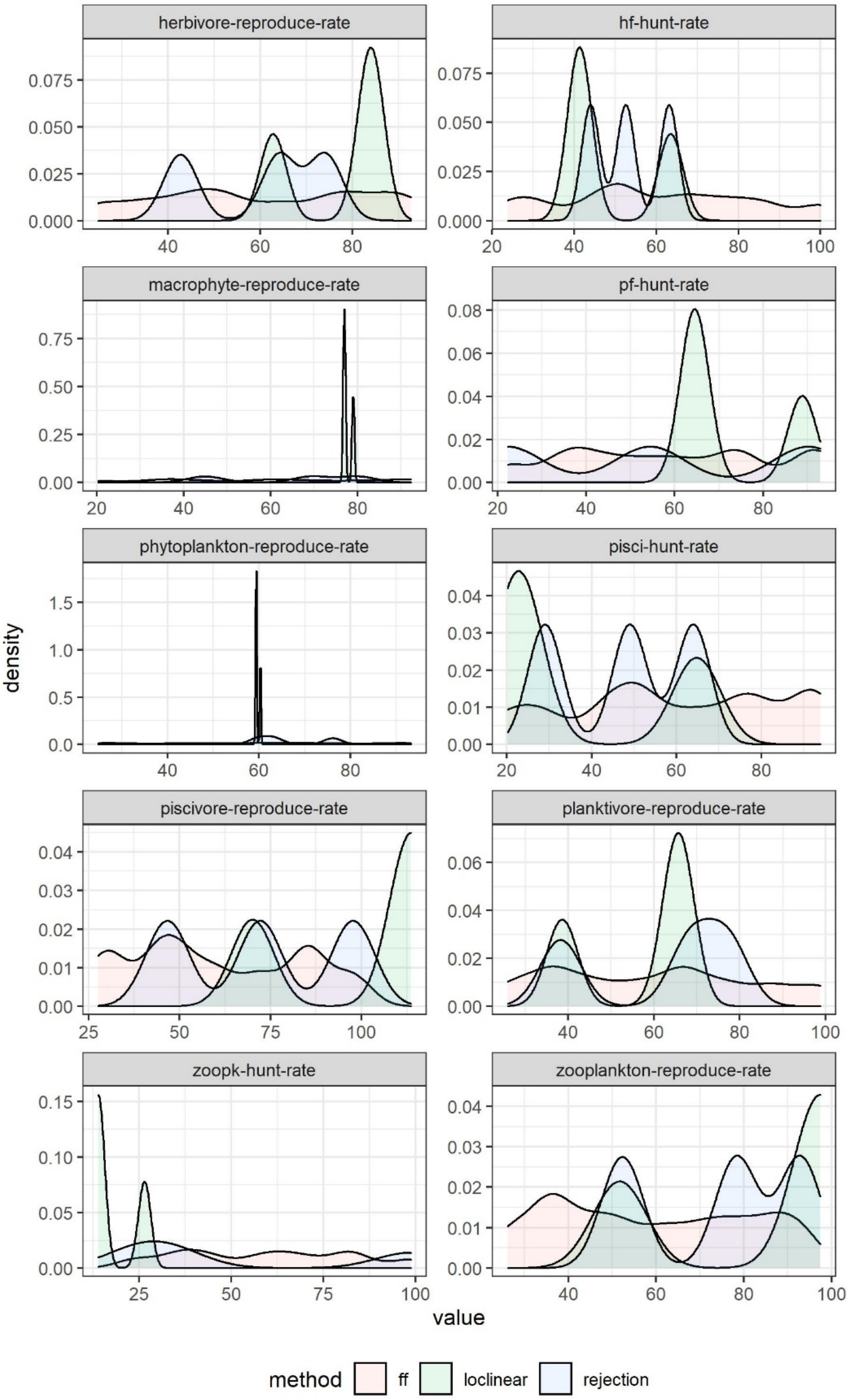

Figure 4-24: Density distribution of metrics against target values using full factor, local linear and rejection methods. The pink transparent areas show all tested parameter ranges in the LHS design. The green transparent areas show the fit ranges of parameters and the blue areas show the rejection parameters against the target.

4.7.2 Dynamic changes contributing to various patterns of equilibria

Based on the 100 experiments described above, data on the six patterns of equilibrium state were filtered for the respective system development pathways and further analysed for their formation mechanisms. The analysis in this subsection deconstructs the stages of change in the composition of the system at a finer resolution of scale and looks for any common emergent patterns of behaviour.

4.7.2.1 Homeostasis of "p+sm"

The ecosystem state with the fewest components is the "p+sm" state, which is shaped by two important events. One was the successive extinction of fishes after Day 1000, and the other was the extinction of zooplankton around Day 6000. The first event led to a rapid rise in the population of submerged plants and the second to a breakthrough and a steady rise in the algal population from a long stable range.

The rapid succession of fish extinctions benefited the abundant nutrient levels in the water and created sufficient space for primary producer numbers to increase, leading to a dramatic rise in zooplankton. After a while, the population of planktivorous fish also increased due to increases in the number of zooplankton and phytoplankton, but the same trend of increase in herbivorous fish gradually created a depressing effect on the population of their food. After about 200 days, the population of piscivorous fish also increased due to the abundance of food, but at this point planktivorous and herbivorous fish, which were declining due to the feedback effects of declining zooplankton and submerged plants, found themselves under simultaneous top-down pressure from piscivorous fish. Inhibited by the pressure and by other stochastic factors such as encounters with predators, planktivorous and herbivorous fish soon became extinct. Piscivorous fish also died out quickly due to lack of prey. Submerged plants increased rapidly after the decline of herbivorous fish and continued to do so until after the extinction of herbivorous fish.

It was difficult to evaluate the cause of the zooplankton extinction in terms of changes in functional group populations. It was relatively unusual that zooplankton responded to an upward pressure reduction following the extinction of planktivorous fish only briefly and did not continue to grow, but declined to extinction. Based on an analysis of the overall pattern of change and the relationships between the various components of the ecosystem, it is reasonable to assume that submerged plants were responsible. The massive growth of submerged plants increased competition for light and space, resulting in slow growth rates and low distribution densities of phytoplankton. Individual zooplankton were not able to access food in terms of both amount and location. Under conditions in which algal growth was slow and impeded by large numbers of submerged plants, it is possible that some of the zooplankton died due to lack of energy intake over several days. Another scenario, which also occurred in other situations, is that the zooplankton population slowly decreased to a set number, and then the phytoplankton population gradually grew, creating a dynamic balance between the two. However, phytoplankton were prevented from development by large numbers of submerged plants, and were unable to respond well to the decline in zooplankton. At Day 5701, the number of zooplankton increased to 17, compared to 112 phytoplankton and 805 submerged plants. Across 961 hectares, these 17 zooplankton would have more difficulty in obtaining food in a timely manner given the rules of mobility and the probability of predation, eventually leading to the group's extinction. With only phytoplankton and submerged plants left, it can be assumed that the two functional groups "p+sm" would gradually reach a competitive equilibrium and then remain very stable.

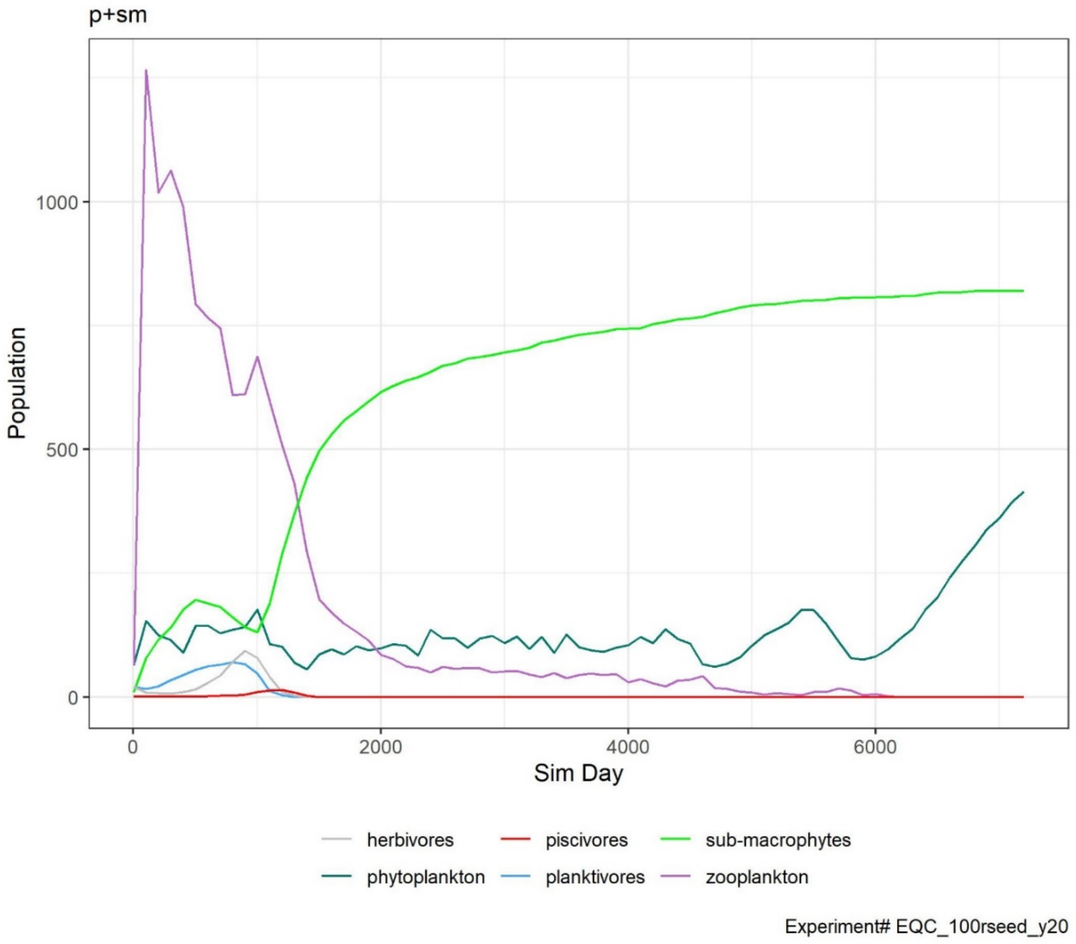

Figure 4-25: Population change of components in experiments that resulted in "p+sm" system composition using random seed 545599574.

4.7.2.2 Homeostasis of "p+z+sm"

In the scenario generated using random seed 18432310, planktivorous fish became extinct on Day 1901 and piscivorous fish on Day 6901. Of the "p+z+sm" states, few reached a steady state and most continued to develop. There are two general scenarios, one in which zooplankton fluctuate over a long period of time in response to fluctuations in submerged plants and herbivorous fish, and another in which the early extinction of herbivorous fish led to a large growth of submerged plants, leading in turn to a slow decline in zooplankton as the growth rate of phytoplankton decreased. In terms of zooplankton populations, the peak that occurred after the period of adaptation had passed almost always followed the peak of herbivorous fish, and the extinction of herbivorous fish also tended to follow their own population peaks. This is interesting, insofar as there is no direct predation between zooplankton and herbivorous fish or submerged plants, but the zooplankton-phytoplankton predation relationship and the competition between phytoplankton and submerged plants created a distinct correlation between them. The submerged plant coverage reduced the growth rate of phytoplankton by reducing light attenuation, while the dominance of submerged plants led to a reduction in the growth and reproduction rate of algae and a dramatic reduction in the population under the grazing pressure of zooplankton. The reduction in algal populations further led to a dramatic decline in zooplankton. In this category, the system state is similar to that of "p+sm", but here the herbivorous fish survive for a longer period, delaying the point at which phytoplankton are stressed by the growth of large numbers of submerged plants. However, the phytoplankton remained under pressure for their survival and the population remained at a low but stable level.

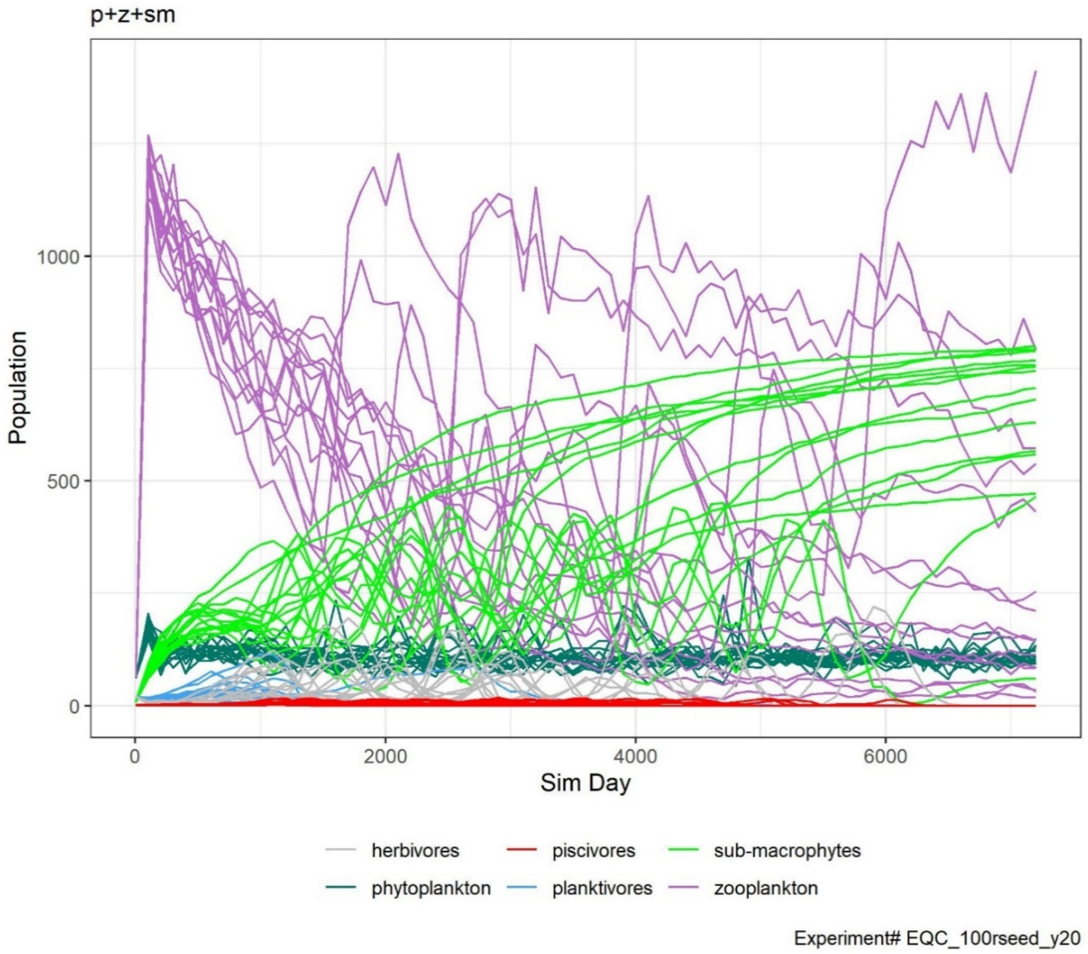

Figure 4-26: Population changes over time in experiments that resulted in the “p+z+sm” system composition. The random seeds that generated the experiments are 1923626584, -15418732, -1126520447, 1482088922, -428611279, -737722944, -1727058838, 1449110742, -41556941, 1332949778, 33916493, 871891006, 1276064229, 745965651, -916241505.

4.7.2.3 Homeostasis of “p+z+sm+pf”

The last systems in the “p+z+sm+pf” state formed a more stable pattern of coexistence earlier than the previous two states. In terms of zooplankton, most systems reached a steady state after 4000 days and showed no significant shift in trends. Compared to the previous “p+z+sm” scenario, the systems here show very early extinctions of herbivorous fish (around 1000 days) and piscivorous fish, a high number of planktivorous fish and consequently a suppressed zooplankton population. Following the demise of piscivorous fish, the relationship between phytoplankton, zooplankton and planktivorous fish was adjusted and balanced. The reduction of zooplankton to around a quarter of their previous population as a result of the massive increase in planktivorous fish greatly reduced the pressure on the number of phytoplankton to be grazed, leading to an increase in their numbers and further sustaining the survival of zooplankton. Due to the increase in the rate of phytoplankton production, the growth of competing submerged plants was not as abundant as it was in the “p+sm” and “p+z+sm” scenarios and was evenly distributed over a range due to the timing of the extinction of herbivorous fish (187-746 on Day 7201). Some planktivorous fish were already low in numbers by year 20, but zooplankton and phytoplankton were still abundant as food sources, so it is unlikely to have wiped out planktivorous fishes in such a short period of time.

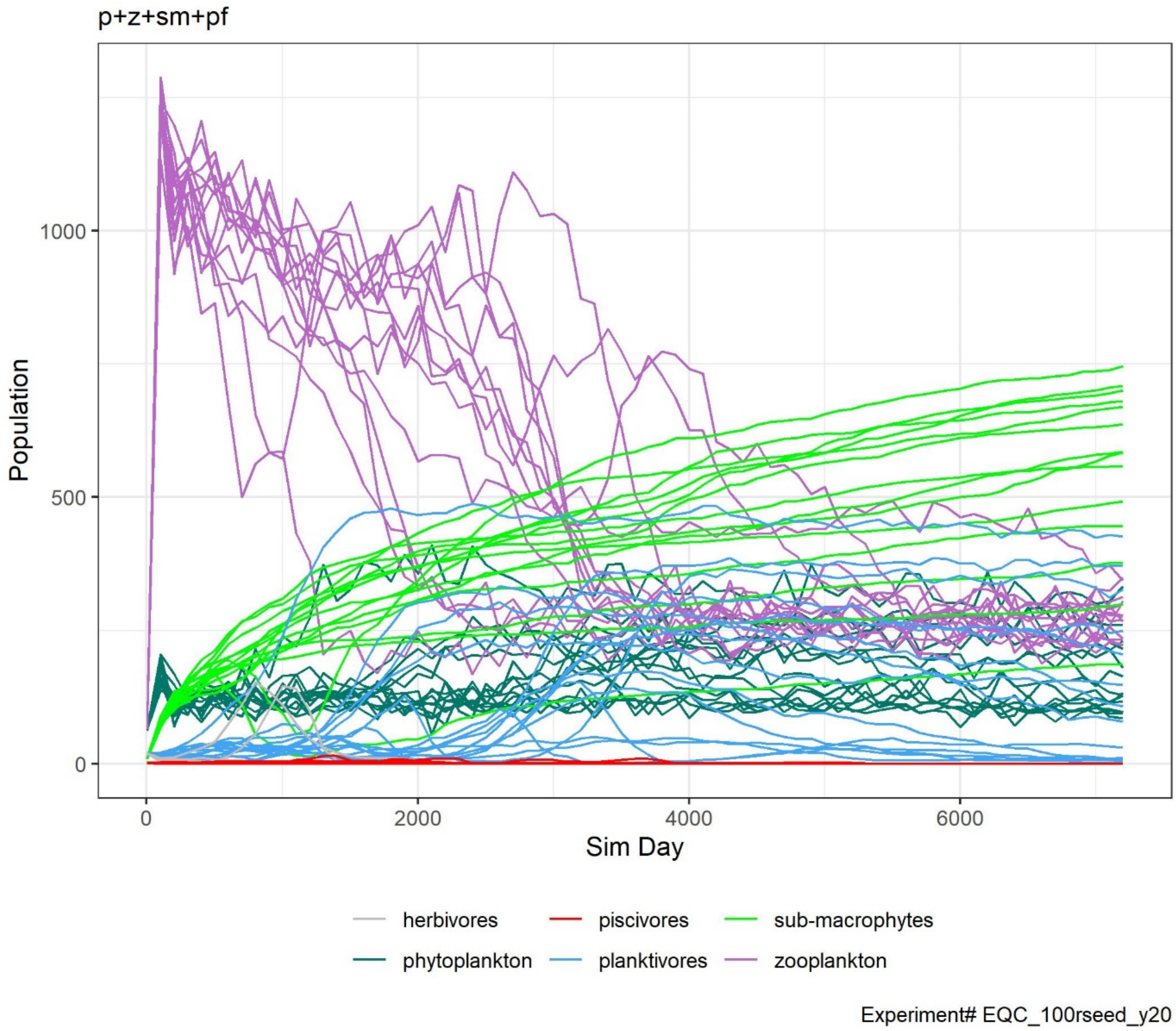

Figure 4-27: Population changes over time in experiments that resulted in the "p+z+sm" system composition. The random seeds that generated the experiments are 180602438, -1610517883, -1514649700, -2093836078, -2014752284, -1048309200, -1988202010, -192996899, -901130779, 1404081424, 41339134, 1193665066.

4.7.2.4 Homeostasis of "p+z+sm+hf"

In this "p+z+sm+hf" system, the ecosystem components entered into a regular dynamic cycle early on and were characterised by the early extinction of planktivorous fish. As found in the "p+z+sm" scenario, zooplankton-phytoplankton and herbivorous fish-submerged plants formed links due to competition between producers. The zooplankton population changed up and down dramatically according to the availability of food. In order to clearly observe the formation of homeostasis in this scenario, I randomly selected a scenario for analysis because of the similarities between the system interactions in this scenario.

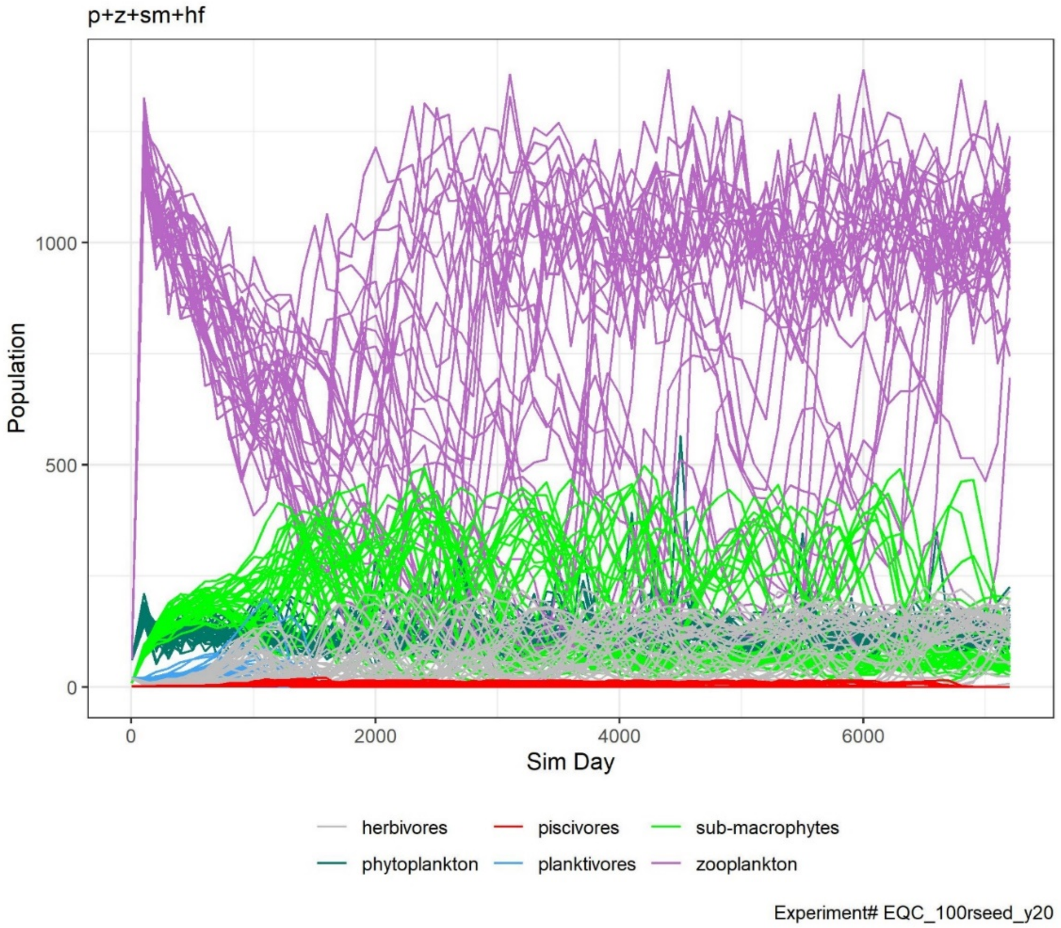

Figure 4-28: Population changes over time in experiments that resulted in the “p+z+sm+hf” system composition. The 33 random seeds that generated the experiments are listed in the end of this section due to large size.

In this scenario, it was the zooplankton (purple line) that were dominant in population terms. Zooplankton experienced a decline and then rose to a higher population size and remained relatively stable. The first population decline in zooplankton was mainly due to grazing by planktivorous fish (blue line). However, at Day 1201 planktivorous fish were exterminated by increasing numbers of piscivorous fish, reducing the downward pressure on zooplankton and creating the first zooplankton population bounce. Fluctuations in the populations of piscivorous and herbivorous fish followed, eventually culminating in the extinction of piscivorous fish on Day 2501 at the lowest point of the fluctuating cycle of herbivorous fish. Compared to other scenarios, the submerged plant population here was affected by greater downward pressure as herbivorous fish became the top predator in the food web. The herbivorous fish population could reach a maximum of 220, whereas after Day 3000 the maximum number of submerged plants was only 137 (Day 5101). This happened because around 500 days after the extinction of the piscivorous fish, the herbivorous fish population grew from its lowest point to over 200, greatly inhibiting the growth of submerged plants. With submerged plants suppressed, phytoplankton were able to grow rapidly because of the space and light they received. Zooplankton, which feed on phytoplankton, therefore grew rapidly to high levels, and despite some lag time correlated positively with changes in the population of phytoplankton. The state of the lake ecosystem remained relatively stable in this series and could be maintained for a long time providing herbivorous fish do not become extinct.

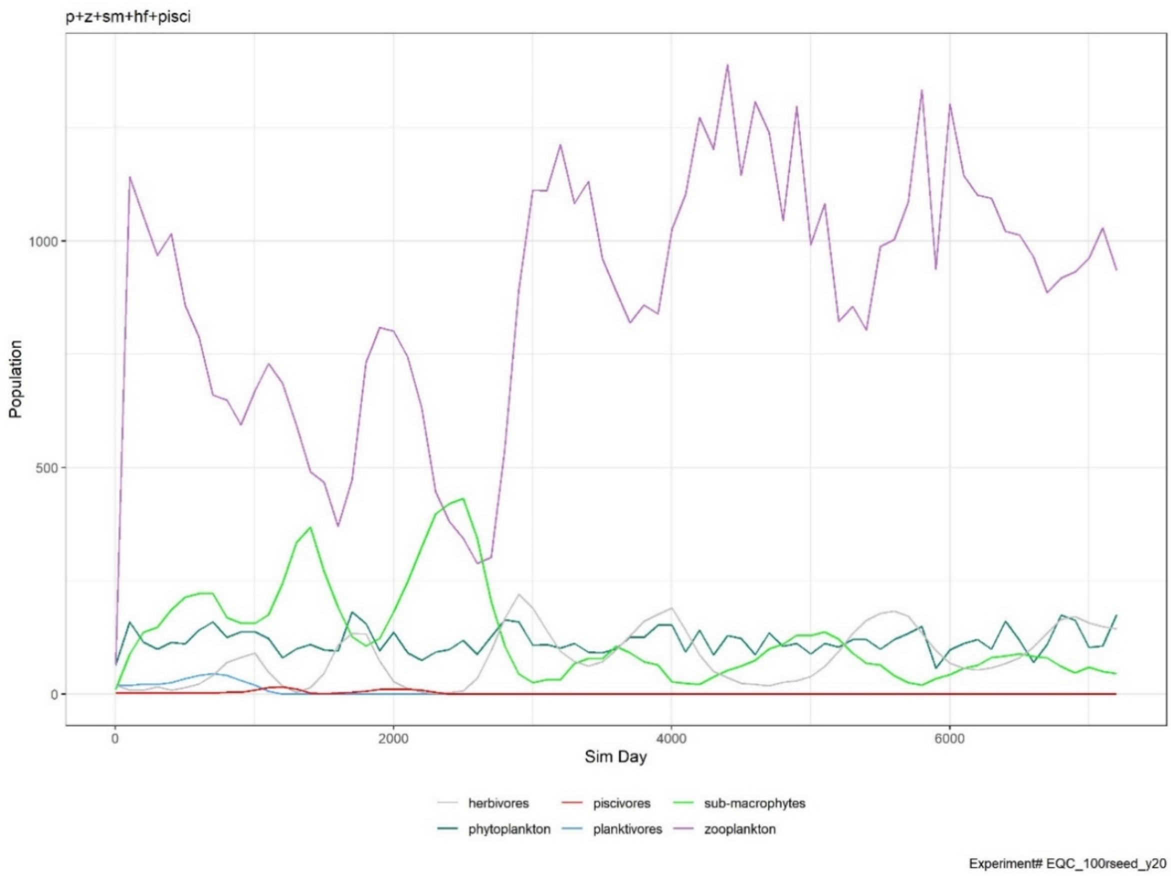

Figure 4-29: Population changes over time in experiments that resulted in the "p+z+sm+hf" system composition, generated by seed -335338721. The random seeds that generated this pattern are -335338721, 229375719, -1797309309, 337959047, 1950967761, -836445367, 898278907, -1571753727, 601740884, 692509364, 1930127150, -263437455, -509383083, 2145391771, -1303367865, -1196075173, 363575445, -1837998399, -332077018, 1996237899, 1103429872, 1654550704, -1588449166, 18432310, -330390789, -1722532767, -2059104482, 1370977418, 1151295625, -1647815409, 232081800, 2100260344, -1688990171

4.7.2.5 Homeostasis of "p+z+sm+pf+hf"

The "p+z+sm+pf+hf" and "p+z+sm+hf" states were formed according to essentially the same mechanism, but during the initial adaptation stage both planktivorous and herbivorous fish escaped the predation of piscivorous fish, meaning that piscivorous fish became extinct first.

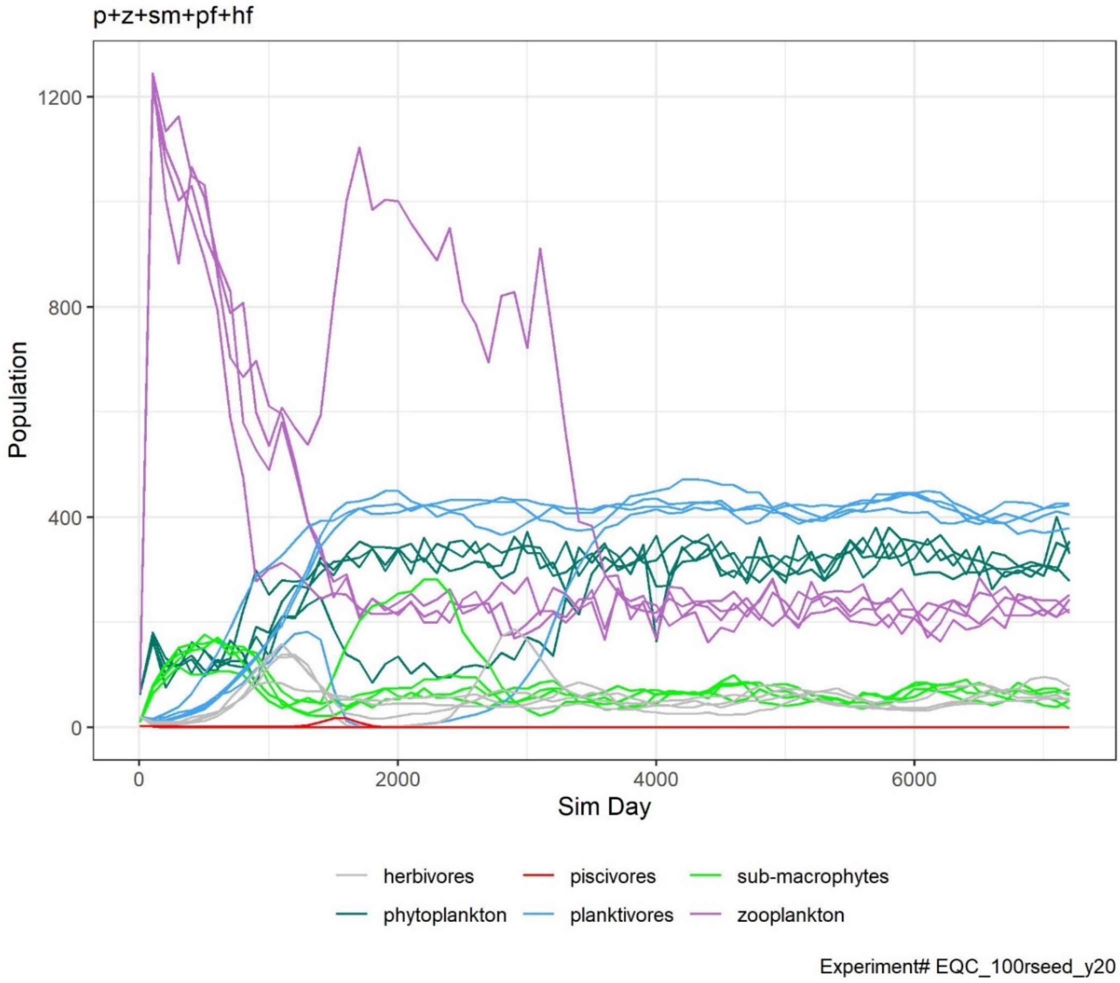

Figure 4-30: Population changes over time in experiments that resulted in the “p+z+sm” system composition. The random seeds that generated the experiments are 950741307, -1894588091, -942030565, 2020098499.

This state is relatively infrequent but seems to have remined stable between Day 4000 and Day 7300. The dominant population in this steady state was planktivorous fish, which fluctuated at around 400. The population curve of planktivorous fish took the form of an 'S' shape, first rising slowly and then more rapidly before reaching a plateau and limiting further growth. When piscivorous fish later became extinct, planktivorous fish would form a similar S-shape later. The only factors limiting the growth of planktivorous fish were bottom-up, such as limits to the number of zooplankton and phytoplankton. The number of zooplankton decreased sharply as the large numbers of planktivorous fish increased, allowing the phytoplankton to grow with less grazing pressure. Within this small food web of phytoplankton-eating fish - zooplankton - phytoplankton, the overall trend in phytoplankton and phytoplankton-eating fish remained the same, in contrast to the number of zooplankton. In the other food chain, herbivorous fish grazed upon submerged plants more freely after the pressure of predators was removed, keeping their numbers at a low level to reach equilibrium and allowing space and resources for phytoplanktons to grow. This steady-state pattern was already relatively smooth by the end of Year 20, and represented a suitable pattern of systemic change for undertaking controlled experiments.

4.7.2.6 Homeostasis of "p+z+sm+hf+pisci"

The " p+z+sm+hf+pisci" state was the most hierarchical in terms of food web relationships, and no system was found in this experiment in which all six functional groups co-existed. The remaining relationships in these systems included zooplankton-phytoplankton and piscivorous fish-herbivorous fish-submerged plants. In terms of population change (Figure 4-31), the magnitude of variations in the components was greater than in the other scenarios. The fluctuation curve for submerged plants (the bright green line) reached a maximum point of around 500, while the minimum point was roughly 50. Variations in zooplankton, the dominant component of the population, were twice as much as they were in submerged plants. It is difficult to conclude whether or not this is a steady state, but each component is restricted to a certain range of variation periodically. The mechanism of the state of this system is analysed below by considering two of the simulations with prominent peaks in phytoplankton abundance.

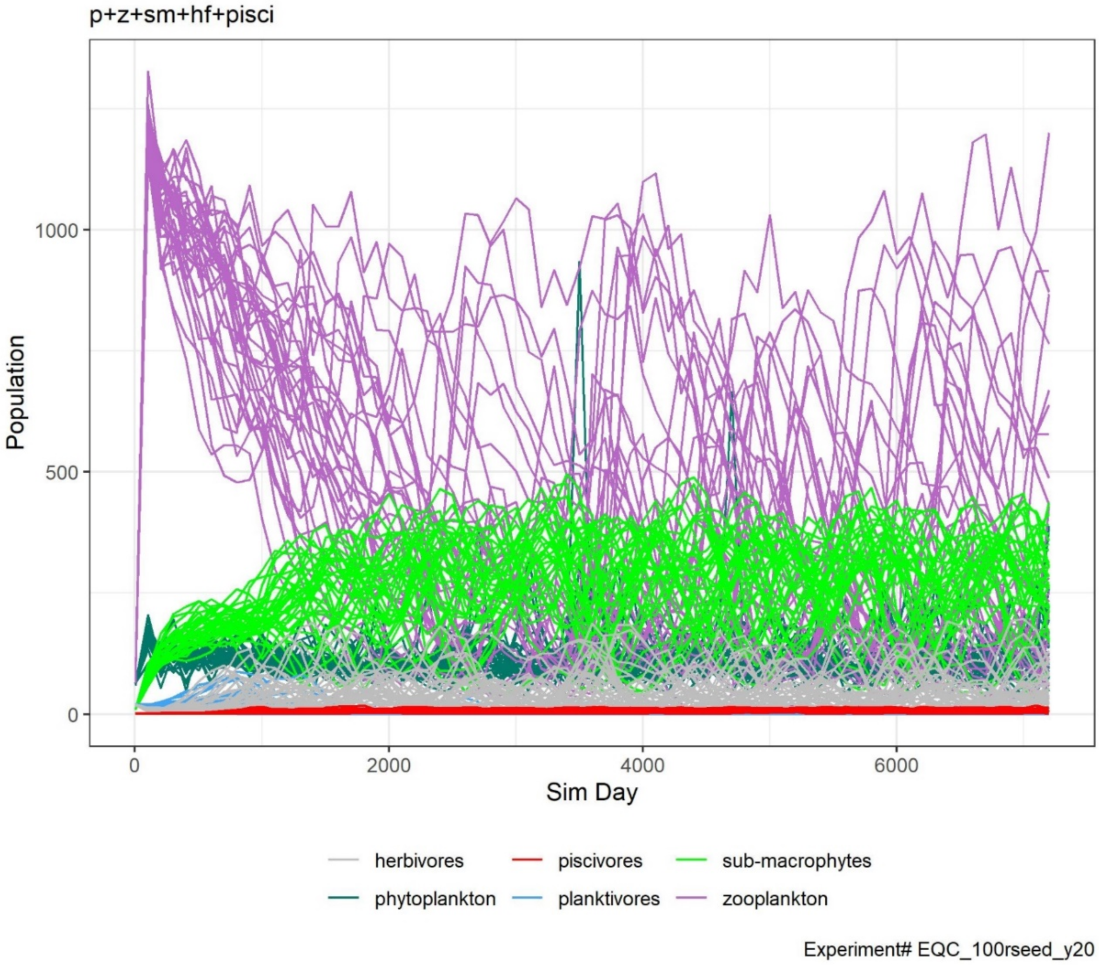

Figure 4-31: Population changes over time in experiments that resulted in the "p+z+sm" system composition. The 33 random seeds that generated the experiments are listed in the end of this section due to their large size.

In both experiments, phytoplankton formed an abrupt peak at around Day 4000 before returning rapidly to its previous average level. For systems in which planktivorous fish became extinct on Day 1201, the phytoplankton peaked on Day 3501, and for systems where planktivorous fish became extinct on Day 2501, the phytoplankton spiked on Day 4701. The time between these two events is 2200 days for one and 2300 days for the other. The extinction of planktivorous fish slowed the downward trend of zooplankton, and with submerged plants under constant grazing pressure from herbivorous fish, the feedback from phytoplankton on the decline in zooplankton numbers was also more rapid, so zooplankton survived. Because zooplankton did not die out, phytoplankton populations were influenced by zooplankton grazing and by competition from submerged plants. Zooplankton were only influenced by phytoplankton so there were no large increases or decreases, as any dramatic changes came from changes in submerged plant populations. Each spike was accompanied by a decline in the submerged plant population, an increase in the herbivorous fish population, and most critically a scarcity of zooplankton. It is reasonable to assume that if these three conditions had not occurred simultaneously, it is likely that zooplankton would have become extinct, as described in the “p+sm” state.

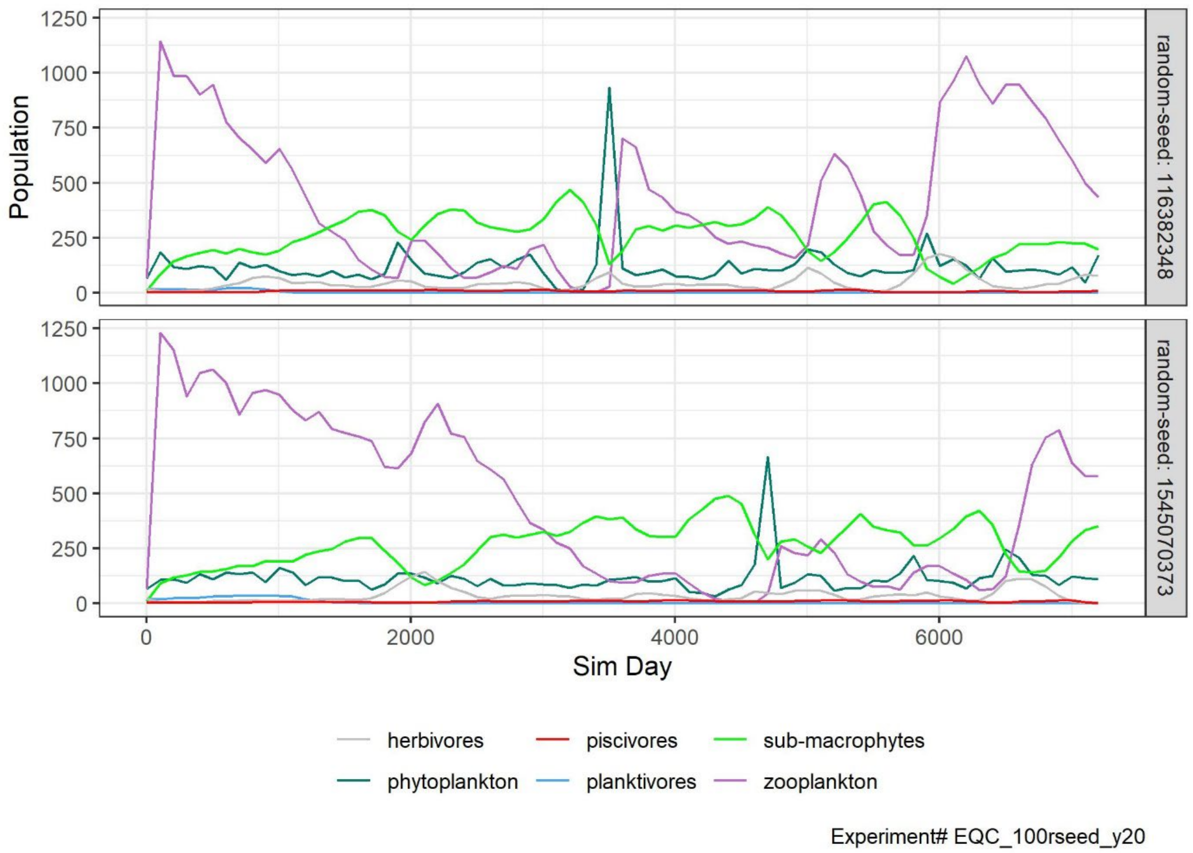

Figure 4-32: Three special cases with extremely high peaks of phytoplankton population (The random seeds that generated this pattern were -376605598, 143948896, 2079287071, 881238975, 826897281, -1828070571,1125087347,761155535,1580760560,-718649879, 1039016332, 1416424260, 116382348, 1545070373, 1720228977, -1693635609, -560480465, -1505887589, -1712858990, 121558985, -364175774, 501750999, -699122299, 1813482280, -1651734717, -874891754, -857298688, 1304991013, 1619402784, 1082871428,-1157874135, -1878117897, -308850860.)

4.7.3 Stochasticity influencing the homeostasis structure

In the previous two subsections, systems generated by different random seeds showed significant differences in functional group demographic changes over time. To further observe the effect of random seeds and their stochastic effect on the simulation of systems with the same parameter settings, the coordinate positions of phytoplankton and zooplankton in the model and the remaining nutrient concentrations in the water body before and after twenty years of ecosystem change (Years 0 and 20) generated by five different random seeds can be seen in Figure 4-33. Results show that initially, even though the random seeds were different, the distribution of both phytoplankton and zooplankton appeared to be even because the number of individuals was the same and individuals were randomly distributed. After 20 years of development, the differences between the systems were shown by the spatial distribution of the communities, the density of distribution and the trophic response of the water body. The nutrient level in the water body also reflects the biomass of the whole ecosystem, showing an up-and-down 'W' pattern (-1974403999, 268024443), a linear decline (1036396851) or a decline followed by an increase (-858908948, 352292986). To summarise, the randomness of the initial set of individual positions and the randomness of the direction in which individuals move and make decisions together determine the eventual highly differentiated system states between the different simulated systems.

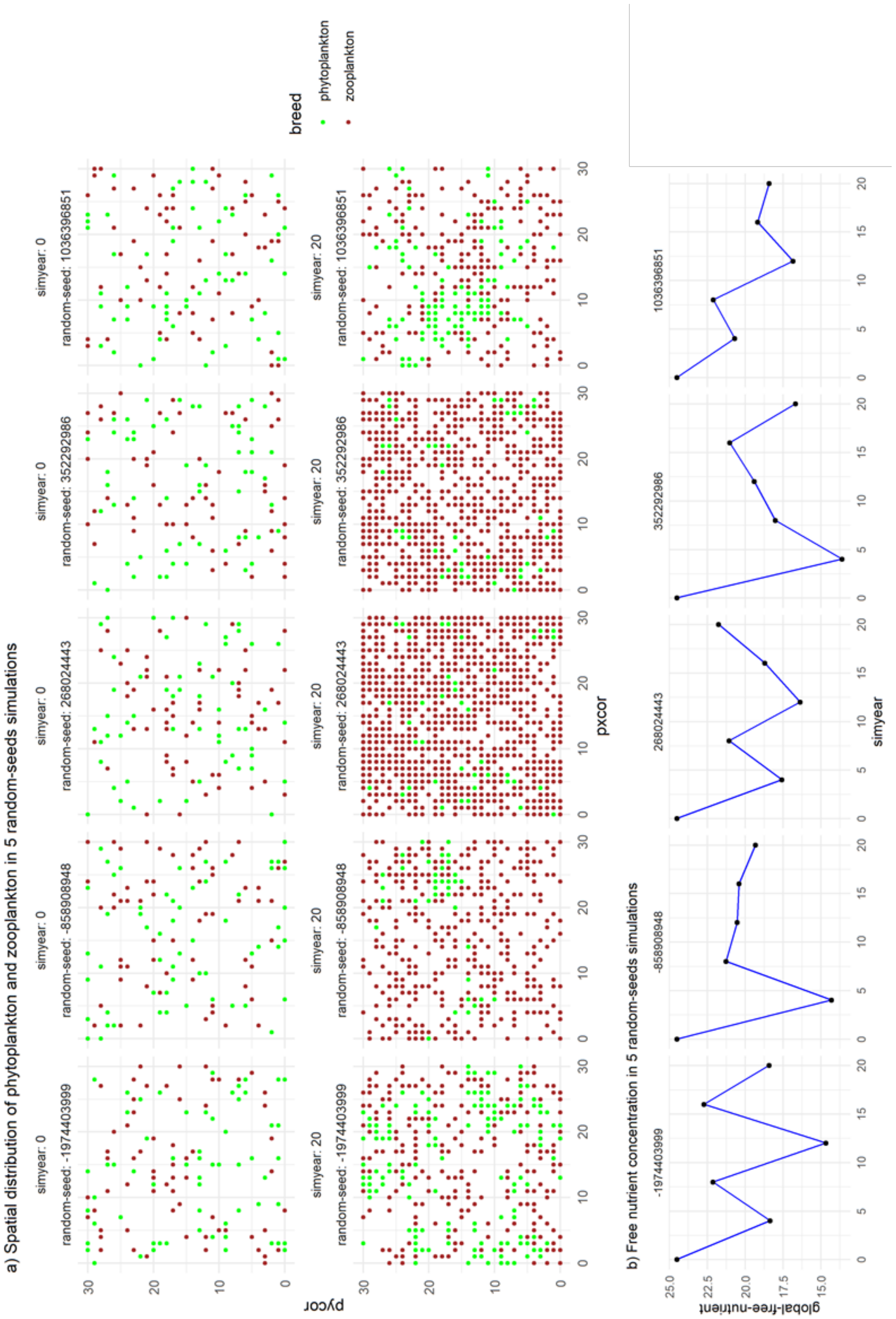

Figure 4-33: Comparison of the spatial distribution of phytoplankton and zooplankton in the ecosystem at the start and 20 years later using 5 Netlogo random seeds as variables (a). Green represents phytoplankton and brown represents zooplankton. Each column shows the results of one random seed simulation, while (b) shows the change in unutilised nutrients in the water (global-free-nutrient) over time in each simulation.

4.8 Discussion

4.8.1 Challenges and limitations of the model

One of the more problematic issues in the development of ABMs is how to balance simplicity with realism. Developing manageable models can maximise the generality, realism and accuracy of our understanding of predicting the transformation of nature, but no model can be constructed or used without some trade-off strategy (Levins, 1966). For ABMs, putting the right amount of detailed rules and parameters as possible into the model based on empirical knowledge may render the model too complex and difficult to understand (Grimm, 1999). Researchers must decide which empirical observations should be entered into the ABMs setup and as well as the appropriate amount of according to the actual needs of the research or the specific experiment. The modelling for this thesis was undertaken to explore the mechanisms of critical transitions in a lake ecosystem, but the balance between simplicity and realism within its aggregation levels was unknown and had to be explored and determined. The approach I used was to try to develop several ABMs of varying complexity, and then to determine which ABM best represented the ecological mechanism of regime shifts under pressure based on the behaviour of the model and my knowledge of the actual ecosystem.

Prior to this version of the model, I tried to model the transition of the ecosystem in Lake Taibai using either more detailed or more concise rules. The more detailed model design gave the model a more realistic ecological relevance, for example by dividing the algae into green algae, cyanobacteria and diatoms, each with different response curves to temperature, light and nutrients, in order to create a more realistic simulation of population change in response to environmental changes. The use of individual body size attributes as criteria for predation was also tried. The reason I decided to remove these designs was that they did not improve the models' explanatory abilities as far as the mechanisms of critical transitions were concerned, and hindered the observation of emergent results at the ecosystem level. The differences between the generic ecological niches of phytoplankton are small compared to the differences between the major functional groups within the ecosystem, and the body size of predators and prey plays a dominant role in simplifying the structure of the food web, even though there was a lack of relevant field observations to calibrate and explain these roles. One of the simplest models I attempted to use was a parametric and behavioural characterisation based on a modification of the wolf-sheep-grass model (Wilensky, 1997). However, this model contains only three trophic levels, and while it is able to simulate ecosystem homeostasis and dynamics, it is unable to capture the major changes in dynamic relationships between the major components of the Lake Taibai system. After rejecting these more complex or simpler models, I eventually settled on the current version of the model and set it up. In this ABM model, some components of the lake ecosystem were replaced by realistic individual behavioural rules and interactions, including mass-energy balance, sediment, faunal communities and nutrient recycling using the palaeoecological approach discussed earlier in the study. Physiological characteristics were also highly simplified, and the role of ecosystem changes on nutrient cycling as well as environmental variables were simplified in the simulated restoration scenarios. Changes between external drivers were manipulated using simple univariate equations, rather than attempting to model the interconnectedness of variables that occurs in real systems. For example, changes in temperature and changes in lake area may have been negatively correlated due to water surface evapotranspiration processes that were not considered in the model. In order to distinguish the role of each external driver as clearly as possible, there was no direct correlation between the external drivers in this model. The influence of human activities on the organisms in lake is seen as being unidirectional, which means that human interference would not be modified by ecosystem changes in the lake. Meanwhile, top predator humans are not included into the ABM of the system, and do not participate in the interactions as the rules of human behaviour cannot be clearly extracted. Lakes in the middle and lower Yangtze River have been exploited by humans for thousands of years, and human food preferences for a particular fish can directly affect their predation pressure and motivation for farming and can alert us to lake water quality because of algal toxins in the water. These are important processes that have not been added to the ecosystem model used in these experiments.

The model assumes that once a functional group becomes extinct, it has no chance to recover. The benefit of keeping the system closed is that it speeds up the formation of dominant ecosystem compositions. In sediments and lakeshore wetland areas of lakes, there are usually seed banks of macrophytes and phytoplankton that ensure the species can rise again when the environment becomes more suitable. However, for modelling purpose, the supplement of plants sprouting from seedbanks adds to the complexity in terms of observing ecosystem state changes, and stabilising feedback slows the transition process.

Given these limitations to the model, I need to be aware of the theoretical limitations of using the ABM as well as the areas in which it works well. The limitations of the model arise in the construction of systems of low complexity, where a two- or one-component system is essentially equivalent to a steady-state equilibrium model built using partial differential equations that include stochasticity, but without the exact parameters of a deterministic model that has undergone an extensive process of calibration. The model is also unable to address the more detailed results of eutrophication, such as competition between wild and domestic fish and changes in bacteria community of the lake. The ABM model I eventually chose to use adequately models the transmission and amplification of changes in the internal structure of complex systems following external influences, generating emergent signals of change at the population level that are related in a nonlinear way to the input signal.

4.8.2 Management implications

The results of the homeostasis simulations show that even the same number of functional groups of ecosystems living in the same environmental conditions in a lake can develop to entirely different steady-state outcomes following inter-biotic and bio-environmental interactions. Lake management researchers should therefore be aware of the limitations of commonly used ecological measures such as population size and biomass for estimating ecosystem structures and states. Despite similar developmental trajectories, neighbouring lakes may not necessarily show similar outcomes in community composition.

The multiple steady-state results of the simulation also suggest that not only critical transitions but also steady states themselves also result from interactions between individual factors or groups within the original system. The formation of homeostasis in a system is based on the interactions between functional group members, population size and spatial location relationships, and is characterised by uncertainty and nonlinearity. Ecosystem states that begin with the same population size and functional group composition can produce seven steady-state patterns by the end of the 5th year, five at the end of the 10th year, and six by the 20th year. From the perspective of system components, systems in the same state may evolve in different patterns, and different patterns may temporarily exist within the same larger pattern as they develop. In some systems, planktivorous fish became extinct first, followed by herbivorous fish, while in others the extinction sequence was reversed, although the same steady-state pattern was eventually reached. The modelling results give us insights into ecosystem management in two main ways. One is that complex systems with the same population of functional groups observed at a given moment are not guaranteed to develop the same homeostasis. Examining other features of ecosystem properties, such as structural properties, feedback loops and spatial heterogeneity can compensate for the limitations inherent in the single perspective. This knowledge helps us to explain why it is difficult to effectively summarise alternative stable states, regime shifts and critical transitions by relying only on the physical properties of ecosystems such as lakes, forests and grasslands or population size and composition. Complex system dynamics change not only in terms of system resilience to state recovery, but also in terms of different pathways to natural recovery, leading to transition processes at different scales that are dominated by different functional groups on longer time scales. Secondly, complex systems with different compositional patterns observed at a given moment may also develop into the same compositional pattern, such as equifinality (as illustrated in subsection 4.7.1). The presence of equifinality is important when it comes to reviewing the mechanisms of eutrophication and water quality management in a region, reminding managers of the importance and limitations of their choice of monitoring indicators.

If the homogeneous parameterised system generated by different random seeds represents a simplification of samples from different parts of a large lake, then the structural changes that occur locally should also be considered as spatially heterogeneous, and therefore influence the direction of the eventual whole-lake state. It has been shown that the bacterioplankton community composition in different areas of Taihu Lake (2427.8 km^2) showed significant spatial differences, forming macrophyte-dominated and phytoplankton-dominated regimes. The functional gene structure approach revealed stronger interspecific interactions within the macrophyte-dominated regime and weaker interspecific interactions within the phytoplankton-dominated regime (Wang et al, 2020). Taihu lake is ten times larger than Taibai lake in area.

Meanwhile, steady-state simulations have shown that less resilient ecosystems may not exhibit the typical alternative stable states, or states that do not persist in the standard dichotomy between turbid and clear water states but instead oscillate between more algae with submerged plants and more algae with fewer submerged plants (such as the “p+z+sm+hf” and “p+z+sm+hf+pisci” states). Similar patterns were reported in empirical lake ecosystems. According to satellite imagery and field measurements, many lakes on the Boreal Plain were often found to shift between clear and turbid water states in which systems are unstable (Bayley et al, 2007). The study concluded that cold winters were responsible for resetting the ecosystem every year.

Chapter 5: Nutrient-driven critical transitions and recovery pathways in Taibai lake ecosystem

5.1 Introduction

A critical transition is a type of abrupt state transition that has received widespread attention in lake ecosystems because of its effect on eutrophication processes, exhibiting sudden outbreaks of algae (Glibert, 2017; Scheffer & Carpenter, 2003). In the presence of constant nutrient load inputs, algal concentrations change rapidly and persistently after surpassing a threshold, creating two distinct response curves to nutrient input drivers before and after each transition. It has been found that many changes in lake ecosystems caused by critical transitions in recent decades have resulted in catastrophic consequences beyond our expectations as well as unpredictable recovery pathways, posing many difficulties for the ecological management of lakes (Folke et al, 2004; Scheffer & Carpenter, 2003; Zhang, 2016). For example, the Veluwemeer in the Netherlands experienced a significant change in terms of the amount of its aquatic vegetation and cyanobacteria between 1961 and 1975 following the construction of a dam, in response to nutrient inputs to the basin (Scheffer, 1998). In China Lake Taibai, which was considered as a case study in Chapter 3, as well as most other MLYB lakes, has shown similar trajectories and similar causes of change. Taibai Lake is also influenced by other external factors, including water level, biomanipulation, storms, flooding and hydrodynamics, and by interactions between the organisms within the lake itself (Scheffer, 1998). The interplay between these factors in lake ecosystems results in dramatic changes in the characteristics of communities such as phytoplankton and submerged plants which are often of interest for researchers. I identified the following questions for further research. Firstly, what roles do functional groups play in ecosystem state transitions? Secondly, how do conditions of environmental change influence patterns of nutrient-driven response to lake ecosystem state? Thirdly, what can be learned about critical transition from these questions?

Among the many global patterns of lake ecosystem change, fold bifurcation is widely recognised as being able to represent the relationship between phytoplankton and submerged plant populations in response to changes in nutrient concentrations under other external forces. This means that the response of phytoplankton populations to nutrient concentrations under specific conditions (such as lake depth) may be asymptotic and essentially almost linear. Under different conditions and different lake depths, this response relationship may be abruptly altered, and the location of the critical point will be influenced by this limiting condition (described in detail in Chapter 2). This conceptual model describes the relationship between the eutrophication-induced critical transitions and their driving forces at the macroscopic level.

To answer the questions, I constructed an ABM to simulate emergent phenomena in steady states from simple individual rules of interaction and provide observations on multiple indicators at various scales, the details of which were illustrated in Chapter 4. This chapter offers parameters for the model specifically in terms of its ecological attributes and the environmental changes taken from the Lake Taibai case study to simulate regime shift processes in the ecosystem as thoroughly as possible. The ABM simulates bi-directional environmental change, with one direction being the eutrophication of the lake over nearly a century and the other being the restoration of Lake Taibai following strict ecological policies that were put in place to protect the lake. Considering the intrinsic uncertainties of the model simulation, the responses of each organism may not match the critical pattern of critical transition in theory (Scheffer, 2009), which is defined as a special form of regime shift. However, simulating ecosystem state changes under external pressure can provide us with a mechanistic approach to improving our understanding of the process of nonlinear changes in modelled ecosystems, ultimately improving our understanding of changes in the internal structure and relationships within the lake ecosystem in the model. In addition, the results of these simulations can provide reasonable strategies and guidance for future water quality restoration management and the sustainable use of all MLYB lakes.

5.2 Methods and data

5.2.1 Ecosystem changes in Taibai lake

5.2.1.1 Setting physical parameters based on empirical evidence

The meteorological station in Huanggang, the nearest city to the lake, recorded annual mean temperatures of between 16.03 and 17.83°C from 1961 to 2005, while in Anqing, another nearby city, temperature changes of between 15.70 and 18.01°C were recorded. Local records show a linear rise in temperature between 1970 and 2005, with an average annual increase of 0.0429°C and 0.0312°C respectively. Meanwhile, according to observed temperature data collected from Chinese meteorological stations (Qian & Zhu, 2001), the region of central China in which Lake Taibai is located experienced an increase in temperature from roughly 1910 until 1950, followed by a slight decline from the 1950s to the 1970s. After this time, temperature has increased over the last 50 years (Figure 5-1).

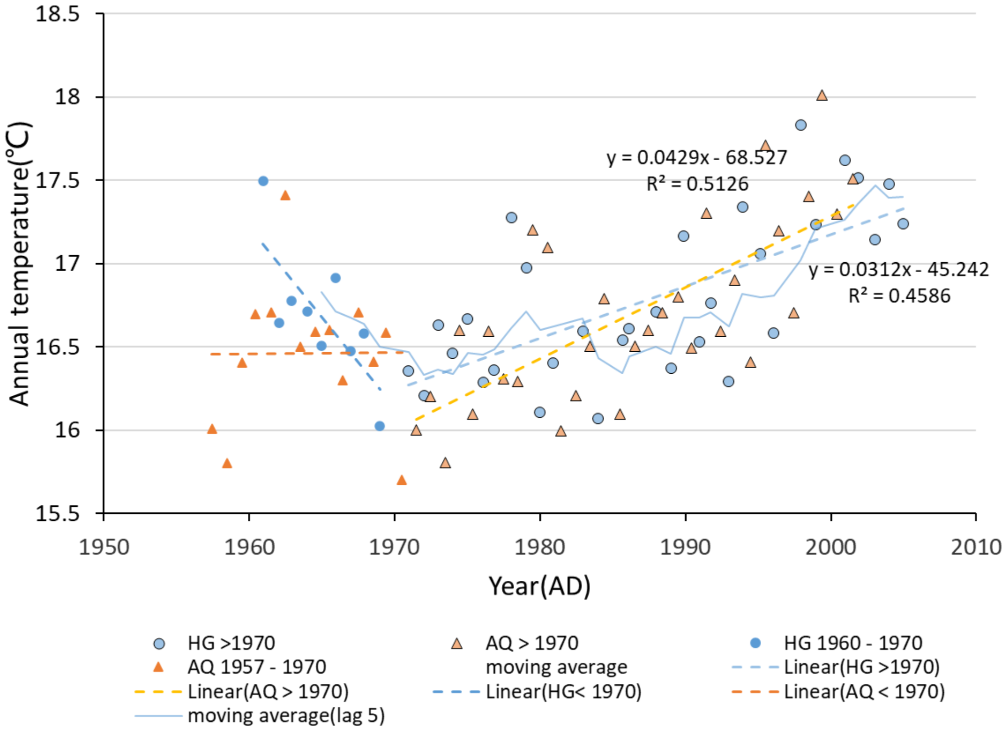

Figure 5-1: Trends of temperature changes in Huanggang (HG) and Anqing (AQ) between 1960-1970 (left) and 1970-2005 (right) respectively. The blue dashes show the linear trends in the HG temperature record and the orange and yellow dashes show the linear trends in the AQ record. The rate of the temperature increased after 1980 near Taibai is 0.035°C/a. A moving average is drawn in a light blue line to show the overall trend of temperature in HG.

The average nutrient concentration change calculated from the increase in TP in Lake Taibai is 38μg/L per year between 2008 and 2019. When the initial nutrient concentration in the model reached 25 µg/L, the annual increase in nutrient concentration was 1.52 times the initial concentration, which equates to an increase of 41.64% of that initial concentration every 100 days.

The area of Lake Taibai was reduced from 83.32 km^2 in 1905 to 27.57 km^2 in 2005 due to land reclamation (Jianghan Floodplain Aquatic Resource Investigation Group, 2001; Liu et al, 2012). Over the fifty years from 1905 to 1955, the lake surface area shrank by an average of 0.4 km^2 per year, representing an annual change of 0.48% of the original lake area. Over the 23 years from 1955 to 1978 linear regression results show that the lake surface area shrank by 1.6 km^2 per year, representing an annual change of 2.51% of the 1955 lake area. As the lake shrank during that time, its temperature increased slightly, but after 1978, temperature changes seem not to be correlated with changes in lake area (Figure 5-2).

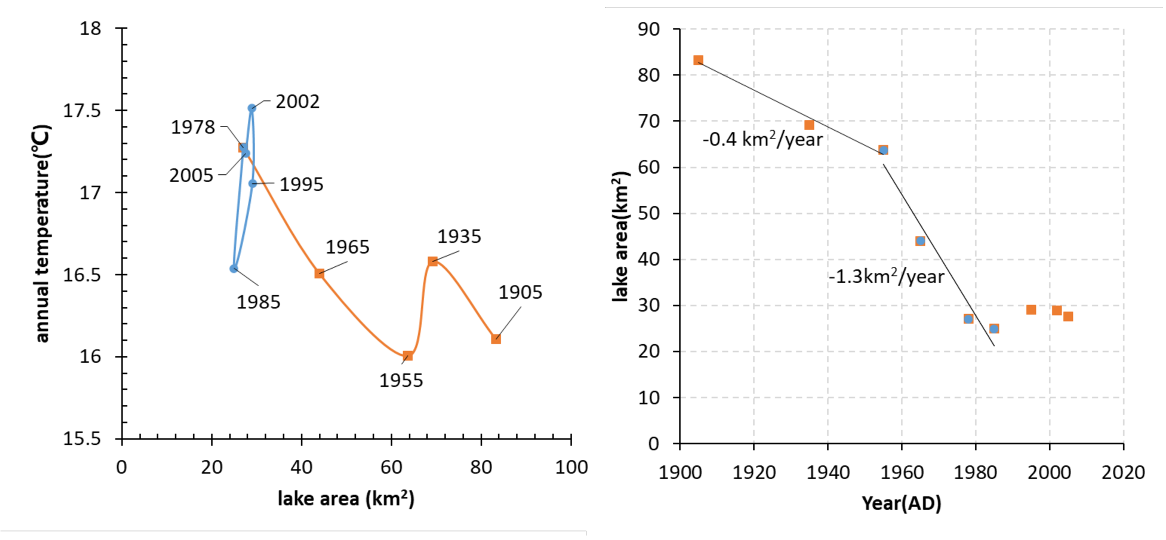

Figure 5-2: Relationship between Taibai Lake area and nearby annual air temperature in Huanggang during the twentieth century (left) and rates of changes (km^2/year) (right). In the left-hand plot, the blue dots represent the states of Taibai after 1978 and the orange dots represent the states of Taibai between 1905 to 1978. The right-hand plot shows trends of lake-area change over time.

5.2.1.2 Setting anthropogenic parameters based on history

According to the Taibai Lake Fishery Survey Report (2001), the Taibai Lake Fishery was established in 1945 under the management of the Huanggang Fisheries Bureau. It was privatised after the 1980s and gradually became one of the most important fish farming bases in Hubei province, with the ability to cultivate fish fry and fish seeds and to sell adult fish. The fishery yield of Lake Taibai shows that before 1980, low-intensity natural fishing methods were used, resulting in cyclical changes in fish catches. After 1988 the fish catch gradually increased, and in 1994 it was reported that 67 hectares of the lake base were deepened during the winter to expand the water volume of the lake and to expand the space for fish and other aquatic organisms (Huang, 1996). In 1995, 65 tonnes of various fish species were introduced, including 41 tonnes of filter-feeding fish, 19 tonnes of herbivorous fish (grass carp, bream and carp), piscivorous fish *Siniperca chuatsi* (75 fish per hectare) and *Channa maculata*, all of which are popular commercial fish in the Chinese market and are generally ready for harvest within one to two years. A ban on fishing came into effect on 1 January 2018 following the 2017 government policy (Ministry of Agriculture Circular [2017] No. 6) regarding the protection of the Yangtze River Basin Aquatic Life Reserve. Lake Taibai has since become a national aquatic germplasm resource reserve and will be completely closed to productive fishing for at least 10 years (until 2028.) From 2018, the management of Lake Taibai has started to transform the lake into a modern and ecologically healthy fishery demonstration base by converting part of the fish farming pools into water purification ponds and expanding the intake pipes and drainage ditches to increase the rate of water exchange.

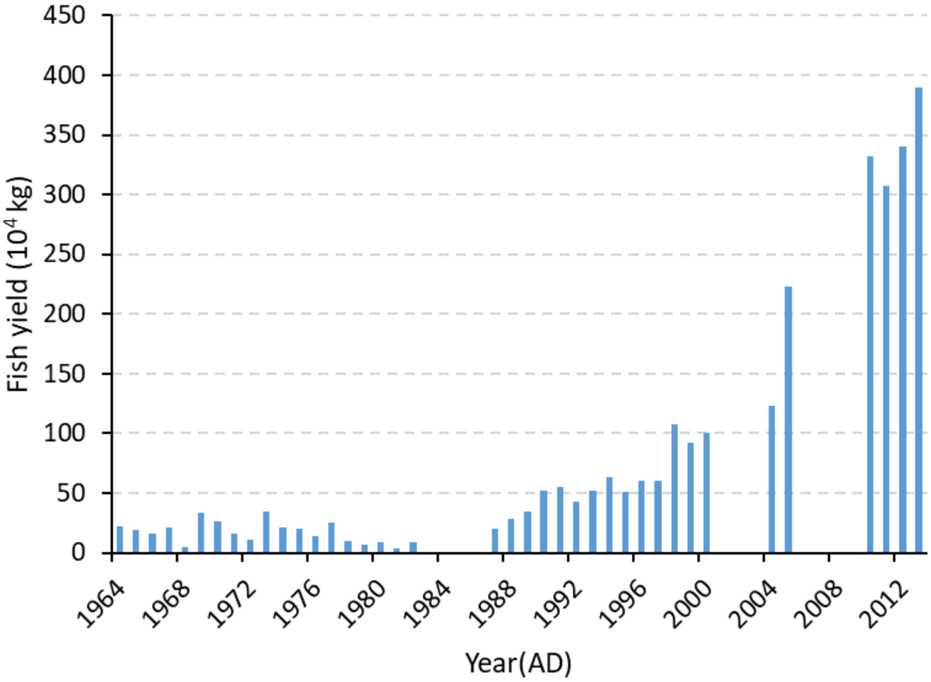

Figure 5-3: Fish yields in Taibai from 1964 to 2012 based on historical records.

Since 2018, cage culture has been banned in Lake Taibai and other lakes in the middle and lower reaches of the Yangtze River, based on the aim of restoring the lake's water quality. However, survey data shows that the TP concentration in Lake Taibai rose to 0.50 mg/L in 2019, which is 5.4 times higher than the TP level in 2008 (0.092 mg/L). This concentration turned out to not to respond to mitigation action immediately. Similar results have been recorded in other MLYB lakes, such as Taihu and Chaohu, where the TP in the water column shows an increasing trend from 2018 to 2020 (Zhu et al, 2021). Meanwhile, according to historical records, the reason why managers of Taibai Lake stocked grass carp and mitten crabs in the 1970s was because of excessive weed and the risk of the lake silting up under the accumulation of organic matter. The artificial intervention was intended to address the adverse results of eutrophication dominated by water plants, but the result was to change the state of Lake Taibai from clear water to turbid water, with large numbers of planktivorous fish being farmed, and to a state in which the risk of algal blooms was greater.

5.2.3 Scenarios for experimentation

The experimental scenarios are divided into three main categories: pilot simulations of eutrophication (Experiment 1), realistic simulations of eutrophication process (Experiment 2) and realistic simulations of recovery pathways (Experiment 3). Experiment 1 was designed to investigate the ecosystem dynamics under nutrient loading pressure in order to address what roles the function groups play in regime shifts. The controlling variables include the amounts of nutrient addition into the system, the addition intervals, the physical property of the lake and the moderating factors involved. Experiment 2 added a variety of environmental drivers to simulate a more realistic scenario of lake changes. Experiment 3 added treatments to the turbid-water system to investigate reasonable pathways for recovery. Numerical analyses were made according to the time series plots showing the population dynamics of organisms and phase plots looking for changes of relationships between species.

Table 5-1: Experiments in each category and number of runs. Details of the scenario settings are described in Appendix D.2.

	Experiment #	**Time span (Sim year)**	**Number of runs**	**Subsection**
Experiment 1	TBNutADD_once_y30	30	1	5.3.1.1
	NUTADDvar_y40	40	10	5.3.1.2
	NUTADD1_vDEPTH_y70, NUTADD0.1_vDEPTH_y70, NUTADD10_vDEPTH_y70, NUTADD20_vDEPTH_y70	70	20	5.3.1.3
	NUTADDTEMP_once_y27	27	1	5.3.1.4
Experiment 2	TBComprehens_v5_y274	274	1	5.3.2
Experiment 3	TBRecNutADD_once_y164	164	1	5.3.3.1
	TBRecNut_once_y80	80	1	5.3.3.2

5.3 Results

5.3.1 Experiment 1: Pilot simulations under nutrient pressure

5.3.1.1 Nutrient-driven only scenario

A slow and long-term nutrient load was applied to the lake ecosystem (Experiment # TBNutADD_once_y30). With a slow increase in total nutrient concentration applied 4548 days (12.5 years) from the start of the simulation, zooplankton populations immediately stopped returning to their initial mean and jumped to new steady-state levels, where they remained for several years. In response to the hike in zooplankton, phytoplankton shifted to a consistently lower population level than before the nutrient load was added (Figure 5-4).

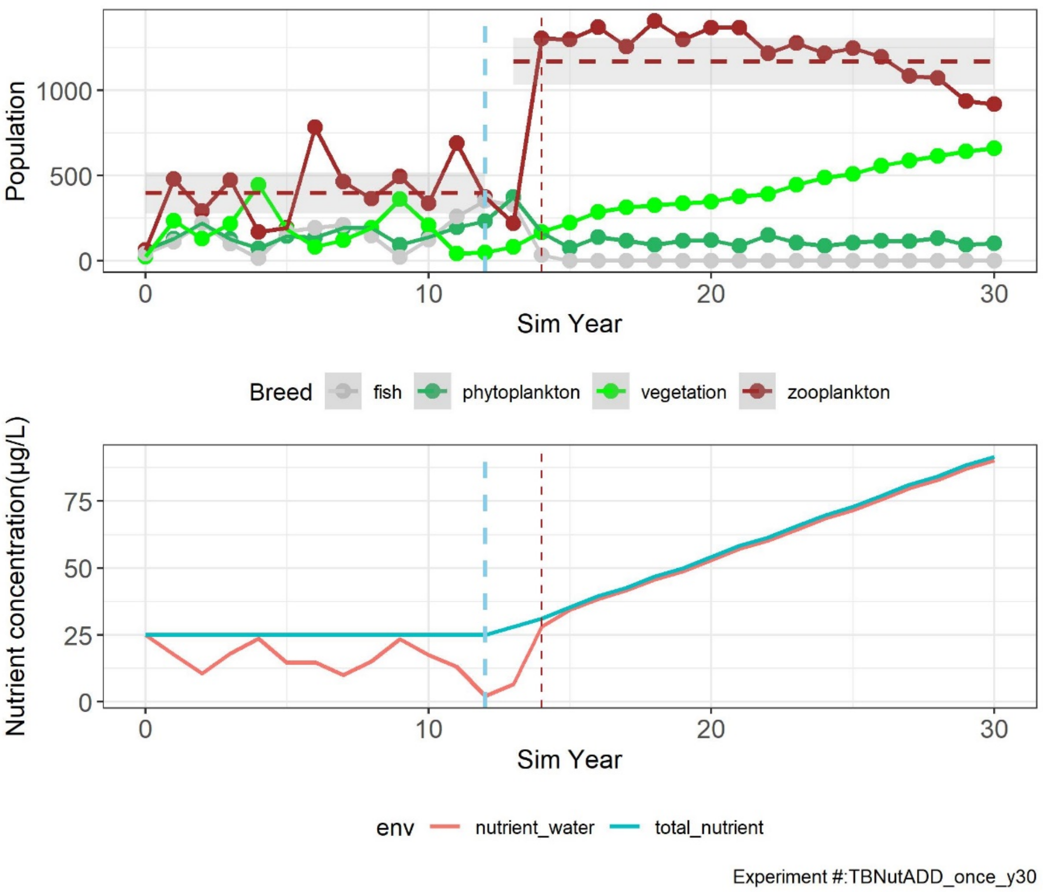

Figure 5-4: Simulated regime shift driven by a gradual increase in total nutrient concentration in system from Year 12 (blue vertical dashes) to Year 14 (brown vertical dashes). The blue dashes in Year 12 represent the start of nutrient change and the brown dashes in Year 14 shows the start of abrupt changes in zooplankton population.

The result is surprising insofar as the nutrient load seemed to promote the growth in population of zooplankton instead of phytoplankton. To confirm the pattern of transition, the response-driver relationship between phytoplankton, zooplankton, macrophytes, fish and in-water nutrient concentration were plotted (Figure 5-5). The relationships were different before and after Year 14, after which time the population of zooplankton suddenly rose. Before the shift, the relationship between phytoplankton population and in-water nutrient concentration was negatively correlated, which then turned into an absence of correlation after Year 14. The relationship between zooplankton population and in-water nutrient concentration was slightly negatively correlated, but shifted clearly after Year 14. In terms of vegetation (submerged macrophytes), the population trend along the gradient of in-water nutrient concentration was positively related, but the slopes of linear regression results lessened after nutrient loading and the regime shift in zooplankton. The relationship between fish and in-water nutrient concentration changed following a similar pattern to the relationship between phytoplankton and in-water nutrients.

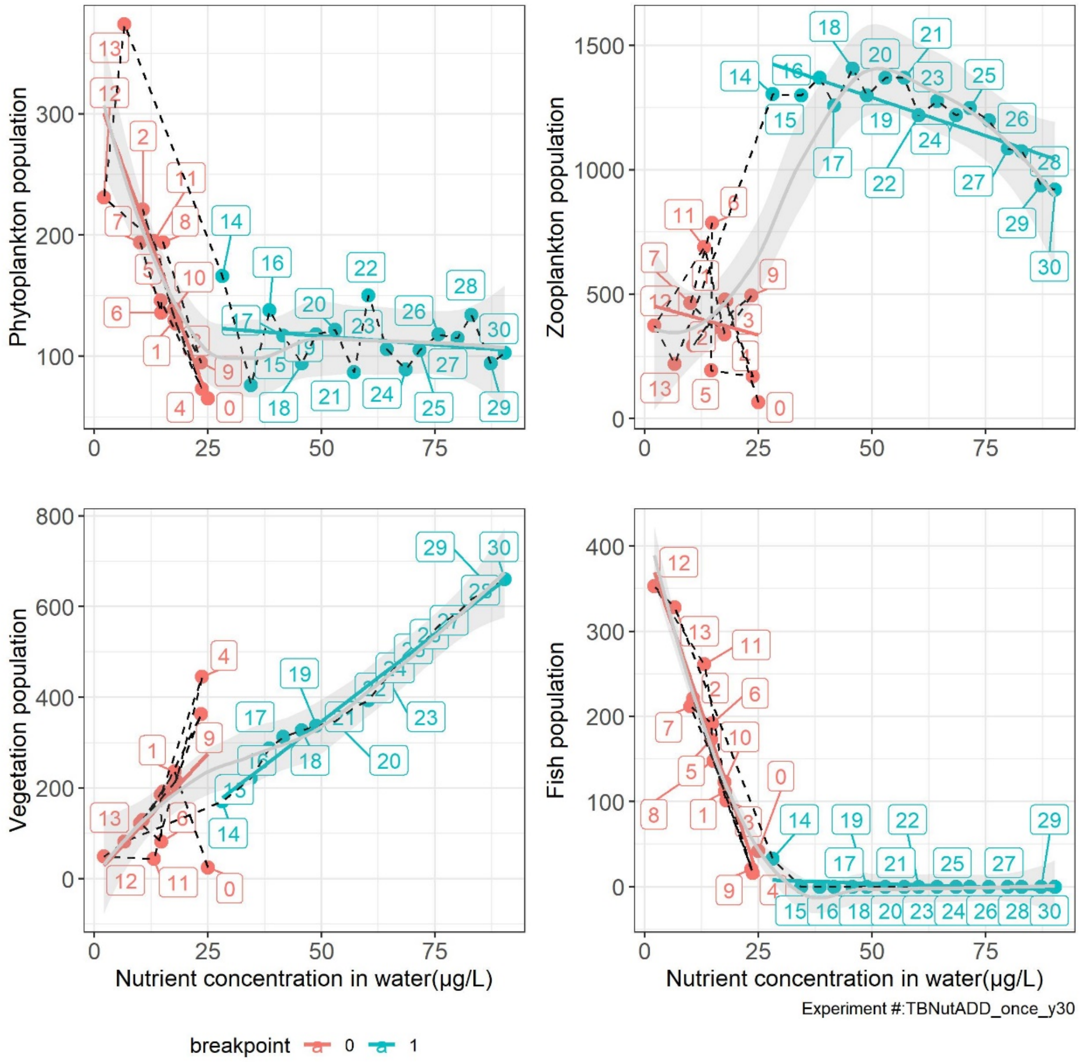

Figure 5-5: Driver-response relationships between functional groups and in-water nutrient concentration before and after breakpoint (Year 14). Black dashes link samples in simulation time order, while the red points represent observations before Year 14 and blue points represent observations after Year 14. Grey lines and shadows represent the smoothed results achieved by using the local polynomial regression fitting method "Loess" (Cleveland et al, 1992). The years are labelled near the points.

The model simulations allowed more changes to other functional groups over the same period to be obtained in order to discover the mechanisms by which the increase in nutrients led to the onset of the critical transition. The analysis also examined the population size, mortality and cause of each community. Population counts show that fish numbers had all declined to the point of extinction by Year 15. Their demise was likely the direct cause of the increase in zooplankton and submerged macrophytes after this time. Given the extinction of fish and the continuing elevated nutrient loads submerged plants, unrestricted by other functional communities, gradually responded to the increase in nutrient concentrations by producing a linear response to proliferation. The abrupt increase in zooplankton numbers was due not only to the lack of predation by planktivorous fish, but also to the constant abundance of food provided by algae that proliferated in response to increased nutrients. Prior to being suppressed by zooplankton, algae rose markedly only once. The combined effect of these two bottom-up and top-down causes resulted in a relative equilibrium in the numbers of phytoplankton, zooplankton and submerged vegetation in an environment that showed increasing nutrient concentrations between Year 14 and Year 22. Submerged vegetation gradually increased, with a consequent increase in nutrient load due to the absence of grazing fish. After Year 25, under the same trend of nutrient change, the continued increase in submerged vegetation encouraged the growth and reproduction rate of phytoplankton, resulting in a decline in population of zooplankton.

The death count and death cause of phytoplankton and zooplankton provide another perspective from which to analyse the reasons why the phytoplankton population remained low. In the top panel of Figure 5-6, The number of algae being grazed fluctuates up and down before increasing to a relatively high level. Following the systemic shift associated with the extinction of fish and the sudden rise in zooplankton, the mean number of grazed algae decreased slightly. After Year 14, the increase in total trophic level contributed to the growth rate of phytoplankton, which continued to be grazed by phytoplankton at higher levels rather than according to the cyclical fluctuations shown previously. The number of zooplankton grazed peaked before Year 14 and fell to zero after the extinction of planktivorous fish. The sudden change in zooplankton population size to higher levels was then followed by an increase in the number of deaths due to the lack of sufficient energy reserves for survival. After Year 27, the zooplankton population and the number of phytoplankton being grazed showed a clear decline, while the number of zooplankton dying of starvation did not change significantly.

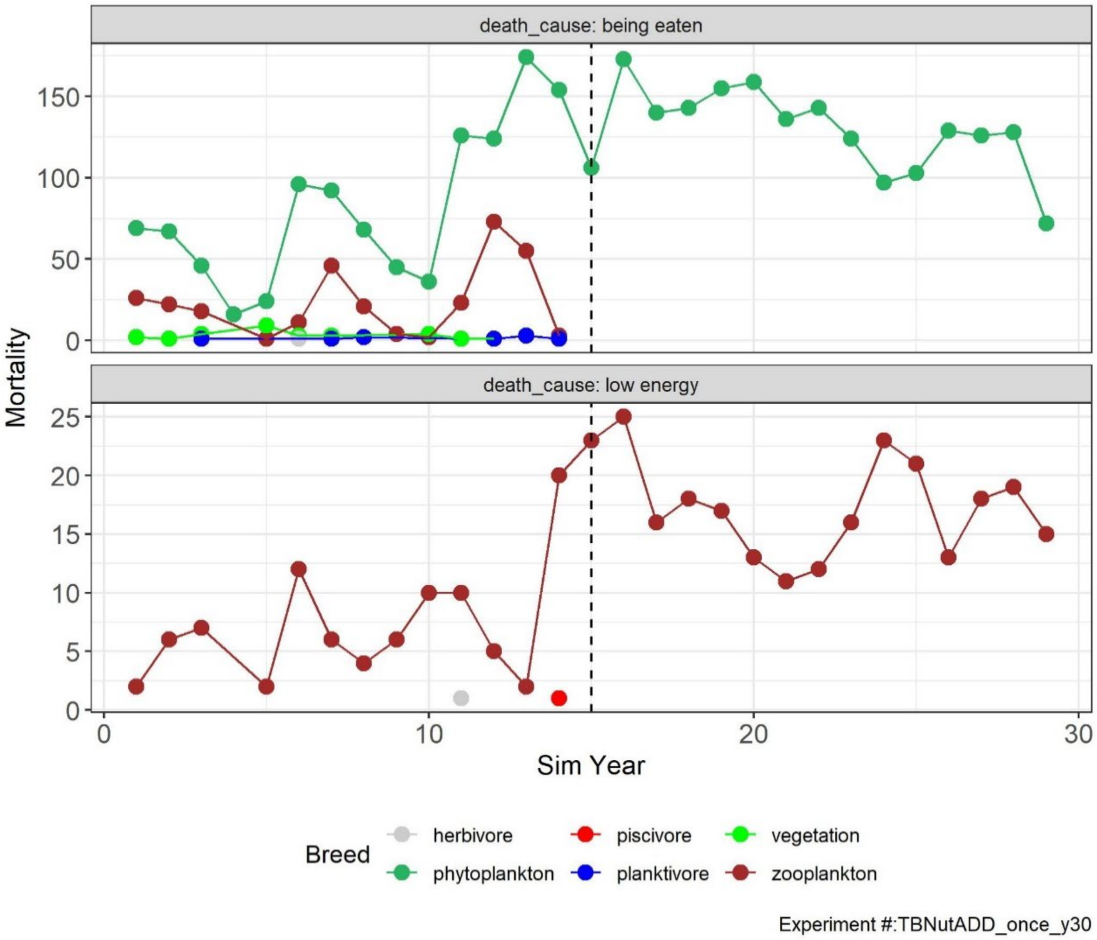

Figure 5-6: Numbers and causes of death of individuals over simulation year. The horizontal axis represents the simulated year, and the vertical axis shows the number of deaths. The top plot shows mortality due to being eaten by predators or grazers, while the bottom plot shows the mortality due to low energy reserve.

Prior to fish extinction, the intensity of predation on herbivorous and planktivorous fish was cyclical. Herbivorous fish became progressively more starved and received less predation pressure over time. For planktivorous fish, the number of starvation deaths remained largely constant over time, while their intensity of predation increased, especially after Day 4500 when a nutrient load was introduced into the system. The mortality cycle length of planktivorous fish was 2000 days, while the cycle for piscivorous fish was roughly 3000 days.

Herbivorous fish did not exhibit any clear cycles. In the end, herbivorous fish died off first, followed by planktivorous and piscivorous fish. The statistics on the number and causes of fish deaths provide a visual overview of the successive extinctions of these three fish groups following increased nutrification.

5.3.1.2 Responses to different amounts of added nutrients

Changes in state caused by different amounts of nutrient being loaded into the system were observed in an experiment that simulated a period of 80 years (experiment NUTADDvar_y40. Since regime shifts did not occur at low nutrient load concentrations in the previous subsection (1.16 µg/L per 100 days), the nutrient load amount added in this experiment was chosen to represent a larger value (10-70 µg/L per 100 days). The metrices of observation remain the population change in each functional group.

The results of the nutrient load gradient experiment showed that the greater the nutrient load per unit time, the earlier the structural transition occurred in population size (Table 5-2). At low nutrient loads, there is a certain probability that steady-state transitions will not occur within 20 years, when the total-nutrient-variation was 10 or 20 µg/L per 100 days. The criterion used to identify a regime shift was either a significant change in the system structure or an evident abrupt change in a population, despite not having undergone a structural change.

Table 5-2 Amount of nutrient load, time of regime shift and proportion of occurrences in experiment #NUTADDvar_y40

Total-nutrient-variation (µg/L per 100 days)	Sim year of regime shift	No regime shift? (among 2 repetitions)
10	38	50%
20	34	50%
40	30,17	0
60	22,16	0
70	16,14	0

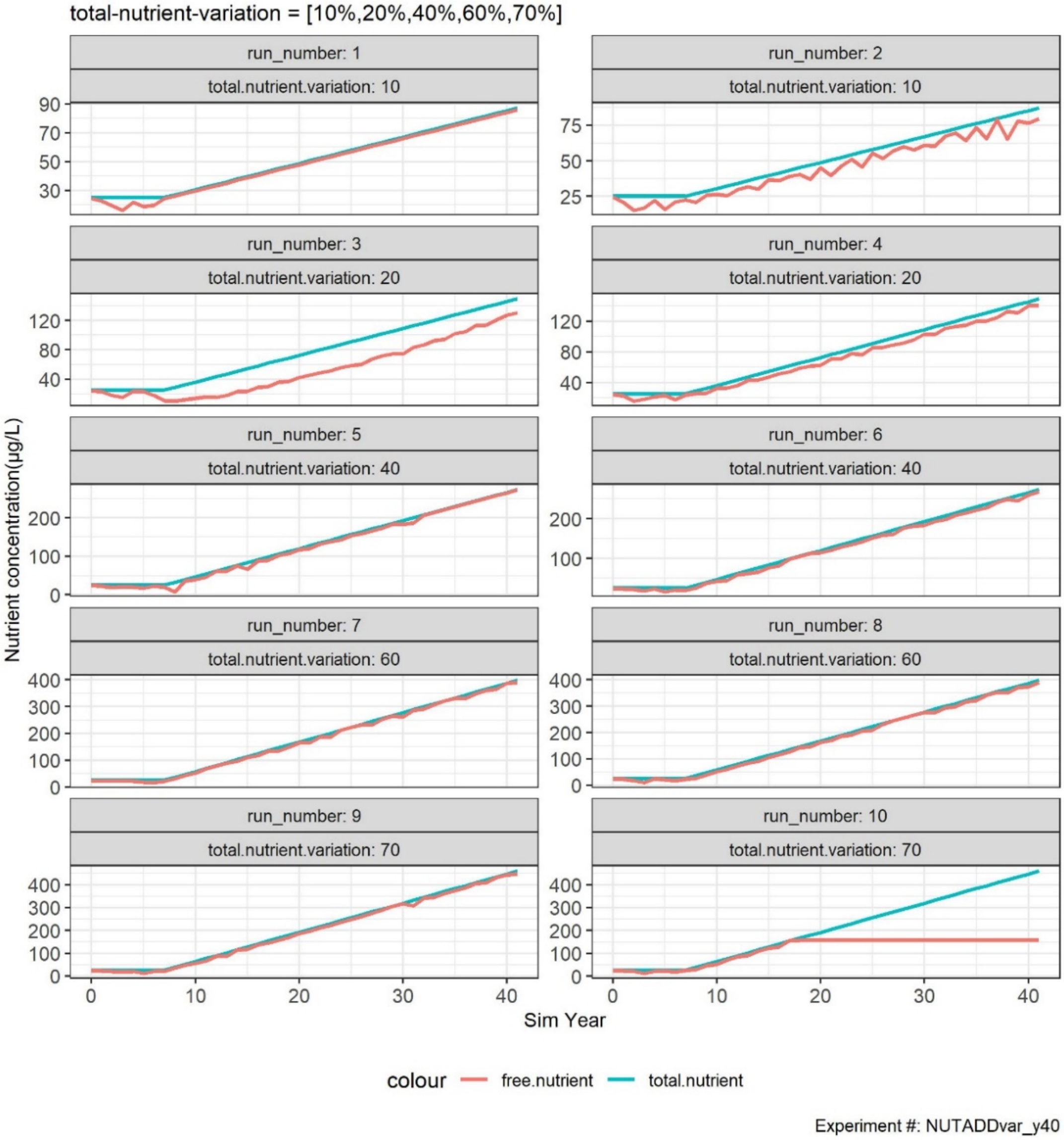

Figure 5-7: Total and free in-water nutrient concentration in experiment #NUTADDvar_y40. The red line shows the trend of total nutrients in the system as having been manipulated to increase after Year 7. The blue line shows trends of free in-water nutrients as a response to the total nutrients.

As there is no control for random seeds, the patterns of state change under the impact of nutrient loading are not identical across all of the simulated systems. For example, some systems produced sudden changes from zooplankton dominance to zooplankton extinction, while others produced structural changes that left only submerged plants, zooplankton and phytoplankton to coexist. A comparative analysis of the results of two experiments (Run-4 and Run-6) selected from these ten experiments showing similar patterns of change demonstrates that from 1953, when nutrient loads began to enter the lake, the regime shift in the lower nutrient load system occurred in 2008 (55 years later), while the regime shift in the double nutrient load system occurred in 1973 (20 years later). In both scenarios, the zooplankton population had already undergone an abrupt shift during the initial phase of nutrient loading into the lake due to the extinction of planktivorous fish (as in the scenario described in the previous subsection). Then, after decades of continued increases in overall nutrient concentrations within the lake, zooplankton suddenly declined and became extinct. Prior to the extinction of zooplankton, the amplitude of population change in phytoplankton had become greater over a period of time, but they too were eventually extinguished. Submerged plants and herbivorous fish, as two other functional groups with a linked relationship, kept their populations negatively correlated upwards and downwards, with amplitudes slowly expanding in response to increasing nutrient loads. In both scenarios, the lake ecosystems in 2020 were dominant by submerged macrophytes with very high nutrient levels (150 μg/L and 275 μg/L).

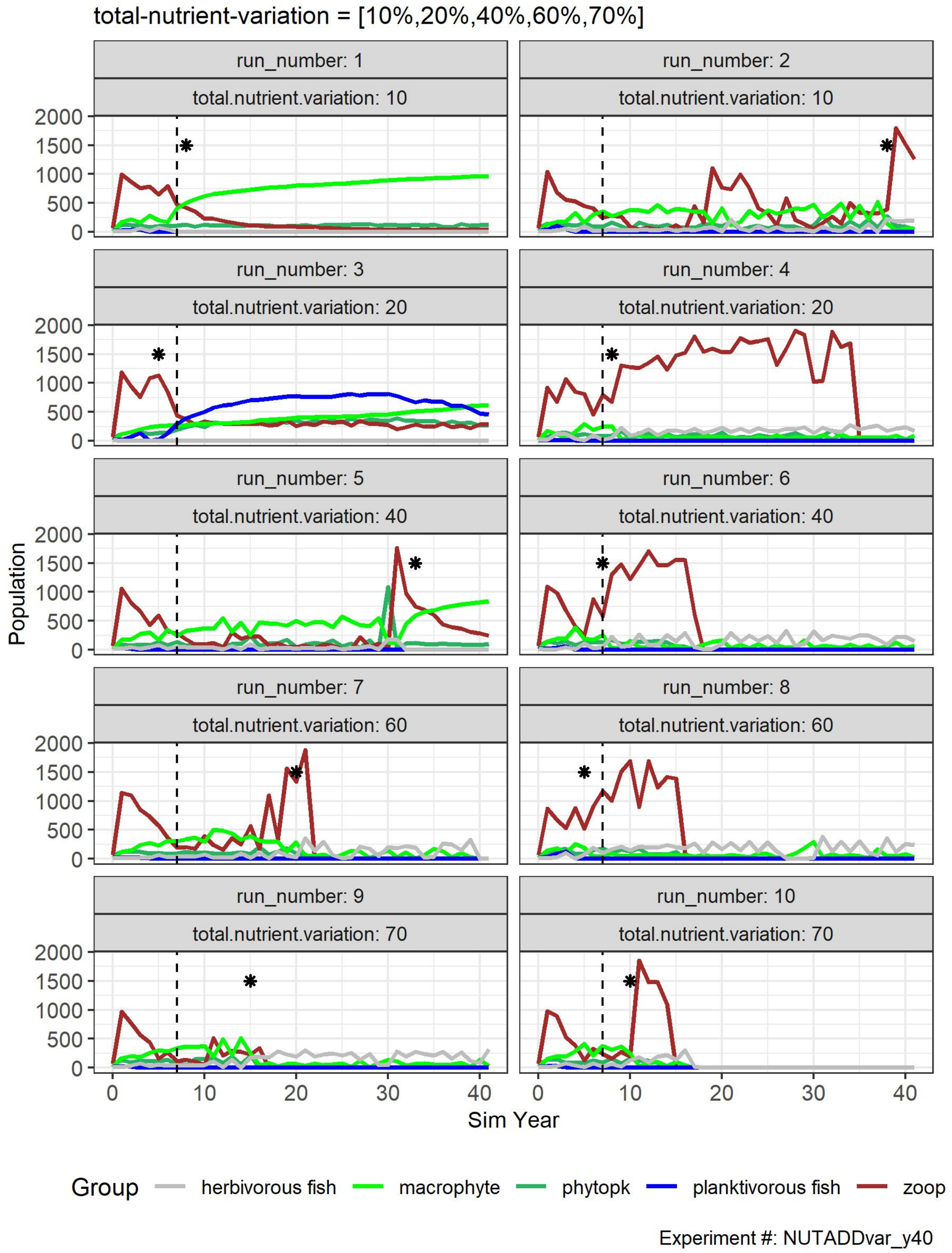

Figure 5-8: Population changes of ecosystem components after different nutrient loadings over 40 years. The brown line represents zooplankton (zoopk), the dark green line represents phytoplankton (phytopk), the light green line represents submerged plants (macrophytes) and the grey line represents herbivorous fish (herbivorous fish). Black asterisks represent the extinction time of piscivores. Black dashes show year 7, when nutrient addition started.

5.3.1.3 Responses to nutrient load at various addition intervals and according to lake depths

The environmental conditions in lakes are differentiated not only by the amount of nutrient load but also by the interval between nutrient load additions and the initial lake depth. In order to investigate the changes in ecosystem state driven by different nutrient loads, single factor experiments on nutrients were conducted under different environmental conditions. The data in this subsection are derived from four sets of experiments, numbered NUTADD10_vDEPTH_y70, NUTADD1_vDEPTH_y70, NUTADD0.1_vDEPTH_y70 and NUTADD20_vDEPTH_y70. These experiments were all generated using the Netlogo random seed = 137, with gradient nutrient input intervals and lake depths set at the same overall nutrient loads.

The results (Figure 5-9) show that the pattern of ecosystem state response to increasing nutrient loads differed from the pattern of response to changes in lake depth. At lake depths of 1.8, 2.6 and 3.4 m, the final states and developmental trajectories of the lake ecosystem were broadly similar, with the dominant functional groups being submerged plants, phytoplankton and zooplankton respectively. In this model of ecosystem development, the greater the depth, the longer the survival of planktivorous and piscivorous fish. At lake depths of 2.2m and 3m, the ecosystem response pattern diverged from the ecosystem development pattern of lakes at other depths, with submerged plants being inhibited by herbivorous fish in most experiments. At a lake depth of 2.2m, zooplankton populations dominated, while at depths of 3m, algal and planktivorous fish populations dominated.

The response of the ecosystem state to increasing total nutrient concentrations also varied according to the trend for the different modes of nutrient loading. At a lake depth of 2.2 m, slow nutrient addition (NutADD0.1) caused a minimal systemic change, and slightly longer intervals of nutrient addition (NutADD1) caused a regime shift in the zooplankton population. NutADD10 added at intervals of 100 days caused a large and increasing variation in the system state, which appeared to be on the verge of a systemic shift. NutADD20 added at 200-day intervals also produced a relatively unstable system state, showing the largest fluctuations and constant variability. At a lake depth of 3 m, an increase in the number of planktivorous fish was observed in the experimental groups with 100- and 200-day addition intervals, while the experimental groups with 1- and 10-day intervals of addition showed very different scenarios, maintaining steady states or an increase in the number of submerged plants and a decrease in the number of planktivorous fish respectively.

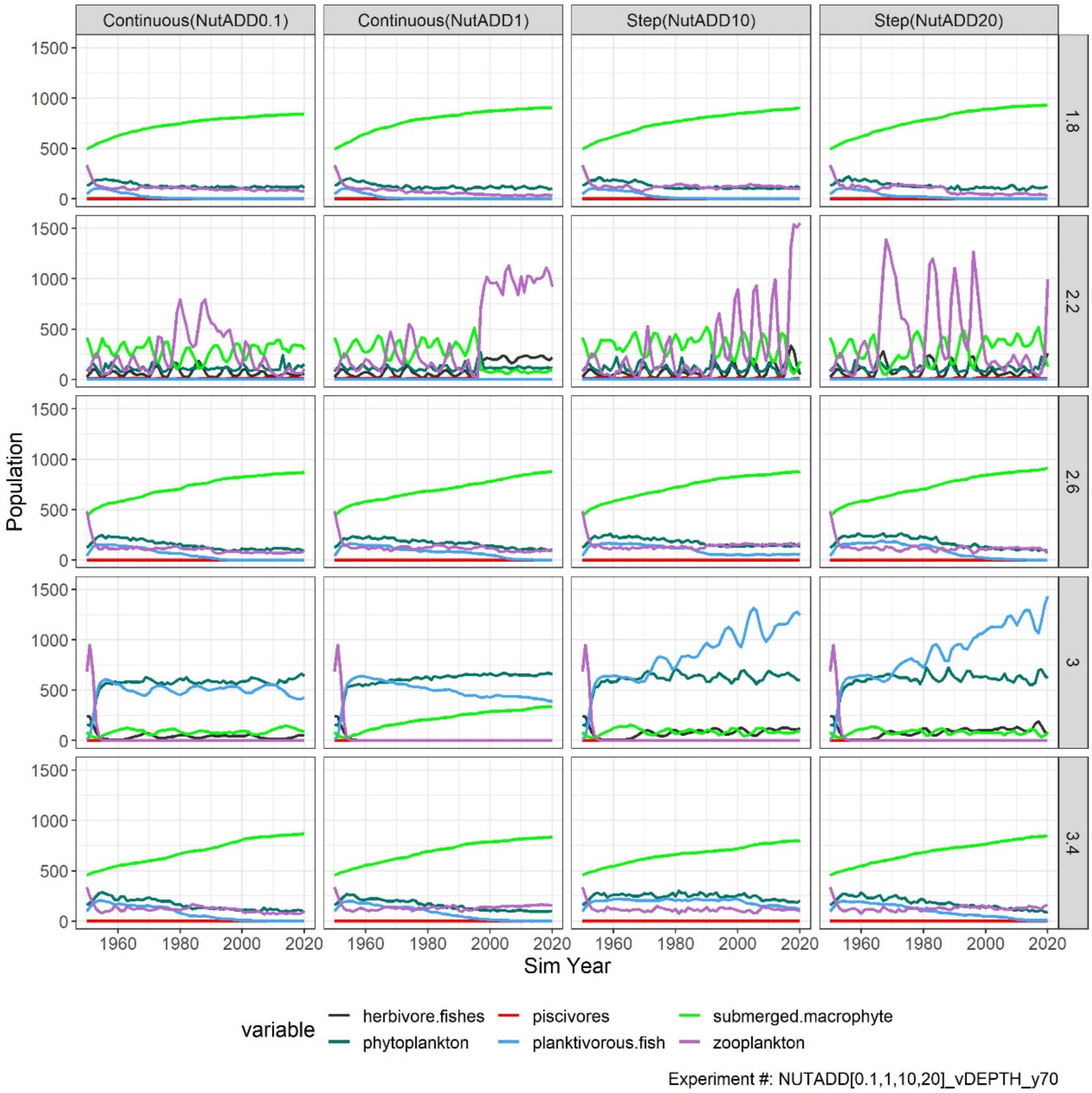

Figure 5-9: Community population under variations in water depth and nutrient loading patterns. The horizontal axis represents the simulation time (years) and the vertical axis represents the population size. The number on the right-hand label of each row is the depth of the lake in metres, and labels on each column show the amount and method of nutrient load addition. NutADD20 represents 20% of the total initial nutrient load every 200 days. The first two additions are labelled as continuous and the last two as periodic. The time periods shown are based on the processes of increasing nutrient load.

The density distribution of zooplankton population numbers at lake depths of 2.2 m gradually became larger in extent as the nutrient addition intervals increased. NutADD20 showed an additional peak at high population levels compared to NutADD0.1, representing the effect of pulsed nutrient inputs on the magnitude of zooplankton population distribution.

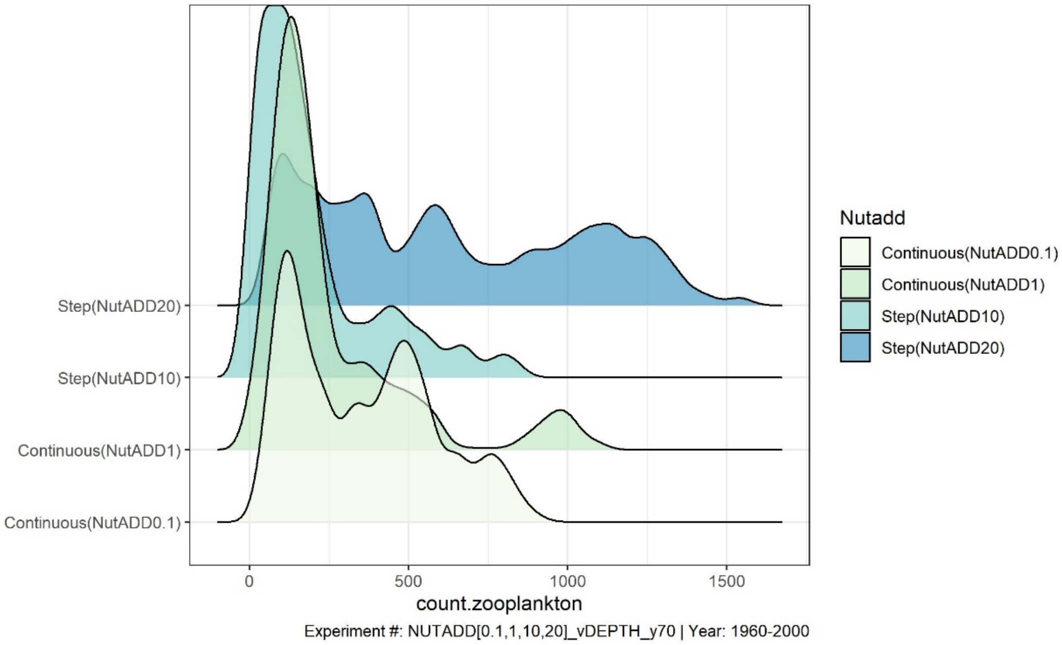

Figure 5-10: Plot showing zooplankton population density resulting from four different frequencies and doses of nutrient loading (simulation results chosen for “ini.water.depth” = 2.2m, random seed = 137). The first light green row corresponds to a 0.1% increase in initial nutrient level per day, the second green row to a 1% increase in initial nutrient level every 10 days, the third light blue row to a 10% increase in initial nutrient level every 100 days, and the fourth dark blue row to a 20% increase in initial nutrient level every 200 days. The horizontal axis is the same for each of the four density distributions.

5.3.1.4 Temperature modulating eutrophication

Based on the continuous addition of nutrient load to the ecosystem at a rate of 0.005 µg/(L-Day), a simulation was conducted with the rise in temperature (0.02°C/day) as a moderating driver between Years 9 and 12. The detailed parameters of experiment NUTADDTEMP_once_y27 are illustrated in Appendix. D.2.

Population dynamics show that after the system stabilised to a state consisting of phytoplankton, zooplankton, planktivorous fish and submerged macrophytes, the increase in total nutrients and temperature did not produce a structural shift in the population size of the system components at that time. The exception to this was a significant increase in the number of planktivorous fish, from 252 at Year 9 to 334 at Year 12, with a slight increase in the number of phytoplankton. There were essentially no significant increasing trends in the abundance of zooplankton and submerged plants. The ratios calculated for each day of biomass (the sum of all biomasses divided by the area of the lake to the number of populations on that day) showed no change in the average mass of zooplankton and phytoplankton in the ecosystem at that time, but the average mass of individual submerged plants increased. This indicates that submerged plants were still in the accumulation of energy phase after the disappearance of herbivorous fish due to their slow growth rate, and had not yet reached the energy level required for reproduction. The concentrations of nutrients in the water column were also in a steady state during this time as the available nutrient concentrations in the water column were directly and negatively correlated with the nutrient concentrations present in the organisms.

After Year 12, the temperature remained at 25°C, and the nutrient load was added to the system gradually, following the same trend. Finally, a structural change occurred before Year 14, with a rapid step increase in phytoplankton concentrations that mirrored the regime shift observed in the algal metrics during the previous fieldwork. As all components of the ecosystem were observed, it could be seen from the change in community numbers that this sudden change was directly caused by the loss of zooplankton, which was associated with the increase in the number of planktivorous fish during the previous period. The increase in planktivorous fish put greater predation pressure on both phytoplankton and zooplankton, but the phytoplankton reacted to the reduction in filter-feeding fish by showing an upward trend in their growth rate from increased nutrients and higher temperatures. The zooplankton, which could not compete with planktivorous fish for energy and were also grazed by the planktivorous fish, gradually declined to extinction.

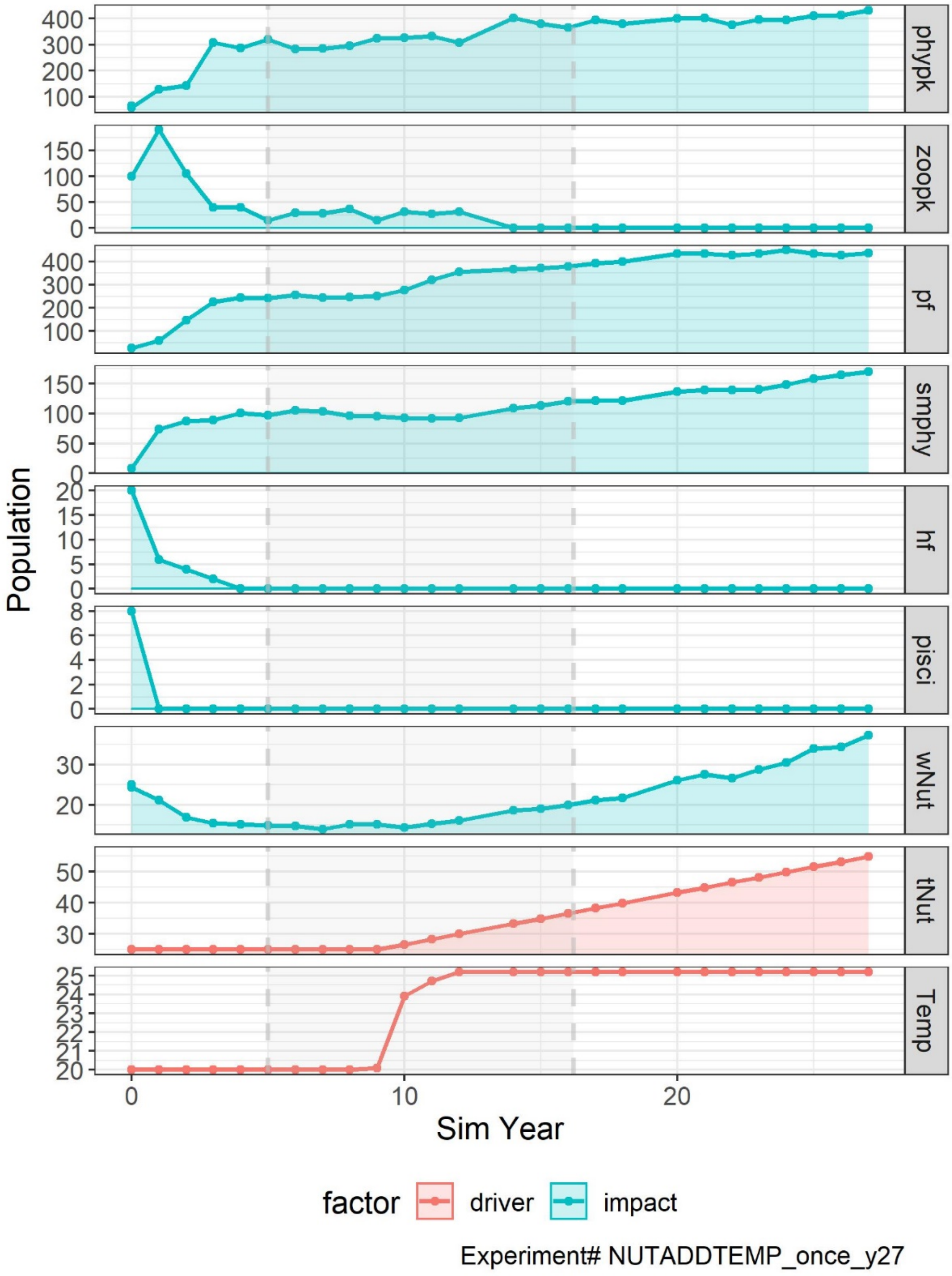

Figure 5-11: Scenario showing Population changes in biotic components and environmental changes in temperature-moderating eutrophication. The horizontal axis represents the simulation time (Sim year) and the vertical axis shows the population. The abbreviation for each component is written on the label to the right of each small window. “Phypk” for phytoplankton, “zoopk” for zooplankton, “pf” for planktivorous fish, “smphy” for submerged plants, “hf” for herbivorous fish, “pisci” for fish-eating fish, “wNut” for the remaining nutrient concentration in the water, “tNut” for the total nutrient concentration and “Temp” for the water temperature.

Phase plots of the relationships between nutrient concentrations and population dynamics show a transition in responses before and after environmental drivers interfered with the states and habitats of the organisms (Figure 5-12). Before Year 9, the level of in-water free nutrient decreased significantly over three years before achieving stability. In the period when both temperature increase and nutrient addition apply (the blue points), the relationship between planktivorous fish and in-water nutrient concentration changed visibly while other relationships remained consistent with previous patterns. After the disappearance of zooplankton in Year 13, phytoplankton became the only food for planktivorous fish. With less energy available, the rise in planktivorous-fish population slowed considerably, while the population of phytoplankton changed cyclically and gradually increased in response to the increased nutrient load. After Year 14, submerged plants reached the threshold of energy for reproduction and their population began to increase with the rise of nutrient concentration in the water. The three functional groups maintained similar responses to the increasing nutrient load (the red points on Figure 5-12), and their population size increased with the eutrophication process. The phase plot did not show any evidence of critical transition based on the driver-response relationship.

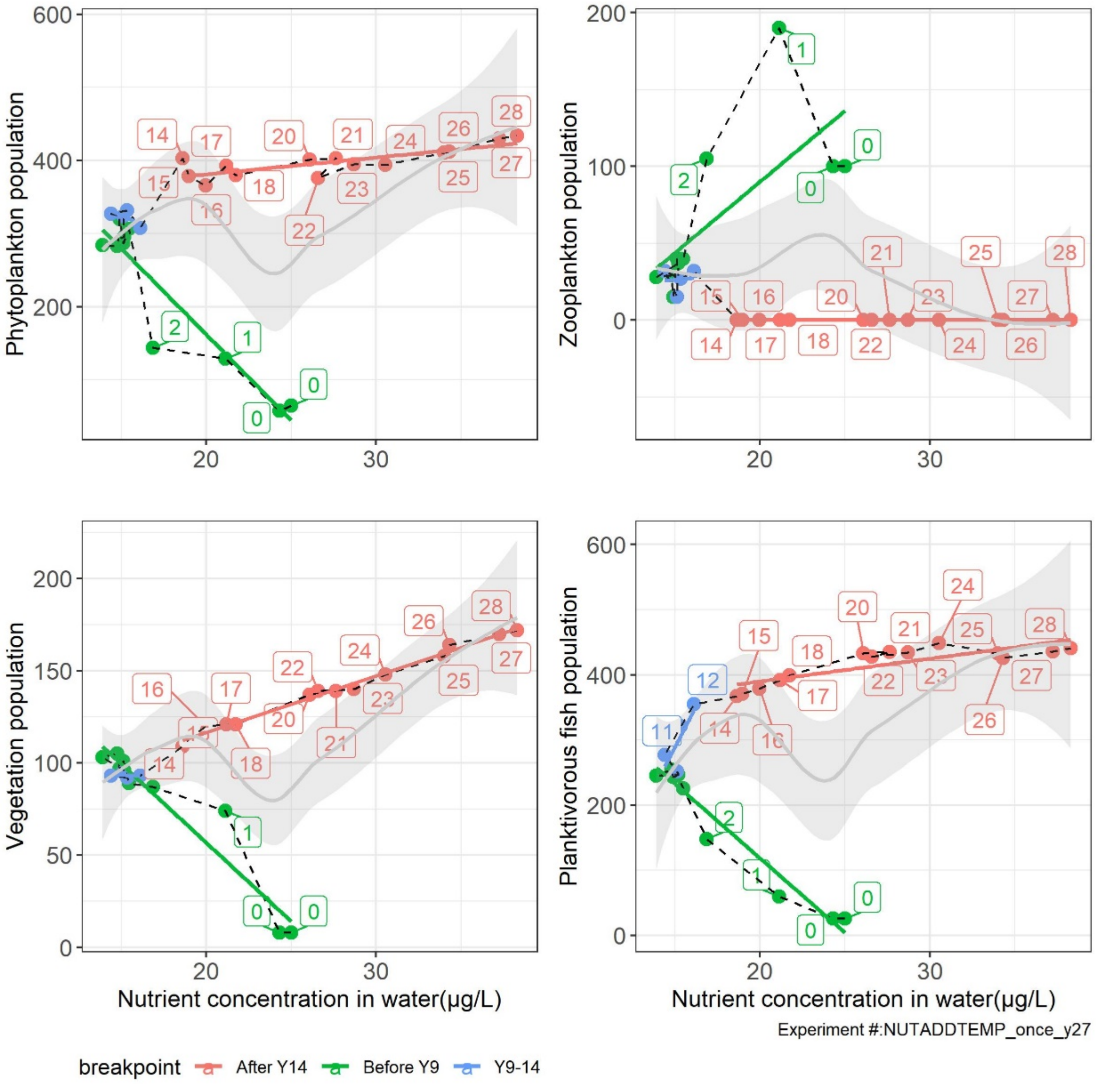

Figure 5-12: Driver-response relationships between functional groups and in-water nutrient concentration before and after breakpoint (Years 9 and 12). Black dashes link samples in order of simulation times. The red points represent observations before Year 9, the green points represent samples between Years 9 and 12 and the blue points represent observations after Year 12. Grey lines and shadows show the results of smoothing all points using the "Loess" method. Simulation years are labelled near points.

5.3.2 Experiment 2: Realistic simulation of eutrophication

To explore the changes in this ecosystem model further under a more realistic scenario of similar environmental change in Lake Taibai, the combined disturbances of continuous nutrient load input, continuous reduction in lake size, temperature increase over time and the release of herbivorous and planktivorous fish into the lake were simulated in Experiment# TBComprehens_v5_y274. After simplification based on the known environmental characteristics of Lake Taibai, a steady input of 1.041 μg/L per 100 days of nutrient load and a reduction in lake area at a rate of 4.5 hectare/a was introduced into the system after 10 years of stable ecosystem operation. After 85 years from the start of simulation, fish were added in a ratio of 2 herbivorous fish and 5 planktivorous fish for 20 years, while water temperature increased slowly, at a rate of 0.05°C, to represent the changes in Taibai Lake described in Section 5.2.1. In Year 95, reclamation ceased and lake size reduction stopped along with it. Changes in ecosystem components (the blue line in the figure below) and response mechanisms were observed under the influence of these environmental changes (red line).

After 10 years of adaptation, the disappearance of herbivorous and piscivorous fish contributed to the composition of phytoplankton, zooplankton, submerged macrophytes and planktivorous fish for the period of eutrophication. After nutrient loads were introduced into the system, submerged macrophytes increased linearly due to a lack of grazers. The zooplankton then died out, causing a reduction in the planktivorous fish population and a change in food sources. After a steady state period during simulation years 30 to 50, the phytoplankton population declined, resulting in a consequent decline in the planktivorous fish population, stimulating an outbreak of phytoplankton growth. Algal blooms led to a subsequent burst in planktivorous fish population. During this period, the nutrient load was steadily imported into the system and the surface area of the lake continued to shrink, increasing both the nutrient concentration in water and the chance of interactions between organisms within the lake. The algae became extinct after being consumed by the sudden elevation of the planktivorous fish population, leading to the subsequent extinction of planktivorous fish. The extinction of algae is rare in a realistic lake ecosystem, and it occurs in the model for the following potential reasons: 1) the natural selection of food size has been neglected and algae can be consumed by all grazers despite physical limitations; 2) algae in the model live in pelagic areas and have no substrates to attach or hide in; 3) in each day, the reproduction of algae is less than the loss from being grazed by more planktivorous fish. Before fish were released in Year 85, only water plants remained in the system. After Year 85, fish were introduced into the system at a rate of 2 herbivorous fish and 5 planktivorous fish every 100 days for 20 years, creating an artificial system based on submerged macrophytes, planktivorous fish and herbivorous fish ("sm+pf+hf"). Nutrient loading and an increasing system temperature continued throughout this period. Submerged plants were suppressed by herbivorous fish, and the herbivorous fish population grew and remained at around 900. The planktivorous fish population was maintained at the same level as the input because there was no food for them. The simulation result is evaluated against reality.

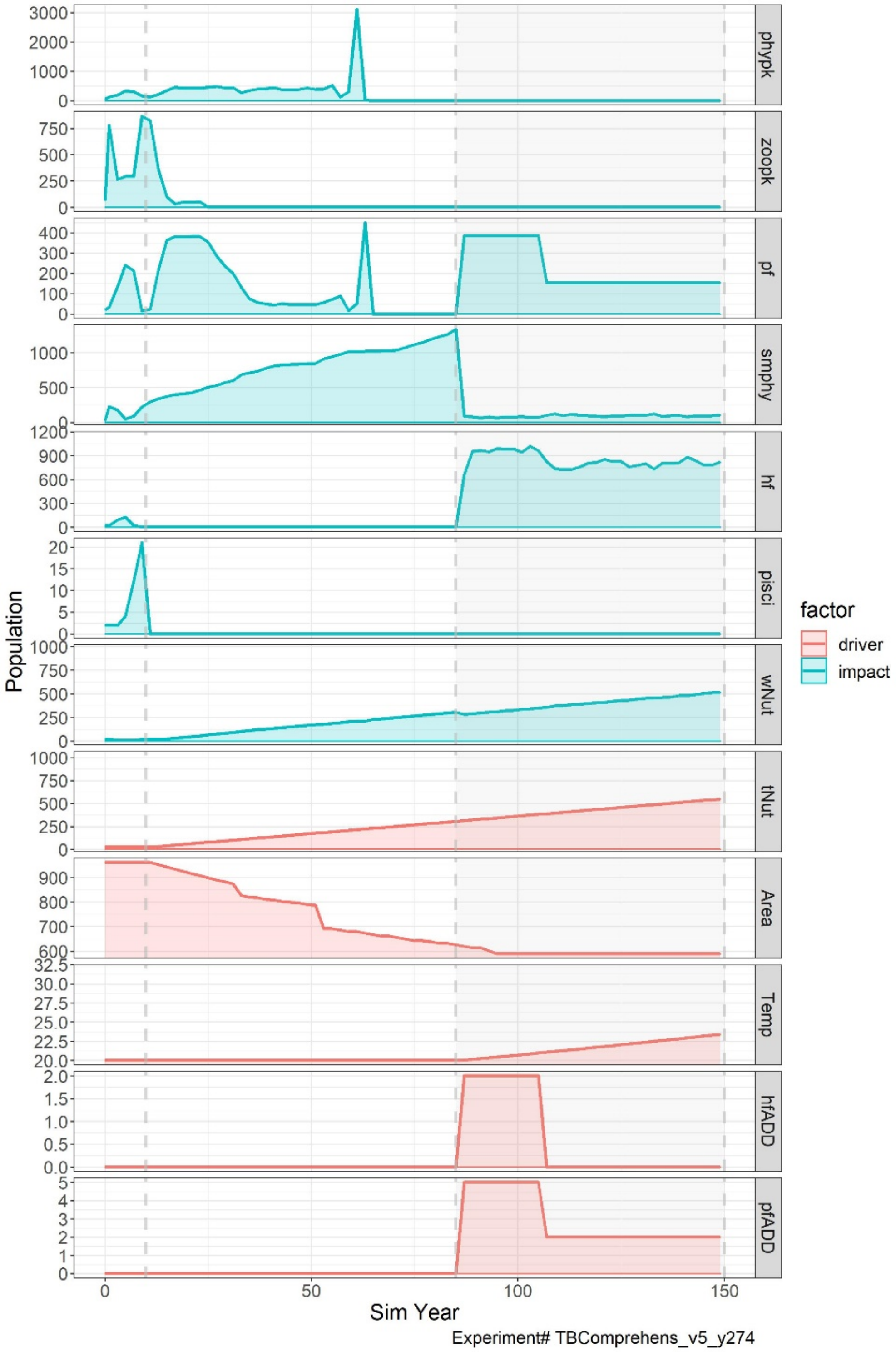

Figure 5-13: Population and environmental changes in experiment #TBComprehens_v5_y274. The pink area shows the period after top-down perturbations

that resulted from the addition of herbivorous and planktivorous fish to the system. The first six panels show populations of functional groups, and the last six show environmental changes among which wNut (free nutrient in water) is dependent on biotic changes. “Area” means lakes area, “Temp” means water temperature, “hfADD” and “pfADD” means the number of added herbivorous and planktivorous fish.

To understand the combined effect of all the factors involved in the model, the influence of each environmental factor on the ecosystem state can be visualised further using multivariate analysis CCA. This analysis quantitatively integrates the relationship between exogenous driving forces and system change in the experiment in the comprehensive model, demonstrating the ecological changes in the group under the overall effect of environmental change. Thirty-seven samples were taken each year from the experiment data and the mean values of the samples represent the yearly system state.

The results of the CCA analysis show that temperature, water nutrient concentrations and lake area have similar arrow lengths, representing similar strengths of influence on change in the community. The sample sites were more evenly influenced over time by the three environmental factors. The distribution of functional groups shows a high degree of overlap between zooplankton and piscivorous fish attributes, with phytoplankton and submerged plants responding more strongly to temperature changes and water column nutrients, showing a slight negative relationship. Site scores, as weighted averages of species scores, show that the ecosystem state is roughly distributed across the three regions over time. The interpreted components of the CCA axis I suggest that the main ecosystem changes depend on lake surface area, temperature and nutrient concentration as I expect, the direction of the axis II may also represent a potential determinant.

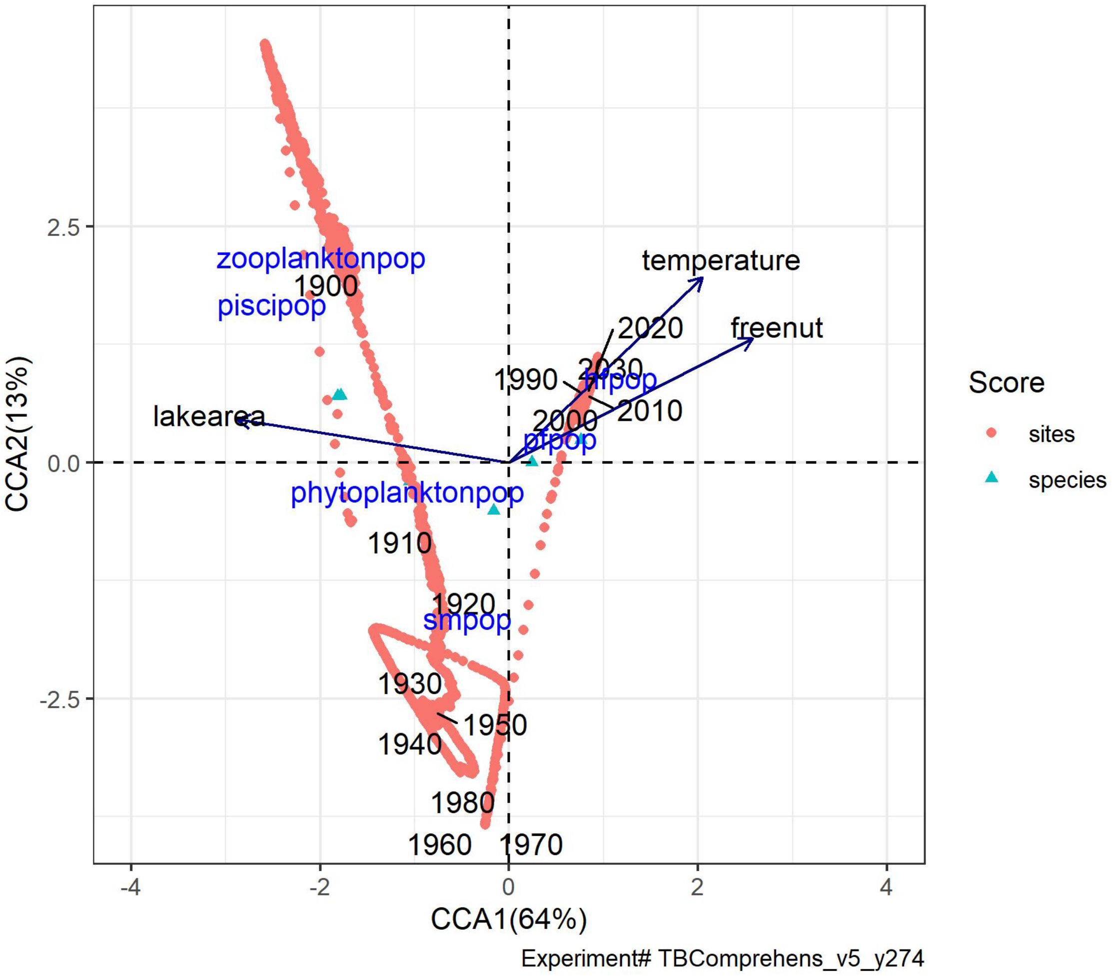

Figure 5-14: CCA biplot with sites (green triangles), species (blue text) and environmental factors (black arrows). Chronological numbers were displayed at a 10-year interval from 1900 to 2020.

In addition to the pattern of ecosystem change, this multiple exogenous driver experiment shows correlations of demographic change between different functional groups. According to the figure and the table, it is evident that zooplankton and piscivorous fish were positioned very close to each other in the CCA space, with piscivorous and herbivorous fish positioned in the same quadrant and submerged plants and phytoplankton in another quadrant. This represents the different response patterns of each functional group to environmental factors.

Table 5-3 Species scores of six functional groups in the CCA result

Abbreviation	Group	CCA1	CCA2	CCA3
phytoplanktonpop	phytoplankton	*-1.0570*	*-0.201547*	*-0.254866*
zooplanktonpop	zooplankton	*-1.7830*	*0.704249*	*0.154440*
smpop	*submerged macrophyte*	*-0.1625*	*-0.511498*	*0.113358*
pfpop	*planktivorous fish*	*0.2422*	*0.002109*	*-0.040639*
hfpop	*herbivorous fish*	*0.7571*	*0.236185*	*-0.009018*
piscipop	*piscivorous fish*	*-1.8155*	*0.702930*	*0.055433*

5.3.3 Experiment 3: Simulating pathways to recovery

5.3.3.1 Recovery with no nutrient load and fish farming

Theoretically, the response of phytoplankton and submerged plants may lag during the recovery of eutrophic states when inputs from external drivers (such as nutrients, fish-farming or surface area changes) either cease or develop in the opposite direction. The experiment referred to in this sub-section is experiment #TBRecNutADD_once_y164. This experiment models a follow-up phase after the nutrient-driven scenario experiment #TBNutADD_once_y30. The variable settings for the turbid water state were estimated based on the stable turbid-water state formed in experiment #TBNutADD_once_y30, after nutrient load stopped and the total nutrient concentration reached 91.624 μg/L. It took 27 simulation years for this stable turbid state to emerge. I subsequently conducted recovery manipulation in order to observe the resulting effects until a new state emerged. Finally, on Day 60,000, about 164 years after the beginning of Experiment # TBNutADD_once_y30), the new state was confirmed as being stable.

Against the background of a gradual increase in nutrient loading, the phytoplankton community remained in numerical dynamic equilibrium, while the number of submerged plants increased in positive correlation to the total nutrient concentration. Until around Day 9450, submerged plants resulted in a decline in zooplankton biomass due to the excessive high density of algal growth and consequent light limitation. After Day 10821, the nutrient loading ceased to grow, and the system returned to a closed state. At this point algal growth came under double pressure and its numbers remained low, while zooplankton gradually decreased to a very low level due to difficulties in finding food. During this period, the three functional groups of the ecosystem completed their re-adaptation and reached a state of equilibrium, resulting in a system in which submerged plants dominated and phytoplankton were low, from around Day 20000 to Day 25000. This simulated ecosystem state is similar to the reconstruction of Lake Taibai in the 1960s, after the construction of the dam and the rebuilding of the lake in a more closed environment and after receiving surface pollution from surrounding agricultural land and domestic sewage. At that time, the fisheries around the lake responded to this state of eutrophication by releasing herbivorous fish and Chinese mitten crabs to clear the water of excess grasses, and by investing in large quantities of planktivorous fish fry as an economic fishery process based on a one- or two-year yield cycle.

The starting point for this manipulation was the desire to restore the ecosystem to its former state, so the manipulation was simplified by adding 50 planktivorous fish and a small number of herbivorous fish to the model's eutrophic steady state.

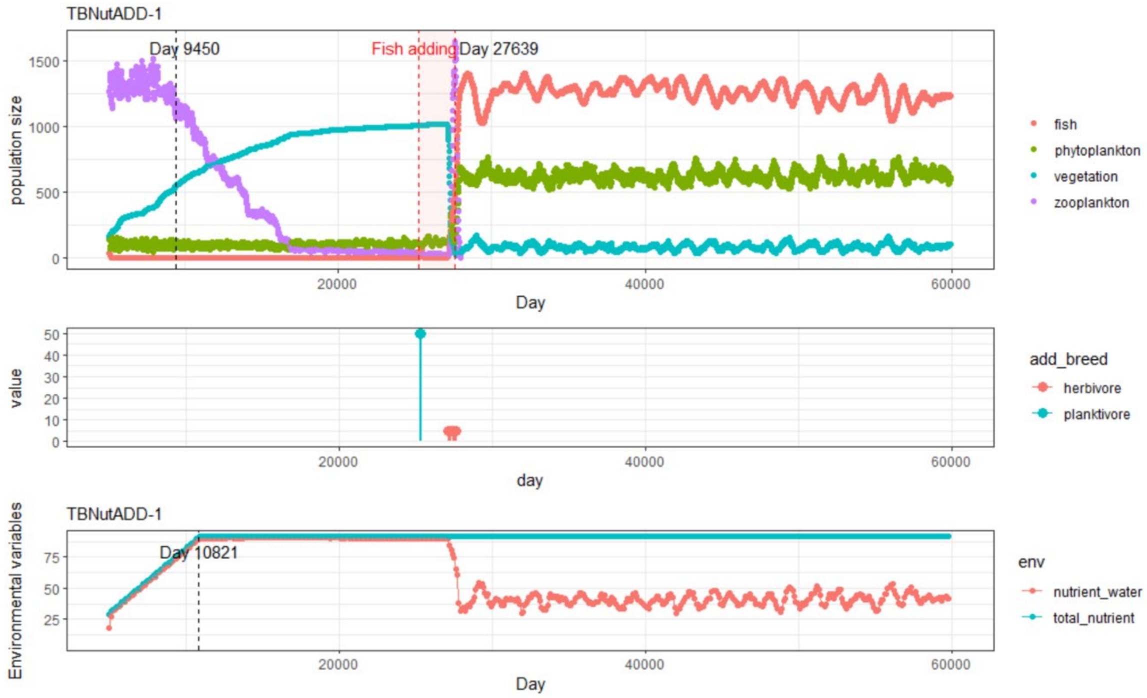

Figure 5-15: Population and environmental changes in the recovery phase based on the addition of planktivorous and herbivorous fish. The top panel shows the trajectory of population change over the simulation time. The middle panel shows the point in time when the means of recovery (the addition of fish) commenced and the amount of fish put in. The lower window shows the change in total nutrient concentrations and the remaining nutrient concentrations in the water of the simulated system over time.

The simulations show that after the introduction of planktivorous and herbivorous fish into the lake, the fish grazed the zooplankton and submerged plants, eventually rendering the zooplankton extinct. However, the zooplankton population rose dramatically, going off the top of the chart in around Year 76 and becoming extinct very soon after this sudden rise. The system consequently underwent a dramatic structural change and was forced to adjust to another steady state based on the dominance of fish, phytoplankton and vegetation. The submerged plant population plummeted to around 1% of its former level and fluctuated periodically henceforth. As zooplankton disappeared, phytoplankton populations rose in a stepwise fashion. Fish reproduced in large numbers by grazing on zooplankton for energy and continued to rely on the rapidly growing phytoplankton in the eutrophic environment to maintain their populations. The fish population consisted of a combination of herbivorous and planktivorous fish, which suppressed the remaining phytoplankton and submerged plants in the system from the top down, forming a relatively stable new equilibrium. The lake at this time was similar to the condition of Lake Taibai according to the 1990s survey, with the fish that were added later dominating the ecosystem, phytoplankton becoming more abundant and submerged plants on the brink of disappearing altogether. Though Lake Taibai has no record of any change in its abundance of zooplankton, the reconstruction of zooplankton subfossils shows that their abundance increased with the trend of eutrophication in Shengjin Lake, another MLYB lake (Cheng et al, 2020).

During these environmental disturbances, the relationship between the submerged plant population and the remaining nutrient concentration in water also changed dramatically. The relationship between submerged plants and residual nutrient concentrations in water shifted immediately after nutrient load input to the lake ceased (the blue points in Figure 5-15 after Year 30). The green dots in the graph, representing the nutrient input phase, show the main trend of increased numbers of submerged plants in response to increasing nutrient concentrations in the water column. After the nutrient load stopped being added (the blue points), the number of submerged plants still increased, albeit more slowly, given the constant nutrient concentration in the water column. The response of submerged plants to the halt in added nutrients during this period was extreme. From Year 74 onwards (the red diamond in the top right corner) the addition of herbivorous and planktivorous fish resulted in a rapid decline in the number of submerged plants, accompanied by a reduction in the remaining nutrient concentration in the water column. After the addition of fish and any other disturbances ceased at Year 76, the residual nutrients in the water column were reduced to half their previous levels with essentially no change in the submerged plant population. The relationship between the submerged plant population and the residual nutrients in the water column formed a stable cycle, which is represented by the new steady state at the far right of the figure. This plot of the relationship clearly shows the areas of convergence of the two different steady states. The steady state represented by the orange dots on the left is the steady state in the initial low nutrient system, while the steady state formed by the blue dots on the right developed after fish were stocked in the lake, while the total nutrient concentration of the system remained high.

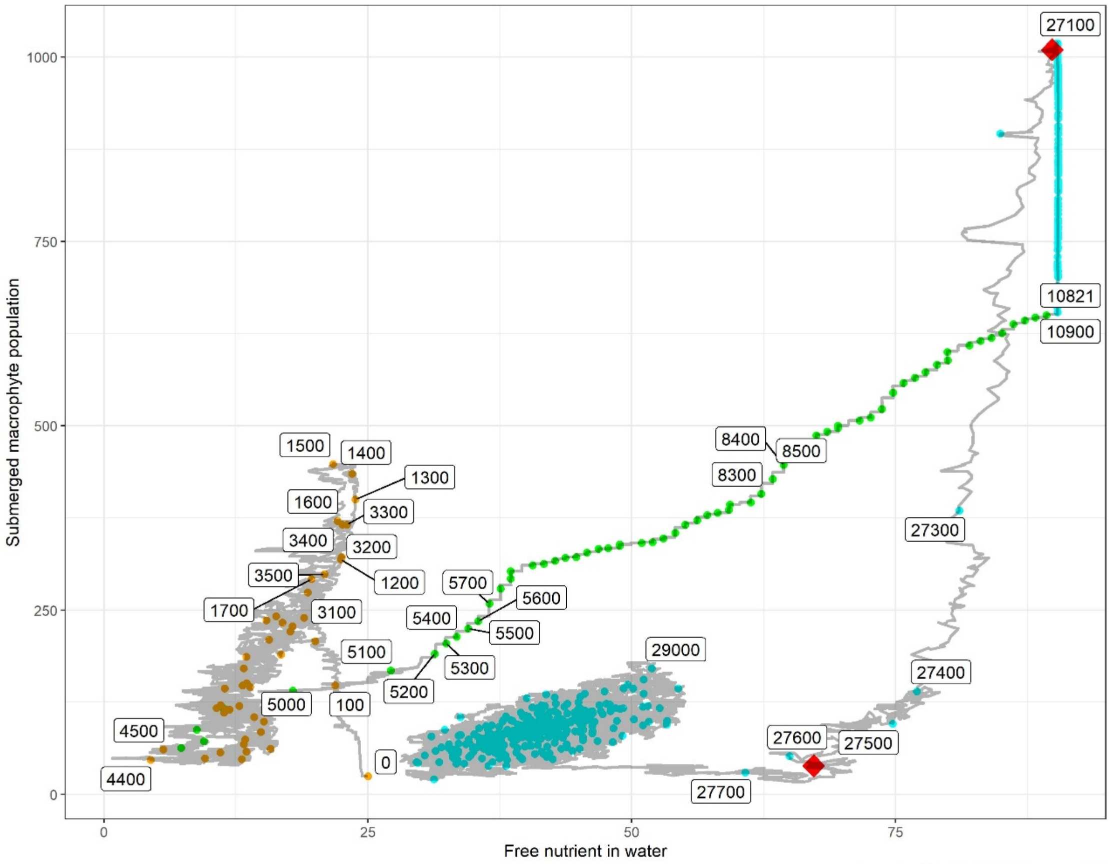

Experiment# TBRecNutADD_once_y164

Figure 5-16: Trajectory plot of the relationship between the submerged plant population and the remaining nutrient concentration in the water over time. The horizontal axis represents the nutrient concentration remaining in the water in the simulated system of the lake other than the biological uptake of nutrients, and the vertical axis is the submerged plant population. The grey lines connect each sample point in time order, with labels on the sample points showing the time of each occurrence in years at nearby points. The orange points are prior to the increase in nutrient loading (before Year 13), the green points represent the time during the nutrient loading process, and the blue points represent the state of the system after nutrient loading stopped (Year 30). The red diamonds represent the start and end times of the fish release process.

The unused nutrient concentration in the water column decreased significantly after the addition of fish, and was negatively correlated with the size of the fish population. The curve of the free nutrient and total nutrient concentration in the lake ecosystem shows three types of response (Figure 5-16). When the total nutrient concentration of the system was constant, the concentration of unutilised nutrients in the water column fluctuated within a certain range. In the simulated ecosystem, stocking fish allowed them to compete and become the dominant functional group in the ecosystem, using more nutrients from the water column and storing them in the organism and causing a reduction in the concentration of unused nutrients in the water. The biomanipulation by fish removal has been used as an effective method in many shallow lakes with a high external nutrient loading (Sondergaard et al, 2007, 2017), but no such management strategies have been applied to MLYB lakes yet.

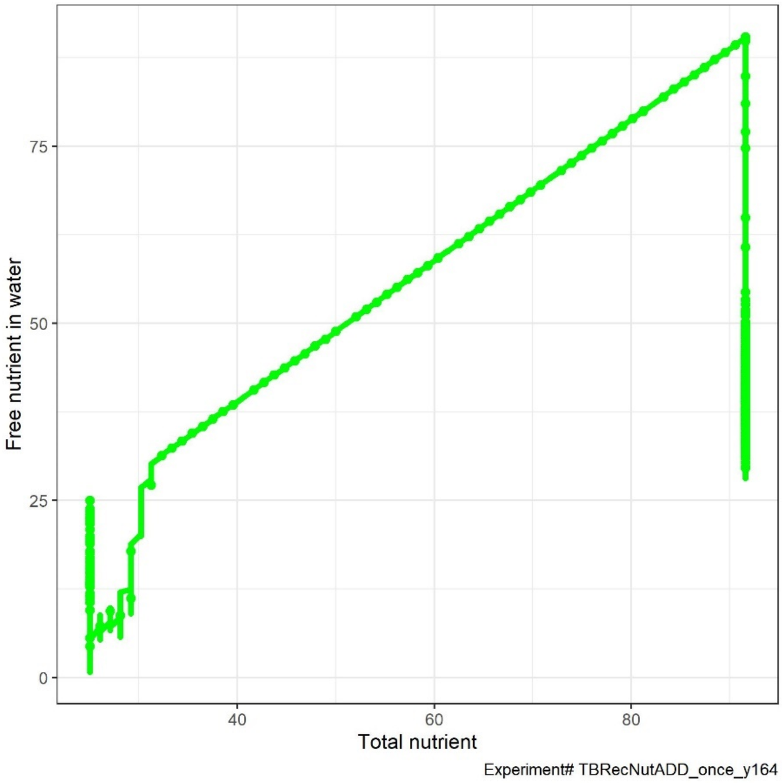

Figure 5-17: The relationship between the total nutrient concentration in the system and the residual nutrient concentration in the water column. The green line connects the points in temporal order.

5.3.3.2 Recovery with reduced total nutrient

Experiment #TBRecNut_once_y80 was designed to simulate the process of de-eutrophication in a system in order to understand how a reduction in the total amount of nutrients would change the remaining levels of nutrients in the water column and the overall state of the ecosystem without disturbing the biome. The eutrophication process was simulated for the first 41 years, and a stable eutrophic state developed for over a decade, with phytoplankton and planktivorous fish as the only components of the system. Immediately after Year41, total nutrients were reduced at a rate of -10% per 100 days until they fell below 20 µg/L. The dependent variables observed represented changes in the population of ecosystem components over time and the remaining nutrient concentration in the water column.

Compared to the total nutrient concentration (84 µg/L), the unused nutrient concentration in the water column of this eutrophic system was low at first, fluctuating between 10 and 15 µg/L. The phytoplankton population did not show any significant trend during the nutrient reduction process, while the planktivorous population decreased linearly along with the total nutrient concentration in the system. As the only two factors in this system were phytoplankton and planktivorous fish, the decline in the planktivorous fish population was entirely due to bottom-up pressure. Meanwhile, total nutrient concentrations and water column nutrient concentrations changed at different rates. The reduction in total nutrient concentration from 84.62 µg/L to 2.76 µg/L was accompanied by a 10.24 µg/L reduction in the residual nutrient concentration of the water column. The reduction in overall nutrients in the system had the effect of stabilising the reduction of the residual nutrient concentration in the water column, with no change in system state or composition. This simulation process is consistent with numerous case histories and large-scale experiments over decades following the removal of phosphorus (Schindler, 2012).

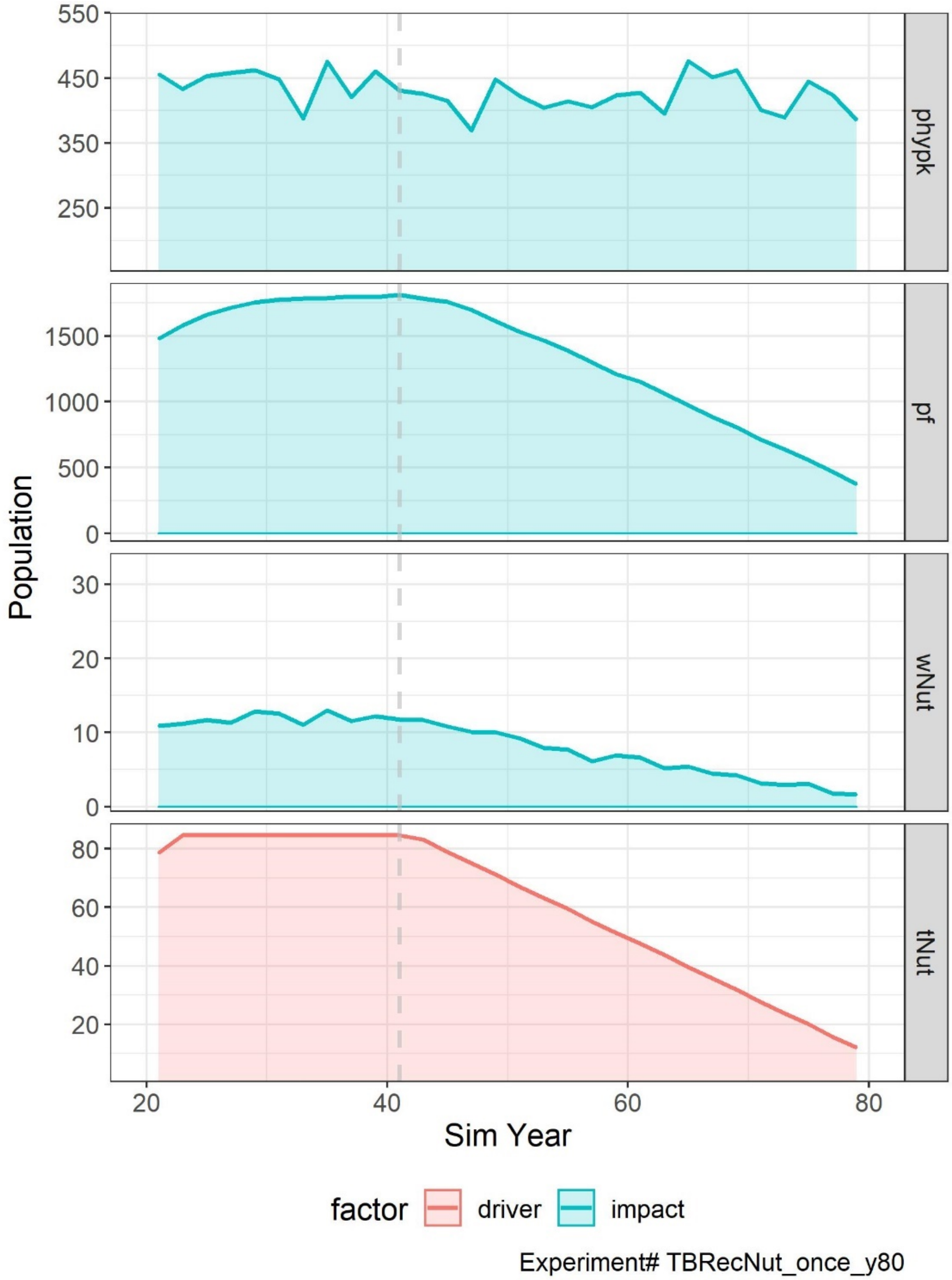

Figure 5-18: Changes in the population of ecosystem components and residual nutrient concentration in the water column over time under a scenario of nutrient concentration reduction only. Red represents changes in driving forces, blue represents changes in dependent variables. “Phypk” represents phytoplankton, “pf” represents phytoplankton-eating fish, “wNut” represents the residual nutrient concentration in the water column, and “tNut “ represents the total nutrient concentration of the system.

Chapter 6: Discussion

6.1 The roles played by the function groups in the transition

The ABM simulations were able to generate and mirror ecosystem transitions in order to acquire a rich dataset of metrices at both aggregated and individual levels. Regime shifts occurred in the above experiments that focused on increases and decreases in the nutrient load, and appeared many times in some systems. In a non-steady state with no external disturbances (Subsection 5.3.1.1), functional groups of ecosystems slowly changed and reconstituted themselves in new numerical proportions. This transition occurred after the cessation of cumulative external drivers over time as a hysteresis. Changes in temperature and nutrients directly stimulated the growth rate of producers, producing bottom-up nonlinear effects such as an increase in phytoplankton that simultaneously promoted an increase in zooplankton and planktivorous fish, while planktivorous fish grazing on zooplankton reduced zooplankton numbers, with zooplankton suffering both an increase and a decrease in abundance. Changes in lake size altered the spatial distances of the food-web components, and therefore the original community balance. As space became smaller, the chances in predator-prey encounters become greater. The submerged macrophytes had a limiting effect on the swimming speed of fish as designed in the model, and the slowing down of fish feeding accelerated the growth of zooplankton, limiting the growth of phytoplankton and having a synergistic effect on the feeding of planktivorous fish.

The dynamic equilibrium of the ecosystem represented in the model is event-stochastic, and the same initial state may end up exhibiting up to seven different system components, most of which continued to maintain a dynamic equilibrium in population size without any external perturbations. This phenomenon helped us to understand the mechanisms of homeostatic ecosystem transitions in terms of our understanding of the generation of steady states. Since the formation of homeostasis itself may result from the gradual accumulation of stochastic events, the probability of the outcome of these events will also change under the influence of gradual environmental change, thereby increasing the probability of the occurrence of another homeostasis, represented by the occurrence of a regime shift. System resilience is expressed at the individual level in terms of the magnitude of variation in population sizes under competition and subsistence constraints, particularly the lower limit, as well as in the structure of the system composition.

Realistic experiments provided useful perspectives to understand the changes that have occurred in lake ecosystems over the past century as revealed by palaeoecology. For example, the algal blooms that emerged from the results of the TBComprehens_v5_y274 experiment occurred under conditions of reduced lake size and progressively higher nutrient concentrations. The mechanism underpinning their appearance was a change in food source for planktivorous fish from two (phytoplankton and zooplankton) to one (phytoplankton), and an increase in nutrient concentration that led to an increase in phytoplankton growth rates. These two factors simultaneously weakened the stability of the planktivorous and phytoplanktonic subsystem, making them both highly vulnerable to extinction during fluctuating cycles.

Meanwhile, individual-based ecosystem models helped me to understand the variation and association of different palaeoecological indicators in complex systems using the results of group interactions. In the palaeoecological evidence from the MLYB lakes Changdang, Taibai, Liangzi and Zhangdu, cladocera subfossil reconstructions reveal that the regime shift in the composition of the zooplankton community was close to and generally later than the time of regime shifts indicated by diatom subfossils in the lakes (Kattel et al, 2016; Ke Zhang et al, 2018), which is similar to the results of some of my own modelling experiments (Subsection 5.3.1.3). Taking Lake Taibai as an example, the changes in the PCA first-axis scores for the diatom communities over time followed a similar trend to the changes in the PCA first-axis scores of the cladocera communities. The trends in the PCA first-axis scores of the chironomid community were similar to those of diatoms and cladocera before the 1960s, but differed from them after the 1960s. These results suggest that algae and zooplankton trends in the Lake Taibai ecosystem have remained relatively similar over the past century, while benthic organisms may have been subject to different effects from zooplankton after the 1960s. Many studies of the biological residues of diatoms, cladoceran and plant macrofossils have already been produced based on MLYB lake sediments, but changes in time series and the environment are independent. The modelling experiments would help understand the interactions and ecological processes in the lakes.

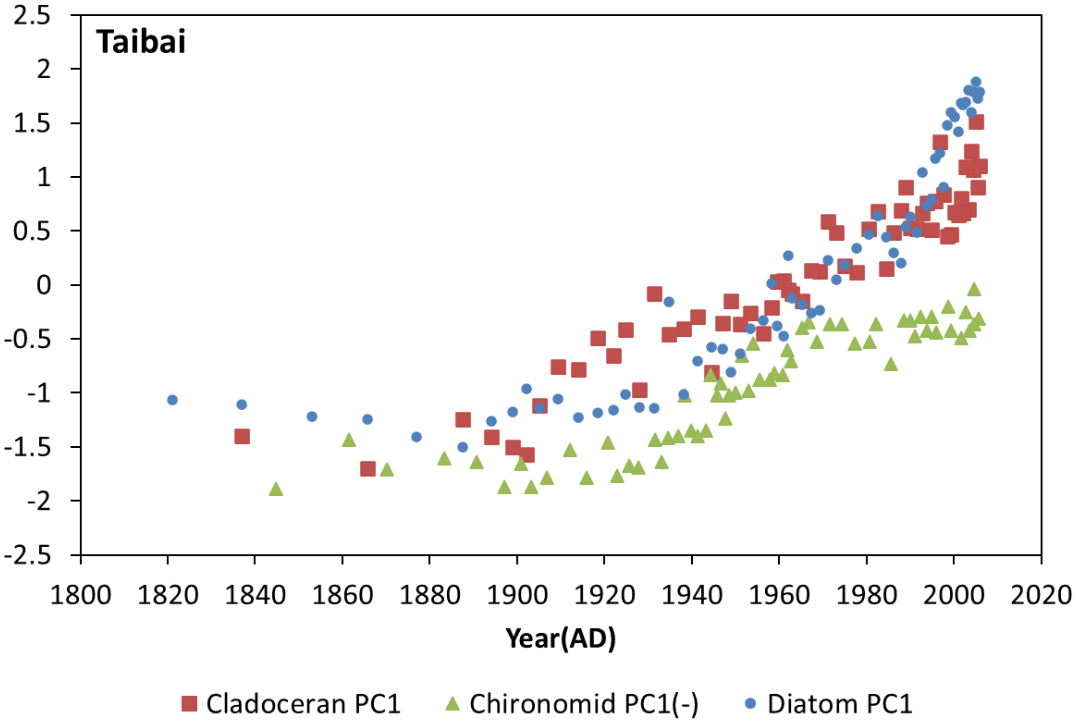

Figure 6-1: Changes in Cladoceran PC1, Chironomid PC1 and Diatom PC1 over time in Taibai Lake. All data were reconstructed using subfossils in sediment cores. Cladoceran and Chironomid PC1 are from unpublished data.

6.2 How environmental changes influence the pattern of driver-response relationship

The results of the steady-state experiments in the previous chapter show that complex systems are highly likely to develop different outcomes even under the same environmental and biological rules. The results of the experiments in this chapter indicate that the intensity of the input of nutrient loading as a disturbance (5.3.1.2), the mode and rate of addition (5.3.1.3), the timing of addition and the presence or absence of supporting factors such as temperature can also lead to different system development outcomes. Other environmental factors, such as lake depth, can alter the pattern of lake ecosystem changes at the ecosystem structural level for the same nutrient change scenario (5.3.1.3).

In the model, ecosystem changes that were due to eutrophication differ from those in practice insofar as increases in nutrient levels directly contribute to increases in the population of grazers, rather than the phytoplankton population, as long as the phytoplankton are suppressed by grazers such as zooplankton or planktivorous fish. The relationship between phytoplankton outbreaks and the exogenous input of nutrients is not straightforward. Lake systems with the same total nutrient load but different nutrient addition patterns may show very different trends over a period of decades. Under conditions of sufficiently slow nutrient addition, homeostasis may even be maintained between ecosystem components. In the experiment in which I attempted to recover via fish farming, nutrient concentrations in the water decreased from 91 µg/L to 25 ~ 50 µg/L after fish became the most dominant community in the system. This experiment illustrates that stocking fish as a method of reducing nutrients in the water column is feasible, but there are a number of constraints that need to be addressed. The conditions include firstly that fish need to be harvested gradually rather than dying and decomposing in the lake, and secondly that no more exogenous nutrients should be added as a result of fish farming. The history of fish farming in Lake Taibai has followed a process of natural farming and intensive farming of Chinese domestic fish while fishermen continued to harvest out the fish and introduce large amounts of nutrients in the form of chemical fertilisers and organic matter into the lake, ultimately resulting in a scenario of severe eutrophication of the lake and a homogenous ecosystem structure.

6.3 Management implications

Consistent with the experiments described in the previous chapter, there is no absolute perfect homeostasis in the complex systems I modelled, but instead there is a relative homeostasis that is always in a process of dynamic fluctuation. The effect of external disturbances on the internal structure of an ecosystem depends on the properties of the disturbance itself, the size of the disturbance, how it is applied and where in the cycle of population dynamics the disturbance is located. The cyclical pattern that emerged in the simulations was similar to the seasonal cycles that occur in natural ecosystems (Hansen & Jeppesen, 1992; Winder & Cloern, 2010), although the annual cycle of phytoplankton appears in the model in cycles of 5-10 simulated years. This periodicity of inter-decadal variation was also manifested in Lake Veluwemeer's changes in vegetation cover in water between 1950 and 1990 (Scheffer, 1998).

In addition, when identifying whether functional groups undergo critical transitions in response to environmental changes, I recognise that the analysis of driver-response relationships is a powerful tool in evaluating systematic relationship change (Andersen et al, 2009; Otto et al, 2018). At the same time, however, the environmental variables used are not necessarily the stereotypical drivers that lead to unidirectional organism responses.

Some environmental indicators, such as the available nutrient concentration in the water, which is the nutrient left after all organisms have taken their share, have a direct feedback effect on changes in biological indicators. In managing lakes, the total nutrient content (total phosphorus, for example) and the residual in-water nutrient content (such as inorganic phosphate) cannot be treated in the same way, as this would lead to huge errors in our assumptions of alternative stable states.

To improve our understanding of the relationships between experimental results and drivers, the experimental setups here were relatively simple, whereas the driver changes that occur in reality are more complex and include comparatively trivial factors. The main purpose of my model is therefore to help researchers understand the nonlinear emergence of ecosystems and to try and make predictions of patterns in possible scenarios based on the mechanisms that are already understood. The different results obtained by modelling different system states under the same environmental change scenarios represent the scientific support for the “One Lake, One Policy” restoration programme for Chinese lake management.

6.4 The ABM model as a tool for assessing ecosystem state shifts

The ABM model is an ecosystem model based on the process of changing ecosystem feedback loops in a lake that have been reconstructed from palaeoecological indicators, sharing the characteristics of expert and emergent models. The expert model refers to the conceptual model of ecosystem feedback mechanisms that I developed prior to the development of the ABM model, based on a phenomenological understanding of the changes in Lake Taibai and its catchment over the past century through analysing changes in the community composition of diatom subfossils in the sediments as well as inferences based on ecological mechanisms. The emergent model is characterised by its ability to reveal system dynamics from simulated individual-level interactions, allowing a multidimensional analysis of the overall processes and mechanisms driving changes in ecosystem state. The most common and universal indicator is the population size of functional groups, followed by the residual nutrient concentration in the water column (the variable “global-free-nutrient” calculated as the total amount of nutrients in the system minus the amount of nutrients that is fixed in the living organisms). The model can also record the spatial distribution characteristics of each agent (Subsection 4.7.2) and measure changes in the strength of interactions at individual scales over time and under different conditions. Models used to explain changes in the state of lake ecosystems, such as PCLake, have been able to produce more realistic predictions of critical transitions based on detection data (Hilt et al, 2018; Nielsen et al, 2014), but the processes and mechanisms of steady-state transition formation have not been explored in as much detail. The simulation of complex systems that do not in themselves aim to produce regime shifts can instead uncover the mechanisms and processes of nonlinear pattern formation during the interaction of individual simulations (Turnbull et al, 2018). The development of customised ABM models for lakes with a palaeoecological reconstruction base can therefore help managers to assess ecosystem state transition mechanisms and predict possible future scenarios.

Meanwhile, mere population changes provide us limited information with which to interpret the processes and causes of ecosystem change without gaining a greater understanding the response patterns of functional groups to environmental change. Functional group populations are important indicators in terms of assessing the state of an ecosystem, but do not provide sufficient information to allow us to analyse the mechanisms of their occurrence (Possingham et al, 2001). For example, in a comprehensive factor-driven eutrophication experiment (Subsection 5.3.2), algal blooms were caused not only by the increasing accumulation of nutrient concentrations in the water column, but also by the extinction of zooplankton, making the link between algae and planktivorous fish overly tight and homogenous. Population models, as a classic simplification of the model used for assessing ecosystems, are able to capture the representation of individual survivorship in individual populations well, but it comes at the cost of discarding other important ecological features at population and ecosystem level, such as individual differences, interactions between populations and relationships across complex systems. While population size is usually used to indicate catastrophic changes of concern to ecosystem management, interactions and feedbacks between populations can explain how the changes occurred. If the aim is just to simulate patterns of change in population size, then the random walk mathematical model (Appendix B.1.4), which simulates changes in palaeoecological indicators, can do this perfectly well. However, population changes that are not correlated will not reflect or be reflected in the emergent behavioural mechanisms of complex systems. This is why the use of individual-based models to simulate changes in lake ecosystems is valuable for ecological conservation, and ABMs can provide modelling recommendations for ecological conservation and risk avoidance in terms of preventing nonlinear behaviour and mitigating catastrophic changes in the system. However, ABMs cannot predict population changes in linear behaviour patterns as accurately as empirical models tuned according to extensive monitoring data.

Given that nonlinear behaviour in lake ecosystems leads to a mismatch between desired goals and actual effectiveness, the need to consider ecosystem change patterns from an ecosystem perspective has grown in practice in recent years. After phosphorus management action between 2015 and 2017 in Lake Taihu, when nutrient load inputs had been reduced, total phosphorus concentrations in the northern region increased in the water column instead of decreasing, and there was no significant downward trend in the concentrations of total dissolved phosphorus (Zhu et al, 2021), which is similar to the Dutch lake management process that took place many decades ago (Sondergaard et al, 2013). The nutrient concentrations in the water column also experienced fluctuations after the simulated nutrient loading ceased in the experiment, and fluctuations were greatest at the beginning of the cessation of the nutrient input phase (in Subsection 5.3.3.1). From the simulation of this ABM ecosystem model, I can see that the causes of changes in eutrophication indicators may be biological and may not be easily detectable. Although nutrient loads and nutrient levels are often used as indicators of eutrophication, biological indicators such as chl-a concentration and diatom composition are more direct indicators of the health of an aquatic ecosystem. Current indicators of eutrophication levels are generally assessed according to nutrient concentrations (TN, TP) or clarity (SD), and lakes with the same nutrient concentration or SD are considered to be in the same eutrophic state, while lakes with a TP of 100 μg/L are considered eutrophic regardless of lake type (Zou et al, 2020). In order to fine-tune China's "one lake, one policy" approach to lake ecology and develop long-term personalised management, more models that reflect the dynamics of the ecosystem should be included as an adjunct to field surveys as well as subdividing the existing eutrophication monitoring and management framework. Before the model is built, it is necessary to simplify the statistical relationships in the empirical data and to identify the main drivers of change in the state of the lake (as was done for Taibai Lake in Chapter 3), drawing on the results of ecological experiments and survey data from the region where the lake is located, as well as on individual ecological knowledge. Once the model has been built, the simulation of steady-state eutrophication and recovery scenarios will allow further testing and verification of our understanding of the mechanisms involved in lake state change. After calibrating the model stage by stage, the lake has additional biological impact indicators that directly reflect the future outlook of the lake's health, such as ecosystem structure, areas of algal aggregation and possible regime-shift scenarios.

6.5 Critical transition caused by the accumulation of relationship changes

This ABM model of ecosystems demonstrates the complexity of the behaviour of community-level phenomena, echoing many community ecology theories of unstable equilibrium. Rosenzweig (1971) proposed that the Paradox of Enrichment, which involves increasing the primary producer energy source of an ecosystem in a predator-prey system or limiting nutrient loads, can cause system instability and ultimately catastrophic changes (such as extinction). In the 1963 experiment by Huffaker, Shea and Herman to create artificial instability in an ecosystem, the food density of herbivorous mites was tripled, leading to the extinction of this herbivorous mite population as well as its predator community of *Acarophagous* mites. This was similar to the relationship between phytoplankton, zooplankton and planktivorous fish in my lake ecosystem, in which an increase in phytoplankton may cause system instability, resulting in the extinction of zooplankton and planktivorous fish. IN my model zooplankton were more capable of escaping predation (based on spatially different daily movement steps), which meant that the predation and reproduction rates of planktivorous fish were low and the system continued to behave as a stable state. The growth of zooplankton as a result of phytoplankton growth can cause the previous equilibrium in the relationship between zooplankton and planktivorous fish to slip into a state of instability, and changes to the number of planktivorous fish can affect the abundance of piscivorous fish and thus the balance of relationships in the rest of the food chain. The formation of such an unstable equilibrium is also related to the periodicity and magnitude of population fluctuations at steady state, probably because the rate of trophic increase is slow enough not to disrupt the balance between functional groups (Subsection 5.3.1.3). It is more often the case that nutritional increases cause food to grow just above the threshold for maintaining the current steady state, leading to a bottom-up increase in the number of food chains and causing a disruption to the inter-functional group equilibrium, resulting in an unstable equilibrium and a new steady state. Nutrient levels increase in the same way, and at the same dose may lead to the emergence of different patterns due to the timing of the addition and the intrinsic population size change cycle, as in the three-species system model built by Suzuki & Yoshida (2015).

Finally, ABM model simulations show that natural stochasticity in complex systems is an important factor in changes to group dynamics. Individual behaviour and decision-making in interactions are characterised by stochasticity, resulting in variations in the population dynamics from day to day. When analysing temporal variation in ecosystems, it is common practice to consider only temporal variation, such as seasonality, environmental stochasticity, external disturbances, environmental stresses and community development. However, the results of models that show spatial heterogeneity remind us that these spatial changes, as well as changes in refuge, dispersal and migration can have an important impact on temporal system changes.

6.6 Community structures determine the components in equilibria

In the analysis of steady-state results, the examination of the relationships between different functional groups is one of best and most often used ways of interpreting population dynamics. The process of allowing a system to develop a steady state on its own is in fact equivalent to the collapse of the composition of functional groups from a less resilient system state to a more resilient state within the larger system. Although changes in system resilience cannot be directly observed, the structural properties of networks between ecosystems play an important role in influencing the resilience of ecosystems. For example, May et al (2008) suggested that in complex systems such as ecosystems and financial systems, catastrophic changes in the overall state of the system may be caused by the way the system is organised, such as from feedback mechanisms within the system. Scheffer et al (2012) argued that the emergence of tipping points in complex systems is characterised by fragile architectures, and that the heterogeneity of components and their degrees of connectivity are two of the main features affecting stability. Wang et al (2019) calculated the network of relationships between diatom genera in several lakes in China using a gradient of change from natural development to anthropogenic influence and found that lakes with greater anthropogenic influence had less network bias and were further from natural network relationships. This variation is also present in a network structure that consists of functional groups in the simulated scenario, as each individual in the modelled network relationships responds differently to external drivers as a result of being in a dynamic network structure that is defined by feedback loops. Changes in how an ecosystem consisting of six functional groups is organised may therefore be one of the most critical clues in the process of analysing homeostasis formation and collapse. I have analysed the network composition and connectivity of my own simple ecosystem, performed tests of modularity by examining the extent to which system nodes can be structured into relatively discrete assemblies and analysed system feedback mechanisms (described more in the next subsection) as a mechanistic explanation for number of the homeostatic states tacked at the end of spin up.

I began by analysing the network of six biological components. This six-component network produced two clustering results based on three network distance measurements (Figure 6-2). Figure 6-2a shows that the network connectivity obtained according to the Newman-Girvan algorithm indicates that the best community division is to divide the six components into four modules, namely submerged plants-herbivorous fish, planktivorous fish-piscivorous fish, zooplankton and phytoplankton. Figure 6-2b shows the clustering tree according to the Fast Greedy and Random Walk algorithms. The best approach to community division is to divide these components into two parts according to connectivity: submerged plants - herbivorous fish - piscivorous fish and phytoplankton - zooplankton - planktivorous fish. The module degrees were 0.0648 and 0.3512, indicating different ways of understanding the construction of the ecosystem as both parts aim to achieve a result in which nodes within the community are more similar and nodes outside the community are less similar. Given that Scheffer et al (2012) concluded that networks with greater modularity and heterogeneity are prone to more gradual changes while networks with greater homogeneity and connectivity are prone to more abrupt changes, the position of the extinction community in the network may determine whether the system is more prone to abrupt or gradual changes in its subsequent development. A comparison of the demographic changes in “p+z+sm+pf” and “p+z+sm+hf” shows that the changes in the components of “p+z+sm+pf” model are relatively more linear. This is in line with the results of the community classification in the left-hand graph, where “p+z+sm+pf” as a node from four communities has greater heterogeneity and modularity than “p+z+sm+hf” as a node from three communities. The reason for the stability of both the “p+z+sm+pf+hf” and “p+z+sm+hf+pisci” states in the community classification of plot (a) may also be due to the structure of the nodes in all four communities. In other words, the stable state reached by the system in this ABM can be inferred and explained in terms of the structure of the ecosystem network in the same way as it can in a real ecosystem.

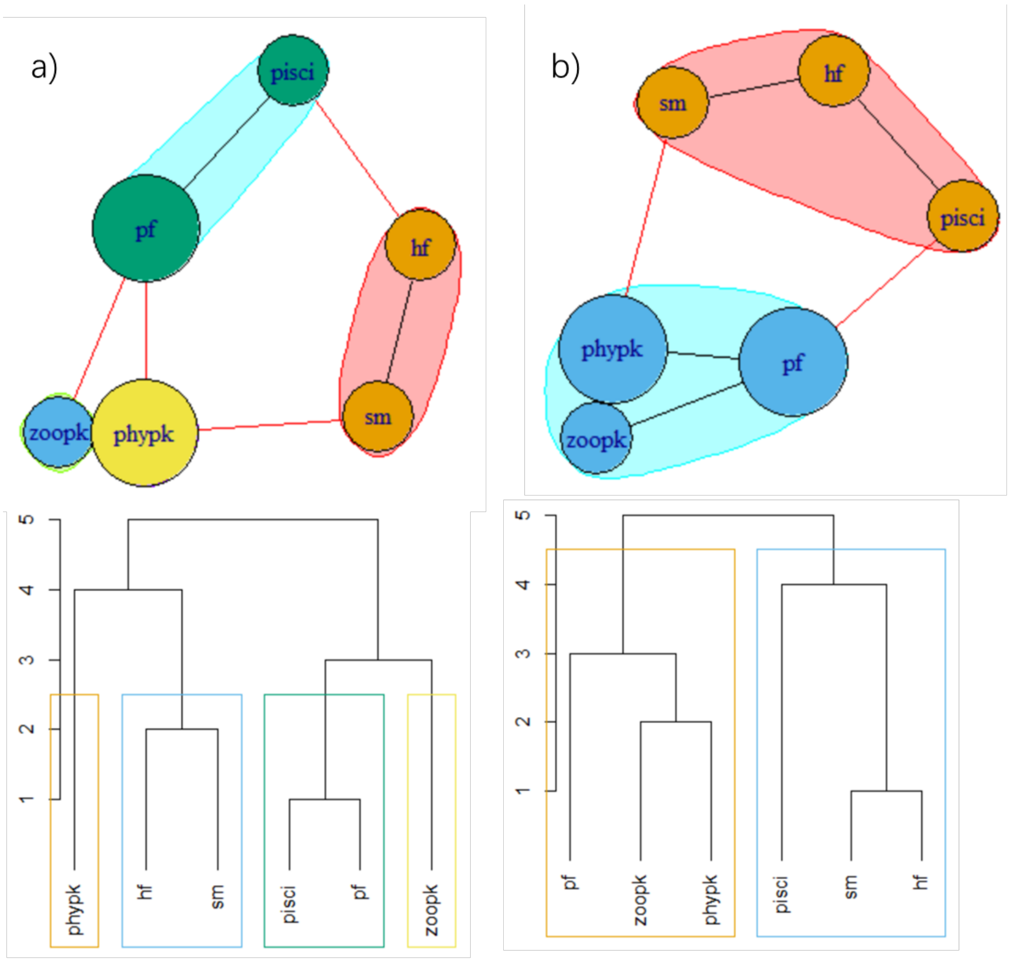

Newman-Girvan algorithm
Modularity = 0.0648

Random Walk & Fast Greedy algorithm
Modularity = 0.3512

Figure 6-2: Modular clustering results and modularity of the lake ecosystem network structure. Transparent coloured shading shows the results of different clustering combinations in which the circled components belong to the same small core network. The fill colour of the community nodes corresponds to the colour of the boxes in the clustering dendrogram, showing the results for the proximity of network relationships. The left column (a) shows the clustering tree diagram and local modularity obtained by the Newman-Girvan algorithm, while the right column (b) shows the clustering tree diagram and local modularity obtained using the Fast Greedy and Random walk algorithms.

In addition to the six natural components of this ABM model, there are three external factors, namely temperature, nutrient and human influence, which are also involved in the ecosystem. The structure of the network is different when these environmental drivers are added, especially as the direct interference of human activities with most ecosystem components gives humans an immediate and central node. Factors relating to nutrient and temperature are more closely related to primary producers because they can only influence system components from the bottom up. Modular clustering of these nine component networks resulted in three groups, the zooplankton-planktivorous fish group, the human-herbivorous fish-piscivorous fish groups and the temperature-nutrient-phytoplankton-submerged macrophyte groups. This means that the groups were divided into the primary producer and impact factor group, the planktonic consumer group and the other group. It is then reasonable to assume that if there is a simulation run that develops to form a structure with four nodes in the primary producer group and a node from the other two communities, this system will likely undergo a critical transition in response to changes in temperature and nutrient.

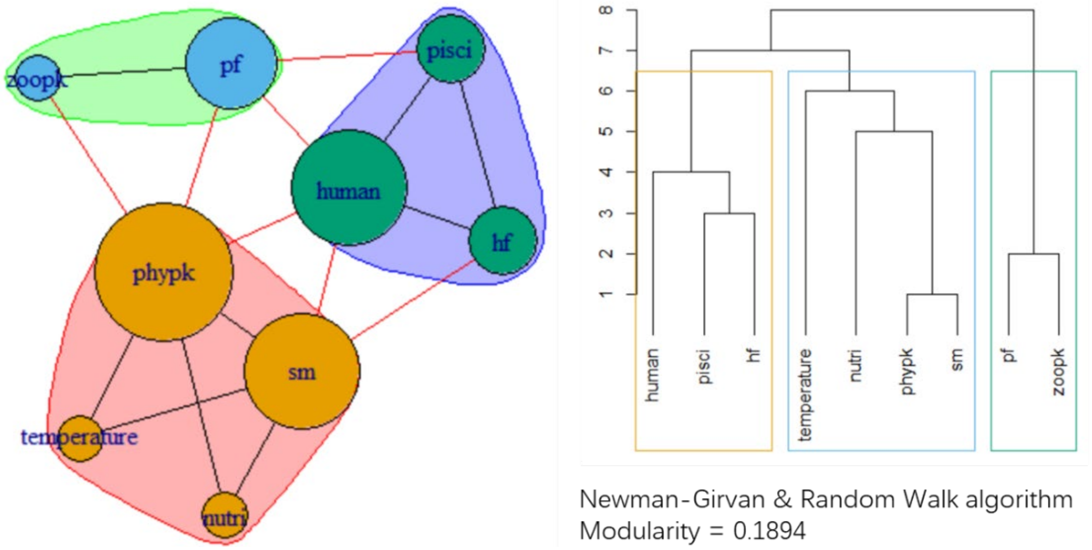

Figure 6-3: Modular clustering results and modularity of the network structure of lake ecosystems under environmental change. Transparent coloured shading indicates the results of different clustering combinations, in which the circled components belong to the same small core network. The fill colour of the community nodes corresponds to the colour of the

boxes in the clustering dendrogram, showing the results for the proximity of network relationships.

6.7 Feedback loops underlying ecosystem resilience

The simulated multiple steady states indicate different combinations of species and population size compositions, the mechanisms of which are attributed to feedback loops. The feedback loops for the six states that appear in the results show that the overall feedback effect is balanced for all homeostasis states (by adding up the + and - signs). The “p+z+sm+hf+pisci” state (f) and the “p+z+sm+hf” state (b) combined count for 33% of runs, and feedback loop diagrams can be analysed to explain the equilibrium mechanisms of other stable states. The six types of steady system state that result in different outcomes may act as the solutions to achieving equilibrium in the system. Besides the initial setting, which includes the number of different groups, the steady state also depends on the closest stable feedback loop structure. Simplifying the relationships between the functional groups in this ABM model into feedback loops can explain more explicitly why ecosystem states are stabilised into different combinatorial patterns, as shown in the feedback loop diagram I applied in Chapter 3.

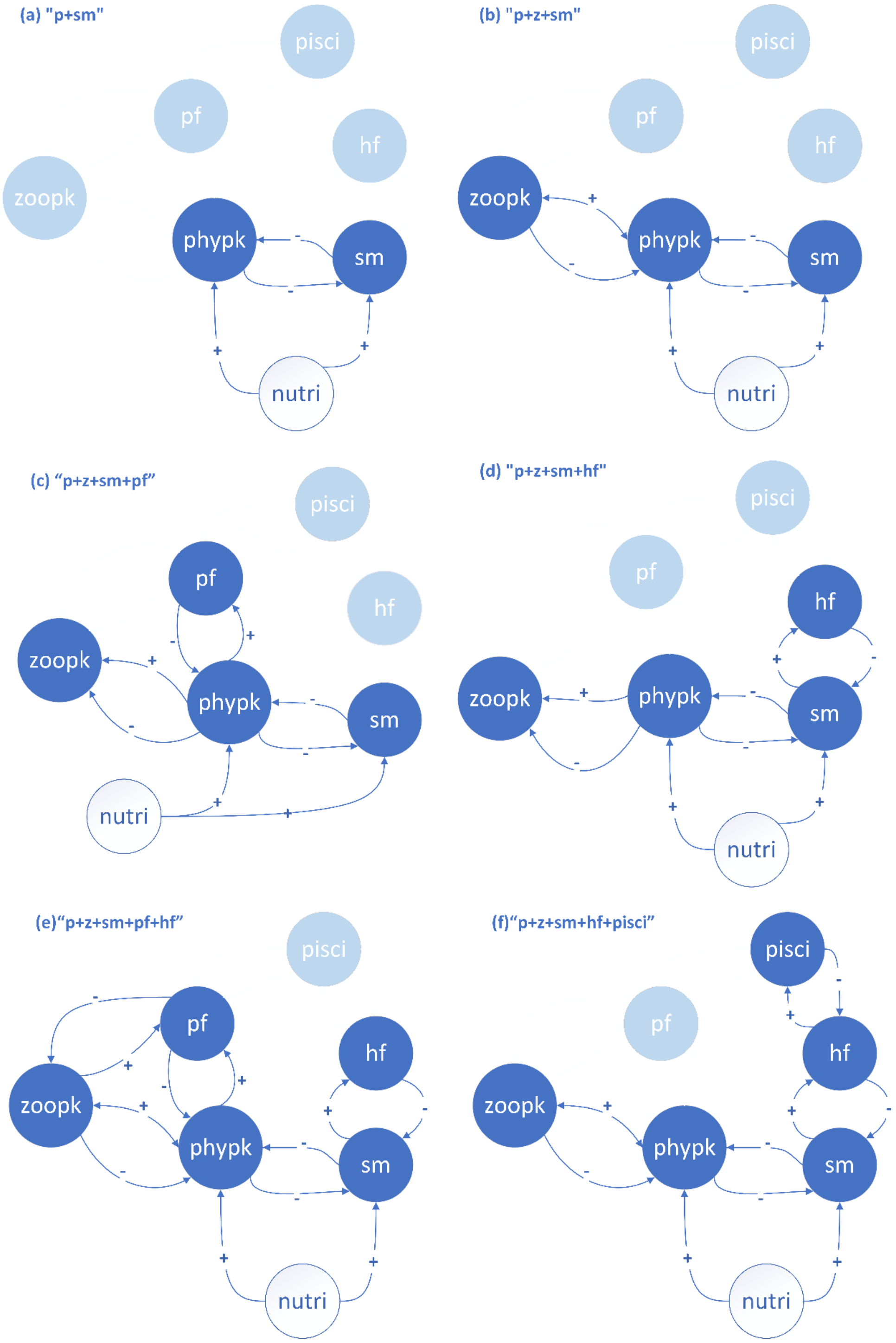

Figure 6-4: Feedback loops in six emergent homeostasis patterns in the model spin up. All biotic elements are shown as nodes, i.e. 'phypk'(phytoplankton), 'zoopk'(zooplankton), 'sm'(submerged macrophyte), 'nutri'(nutrient), 'pf'(planktivorous fish), 'hf'(herbivorous fish), 'pisci' (piscivorous fish). Dark blue circles show components involved in feedbacks while light blue circles are extinct on its panel. The '+' sign represents a positive effect to the population growth of the object pointed to by the arrow, and '-' represents a negative effect in the population size of the object pointed to by the arrow.

6.8 Ecological recovery pathways in MLYB lakes

The experiments described above were used to simulate two pathways of recovery from eutrophication. One is a zooplankton-dominated eutrophic lake system comprising phytoplankton, zooplankton, submerged plants and fish. After nutrient loading ceased, the composition of the system gradually changed to a new steady state dominated by submerged plants. However, there was no significant decrease in water column nutrient concentrations. After the introduction of herbivorous fish and planktivorous fish, there was a significant decrease in water column nutrient concentrations, an increase in total ecosystem biomass and an increase in algal abundance, resulting in a fish-dominated steady state (Subsection 5.3.2). This experiment shows that natural fish behaviour is beneficial to eutrophic lake systems in reducing water column nutrient levels. The direct reduction of total nutrient concentrations was also attempted in a hypereutrophic lake consisting of phytoplankton and planktivorous fish, simulating realistic dredging of the substrate, or water purification and filtration treatments (Subsection 5.3.3). The results showed that a direct reduction in total nutrient concentrations directly reduces nutrient levels in the water column, but that there was no reduction in phytoplankton abundance over time (a 40-year simulation period). Both initial ecosystem states are common in MLYB lakes, so both simulations have practical implications for ecological restoration pathways in the lakes. When restoring a body of water from its initial eutrophic state, a reduction in nutrient concentrations in the water body will not necessarily result in the reduction of algae.

Similarly, an increase in algal abundance may also result from a decrease in zooplankton, accompanied by a decrease in the nutrient concentration of the water column. A combination of physicochemical (such as water purification) and biological (such as appropriate fishing) approaches is therefore required to reduce both the nutrient level of the water column and the algal population.

Conclusion

7.1 Responses, drivers, and mechanism of ecological transitions in the MLYB lakes

In the literature review chapter, at least thirteen lakes in MLYB were found to have undergone regime shifts and turned into turbid-water states along the eutrophication process in the last century. The ecological responses in studies include water quality, algae, cladoceran, chironomid, fish, pollen and macrofossil of submerged macrophyte from observation and subfossil reconstruction. The drivers contributing to regime shifts include nutrient loading, fish stocking, hydrological regulation, weeding, warming, droughts and floods. Multiple Factor Analysis of the properties of thirteen lakes in MLYB shows nutrient levels of phosphorus and nitrogen as the most influential to the occurrence time of regime shifts. Other influential properties in the investigation list are SD, water level, lake area, longitude, and drainage ratio.

Then ecological transitions were detected, and the detailed response, drivers and mechanisms were explored in a case study. I reconstructed diatom communities from sediment cores in Lake Taibai using palaeolimnological methods to reveal the history of state transitions in the lake ecosystem on the multidecadal scale. Algorithms using sequential *t* and *F* statistics detected breakpoints in the time series of diatom assemblages, in 1994-1996, 1974-1977, 1952-1956, and 1931-1934 respectively. The regression statistics suggest that the relationships between hydrodynamic and aquacultural ecosystems fit better in the breakpoint regression model and the relationship between nutrient loading and ecosystem state are more suited to the linear model, indicating different patterns of response-driver relationship. Breakpoint detection, regression analysis and feedback loops help the researcher understand the process of environmental and ecological changes derived from historical records or monitoring data. Feedback loop diagrams were created to present the varying interactions between major functioning system groups, i.e., phytoplankton, zooplankton, fish, and submerged macrophytes and the external drivers, i.e., turbulence, turbidity, nutrients, and artificial diets in different periods. The whole set of methods is comparatively novel, providing an example for studying drivers, responses and mechanisms of ecological regime shifts in aquatic ecosystems.

7.2 Testing the hypothesised mechanism of regime shifts using an ABM of the lake ecosystem

Based on the hypothesised mechanism of regime shifts depicted in feedback loops of functional groups in the lake, an agent-based model was constructed using the Netlogo platform for testing if the feedback loops can lead to the emergence of critical transition. The hypothesis mechanism proved feasible to generate critical transitions. The slow drivers in the model are designed as nutrient only, water depth only, nutrient and temperature, and a combination of nutrient, temperature, fish stocking and lake area. As nutrient was regarded as a dominant driver of eutrophication, more experiments were designed to investigate the ecological effects of different amounts of nutrient addition, various intervals of nutrient addition, and concurrent modifying factors of temperature or water depth. The application of gradual and constant nutrient load caused critical transitions in the simulated system and the more intense nutrient loads drove the earlier critical transitions. Besides, the frequency of nutrient loading seems important in generating critical transitions. At a constant total volume, neither continuous small daily additions nor large doses of additions every 200 days produced a clear critical transition, while a critical transition occurred when nutrients were added every ten days. Thus the effect of the application frequency of nutrient loads on ecosystem state changes can be very important for ecosystem management though it has rarely been mentioned in previous studies. Modifying temperature in the process of eutrophication did not significantly influence the occurrence of critical transitions in the model. Changing water depth could alter the relation between the ecosystem states and drivers from gradual-response patterns into nonlinear-response patterns.

The process of state-threshold regime shifts in the model was usually composed of three steps. Firstly, drivers caused gradual and direct responses of one or several components, e.g. nutrient loading makes the growth rates of algae and macrophyte rise. Then, secondary effects followed the direct responses, e.g., zooplankton grazes more algae so that their population gets larger. After this step, the system became unstable due to the increased amplitude of variation under the influence of drivers. This made extinction more possible for components in the ecosystem and pushed the system into a structurally different state, which usually took some time to reach a new equilibrium. The driver-threshold regime shifts may result mainly from the first step under strong disturbance.

7.3 Reflection on empirical study and modelling of ecological regime shifts in lakes

Combining paleoecological analysis with agent-based modelling is a new approach to investigating long-term ecological changes in lakes. This approach takes advantage of both long-term records in sediment cores and the experimental simulation of models to better understand the interactions between drivers and ecosystem components. In extensive model spin-ups and control experiments, besides the tested hypothesis of mechanism in the subsection above, I obtained the following knowledge that is important and new to the study of ecological regime shifts.

1. Equilibrium is the result of interactions among functional groups, initial conditions, and individual decisions. The equilibrium is key for the formation of a regime shift or critical transition instead of a continuous change and requires a stable structure of ecosystem feedback loops.
2. The ecosystem state-driver relationships have been modelled in varying physical environments. The hypothesis that physical attributes, e.g., water depth, can alter the changing patterns of ecosystem states responding to dominant drivers was

tested. There appeared both linear and nonlinear changes in ecosystem state-driver relationships when the depth of the lake varied though the way physical attributes influence the relationship was not as expected. Besides, contrary to intuitive thinking, the correlation between nutrient concentration in the water column and the population density of algae is often negative, especially after the reduction of total nutrient concentrations in the system.

3. Stocking fish can accelerate the use of nutrients from the water and transfer nutrients into the organisms, thus causing a reduction in the unused nutrients in the water. Removing fish, especially after stocking, proves as an effective method to rapidly reduce nutrient concentrations in the lake.
4. Calibrating and validating agent-based models against empirical data is difficult and needs interdisciplinary methods. The ABM is pattern-oriented and spatially explicit, which means the spatial distribution of agents determines the dynamics and development of ecosystem states. The robustness of the model fitting to data partly depends on the innate spatial stochasticity. To compare the changing pattern of the model and Taibai Lake, I used the CCA multivariate analysis method for the modelling results. The analysis shows that temperature, nutrient concentrations and lake area have similar strengths of influence on the community changes, which is consistent with empirical findings.

References

Abar, S., Theodoropoulos, G. K., Lemarinier, P., & O'Hare, G. M. P. (2017). Agent Based Modelling and Simulation tools: A review of the state-of-art software. *Computer Science Review*, *24*, 13–33. https://doi.org/10.1016/j.cosrev.2017.03.001

Ampel, L., Wohlfarth, B., Risberg, J., Veres, D., Leng, M. J., & Tillman, P. K. (2010). Diatom assemblage dynamics during abrupt climate change: The response of lacustrine diatoms to Dansgaard-Oeschger cycles during the last glacial period. *Journal of Paleolimnology*, *44*(2), 397–404. https://doi.org/10.1007/s10933-009-9350-7

Andersen, T., Carstensen, J., Hernandez-Garcia, E., & Duarte, C. M. (2009). Ecological thresholds and regime shifts: approaches to identification. *Trends in Ecology & Evolution*, *24*(1), 49–57. https://doi.org/10.1016/j.tree.2008.07.014

Ansari, A. A., Gill, S. S., & Khan, F. A. (2011). Eutrophication: Threat to aquatic ecosystems. In *Eutrophication: Causes, Consequences and Control*. https://doi.org/10.1007/978-90-481-9625-8-7

Appleby, P. G. (2008). Three decades of dating recent sediments by fallout radionuclides: a review. *The Holocene*, *18*(1), 83–93. https://doi.org/10.1177/0959683607085598

Battarbee, R., Jones, V., Flower, R., Cameron, N., Bennion, H., Carvalho, L., & Juggins, S. (2001). Diatoms. In J. Smol, H. J. Birks, W. Last, R. Bradley, & K. Alverson (Eds.), *Tracking Environmental Change Using Lake Sediments* (Vol. 3, pp. 155–202). Springer Netherlands. https://doi.org/10.1007/0-306-47668-1_8

Bayley, S. E., Creed, I. F., Sass, G. Z., & Wong, A. S. (2007). Frequent regime shifts in trophic states in shallow lakes on the Boreal Plain: Alternative 'unstable' states? *Limnology and Oceanography*, *52*(5), 2002–2012. https://doi.org/10.4319/lo.2007.52.5.2002

Beck, H. E., Zimmermann, N. E., McVicar, T. R., Vergopolan, N., Berg, A., & Wood, E. F. (2018). Present and future köppen-geiger climate classification maps at 1-km resolution. *Scientific Data*, *5*, 1–12. https://doi.org/10.1038/sdata.2018.214

Bégin, P. N., Tanabe, Y., Kumagai, M., Culley, A. I., Paquette, M., Sarrazin, D., Uchida, M., & Vincent, W. F. (2020). Extreme warming and regime shift toward amplified variability in a far northern lake. *Limnology and Oceanography*, 1–13. https://doi.org/10.1002/lno.11546

Bennett, K. D. (1996). Determination of the number of zones in a biostratigraphical sequence. *New Phytologist*, *132*(1), 155–170. https://doi.org/10.1111/j.1469-8137.1996.tb04521.x

Biggs, R., Peterson, G. D., & Rocha, J. C. (2018). The regime shifts database: A framework for analyzing regime shifts in social-ecological systems. *Ecology and Society*, *23*(3).

https://doi.org/10.5751/ES-10264-230309

Blaauw, M., Bennett, K. D., & Christen, J. A. (2010). Random walk simulations of fossil proxy data. *Holocene*, *20*(4), 645–649. https://doi.org/10.1177/0959683609355180

BLINDOW, I., ANDERSSON, G., HARGEBY, A., & JOHANSSON, S. (1993). Long-term pattern of alternative stable states in two shallow eutrophic lakes. *Freshwater Biology*. https://doi.org/10.1111/j.1365-2427.1993.tb00796.x

Briske, D. D., Washington-Allen, R. A., Johnson, C. R., Lockwood, J. A., Lockwood, D. R., Stringham, T. K., & Shugart, H. H. (2010). Catastrophic thresholds: A synthesis of concepts, perspectives, and applications. *Ecology and Society*, *15*(3). https://www.scopus.com/inward/record.uri?eid=2-s2.0-77958453241&partnerID=40&md5=6609097f82036ed4a8d48c24fcdcfde4

Bronmark, C., & Hansson, L.-A. (2005). *The Biology of lakes and ponds - Second Edition*.

Cao, Y., Langdon, P., Chen, X., Huang, C., Yan, Y., Yang, J., & Zeng, L. (2020). Regime shifts in shallow lake ecosystems along an urban-rural gradient in central China. *Science of the Total Environment*, *733*, 139309. https://doi.org/10.1016/j.scitotenv.2020.139309

Capon, S. J., Lynch, A. J. J., Bond, N., Chessman, B. C., Davis, J., Davidson, N., Finlayson, M., Gell, P. A., Hohnberg, D., Humphrey, C., Kingsford, R. T., Nielsen, D., Thomson, J. R., Ward, K., & Nally, R. Mac. (2015). Regime shifts, thresholds and multiple stable states in freshwater ecosystems; a critical appraisal of the evidence. *Science of the Total Environment*, *534*, 122–130. https://doi.org/10.1016/j.scitotenv.2015.02.045

Carpenter, S. R., Cole, J. J., Pace, M. L., Batt, R., Brock, W. a., Cline, T., Coloso, J., Hodgson, J. R., Kitchell, J. F., Seekell, D. a., Smith, L., & Weidel, B. (2011). Early Warnings of Regime Shifts: A Whole-Ecosystem Experiment. *Science*, *332*(6033), 1079–1082. https://doi.org/10.1126/science.1203672

Chen, J. (2020). Future of the Yangtze River. In *Evolution and Water Resources Utilization of the Yangtze River* (pp. 461–468). Springer Singapore. https://doi.org/10.1007/978-981-13-7872-0_9

Cheng, L., Xue, B., Yao, S., & Liu, J. (2020). Response of Cladocera fauna to environmental change based on sediments from Shengjin Lake, a Yangtze River-connected lake in China. *Quaternary International*, *536*, 52–59. https://doi.org/https://doi.org/10.1016/j.quaint.2019.11.044

Chiverrell, R. C., Sear, D. A., Warburton, J., Macdonald, N., Schillereff, D. N., Dearing, J. A., Croudace, I. W., Brown, J., & Bradley, J. (2019). Using lake sediment archives to improve understanding of flood magnitude and frequency: Recent extreme flooding in northwest UK. *Earth Surface Processes and Landforms*, *44*(12), 2366–2376. https://doi.org/10.1002/esp.4650

Clauset, A., Newman, M. E. J., & Moore, C. (2004). Finding community structure in very large networks. *Physical Review E*, *70*(6), 066111. https://doi.org/10.1103/PhysRevE.70.066111

Cleveland, W. S., Grosse, E., & Shyu, W. M. (1992). Local Regression Models. In J. M. Chambers & T. J. Hastie (Eds.), *Statistical Models in S* (1st Editio, p. 68). Routledge. https://doi.org/10.1201/9780203738535

Collie, J. S., Richardson, K., & Steele, J. H. (2004). Regime shifts: Can ecological theory illuminate the mechanisms? *Progress in Oceanography*, *60*(2–4), 281–302. https://doi.org/http://dx.doi.org/10.1016/j.pocean.2004.02.013

Contamin, R., Ellison, A. M., Contamin, R., Ellison, A. M., & Ellison, A. M. (2009). Indicators of regime shifts in ecological systems: what do we need to know and when do we need to know it? *Ecological Applications*, *19*(3), 799–816. https://doi.org/10.1890/08-0109.1

Cornell, S. J., Suprunenko, Y. F., Finkelshtein, D., Somervuo, P., & Ovaskainen, O. (2019). A unified framework for analysis of individual-based models in ecology and beyond. *Nature Communications*, *10*(1), 1–14. https://doi.org/10.1038/s41467-019-12172-y

Dakos, V., & Bascompte, J. (2014). Critical slowing down as early warning for the onset of collapse in mutualistic communities. *Proceedings of the National Academy of Sciences of the United States of America*, *111*(49), 17546–17551. http://www.pnas.org/content/111/49/17546.full.pdf

Dauta, A., Devaux, J., Piquemal, F., & Boumnich, L. (1990). Growth rate of four freshwater algae in relation to light and temperature. *Hydrobiologia*, *207*(1), 221–226. https://doi.org/10.1007/BF00041459

DeAngelis, D. L., & Mooij, W. M. (2005). Individual-based modeling of ecological and evolutionary processes. *Annual Review of Ecology, Evolution, and Systematics*, *36*(December), 147–168. https://doi.org/10.1146/annurev.ecolsys.36.102003.152644

DeAngelis, D. L., Post, W. M., & Travis, C. C. (1986). *Positive Feedback in Natural Systems* (Vol. 15). Springer Berlin Heidelberg. https://doi.org/10.1007/978-3-642-82625-2

Dearing, J. A. (1997). Sedimentary indicators of lake-level changes in the humid temperate zone: A critical review. *Journal of Paleolimnology*, *18*(1), 1–14. https://doi.org/Doi 10.1023/A:1007916210820

Dearing, J. A. (2013). Why Future Earth needs lake sediment studies. *Journal of Paleolimnology*, *49*(3), 537–545. https://doi.org/DOI 10.1007/s10933-013-9690-1

Dearing, J. A., Jones, R. T., Shen, J., Yang, X., Boyle, J. F., Foster, G. C., Crook, D. S., & Elvin, M. J. D. (2008). Using multiple archives to understand past and present climate-human-environment interactions: the lake Erhai catchment, Yunnan Province, China. *Journal of Paleolimnology*, *40*(1), 3–31. https://doi.org/DOI 10.1007/s10933-007-9182-2

Dent, C. L., Cumming, G. S., & Carpenter, S. R. (2002). Multiple states in river and lake ecosystems. *Philosophical Transactions of the Royal Society of London Series B-Biological Sciences*, *357*(1421), 635–645. https://doi.org/10.1098/rstb.2001.0991

deYoung, B., Barange, M., Beaugrand, G., Harris, R., Perry, R. I., Scheffer, M., & Werner, F. (2008). Regime shifts in marine ecosystems: detection, prediction and management. *Trends in Ecology & Evolution*, *23*(7), 402–409. https://doi.org/10.1016/j.tree.2008.03.008

Doncaster, C. P., Chávez, V. A., Viguier, C., Wang, R., Zhang, E., Dong, X., Dearing, J. A., Langdon, P. G., & Dyke, J. G. (2016). Early warning of critical transitions in biodiversity from compositional disorder. *Ecology*, *97*(11), 3079–3090. https://doi.org/10.1002/ecy.1558

Dong, Y., Zheng, W., Zhang, C., Xu, M., Wang, R., Wu, X., & Li, Y. (2021). *Temporal and spatial differences of lake ecosystem regime shift in China*. Journal of Lake Sciences. https://doi.org/10.18307/2021.0403

Downing, J. A., & Rath, L. C. (1988). Spatial patchiness in the lacustrine sedimentary environment. *Limnology and Oceanography*, *33*(3), 447–458. https://doi.org/10.4319/lo.1988.33.3.0447

Earth’s boundaries? (2009, September 23). *Nature*, *461*(7263), 447–448. https://doi.org/10.1038/461447b

Ferber, J. (1999). *Multi-agent systems - an introduction to distributed artificial intelligence*.

Folke, C., Carpenter, S., Walker, B., Scheffer, M., Elmqvist, T., Gunderson, L., & Holling, C. S. (2004a). Regime shifts, resilience, and biodiversity in ecosystem management. In *Annual Review of Ecology, Evolution, and Systematics* (Vol. 35). https://doi.org/10.1146/annurev.ecolsys.35.021103.105711

Folke, C., Carpenter, S., Walker, B., Scheffer, M., Elmqvist, T., Gunderson, L., & Holling, C. S. (2004b). Regime Shifts, Resilience, and Biodiversity in Ecosystem Management. *Annual Review of Ecology, Evolution, and Systematics*, *35*(1), 557–581. https://doi.org/10.1146/annurev.ecolsys.35.021103.105711

Forbes, S. a. (1887). The lake as a microcosm. *Forbes*, *15*(537), 77–87.

Gal, G., & Anderson, W. (2010). A novel approach to detecting a regime shift in a lake ecosystem. *Methods in Ecology and Evolution*, *1*(1), 45–52. https://doi.org/10.1111/j.2041-210X.2009.00006.x

Gao, C., & Zhang, T. (2010). Eutrophication in a Chinese context: Understanding various physical and socio-economic aspects. *Ambio*, *39*(5), 385–393. https://doi.org/10.1007/s13280-010-0040-5

Glibert, P. M. (2017). Eutrophication, harmful algae and biodiversity — Challenging paradigms in a world of complex nutrient changes. *Marine Pollution Bulletin*, *124*(2), 591–606. https://doi.org/10.1016/j.marpolbul.2017.04.027

Goldman, J. C., & Carpenter, E. J. (1974). A kinetic approach to the effect of temperature on algal growth. *Limnology and Oceanography*, *19*(5), 756–766. https://doi.org/10.4319/lo.1974.19.5.0756

Grasman, R. P. P. P., van der Maas, H. L. J., & Wagenmakers, E. J. (2009). Fitting the cusp catastrophe in R: A cusp package primer. *Journal of Statistical Software*, *32*(8), 1–27. https://doi.org/10.18637/jss.v032.i08

Griffith, C. S., Long, B. L., & Sept, J. M. (2010). HOMINIDS: An agent-based spatial simulation model to evaluate behavioral patterns of early Pleistocene hominids. *Ecological Modelling*, *221*(5), 738–760. https://doi.org/10.1016/j.ecolmodel.2009.11.009

Grimm, V. (1999). Ten years of individual-based modelling in ecology: What have we learned and what could we learn in the future? *Ecological Modelling*, *115*(2–3), 129–148. https://doi.org/10.1016/S0304-3800(98)00188-4

Groffman, P. M., Baron, J. S., Blett, T., Gold, A. J., Goodman, I., Gunderson, L. H., Levinson, B. M., Palmer, M. A., Paerl, H. W., Peterson, G. D., Poff, N. L. R., Rejeski, D. W., Reynolds, J. F., Turner, M. G., Weathers, K. C., & Wiens, J. (2006). Ecological thresholds: The key to successful environmental management or an important concept with no practical application? *Ecosystems*, *9*(1), 1–13. https://doi.org/10.1007/s10021-003-0142-z

Gui, J., Tang, Q., Li, Z., Liu, J., & De Silva, S. S. (2018). *Aquaculture in China: Success Stories and Modern Trends* (J. Gui, Q. Tang, Z. Li, J. Liu, & S. S. De Silva (Eds.)). Wiley-Blackwell. https://books.google.co.uk/books?hl=en&lr=&id=QQ5TDwAAQBAJ&oi=fnd&pg=PP2&dq=Aquaculture+in+China:+Success+Stories+and+Modern+Trends&ots=mz_axshrQW&sig=CluNNqsOmhm31BAtDKm-rUkJ6E0&redir_esc=y#v=onepage&q=Aquaculture in China%3A Success Stories and Modern T

Guo, C., Zhu, G., Qin, B., Zhang, Y., Zhu, M., Xu, H., Chen, Y., & Paerl, H. W. (2019). Climate exerts a greater modulating effect on the phytoplankton community after 2007 in eutrophic Lake Taihu, China: Evidence from 25 years of recordings. *Ecological Indicators*, *105*(January), 82–91. https://doi.org/10.1016/j.ecolind.2019.05.034

Guo, W., Yu, M., Liu, Q., Wu, J., & Li, X. (2015). Vernalization Process and the Relationship between Inductive Low Temperature in Microcystis aeruginosa in Dianchi Lake. *Ecology and Environmental Sciences*, *24*(12), 2022–2026. https://doi.org/10.16258/j.cnki.1674-5906.2015.12.015

Haddaway, N. R., Macura, B., Whaley, P., & Pullin, A. S. (2018). ROSES Reporting standards for Systematic Evidence Syntheses: Pro forma, flow-diagram and descriptive summary of the plan and conduct of environmental systematic reviews and systematic maps.

Environmental Evidence, *7*(1), 4–11. https://doi.org/10.1186/s13750-018-0121-7

Hansen, A. M., & Jeppesen, E. (1992). Changes in the Abundance and Composition of Cyclopoid Copepods Following Fish Manipulation in Eutrophic Lake Vaeng, Denmark. *Freshwater Biology*, *28*(2), 183–193.

Hare, S. R., & Mantua, N. J. (2000). Empirical evidence for North Pacific regime shifts in 1977 and 1989. *Progress in Oceanography*, *47*(2–4), 103–145. https://doi.org/Doi 10.1016/S0079-6611(00)00033-1

Harfoot, M. B. J., Newbold, T., Tittensor, D. P., Emmott, S., Hutton, J., Lyutsarev, V., Smith, M. J., Scharlemann, J. P. W., & Purves, D. W. (2014). Emergent Global Patterns of Ecosystem Structure and Function from a Mechanistic General Ecosystem Model. *Plos Biology*, *12*(4). https://doi.org/ARTN e1001841 10.1371/journal.pbio.1001841

Heggen, M. P., Birks, H. H., Heiri, O., Grytnes, J. A., & Birks, H. J. B. (2012). Are fossil assemblages in a single sediment core from a small lake representative of total deposition of mite, chironomid, and plant macrofossil remains? *Journal of Paleolimnology*, *48*(4), 669–691. https://doi.org/10.1007/s10933-012-9637-y

Hillebrand, H., Donohue, I., Harpole, W. S., Hodapp, D., Kucera, M., Lewandowska, A. M., Merder, J., Montoya, J. M., & Freund, J. A. (2020). Thresholds for ecological responses to global change do not emerge from empirical data. *Nature Ecology and Evolution*, *4*(11), 1502–1509. https://doi.org/10.1038/s41559-020-1256-9

Hilt, S., Nunez, M. M. A., Bakker, E. S., Blindow, I., Davidson, T. A., Gillefalk, M., Hansson, L. A., Janse, J. H., Janssen, A. B. G., Jeppesen, E., Kabus, T., Kelly, A., Kohler, J., Lauridsen, T. L., Mooij, W. M., Noordhuis, R., Phillips, G., Rucker, J., Schuster, H. H., … Sayer, C. D. (2018). Response of Submerged Macrophyte Communities to External and Internal Restoration Measures in North Temperate Shallow Lakes. *Frontiers in Plant Science*, *9*.

Holling, C. S. (1973). Resilience and stability of ecological systems. *Annual Review of Ecology and Systematics*, *4*(1), 1–23. https://doi.org/10.1146/annurev.es.04.110173.000245

Huang, J., Zhang, Y., Arhonditsis, G. B., Gao, J., Chen, Q., Wu, N., Dong, F., & Shi, W. (2019). How successful are the restoration efforts of China's lakes and reservoirs? *Environment International*, *123*(November 2018), 96–103. https://doi.org/10.1016/j.envint.2018.11.048

Huang, Z. (1996). Taibai Lake Fisheries Exploitation Forms and Experiences. *Inland Aquaculture*, *1*, 9–10.

Janse, J. H., Scheffer, M., Lijklema, L., Van Liere, L., Sloot, J. S., & Mooij, W. M. (2010). Estimating the critical phosphorus loading of shallow lakes with the ecosystem model PCLake: Sensitivity, calibration and uncertainty. *Ecological Modelling*, *221*(4), 654–665. https://doi.org/10.1016/j.ecolmodel.2009.07.023

Jansen, M. J. W. (1999). Analysis of variance designs for model output. *Computer Physics Communications*, *117*(1), 35–43. https://doi.org/10.1016/S0010-4655(98)00154-4

Janssen, A. B. G., Arhonditsis, G. B., Beusen, A., Bolding, K., Bruce, L., Bruggeman, J., Couture, R.-M., Downing, A. S., Alex Elliott, J., Frassl, M. A., Gal, G., Gerla, D. J., Hipsey, M. R., Hu, F., Ives, S. C., Janse, J. H., Jeppesen, E., Jöhnk, K. D., Kneis, D., … Mooij, W. M. (2015). Exploring, exploiting and evolving diversity of aquatic ecosystem models: a community perspective. *Aquatic Ecology*, *49*(4), 513–548. https://doi.org/10.1007/s10452-015-9544-1

Jeppesen, E, Appelt, M., Hastrup, K., Gronnow, B., Mosbech, A., Smol, J. P., & Davidson, T. A. (2018). Living in an oasis: Rapid transformations, resilience, and resistance in the North Water Area societies and ecosystems. *Ambio*, *47*, 296–309. https://link.springer.com/content/pdf/10.1007%2Fs13280-018-1034-y.pdf

Jeppesen, E, Jensen, J. P., Jensen, C., Faafeng, B., Hessen, D. O., Sondergaard, M., Lauridsen, T., Brettum, P., & Christoffersen, K. (2003). The impact of nutrient state and lake depth on top-down control in the pelagic zone of lakes: A study of 466 lakes from the temperate zone to the arctic. *Ecosystems*, *6*(4), 313–325. https://doi.org/10.1007/PL00021503

Jeppesen, E, Jeppesen, E., Leavitt, P., Leavitt, P., Jensen, J. P., & Jensen, J. P. (2001). Functional ecology and\npalaeolimnology: using\ncladoceran remains to\nreconstruct anthropogenic impact. *Trends in Ecology & Evolution*, *16*(4), 191–198.

Jeppesen, E, Sondergaard, M., Meerhoff, M., Lauridsen, T. L., & Jensen, J. P. (2007). Shallow lake restoration by nutrient loading reduction - some recent findings and challenges ahead. *Hydrobiologia*, *584*, 239–252. https://doi.org/10.1007/s10750-007-0596-7

Jeppesen, Erik. (1998). The Structuring Role of Submerged Macrophytes in Lakes. In Erik Jeppesen, M. Søndergaard, M. Søndergaard, & K. Christoffersen (Eds.), *Ecological studies* (Vol. 131, Issue vol. 131). Springer New York. https://doi.org/10.1007/978-1-4612-0695-8

Jian, Y. (2001). A comparative study of aquatic plant diversity of Haikou,Taibai and Wushan Lake in Hubei Province of China. *Acta Ecologica Sinica*.

Jianghan Floodplain Aquatic Resource Investigation Group. (2001). *Comprehensive Investigation Report on Taibai Lake Aquatic Resource*.

Jin, X., & Tu, Q. (1990). *Code for Field Survey of Lake Eutrophication*.

Jørgensen, S. E., & Fath, B. D. (2011). *Fundamentals of Ecological Modelling:Applications in Environmental Management and Research(Fourth Edition)*. Elsevier B. V.

Joseph Seckbach, & Kociolek, J. P. (2011). *The Diatom World* (J. Seckbach & P. Kociolek (Eds.); Vol. 19). Springer Netherlands. https://doi.org/10.1007/978-94-007-1327-7

Ju, T., Xing, G., Chen, X., & Zhang, S. (2009). Correction for Ju et al., Reducing environmental risk by improving N management in intensive Chinese agricultural systems. *Proceedings of the National Academy of Sciences*, *106*(19), 8077–8077. https://doi.org/10.1073/pnas.0902655106

Kankaala, P., Arvola, L., Hiltunen, M., Huotari, J., Jones, R. I., Nykänen, H., Ojala, A., Olin, M., Peltomaa, E., Peura, S., Rask, M., Tulonen, T., & Vesala, S. (2019). Ecosystem responses to increased organic carbon concentration: comparing results based on long-term monitoring and whole-lake experimentation. *Inland Waters*. https://doi.org/10.1080/20442041.2019.1600938

Kattel, G. R., Dong, X., & Yang, X. (2016). A century-scale, human-induced ecohydrological evolution of wetlands of two large river basins in Australia (Murray) and China (Yangtze). *Hydrology and Earth System Sciences*, *20*(6), 2151–2168. https://doi.org/10.5194/hess-20-2151-2016

Kéfi, S., Guttal, V., Brock, W. A., Carpenter, S. R., Ellison, A. M., Livina, V. N., Seekell, D. A., Scheffer, M., van Nes, E. H., Dakos, V., Kefi, S., Guttal, V., Brock, W. A., Carpenter, S. R., Ellison, A. M., Livina, V. N., Seekell, D. A., Scheffer, M., van Nes, E. H., & Dakos, V. (2014). Early Warning Signals of Ecological Transitions: Methods for Spatial Patterns. *Plos One*, *9*(3), e92097. https://doi.org/10.1371/journal.pone.0092097

Kefi, S., Holmgren, M., & Scheffer, M. (2016). When can positive interactions cause alternative stable states in ecosystems? *Functional Ecology*, *30*(1), 88–97. https://doi.org/10.1111/1365-2435.12601

Kinzig, A P, Ryan, P., Etienne, M., Allison, H., Elmqvist, T., & Walker, B. H. (2006). Resilience and regime shifts: Assessing cascading effects. *Ecology and Society*, *11*(1), 23. https://doi.org/Artn 20

Kinzig, Ann P., Ryan, P., Etienne, M., Allison, H., Elmqvist, T., & Walker, B. H. (2006). Resilience and regime shifts: Assessing cascading effects. *Ecology and Society*, *11*(1), 23. https://doi.org/Artn 20

Kong, F., & Gao, G. (2005). Hypothesis on cyanobacteria bloom-forming mechanism in large shallow eutrophic lakes. *ACTA ECOLOGICA SINICA*, *25*(3), 590–595.

Kong, X., He, Q., Yang, B., He, W., Xu, F., Janssen, A. B. G., Kuiper, J. J., van Gerven, L. P. A., Qin, N., Jiang, Y., Liu, W., Yang, C., Bai, Z., Zhang, M., Kong, F., Janse, J. H., & Mooij, W. M. (2017). Hydrological regulation drives regime shifts: evidence from paleolimnology and ecosystem modeling of a large shallow Chinese lake. *Glob Chang Biol*, *23*(2), 737–754. https://doi.org/10.1111/gcb.13416

Krammer, K., & Lange-Bertalot, H. (2008). Bacillariophyceae(1-4Teil). In *Süßwasserflora von Mitteleuropa*. durchgesehener Nachdruck.

Krause, A. E., Frank, K. A., Mason, D. M., Ulanowicz, R. E., & Taylor, W. W. (2003). Compartments revealed in food-web structure. *Nature*, *426*(6964), 282–285. https://doi.org/10.1038/nature02115

Kuehn, C. (2011). A mathematical framework for critical transitions: Bifurcations, fast-slow systems and stochastic dynamics. *Physica D-Nonlinear Phenomena*, *240*(12), 1020–1035. https://doi.org/10.1016/j.physd.2011.02.012

Kuiper, J. J., van Altena, C., De Ruiter, P. C., van Gerven, L. P. a., Janse, J. H., & Mooij, W. M. (2015). Food-web stability signals critical transitions in temperate shallow lakes. *Nature Communications*, *6*, 7727. https://doi.org/10.1038/ncomms8727

Li, D., He, P., Xu, J., & Hou, L. (2020). Research basis of ecological thresholds and regime shifts in China. *Chinese Journal of Applied Ecology*, *31*(6), 2015–2028.

Li, H., Mynett, A., Penning, E., & Qi, H. (2010). Revealing spatial pattern dynamics in aquatic ecosystem modelling with Multi-Agent Systems in Lake Veluwe. *Ecological Informatics*, *5*(2), 97–107. https://doi.org/10.1016/j.ecoinf.2009.08.003

Li, W., & Lian, G. (1996). Light demand for brood-bud germination of submerged plant. *Journal of Lake Sciences*, *8*(Z1), 25–30. http://epub.cnki.net/grid2008/brief/detailj.aspx?filename=GCLX200009002135&dbname=CPFD2000

Li, W. W. (1997). Multiplicity of Stable States in Shallow Lakes and its Application. 湖泊科学, *9*(2), 97–104.

Liu, E., Yang, X., Shen, J., Dong, X., Zhang, E., & Wang, S. (2007). Environmental response to climate and human impact during the last 400 years in Taibai Lake catchment, middle reach of Yangtze River, China. *Sci Total Environ*, *385*(1–3), 196–207. https://doi.org/10.1016/j.scitotenv.2007.06.041

Liu, J., & Xie, P. (1999). Unraveling the enigma of the disappearance of water bloom from the east lake (Lake Donghu) of Wuhan. *Resources and Environment in the Yangtze Basin*, *8*(3).

Liu, Q., Yang, X., Anderson, J., & Liu, E. (2012). Diatom ecological response to altered hydrological forcing of a shallow lake on the Yangtze floodplain, SE China. *Ecohydrology*, *268*(May 2011), 256–268. https://doi.org/10.1002/eco.2

Liu, Q., Yang, X. D., Anderson, N. J., Liu, E. F., Dong, X. H., Anderson, J., Liu, E. F., Qian, L., Xiangdong, Y., Anderson, N. J., Enfeng, L., Xuhui, D., Liu, Q., Yang, X. D., Anderson, J., & Liu1, E. (2012). Diatom ecological response to altered hydrological forcing of a shallow lake on the Yangtze floodplain, SE China. *Ecohydrology*, *5*(3), 256–268. https://doi.org/10.1002/eco.2

Mac Nally, R., Albano, C., & Fleishman, E. (2014). A scrutiny of the evidence for pressure-induced state shifts in estuarine and nearshore ecosystems. In *Austral Ecology*. https://doi.org/10.1111/aec.12162

Marín, V. H. (1997). General System Theory and the Ecosystem Concept. *Bulletin of the Ecological Society of America*, *78*(1), 102–104. http://www.jstor.org/stable/20168127

Martin, R., & Schlüter, M. (2015). Combining system dynamics and agent-based modeling to analyze social-ecological interactions—an example from modeling restoration of a shallow lake. *Frontiers in Environmental Science*, *3*(66). https://doi.org/10.3389/fenvs.2015.00066

Martin, R., Schlüter, M., & Blenckner, T. (2020). The importance of transient social dynamics for restoring ecosystems beyond ecological tipping points. *Proceedings of the National Academy of Sciences of the United States of America*. https://doi.org/10.1073/pnas.1817154117

Martin, R., & Thomas, S. A. (2016). Analyzing regime shifts in agent-based models with equation-free analysis. *Environmental Modelling and Software for Supporting a Sustainable Future, Proceedings - 8th International Congress on Environmental Modelling and Software, IEMSs 2016*.

May, R. M. (1977). Thresholds and Breakpoints in Ecosystems with a Multiplicity of Stable States. *Nature*, *269*(5628), 471–477. https://doi.org/10.1038/269471a0

Meijer, M. L. (2000). *Biomanipulation in the Netherlands : 15 years of experience*.

Ministry of Ecology and Environment of PRC. (2020). *Lake Nutrient Standards-Central and Eastern Lakes （Total phosphorus, total nitrogen and Chl a）2020*. https://doi.org/000014672/2020-01882

Montoya, J. M., Donohue, I., & Pimm, S. L. (2018). Planetary Boundaries for Biodiversity: Implausible Science, Pernicious Policies. *Trends in Ecology and Evolution*, *33*(2), 71–73. https://doi.org/10.1016/j.tree.2017.10.004

Morris, M. D. (1991). Factorial Sampling Plans for Preliminary Computational Experiments. *Technometrics*, *33*(2), 161–174. https://doi.org/10.1080/00401706.1991.10484804

Nanjing Institute of Geographical and Limnological science CAS. (2019). *Survey Report of Chinese Lakes [中国湖泊调查报告]*. 科学出版社. https://books.google.co.uk/books?id=fca2zQEACAAJ

Neutel, A. M., & Thorne, M. A. S. (2014). Interaction strengths in balanced carbon cycles and the absence of a relation between ecosystem complexity and stability. *Ecology Letters*, *17*(6), 651–661. https://doi.org/10.1111/ele.12266

Newman, M. E. J., & Girvan, M. (2004). Finding and evaluating community structure in networks. *Physical Review E - Statistical, Nonlinear, and Soft Matter Physics*, *69*(2 2), 1–

15. https://doi.org/10.1103/PhysRevE.69.026113

Nielsen, A., Trolle, D., Bjerring, R., Sondergaard, M., Olesen, J. E., Janse, J. H., Mooij, W. M., & Jeppesen, E. (2014). Effects of climate and nutrient load on the water quality of shallow lakes assessed through ensemble runs by PCLake. *Ecological Applications*, *24*(8), 1926–1944.

Nunes, M. A., & Prangle, D. (2015). abctools: An R package for tuning approximate bayesian computation analyses. *R Journal*, *7*(2), 189–205. https://doi.org/10.32614/rj-2015-030

Odum, E. P. (1953). Fundamentals of Ecology. In L. Robin, S. Sörlin, & P. Warde (Eds.), *The Future of Nature: Documents of Global Change* (pp. 233–244). Yale University Press. https://doi.org/10.12987/9780300188479-022

Otto, S. A., Kadin, M., Casini, M., Torres, M. A., & Blenckner, T. (2018). A quantitative framework for selecting and validating food web indicators. *Ecological Indicators*, *84*, 619–631. https://doi.org/10.1016/j.ecolind.2017.05.045

Pace, M. L., Carpenter, S. R., Johnson, R. A., & Kurtzweil, J. T. (2013). Zooplankton provide early warnings of a regime shift in a whole lake manipulation. *Limnology and Oceanography*. https://doi.org/10.4319/lo.2013.58.2.0525

Pagès, J. (2002). Analyse factorielle multiple appliquée aux variables qualitatives et aux données mixtes. *Revue Des Statistiques Appliquées*, *50*, 5–37.

Pan, B. Z., Wang, H. Z., Pusch, M. T., & Wang, H. J. (2015). Macroinvertebrate responses to regime shifts caused by eutrophication in subtropical shallow lakes. *Freshwater Science*, *34*(3), 942–952. https://doi.org/10.1086/682077

Perry, G. L. W., Wainwright, J., Etherington, T. R., & Wilmshurst, J. M. (2016). Experimental simulation: Using generative modeling and palaeoecological data to understand human-environment interactions. *Frontiers in Ecology and Evolution*, *4*(OCT), 1–14. https://doi.org/10.3389/fevo.2016.00109

Peterson, C. H. (1984). Does a Rigorous Criterion for Environmental Identity Preclude the Existence of Multiple Stable Points? *The American Naturalist*. https://doi.org/10.1086/284256

Peterson, G. D., Biggs, R., Rocha, J. C., Peterson, G. D., & Biggs, R. (2015). *Regime Shifts in the Anthropocene : Drivers , Risks , and Resilience Regime Shifts in the Anthropocene : Drivers , Risks , and Resilience*. *AUGUST*. https://doi.org/10.1371/journal.pone.0134639

Petraitis, P. (2013). Multiple Stable States in Natural Ecosystems. In *Multiple Stable States in Natural Ecosystems*. https://doi.org/10.1093/acprof:osobl/9780199569342.001.0001

Pons, P., & Latapy, M. (2005). Computing communities in large networks using random walks. *Lecture Notes in Computer Science (Including Subseries Lecture Notes in Artificial*

Intelligence and Lecture Notes in Bioinformatics), *3733 LNCS*, 284–293. https://doi.org/10.1007/11569596_31

Possingham, H. P., Lindenmayer, D. B., & McCarthy, M. A. (2001). Population Viability Analysis. In S. A. Levin (Ed.), *Encyclopedia of Biodiversity* (pp. 831–843). Elsevier. https://doi.org/https://doi.org/10.1016/B0-12-226865-2/00356-4

Qian, W., & Zhu, Y. (2001). Climate change in China from 1880 to 1998 and its impact on the environmental condition. *Climatic Change*, *50*(4), 419–444. https://doi.org/10.1023/A:1010673212131

Qin, BoQiang, Gao, G., Zhu, G., Zhang, Y., Song, Y., Tang, X., Xu, H., & Deng, J. (2013). Lake eutrophication and its ecosystem response. *Chinese Science Bulletin*, *58*(9), 961–970. https://doi.org/10.1007/s11434-012-5560-x

Qin, Boqiang, Yang, L., Chen, F., Zhu, G., Zhang, L., & Chen, Y. (2006). Mechanism and control of lake eutrophication. *Chinese Science Bulletin*, *51*(19), 2401–2412. https://doi.org/10.1007/s11434-006-2096-y

Randsalu-Wendrup, L., Conley, D. J., Carstensen, J., & Fritz, S. C. (2016). Paleolimnological records of regime shifts in lakes in response to climate change and anthropogenic activities. *Journal of Paleolimnology*, *56*(1), 1–14. https://doi.org/10.1007/s10933-016-9884-4

Randsalu-Wendrup, L., Conley, D. J., Carstensen, J., Snowball, I., Jessen, C., & Fritz, S. C. (2012). Ecological Regime Shifts in Lake Kälksjön, Sweden, in Response to Abrupt Climate Change Around the 8.2 ka Cooling Event. *Ecosystems*, *15*(8), 1336–1350. https://doi.org/10.1007/s10021-012-9588-1

Ratajczak, Z., Carpenter, S. R., Ives, A. R., Kucharik, C. J., Ramiadantsoa, T., Stegner, M. A., Williams, J. W., Zhang, J., & Turner, M. G. (2018). Abrupt Change in Ecological Systems: Inference and Diagnosis. *Trends in Ecology & Evolution*, *33*(7), 513–526. https://doi.org/10.1016/j.tree.2018.04.013

Reid, M. A., & Ogden, R. W. (2009). Factors affecting diatom distribution in floodplain lakes of the southeast Murray Basin, Australia and implications for palaeolimnological studies. *Journal of Paleolimnology*, *41*(3), 453–470. https://doi.org/10.1007/s10933-008-9236-0

Reynaud, A., & Lanzanova, D. (2017). A Global Meta-Analysis of the Value of Ecosystem Services Provided by Lakes. *Ecological Economics*, *137*, 184–194. https://doi.org/10.1016/j.ecolecon,2017.03.001

Rocha, J., Biggs, R. (Oonsie), Peterson, G., & Carpenter, S. (2017). *Freshwater Eutrophication*. Regime Shifts Database. www.regimeshifts.org

Rocha, J. C., Peterson, G. D., & Biggs, R. (2015). Regime shifts in the anthropocene: drivers, risks, and resilience. *Plos One*, *10*(8), e0134639. https://doi.org/10.1371/journal.pone.0134639

Rockström, J., Steffen, W., Noone, K., Persson, Å., Chapin, F. S., Lambin, E. F., Lenton, T. M., Scheffer, M., Folke, C., Schellnhuber, H. J., Nykvist, B., De Wit, C. A., Hughes, T., Van Der Leeuw, S., Rodhe, H., Sörlin, S., Snyder, P. K., Costanza, R., Svedin, U., … Foley, J. A. (2009). A safe operating space for humanity. *Nature*, *461*(7263), 472–475. https://doi.org/10.1038/461472a

Rodionov, S. N. (2004). A sequential algorithm for testing climate regime shifts. *Geophysical Research Letters*, *31*(9). https://doi.org/Artn L0920410.1029/2004gl019448

Rosenzweig, M. L. (1971). Paradox of enrichment: Destabilization of exploitation ecosystems in ecological time. *Science*, *171*(3969), 385–387. https://doi.org/10.1126/science.171.3969.385

Salecker, J., Sciaini, M., Meyer, K. M., & Wiegand, K. (2019). The nlrx r package: A next-generation framework for reproducible NetLogo model analyses. *Methods in Ecology and Evolution*, *10*(11), 1854–1863. https://doi.org/10.1111/2041-210X.13286

Salgado, J., Vélez, M. I., González-Arango, C., Rose, N. L., Yang, H., Huguet, C., Camacho, J. S., & O'Dea, A. (2020). A century of limnological evolution and interactive threats in the Panama Canal: Long-term assessments from a shallow basin. *Science of The Total Environment*, *729*, 138444. https://doi.org/10.1016/j.scitotenv.2020.138444

Sand-Jensen, K., & Søndergaard, M. (1981). Phytoplankton and Epiphyte Development and Their Shading Effect on Submerged Macrophytes in Lakes of Different Nutrient Status. *Internationale Revue Der Gesamten Hydrobiologie Und Hydrographie*, *66*(4), 529–552. https://doi.org/10.1002/iroh.19810660406

Saunders, P. T. (1980). An Introduction to Catastrophe Theory. In *An Introduction to Catastrophe Theory*. Cambridge University Press. https://doi.org/10.1017/cbo9781139171533

Sayer, C. D., Hoare, D. J., Simpson, G. L., Henderson, A. C. G., Liptrot, E. R., Jackson, M. J., Appleby, P. G., Boyle, J. F., Jones, J. I., & Waldock, M. J. (2006). TBT causes regime shift in shallow lakes. *Environmental Science and Technology*, *40*(17), 5269–5275. https://doi.org/10.1021/es060161o

Schallenberg, M., de Winton, M. D., Verburg, P., Kelly, D. J., Hamill, K. D., & Hamilton, D. P. (2013). Ecosystem Services of Lakes. *Ecosystem Services in New Zealand: Conditions and Trends*, 203–225.

Scheffer, M. (1989). Alternative stable states in eutrophic, shallow freshwater systems: A minimal model. *Hydrobiological Bulletin*, *23*(1), 73–83. https://doi.org/10.1007/BF02286429

Scheffer, M. (1990). Multiplicity of Stable States in Fresh-Water Systems. *Hydrobiologia*, *200*, 475–486. https://doi.org/Doi 10.1007/Bf02530365

Scheffer, M, Hosper, S. H., Meijer, M.-L., Moss, B., & Jeppesen, E. (1993). Alternative equilibria in shallow lakes. *Trends in Ecology & Evolution*, *8*(8), 275–279. https://doi.org/10.1016/0169-5347(93)90254-M

Scheffer, Marten. (1990). Multiplicity of stable states in freshwater systems. *Hydrobiologia*, *200*, 475–486.

Scheffer, Marten. (1998). Ecology of Shallow Lakes. In *Population and Community BiologySeries* (1998th ed., Vol. 68, Issue 1). Chapman and Hall. https://doi.org/10.1016/S0304-3770(00)00103-0

Scheffer, Marten. (2009). *Critical Transitions in Nature and Society*. Princeton University Press. https://doi.org/10.2307/j.ctv173f1g1

Scheffer, Marten, Baveco, J. M., Deangelis, D. L., Rose, K. A., & Vannes, E. H. (1995). Super-Individuals a Simple Solution for Modeling Large Populations on an Individual Basis. *Ecological Modelling*, *80*(2–3), 161–170. https://doi.org/10.1016/0304-3800(94)00055-M

Scheffer, Marten, Carpenter, S., Foley, J. A., Folke, C., & Walker, B. (2001). Catastrophic shifts in ecosystems. *Nature*, *413*(6856), 591–596. https://doi.org/10.1038/35098000

Scheffer, Marten, & Carpenter, S. R. (2003). Catastrophic regime shifts in ecosystems: linking theory to observation. *Trends in Ecology & Evolution*, *18*(12), 648–656. https://doi.org/10.1016/j.tree.2003.09.002

Scheffer, Marten, Carpenter, S. R., Lenton, T. M., Bascompte, J., Brock, W., Dakos, V., van de Koppel, J., van de Leemput, I. a., Levin, S. a., van Nes, E. H., Pascual, M., & Vandermeer, J. (2012). Anticipating Critical Transitions. *Science*, *338*(6105), 344–348. https://doi.org/10.1126/science.1225244

Scheffer, Marten, & Jeppesen, E. (2007). Regime shifts in shallow lakes. *Ecosystems*, *10*, 1–3. https://doi.org/10.1007/s10021-006-9002-y

Scheffer, Marten, & Van Nes, E. H. (2004). Mechanisms for marine regime shifts: Can we use lakes as microcosms for oceans? *Progress in Oceanography*, *60*(2–4), 303–319. https://doi.org/10.1016/j.pocean.2004.02.008

Schindler, D. W. (2012). The dilemma of controlling cultural eutrophication of lakes. *Proceedings of the Royal Society B: Biological Sciences*, *279*(1746), 4322–4333. https://doi.org/10.1098/rspb.2012.1032

Schroder, A., Persson, L., & De Roos, A. M. (2005). Direct experimental evidence for alternative stable states: a review. *Oikos*, *110*(1), 3–19. https://doi.org/DOI

10.1111/j.0030-1299.2005.13962.x

Seekell, D., Cline, T., Carpenter, S., & Pace, M. (2013). Evidence of alternate attractors from a whole-ecosystem regime shift experiment. *Theoretical Ecology*, *6*(3), 385–394. https://doi.org/10.1007/s12080-013-0183-7

Sibly, R. M., Grimm, V., Martin, B. T., Johnston, A. S. A., Topping, C. J., Calow, P., Nabe-nielsen, J., Thorbek, P., & Deangelis, D. L. (2013). Representing the acquisition and use of energy by individuals in agent-based models of animal populations. *Methods in Ecology and Evolution*, *4*, 151–161. https://doi.org/10.1111/2041-210x.12002

Smith, V. H., & Schindler, D. W. (2009). Eutrophication science: where do we go from here? *Trends in Ecology and Evolution*, *24*(4), 201–207. https://doi.org/10.1016/j.tree.2008.11.009

Smol, J. P., Birks, H. J. B., & Last, W. M. (2002). Tracking environmental change using lake sediments. Volume 3, Terrestrial, algal, and siliceous indicators. In *Developments in paleoenvironmental research;* (Issue vol. 3). Kluwer Academic.

Smol, J. P., Wolfe, A. P., Birks, H. J. B., Douglas, M. S. V, Jones, V. J., Korhola, A., Pienitz, R., Ruhland, K., Sorvari, S., Antoniades, D., Brooks, S. J., Fallu, M. A., Hughes, M., Keatley, B. E., Laing, T. E., Michelutti, N., Nazarova, L., Nyman, M., Paterson, A. M., … Weckstrom, J. (2005). Climate-driven regime shifts in the biological communities of arctic lakes. *Proceedings of the National Academy of Sciences of the United States of America*, *102*(12), 4397–4402. https://doi.org/10.1073/pnas.0500245102

Sondergaard, M., Bjerring, R., & Jeppesen, E. (2013). Persistent internal phosphorus loading during summer in shallow eutrophic lakes. *Hydrobiologia*, *710*(1), 95–107.

Sondergaard, M., Jeppesen, E., Lauridsen, T. L., Skov, C., Van Nes, E. H., Roijackers, R., Lammens, E., & Portielje, R. (2007). Lake restoration: successes, failures and long-term effects. *Journal of Applied Ecology*, *44*(6), 1095–1105.

Sondergaard, M., Lauridsen, T. L., Johansson, L. S., & Jeppesen, E. (2017). Repeated Fish Removal to Restore Lakes: Case Study of Lake Vaeng, Denmark-Two Biomanipulations during 30 Years of Monitoring. *Water*, *9*(1).

Sondergaard, M., Liboriussen, L., Pedersen, A. R., & Jeppesen, E. (2008). Lake Restoration by Fish Removal: Short- and Long-Term Effects in 36 Danish Lakes. *Ecosystems*, *11*(8), 1291–1305.

Spears, B. M., Futter, M. N., Jeppesen, E., Huser, B. J., Ives, S., Davidson, T. A., Adrian, R., Angeler, D. G., Burthe, S. J., Carvalho, L., Daunt, F., Gsell, A. S., Hessen, D. O., Janssen, A. B. G., Mackay, E. B., May, L., Moorhouse, H., Olsen, S., Sondergaard, M., … Thackeray, S. J. (2017). Ecological resilience in lakes and the conjunction fallacy. *Nature Ecology & Evolution*, *1*(11), 1616–1624.

Standish, R. J., Hobbs, R. J., Mayfield, M. M., Bestelmeyer, B. T., Suding, K. N., Battaglia, L. L., Eviner, V., Hawkes, C. V, Temperton, V. M., Cramer, V. A., Harris, J. A., Funk, J. L., & Thomas, P. A. (2014). Resilience in ecology: Abstraction, distraction, or where the action is? *Biological Conservation*, *177*, 43–51. https://doi.org/10.1016/j.biocon.2014.06.008

Su, Han, Liu, X., & Liu, Y. (2016). Build-in uncertainty in agent-based model and its impact on social-ecological system decision-making under deep uncertainty. *Environmental Modelling and Software for Supporting a Sustainable Future, Proceedings - 8th International Congress on Environmental Modelling and Software, IEMSs 2016*, *4*, 1020–1026.

Su, Haojie, Wang, R., Feng, Y., Li, Y., Li, Y., Chen, J., Xu, C., Wang, S., Fang, J., & Xie, P. (2020). Long-term empirical evidence, early warning signals and multiple drivers of regime shifts in a lake ecosystem. *Journal of Ecology*, *October*, 1–13. https://doi.org/10.1111/1365-2745.13544

Su, Haojie, Wu, Y., Xia, W., Yang, L., Chen, J., Han, W., Fang, J., & Xie, P. (2019). Stoichiometric mechanisms of regime shifts in freshwater ecosystem. *Water Research*, *149*, 302–310. https://doi.org/10.1016/j.watres.2018.11.024

Suding, K. N., & Hobbs, R. J. (2009). Threshold models in restoration and conservation: a developing framework. *Trends in Ecology & Evolution*, *24*(5), 271–279. https://doi.org/10.1016/j.tree.2008.11.012

Suzuki, K., & Yoshida, T. (2015). Ecological resilience of population cycles: A dynamic perspective of regime shift. *Journal of Theoretical Biology*, *370*, 103–115. https://doi.org/10.1016/j.jtbi.2015.01.026

Tansley, A. G. (1935). The Use and Abuse of Vegetation Concepts and Terms. In *Ecology* (Vol. 16, Issue 3, pp. 284–307). http://isites.harvard.edu/fs/docs/icb.topic97823.files/III/October_30/tansley_-_use_and_abuse.pdf

Tansley, A. G. G. (1935). The Use and Abuse of Vegetational Concepts and Terms. *Ecology*, *16*(3), 284–307. https://doi.org/10.2307/1930070

Tao, H., Pan, J., Shen, Y., Li, W., Huang, F., & Zhao, H. (2012). Phosphorus threshold for the shift between grass- and algae-stable states in Dahong Harbor of Gehu Lake. *Chinese Journal of Applied Ecology*, *23*(1), 264–270.

Tátrai, I., Gyrgy, Á. I., Mátys, K., Korponai, J., Pomogyi, P., Vári, Á., Józsa, V., & Boros, G. (2011). Intrinsic processes causing periodic changes in stability in a shallow biomanipulated lake. *Marine and Freshwater Research*. https://doi.org/10.1071/MF10245

Thiele, J. C. (2014). *Towards Rigorous Agent-Based Modelling Linking, Extending, and Using Existing Software Platforms*. Georg-August-Universität Göttingen.

Thom, R. (1975). *Structural Stability and Morphogenesis: an outline of a general theory of models*.

Torigoe, M., Islam, T., Kakinuma, H., Fung, C. C. A., Isomura, T., Shimazaki, H., Aoki, T., Fukai, T., & Okamoto, H. (2021). Zebrafish capable of generating future state prediction error show improved active avoidance behavior in virtual reality. *Nature Communications*, *12*(1), 1–21. https://doi.org/10.1038/s41467-021-26010-7

Turnbull, L., Hütt, M., Ioannides, A. A., Kininmonth, S., Poeppl, R., Tockner, K., Bracken, L. J., Keesstra, S., Liu, L., Masselink, R., & Parsons, A. J. (2018). *Connectivity and complex systems : learning from a multi-disciplinary perspective*.

van der Vaart, E., Johnston, A. S. A., & Sibly, R. M. (2016). Predicting how many animals will be where: How to build, calibrate and evaluate individual-based models. *Ecological Modelling*. https://doi.org/10.1016/j.ecolmodel.2015.08.012

van Nes, E. H., Scheffer, M., van den Berg, M. S., & Coops, H. (2002). Aquatic macrophytes: restore, eradicate or is there a compromise? *Aquatic Botany*, *72*(3–4), 387–403. https://doi.org/Pii S0304-3770(01)00212-1Doi 10.1016/S0304-3770(01)00212-1

van Nes, E. H., Scheffer, M., van den Berg, M. S., & Coops, H. (2003). Charisma: a spatial explicit simulation model of submerged macrophytes. *Ecological Modelling*, *159*(2–3), 103–116. https://doi.org/Pii S0304-3800(02)00275-2Doi 10.1016/S0304-3800(02)00275-2

Veraart, A. J., Faassen, E. J., Dakos, V., van Nes, E. H., Lurling, M., & Scheffer, M. (2012). Recovery rates reflect distance to a tipping point in a living system (vol 481, pg 357, 2012). *Nature*, *481*(7394), 404. https://doi.org/10.1038/nature11029

Volterra, V. (1926). Fluctuations in the Abundance of a Species considered Mathematically1. *Nature*, *118*(2972), 558–560. https://doi.org/10.1038/118558a0

Wang, D., Feng, X., Zhou, L., Hao, J., & Xu, X. (2008). Relationship between blue algal bloom and water temperature in Lake Taihu based on MODIS. *Journal of Lake Sciences*, *20*(2), 173–178.

Wang, H. J., Wang, H. Z., Liang, X. M., & Wu, S. K. (2014). Total phosphorus thresholds for regime shifts are nearly equal in subtropical and temperate shallow lakes with moderate depths and areas. *Freshwater Biology*. https://doi.org/10.1111/fwb.12372

Wang, R., Dearing, J. A., Doncaster, C. P., Yang, X., Zhang, E., Langdon, P. G., Yang, H., Dong, X., Hu, Z., Xu, M., Zhao, Y., & Shen, J. (2019). Network parameters quantify loss of assemblage structure in human-impacted lake ecosystems. *Global Change Biology*, *25*(11), 3871–3882. https://doi.org/10.1111/gcb.14776

Wang, R., Dearing, J. a., Langdon, P. G., Zhang, E., Yang, X., Dakos, V., & Scheffer, M. (2012). Flickering gives early warning signals of a critical transition to a eutrophic lake state. *Nature*, *492*(7429), 419–422. https://doi.org/10.1038/nature11655

Wang, S., Meng, W., Jin, X., Zheng, B., Zhang, L., & Xi, H. (2015). Ecological security problems of the major key lakes in China. *Environmental Earth Sciences*, *74*(5), 3825–3837. https://doi.org/10.1007/s12665-015-4191-3

Wang, Y., Cao, X., Zeng, J., Li, H., Zhao, D., & Wu, Q. L. (2020). Distinct shifts in bacterioplankton community composition and functional gene structure between macrophyte- and phytoplankton-dominated regimes in a large shallow lake. *Limnology and Oceanography*, *65*(S1), S208–S219. https://doi.org/10.1002/lno.11373

Wetzel, R. G. (2001). Limnology, Lake and River Ecosystems. In *Journal of Phycology* (Vol. 37). Academic Press. https://doi.org/10.1046/j.1529-8817.2001.37602.x

Wilensky, U. (1997). *NetLogo Wolf Sheep Predation model*. Center for Connected Learning and Computer-Based Modeling, Northwestern University.

Wilensky, U., & Reisman, K. (1998). Connected Science: Learning Biology through Constructing and Testing Computational Theories -- an Embodied Modeling Approach. *InterJournal of Complex Systems*, 1–12.

Wilkinson, G. M., Carpenter, S. R., Cole, J. J., Pace, M. L., Batt, R. D., Buelo, C. D., & Kurtzweil, J. T. (2018). Early warning signals precede cyanobacterial blooms in multiple whole-lake experiments. *Ecological Monographs*, *88*(2), 188–203. https://doi.org/10.1002/ecm.1286

Winder, M., & Cloern, J. E. (2010). The annual cycles of phytoplankton biomass. *Philosophical Transactions of the Royal Society B-Biological Sciences*, *365*(1555), 3215–3226. https://doi.org/10.1098/rstb.2010.0125

Xie, P., & Liu, J. (2001). Practical success of biomanipulation using filter-feeding Fish to control cyanobacteria blooms: a synthesis of decades of research and application in a subtropical hypereutrophic lake. In *TheScientificWorldJournal*. https://doi.org/10.1100/tsw.2001.67

Xu, H., Paerl, H., Qin, B., Zhu, G., Hall, N., & Wu, Y. (2015). Determining critical nutrient thresholds needed to control harmful cyanobacterial blooms in eutrophic Lake Taihu, China. *Environmental Science and Technology*, *49*(2), 1051–1059. https://doi.org/10.1021/es503744q

Xu, M, Dong, X. H., Yang, X. D., Chen, X., Zhang, Q. H., Liu, Q., Wang, R., Yao, M., Davidson, T. A., & Jeppesen, E. (2017). Recent Sedimentation Rates of Shallow Lakes in the Middle and Lower Reaches of the Yangtze River: Patterns, Controlling Factors and Implications for Lake Management. *Water*, *9*(8). https://doi.org/ARTN 61710.3390/w9080617

Xu, Min, Wang, R., Dong, X., & Yang, X. (2019). A palaeolimnological perspective to understand regime-shift dynamics in two Yangtze-basin lakes. *Biology Letters*, *15*(11). https://doi.org/10.1098/rsbl.2019.0447

Xu, X., Zhang, Y., Chen, Q., Li, N., Shi, K., & Zhang, Y. (2020). Regime shifts in shallow lakes observed by remote sensing and the implications for management. *Ecological Indicators*, *113*(October 2019). https://doi.org/10.1016/j.ecolind.2020.106285

Xue, J. T., Li, J. J., Dang, X. Y., Meyers, P. A., & Huang, X. Y. (2017). Paleohydrological changes over the last 4000 years in the middle and lower reaches of the Yangtze River: Evidence from particle size and n-alkanes from Longgan Lake. *Holocene*, *27*(9), 1318–1324. https://doi.org/10.1177/0959683616687386

Yang, X D, Shen, J., Dong, X. H., Liu, E. F., & Wang, S. M. (2006). Historical trophic evolutions and their ecological responses from shallow lakes in the middle and lower reaches of the Yangtze River: Case studies on Longgan Lake and Taibai Lake. *Science in China Series D-Earth Sciences*, *49*, 51–61. https://doi.org/10.1007/s11430-006-8105-9

Yang, Xiangdong D, Shen, J., Dong, X. H., Liu, E. F., Wang, S. M., XiangDong, Y., Ji, S., Xuhui, D., Yang, X. D., Shen, J., Dong, X. H., Liu, E. F., & Wang, S. M. (2006). Historical trophic evolutions and their ecological responses from shallow lakes in the middle and lower reaches of the Yangtze River: Case studies on Longgan Lake and Taibai Lake. *Science in China Series D*, *49*(S1), 51–61. https://doi.org/10.1007/s11430-006-8105-9

Yang, Y., Yin, X., Yang, Z., Sun, T., & Xu, C. (2018). Detection of regime shifts in a shallow lake ecosystem based on multi-proxy paleolimnological indicators. *Ecological Indicators*, *92*(August 2016), 312–321. https://doi.org/10.1016/j.ecolind.2017.05.059

Zeeman, E. C. (1976). Catastrophe Theory. *Scientific American*, *234*(4), 65–83. https://doi.org/10.1038/scientificamerican0476-65

Zeileis, A., Kleiber, C., Kramer, W., Hornik, K., Walter, K., Hornik, K., Kramer, W., Hornik, K., Walter, K., & Hornik, K. (2003). Testing and dating of structural changes in practice. *Computational Statistics & Data Analysis*, *44*(1–2), 109–123. https://doi.org/10.1016/s0167-9473(03)00030-6

Zhang, C., Ni, Z., & Tang, H. (2020). Tracking ecosystem regime shifts in Lake Xijiu(Taihu Basin) based on chironomid sub-fossil assemblages. *Journal of Lake Sciences*, *32*(2), 587–595.

Zhang, K. (2016). Regime shifts and resilience in China’s coastal ecosystems. *Ambio*, *45*(1), 89–98. https://doi.org/10.1007/s13280-015-0692-2

Zhang, Ke, Dong, X., Yang, X., Kattel, G., Zhao, Y., & Wang, R. (2018). Ecological shift and resilience in China’s lake systems during the last two centuries. *Global and Planetary Change*, *165*(January), 147–159. https://doi.org/10.1016/j.gloplacha.2018.03.013

Zhang, Ke, Yang, X., Xu, M., Lin, Q., Kattel, G., & Shen, J. (2018). Confronting challenges of managing degraded lake ecosystems in the Anthropocene, exemplified from the Yangtze River Basin in China. *Anthropocene*, *24*, 30–39. https://doi.org/10.1016/j.ancene.2018.11.001

Zhang, S. Y., Liu, A. F., Ma, J. M., Zhou, Q. H., Xu, D., Cheng, S. P., Zhao, Q., & Wu, Z. Bin. (2010). Changes in physicochemical and biological factors during regime shifts in a restoration demonstration of macrophytes in a small hypereutrophic Chinese lake. *Ecological Engineering*, *36*(12), 1611–1619. https://doi.org/10.1016/j.ecoleng.2010.05.006

Zhang, Y., Gao, Y., Wu, F., & Huo, S. (2018). Characteristics of Ecological Effects in the Eastern Shallow Lakes, China. *Research of Environmental Sciences*, *31*, 878–885. https://doi.org/10.13198/j.issn.1001-6929.2017.03.99

Zhao, L. (2013). *The regime shifts and inversion of catastrophic driving factors in the ecosystems of Yilong lake, Yunnan*. 中国科学院研究生院.

Zhao, L., Wang, M., Liang, Z., & Zhou, Q. (2020). Identification of regime shifts and their potential drivers in the shallow eutrophic Lake Yilong, Southwest China. *Sustainability (Switzerland)*, *12*(9), 1–12. https://doi.org/10.3390/su12093704

Zhao, Y., Wang, R., Yang, X., Dong, X., & Xu, M. (2016). Regime shifts revealed by paleoecological records in Lake Taibai's ecosystem in the middle and lower Yangtze River Basin during the last century. *Journal of Lake Sciences*, *28*(6), 1381–1390. https://doi.org/10.18307/2016.0624

Zhen, W., Genbao, L., Gaohong, W., Yinwu, S., & Yongding, L. (2011). Application of Fuzzy Synthetic Evaluation on the Regime Shift Phases of Lake Erhai. *Chinese Journal of Hydroecology*, *32*(3).

Zhu, G., Qin, B., Zhang, Y., Li, Y., Zhu, M., Xu, H., & Zhang, Y. (2021). Fluctuation of phosphorus concentration in Lake Taihu in the past 70 years and future control strategy. *Journal of Lake Sciences*, *33*(4), 957–973. https://doi.org/10.18307/2021.0401

Zou, W., Zhu, G., Cai, Y., Vilmi, A., Xu, H., Zhu, M., Gong, Z., Zhang, Y., & Qin, B. (2020). Relationships between nutrient, chlorophyll a and Secchi depth in lakes of the Chinese Eastern Plains ecoregion: Implications for eutrophication management. *Journal of Environmental Management*, *260*(January), 109923. https://doi.org/10.1016/j.jenvman.2019.109923

Appendices

Appendix A Model Development Procedures

The procedure for the development of my model combines a general routine of ecosystem modelling with the specific goal of modelling and understanding the mechanisms of critical transitions and regime shifts in lake ecosystems during the last century. It starts with defining the precise problem to be studied in the system. The problem that I wish to address with this model is how micro-level interactions between ecologically functional groups and exogenous drivers lead to critical transitions occurring in a lake ecosystem. Specifically, the driving forces can be nutrient loading, lake size, hydrodynamics and the addition of fish, while critical ecosystem transitions can be assessed by determining the outbreaks and extinctions of biological communities.

The next step is to design the model structure. The mechanisms of inter-biotic and environment-biotic interactions are key factors in the ecosystem mechanism model, so a feedback loop diagram based on the reconstruction of Lake Taibai was used as a basic model structure. On the basis of this structure, concepts were selected, added, simplified and connected. For example, to facilitate external validation, the driving forces of the problem and the measurements of ecosystem state needed to be identified. The third step was to search for mathematical formulae and ranges of applicable parameters in terms of individual ecology, which will become a key part of the rules by which individuals perceive and adapt to their environment. Examples of individual ecology-based equations that were used include empirical equations for photosynthetic efficiency as a function of temperature, and metabolic rate as a function of organism mass. These equations have some adjustable parameters and terms, the range of which was determined by a combination of ecological experimental results and simulations.

The model design can then be implemented in a computer language (step 4), which requires the implementation of algorithms based on the syntax of the computer language. In this step, other models can be consulted for ideas. For example, predators do not hunt constantly throughout the day, and it is not clear how specific feeding limits relates to other body metrics. I referred to the wolf-sheep model of predation probability (Wilensky, 1997), in which the predator (the wolf) first decides whether or not to feed on sheep by comparing a random number between 0 and 100 to the predation probability (as a percentage) when it encounters food. The resulting macro-level outcome shows that the predator’s probability to attack is controlled. Another example is the avoidance of obstacles. When designing a reclamation scenario, a certain portion of the lake becomes land, which meant that allowing fish and phytoplankton in the water to avoid any irregularly shaped land was a problem. The model references a movement algorithm in an ABM that simulates the Chicago Lake food web (Appendix B.2.5), allowing the agent to judge what the next step is about to be on land by moving forward a large enough distance to basically get around the obstacle. The algorithmic statements in my model reference these models, allowing the results to function as intended.

The fifth step in the modelling process is validation. That involves the internal testing of the model's logic and the evaluation of its behaviour (Jørgensen & Fath, 2011). In Check #1, the model needs to be checked in the following areas: 1) Is the model stable in the long term? 2) Do all agents' behaviours conform to the model rules in the design? 3) Do the model responses conform to expectations? 3) Are the units in all equations consistent? 4) Do patterns of change at system level emerge from the agents' behaviours? 5) Does the ABM reproduce the observed patterns robustly? The validation results demonstrate the behaviour and effectiveness of the model at the micro- and macro-scale, and any anomalies in performance can be modified retrospectively at this step. After several rounds of modification, the model largely met the pattern of the lake ecosystem expected from the previous theoretical model designs. The validation results are recorded in Appendix A. The model is then ready to proceed to the next steps, namely parameter tuning and performance testing.

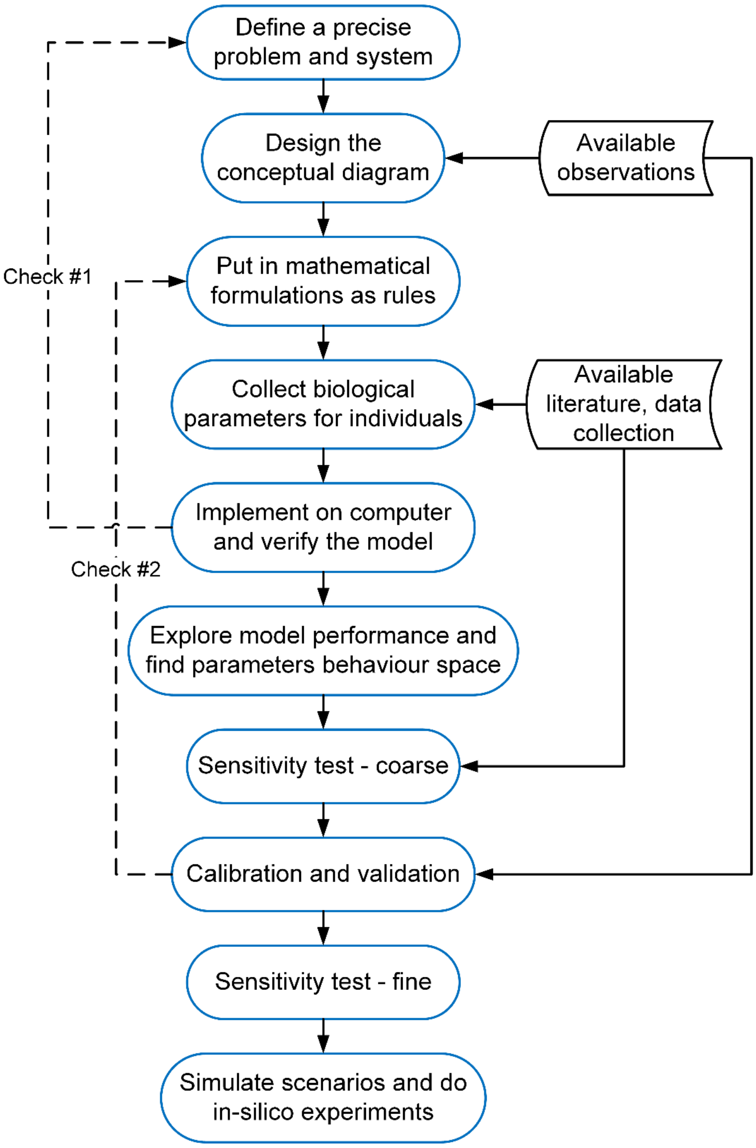

Figure Apx 1: The general modelling procedure used in the development of my ABMs. Developed and adapted from protocols in Jørgensen & Fath (2011).

In step 6, an attempt is made to find a range within the multidimensional space of parameters that is suitable for the purpose of simulation. For example, in the absence of perturbations, the functional groups in the simulated system should gradually converge to a steady state and the system should simulate multiple steady states effectively. Any parameters that lead to the extinction of all components of the system would therefore be excluded at this stage, and the process then involves running each structural parameter through the model several times with different values, synthesising the resulting extinction parameters to frame a parameter interval that would result in a steady-state ecosystem. The range of parameters was collected from existing literature and experiments to reduce the computational effort and testing run time for parameter sweeps. The model parameters that were tested included basic environmental parameters, initial population size parameters, individual ecological characteristics parameters and predation relationship parameters, a total of 19 parameters in all. The basic environmental parameters include water temperature, water depth and total nutrient concentration of the system. The initial population parameters include the initial number of agents in each functional group, the individual ecological characteristics parameters mainly involve the reproduction rate of each functional group, and the predation relationship parameters reflect the predation rate of each functional group.

From Step 7 (“sensitivity test-coarse”) to Step 10 (“simulate scenarios”), the community assembly patterns of the ecosystem simulated by the ABM model and the patterns of response to external drives were systematically evaluated, and changes in the state of the system dynamics in equilibrium and under perturbation were observed. To facilitate replication and use by peer developers, the model description uses part of the Overview, Design, and Details (ODD protocol)(Grimm et al, 2006) and an extended version of ODD + D (plus human decision making) (Müller et al, 2013). An overview of the model, design concepts, parameters and variables, details of the main simulation processes and the lifecycle of the agent are included in this list.

Appendix B : Reference models for ABM development

Using publicly available models provides algorithms that can be used towards a specific goal. To investigate the mechanism of critical transitions in lake ecosystems, useful models, especially ABMs relating to lake ecosystems or interactions in biological communities, were searched for reference and gathered together in this section.

B.1 Generic models

B.1.1 Multiple stable states of a single population

To produce a one-dimensional system that reaches an equilibrium and then remains stable, the variable of population N can be controlled by the logistic growth equation:

$$\frac{dN}{dt} = C_1 \times N - C_2 \times N^2$$

where population reaches a stable equilibrium at C_1/C_2. For ABMs where the growth rate is applied to each individual agent, the equation can be further simplified as:

$$\left(\frac{dN}{dt}\right)_i = C_1 - C_2 \times N$$

The parameter i represents one of the agents, and its individual growth-rate is related to the population to which it belongs. Here, growth rate no longer strictly stands for the number the agent would become when $C_1 - C_2$ is not an integer but may stand for energy or body mass, which in turn would lead to reproduction of the agent. This equation shows that with one negative parameter of feedback the population can reach a stable state by limiting its own growing rate.

B.1.2 A mathematical framework for critical transitions

The use of the mathematical theory of fast-slow systems is suggested to naturally define critical transitions (Kuehn, 2011). Attributes of critical transitions have been summarised from observations as:

(1) An abrupt qualitative change in the dynamical system occurs.

(2) The change occurs rapidly in comparison to the regular dynamics.

(3) The system crosses a particular threshold near a transition.

(4) The new state of the system is significantly different from its previous state.

(5) The data have a major deterministic component with small “random fluctuations”.

(6) Prior to the transition, the system recovers slowly from perturbations such as “critical slowing down”.

(7) Prior to the transition, the variance of the system increases as the transition is approached.

(8) Prior to the transition, noisy fluctuations become more asymmetric.

(9) Prior to the transition, autocorrelation increases.

Deterministic and stochastic dynamic systems were then developed in which slow changes drove the system towards a more rapid bifurcation in the subsystem. The fold critical transitions were modelled as follows

$$dx_\tau = \frac{1}{\epsilon}(y - x^2)d_\tau + \frac{\sigma}{\sqrt{\epsilon}}dW_\tau$$

$$dy_\tau = g(x_\tau, y_\tau)d\tau$$

where W_τ is standard Brownian motion. When responses occur on the fast time scale $t = \tau/\epsilon$, and the the singular limit $\epsilon \to 0$, the variation is

$$dx_t = (y - x^2)dt + \sigma dW_t$$

The mathematical model summarises the characteristics of critical transitions in natural systems and uses the deterministic and stochastic equations to simulate and synthesise the "slow" driving force and "fast" change in this phenomenon respectively. In my ABM development process, I mainly refer to observations 1-4, which describe the characteristics of the critical transition phenomenon. The early warning signals are not always observed and cannot represent all changes before the transition.

B.1.3 Wolf Sheep Predation model in NetLogo

A modified version of the classical Lotka-Volterra model is used in this agent-based model as a theoretical foundation. The original Lotka-Volterra predation equations describe changes in the densities of the prey population (N_1) and the predator population (N_2) (Volterra, 1926).

$$\frac{dN_1}{dt} = b_1N_1 - k_1N_1N_2 \tag{1}$$

$$\frac{dN_2}{dt} = k_2N_1N_2 - d_2N_2 \tag{2}$$

In these equations, b_1 is the birth rate of the prey, d_2 is the death rate of the predators, and k_1 and k_2 are constants. For prey (equation 1), the first term (b_1N_1) is a multiplication of the prey birth rate and the density of the prey population, yielding the increase in density due to new prey births. In the second term ($k_1N_1N_2$), the frequency of interaction between the prey and predator populations is determined, yielding the decrease in prey density due to consumption of prey by predators. The rate of change in the density of the prey population is thus computed by subtracting the total effect of prey deaths from the total effect of prey births. For predator (equation 2), on the contrast, relies on the interactions with prey to increase population size, while the deaths are only dependent on its own.

To simulate characteristic properties of predator-prey population dynamics in view of individuals, the Lotka-Volterra equation was enhanced with other theories to increase the stability and a Lotka-Volterra-like behaviour was implemented in StarLogoT simulating the population dynamics of wolf-sheep on grass (Wilensky, 1997; Wilensky & Reisman, 1998).

B.1.4 Random-walk simulation of palaeoecological records

Blaauw et al (2010) simulated fossil proxy time series using the Random Walk algorithm, and found the simple procedures can generate results that resembling the patterns usually identified in palaeoecological data, such as abrupt events, long-term trends, quasi-cyclic behaviour, extinction and immigration. Four environmental factors were given values from a normal distribution with mean of 100 and standard deviation 0.2. Assuming that ecosystem changes are driven by specific environmental factors, the responses of biological proxies to the environmental variables were generated in random patterns, all within a normal distribution with an optimum and range. The combined effects of environmental factors on the biological species and community generated nonlinear changes in proxy abundances were based on the initial population sampled from a negative binomial distribution.

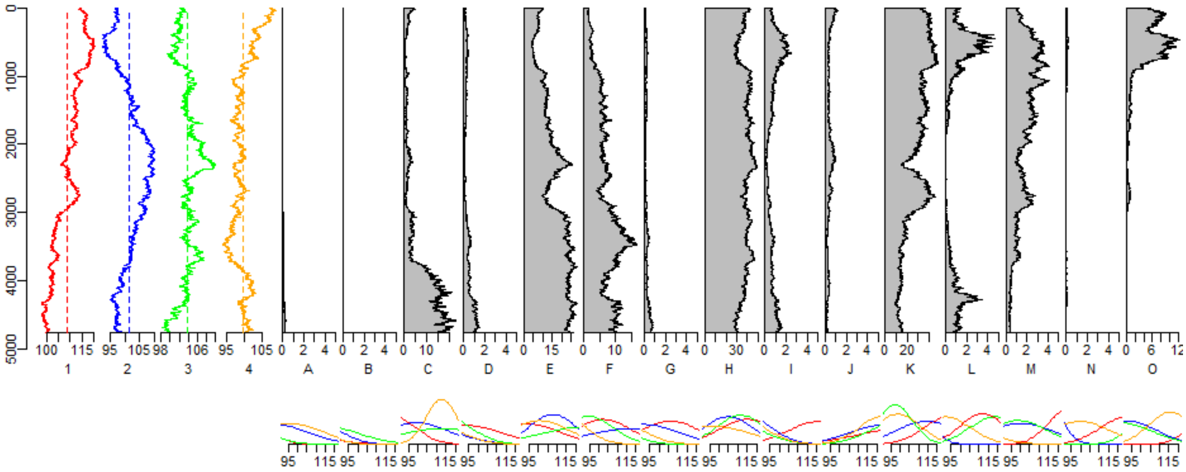

Figure Apx 2: Results of random walk simulation of proxy reactions to random environmental factors generated by RandomEnv package (setseed = 666)

Although the interdependence between environmental forcing factors and competition between species were intentionally excluded, the random-walk simulation showed a deterministic way of generating palaeoecological records visually. The R codes of the simulation functions are openly accessible online. This simulation combined Pressure-State-Response framework with palaeoecological evidence using computational techniques. The

Random Walk algorithm is naturally implemented in ABMs when individuals in the same breed aggregate, showing the strength of the ABM in modelling empirical natural systems.

B.2 ABMs simulating lake ecosystems

B.2.1 Modelling spatial population dynamics of aquatic plant growth using MAS

An MAS was used to model aquatic plant population in Lake Velwe based on expert biological knowledge, GIS maps and environmental conditions (Li et al, 2010). The main goal of the MAS was to explore the colonization of submerged plant *Cs* in Lake Veluwe in the Netherlands. The model consisted of plant agents, environmental backgrounds and animal influences. The plants were *Potamogeton pectinatus* (*Pp*) and *Chara aspera* (*Cs*) and environmental factors included flow pattern, light visibility, water temperature, water depth and wind. Animal influences came from water birds. The data on spatial area and the annual densities of macrophytes were measured using remote sensing images in 1994, 1997 and 1999, while average water depth and average flow velocity were calculated from bathymetry data using the Delft3D software package. The variables of plant *Pp* and *Cs* were height and density. The rules of agent behaviours were controlled by differential equations including germination, growth, species interactions, spatial extension and seed dispersal.

The model ran from 1994 to 2001, with occupation percentages and spatial patterns captured and compared with the observed plant coverage pattern. The result showed that in most years MAS could predict *Cs* spatial patterns with high accuracy (>70% correct). This application of MAS showed that the development of spatial patterns could be accurately modelled as long as the mechanisms and the mathematical formulation of processes are well understood.

B.2.2 LimnoSES as a hybrid model for social-ecological system

The main purpose of the LimnoSES model is to simulate social-ecological feedback in lake use and management systems in which ecological regime shifts can occur between turbid and the clear water states (Martin & Schlüter, 2015). The model consists of a social and an ecological submodel which employ agent-based modeling and dynamic system modeling respectively. The ecological submodel uses a minimal model by Scheffer (1989), representing two fish populations of piscivorous fish (pike) and its prey (bream), as well as macrophytes and nutrients. In the model, the lake ecosystem operated on a daily time steps and showed bi-stability of fish densities in response to nutrient amounts. The social submodel ran on annual time steps, and was used to givern policies on sewage treatment. The input and output of the model were not as precise as other deterministic models, as it was a coupled system that aimed to investigate links between social and ecological compartments.

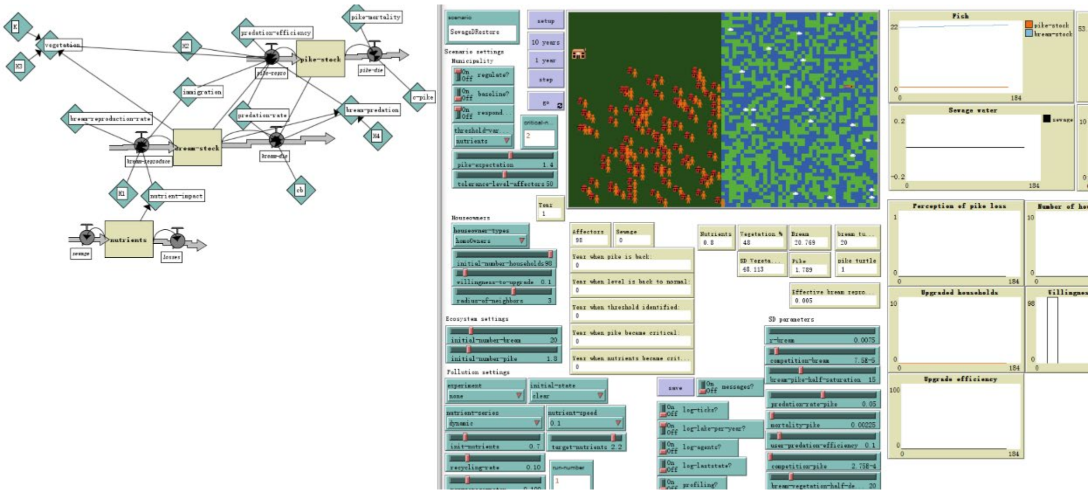

scenario: SewageDRestore

Scenario settings

Municipality

On/Off regulate?

On/Off baseline?

On/Off respond...

threshold-var...: nutrients

critical-n...: 2

pike-expectation 1.4

tolerance-level-affectors 50

Year: 1

Houseowners

houseowner-types: homeOwners

initial-number-households 98

willingness-to-upgrade 0.1

radius-of-neighbors 3

Ecosystem settings

initial-number-bream 20

initial-number-pike 1.8

Pollution settings

experiment: none

initial-state: clear

nutrient-series: dynamic

nutrient-speed: 0.1

init-nutrients 0.7

target-nutrients 2.2

recycling-rate 0.10

run-number: 1

Affectors: 98

Sewage: 0

Year when pike is back: 0

Year when level is back to normal: 0

Year when threshold identified: 0

Year when pike became critical: 0

Year when nutrients became crit...: 0

Nutrients: 0.8

Vegetation %: 48

Bream: 20.769

bream tu...: 20

SD Vegeta...: 48.113

Pike: 1.789

pike turtle: 1

Effective bream repro...: 0.005

SD parameters

r-bream 0.0075

competition-bream 7.5E-5

bream-pike-half-saturation 15

predation-rate-pike 0.05

mortality-pike 0.00225

user-predation-efficiency 0.1

competition-pike 2.75E-4

bream-vegetation-half-de... 20

On/Off messages?

On/Off log-ticks?

On/Off log-lake-per-year?

On/Off log-agents?

On/Off log-laststate?

On/Off profiling?

Figure Apx 3: Conceptual graph of the hybrid LimnoSES model, with the SDM module on the left and the ABM module on the right

The LimnoSES model was implemented in Netlogo and documented using ODD+D protocol, which provided me with an example of how to develop a replicable ABM for ecological regime shifts and simulations under specific scenarios.

B.2.3 PCLake to simulate a critical transition of a shallow lake

Kuiper et al (2015) developed an integrated dynamic model for shallow lakes using PCLake. The main purpose of the model was to identify critical levels of environmental change beyond which ecosystems underwent radical shifts in terms of their functioning. Key ecological processes included closed cycles of nutrients and matter, benthic-pelagic coupling, stoichiometry, food-web dynamics and trophic cascades. The model was run for a range of nutrient loadings from oligotrophic to hypotrophic conditions to simulate the typical loading history of shallow lakes in the temperate zone since the 1950s. In each run, the seasonal equilibrium was firstly reached, and the average chl-a concentration was used to define the state of the lake ecosystem. The food-web stability was assessed using the diagonal strength metric, representing the minimum degree of relative intraspecific interaction needed for matrix stability. This study showed that food-web stability can signal critical transitions in a shallow lake ecosystem, and that only few trophic interactions (between diatoms, zooplankton and detritus) determine the deterioration of the stabiity of the food-web.

B.2.4 Using GEM Madingley to capture the emergence of ecosystem properties

The General Ecosystem Model (GEM) Madingley model mainly aims to capture the emergence of higher-level ecosystem properties using individual-based rules (Harfoot et al, 2014). The model uses a trait-based approach in which individuals are characterized by their functional traits instead of their taxonomic identity. The core biological and ecological processes that are considered necessary for the model to predict ecosystem-level properties include primary production for autotrophs, and eating, metabolism, growth, reproduction, dispersal and mortality for heterotrophs. Both marine and terrestrial environments were modelled but freshwater ecosystems were excluded.

The spatial extents of this GEM are global grid cells of at least a $1° \times 1°$ size, while the temporal length is at least 100 years. Environmental conditions in each grid cell are taken as model inputs from publicly available datasets, and these are air temperature, precipitation, soil water availability, number of frost days, seasonality of primary productivity (in terrestrial ecosystems) and sea-surface temperature, NPP and ocean current velocity (in marine ecosystems). The outputs compute the biomass and the abundance densities of organisms by functional group to indicate the state of ecosystems.

The code of the Madingley model is openly accessible in C# (https://madingley.github.io/). From the Madingley model I learned that modelling the role of individuals in ecosystems in terms of their traits is more useful than modelling them in terms of their taxonomic identity when there are limited taxonomic knowledge and data available. This is because the functional traits of organisms are often directly relevant to ecosystem functions and ecosystem services, helping to show emergence across a broad range of scales.

B.2.5 Topographic Variability and Stability in Lake Food Webs

The Topographic Variability and Stability in Lake Food Webs (LFW) model describes one aspect of the Lake Michigan Food Web Interactions (Krause et al, 2003), by extending and modifying code from the Wolf Sheep Predation model. As this model was developed for education purposes in order to observe species invasion in a stable lake food web, the annotations are elaborate and provide easy approaches for adjusting the parameters and interactions based on the food web being studied. The food web contains mainly predator-prey relationships between certain species and functional groups, e.g. zooplankton eat phytoplankton, molluscs eat phytoplankton, and round gobys eat Opossum Shrimp. The users can edit the food web in the interface and insert obstacles for predators or grazers.

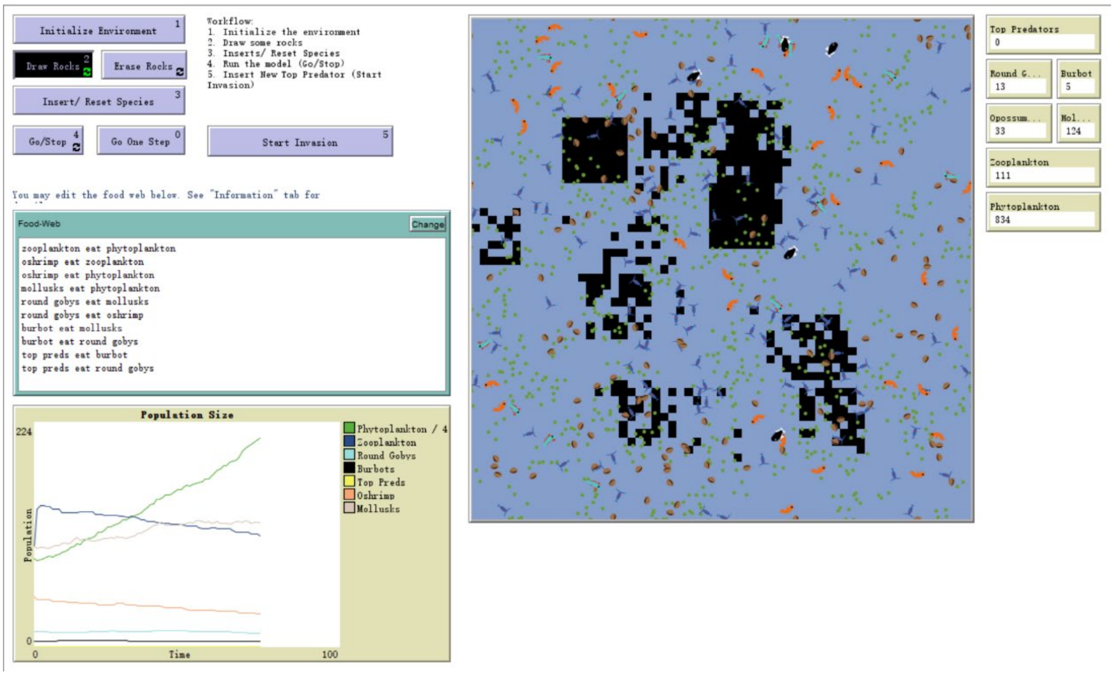

Workflow:
1. Initialize the environment
2. Draw some rocks
3. Inserts/ Reset Species
4. Run the model (Go/Stop)
5. Insert New Top Predator (Start Invasion)

You may edit the food web below. See "Information" tab for

```
zooplankton eat phytoplankton
oshrimp eat zooplankton
oshrimp eat phytoplankton
mollusks eat phytoplankton
round gobys eat mollusks
round gobys eat oshrimp
burbot eat mollusks
burbot eat round gobys
top preds eat burbot
top preds eat round gobys
```

Top Predators 0
Round G... 13
Burbot 5
Opossum... 33
Mol... 124
Zooplankton 111
Phytoplankton 834

Figure Apx 4: The Netlogo interface of the LFW model after setting up organisms and obstacles

The input in this model was the species and relationships between them in the food web. The output was the population sizes of the groups. The LFW model presents a stable lake ecosystem in which multiple species interact with each other and with the physical environment. The idea of using different moving speeds to limit the predation ability of various agents makes the model more realistic than the Wolf Sheep model, which can be referred in our model.

B.2.6 CHARISMA model studying submerged macrophytes

CHARISMA is a spatially explicit agent-based model that is used to study submerged macrophytes in aquatic ecosystems(van Nes et al, 2002, 2003). It mainly aims to answer these questions: 1) Could the results of laboratory experiments such as photosynthesis measurements explain what I see in the field? 2) Which physiological features make *Potamogeton pectinatus* a better competitor than *Chara* in turbid water? 3) Which processes and parameters are most important in explaining the growth of macrophytes? 4) What could I infer if I compare competition between species in different climates? 5) What hypotheses relating to the mechanisms of alternative stable states in lakes can be generated?

CHARISMA is a multi-species model based on seasonal cycles, and the default model includes two species, *Potamogeton* and *Chara*. The main procedures include growth, respiration, primary production, mortality, grazing and seasonal die-off of vegetation, as well as setting environment conditions in terms of light, effective irradiation, temperature, water depth, water level, bicarbonate and limiting nutrients. The input of the model is the physiological data of macrophyte species and other environmental variables. The output of the model is the spatial and temporal patterns of macrophytes, which can then be compared with field data. The rules of the model are made up from factors relating to the vegetation and environment, and the model makes extensive use of Hill Functions and Monod equations (also referred to as Michaelis-Menten equations) to simulate resource limitation.

In the CHARISMA model, the temperature dependency of photosynthesis is formulated as an equation:

$$f(T) = S\frac{T^{p_T}}{H_T^{p_T} + T^{p_T}}$$

Where T=temperature of water (℃); S=temperature factor (1.35); p_T=power of Hill function (3 for *Potamogeton*); H_T= half-saturation of temperature effect (14 for *Potamogeton*). As well as temperature, the efficiency of photosynthesis also relies on environmental factors such as in situ light (I), the distance (D) from the tissue to the top of the plant, bicarbonate concentration (C) and limiting nutrient concentration (N), which can be expressed as:

$$P = P_{max} f(I) f(T) f(D) f(C) f(N)$$

The parameter P_{max} represents the daily production of the plant top at 20℃ with no light limitations. Other ecological effects use either Monod or Hill function and are then fitted to the data.

As the model was implemented in Borland Delphi 4.0 and supported in the Windows 95 environment, it is difficult to directly use any codes from the model. However, the model provides excellent ideas on how to construct a life cycle of macrophytes in an aquatic ecosystem, and offers useful functions to represent the mixed effects of various factors to which I can refer in the development of different models.

Appendix C : Model verification

As a preliminary check, verification is conducted answering questions presented below to make sure that the model lies within the primary expectation and design concepts. The verification methods include a visual check on the graphical user interface (GUI), testing extreme values and checking codes and coding structures.

The model verification process answers the following main questions:

1) What is the approximate lifespan of each individual?

2) Are phytoplankton and submerged plants able to grow on their own and do they follow an approximate logistic growth curve?

3) Can each consumer group of agents coexist with its food?

4) Do the results of individual responses to environmental change match the simulation equations?

5) Do the group properties of individual agents change in response to environmental change in a way that is consistent with ecological experience? The answers to these questions were tested through model runs, and the unsatisfactory parts were adjusted mechanically or parametrically until the model behaved as expected. The following subsections present the results of the verified patterns.

C.1 Testing code functions and procedure

The codes were checked in hierarchical order. The functions of “setup” and “go” were checked first, followed by the functions the support them. The method used to check the functions was to compare the model outputs with and without the tested functions. For example, the “setup” function consists of function “*ca*”, “*clear-all-plots*”, “*setseed*”, “*initialize-parameters*”, “*setup-drivers*”, “*create-function-groups*”, “*set-water*”, “*show-existence*”, “ *system-dynamics-setup*”, “*count-amounts*”, “*save-scenario-to-csv*”, “*reset-ticks*” and text output. These factors ordered cleaning, setting up random seeds, setting ecological parameters, setting parameters for drivers, creating function groups of organisms, defining available water areas for organisms, showing the existence of individual energy, setting up the SDM environmental model, measuring the counts of individuals, saving data to spreadsheet and resetting time at the beginning of each run. The following are code was used to run the “setup” procedure.

```
to setup
  ca
  clear-all-plots
  setseed
  initialize-parameters             ;; initialize constants of variables
  set year initial-year
  setup-drivers
  create-function-groups
  set-water
  ;; setup agents' vars based on function groups
  output-type “This scope of lake is formed by “ output-type world-width output-
type “ x “ output-type world-height output-print “ patches.”
```

```
  output-type “Phytoplankton are initially set in agents of size “ output-type
phytoplankton-size-default output-print “ .”
  output-type “The depth of the lake is initially set as “ output-type ini-water-
depth output-print “ m.” output-type “Initial Water temperature “ output-type ini-
water-temperature output-type “ celcius degree.”
  if global-free-nutrient > 1 [ set nutrientclear? False ]
  show-existence
  system-dynamics-setup
  count-amounts
  if logData = TRUE [ save-scenario-to-csv ]
  reset-ticks
end
```

The *“go”* function gives commands on organisms in the order of primary producers, primary consumers, and secondary consumers. It consists of function “*reset-counts*”, “*set-drivers-scenario*”, “*setup-drivers*”, “*system-dynamic*” , “*consumer-life*”, “*plant-grow*”, “*phytoplankton-reproduction*” , “*die-decomposite*”, “*tick*”. Since the “*go*” function is usually run iteratively, these functions support the life cycles of organisms and data measurements. For example, the *“reset-counts”* function helps to reset the variables that are used to record mortality and addition of agents to zero at the start of every day, which can be verified by checking if the variation of mortality and population matches.

```
to go
  reset-counts
  ask turtles [ set last-energy energy]
  ask patches [
    set pcolor scale-color cyan global-free-nutrient 100 0
    if refuge? = TRUE [ set pcolor black]
    if water? = FALSE [ set pcolor brown]]
  set-drivers-scenario
```

```
  setup-drivers
  system-dynamic
 ask phytoplankton [
   count-amounts
   plant-grow
   phytoplankton-reproduction
   die-decomposite]
 ask submerged-macrophytes [
  count-amounts
  plant-grow
  macrophyte-reproduction
  die-decomposite]
 consumer-life
   show-existence
   if logData = TRUE [ keep-log]
   ask turtles [ set age age + 1]
   tick
   set year int (ticks / 365) + initial-year
end
```

C.2 Testing community-level behaviour

The maximum population sizes in nominal clear-water environment depend on the efficiency of energy assimilation at the trophic levels. The growth rates of algae and macrophytes gradually slowed down when the population sizes approached ca. 3000 and 900 respectively, as they were constrained by density limits. In a system composed only of algae and zooplankton, they finally arrive at a dynamic steady state with population ratio of 1:50. In a system composed only of submerged macrophytes and herbivorous fish, similar oscillations appear after the initial stage and the population sizes are closer in number between macrophyte and herbivores than they were between algae and zooplankton. In contrast to the strong intrinsic sensitivity and stochasticity in systems that have six components, individual communities can always reach a balance with their environment or neighbours after initial adaptation, when a single group or predator-prey pairs live alone in the model.

Single group scenario 1: only algae

Predator-prey scenario 1: algae and zooplankton

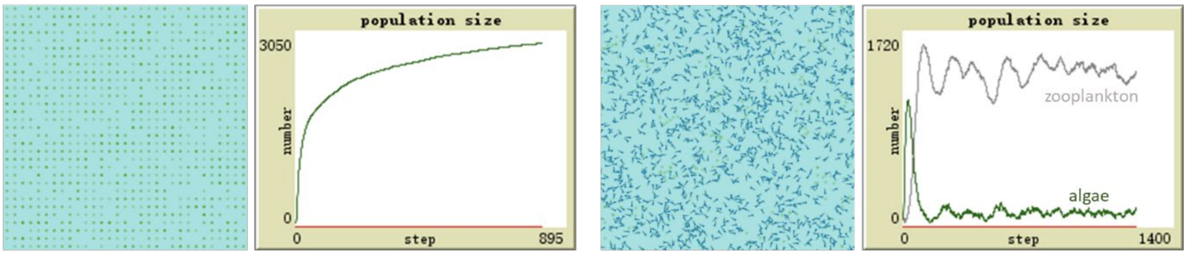

Single group scenario 2: only macrophyte

Predator-prey scenario 2: macrophyte and herbivorous fish

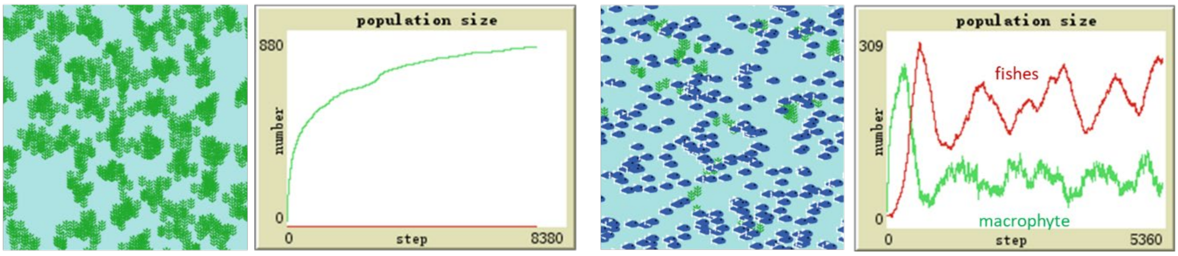

Figure Apx 5: Spatial distribution and population size of each single group scenario and predator-prey scenario upon approaching steady states

Meanwhile, experiments were done on gradient trends in the component populations of the ecosystem at different total nutrient concentrations. The results are shown in Figure Apx 6.

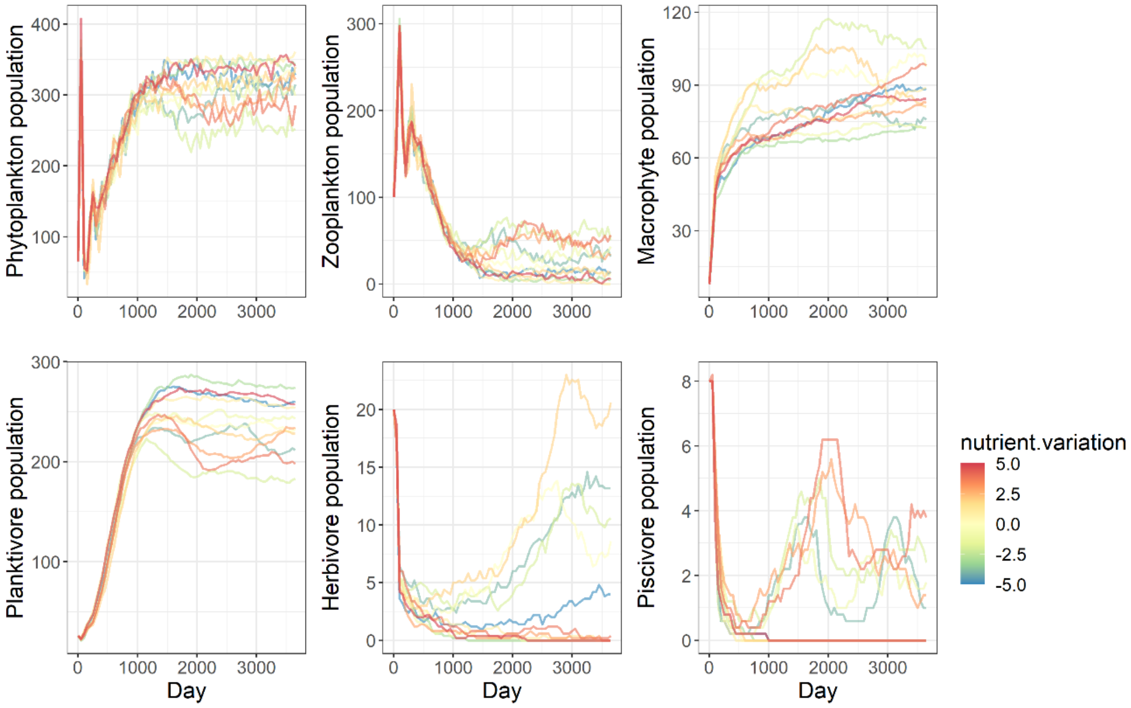

Figure Apx 6: Population changes on the gradient of total nutrients in the whole system. The value of nutrient variations (±5 μg/L) is based on the standard nutrient level of 25μg/L. Different colours in the spectrum represent different runs with varying total nutrients.

Appendix D : Model parameterisation in multiple scenarios

D.1 Parameterisation of internal attributes

For the ecosystem model, the first parameters to be determined were the components of individual behavioural rules, including the processes of energy intake, energy consumption and nutrient cycling. The number of parameters in this model is very large, and some of the biologically based parameters mentioned in the previous section on ODD descriptions will not be repeated here. The remaining adjustable parameters were selected after model tuning as a set of ecosystem states that would allow for reasonable and flexible changes to the model's stable output.

Table Apx 1: Parameters defining main attributes of the modelled ecosystem

Code	Abbrev.	Unit	Nominal value
phytoplankton-reproduce-rate	RR_p	%	80
macrophyte-reproduce-rate	RR_{sm}	%	50
zooplankton-reproduce-rate	RR_z	%	60
planktivore-reproduce-rate	RR_{pf}	%	40
herbivore-reproduce-rate	RR_{hf}	%	40
piscivore-reproduce-rate	RR_{pis}	%	20
zooplankton-reproduce-energy	Er_z	J	140
planktivore-reproduce-energy	Er_{pf}	J	460
herbivore-reproduce-energy	Er_{hf}	J	460
piscivore-reproduce-energy	Er_{pis}	J	540
nutrient-concentration-in-phytoplankton	NC_{phyp}	g/g	5
nutrient-concentration-in-zooplankton	NC_z	g/g	5
nutrient-concentration-in-sm	NC_{sm}	g/g	10
nutrient-concentration-in-fish	NC_f	g/g	10

D.2 Parameterisation of experiments

Table Apx 2: Experiment numbers, repetitions, parameters and variable settings used in chapters 4 and 5. The descriptions "[a b c]" means that the variable takes itsvalues from a to c, with an interval of b.

Experiment#	**Rep**	**Constants**	**Variables**	**Perturbation phase**
EQC_100rseed_y20	1	Nominal clear state	100 random seeds	No perturbation
EQC_fixrseed137_y20	100	Nominal clear state; random-seed =137	None	No perturbation
EQC_5rseed_y20	1	Nominal clear state	5 random seeds	No perturbation
NUTADDTEMP_once_y27	1	Nominal clear state(modified); macrophyte-start-amount =8; planktivore-fish-start-amount = 26; piscivore-start-amount = 8	None	Environmental change starting after Day 3280; Temperature change stopping at Day 4230 when nutrient adding continued
TBNutADD_once_y30	1	Nominal clear state(modified); total-nutrient-variation = 4.164% per 90 day	None	Nutrient load starting at Day 4548
NUTADD1-vperturtiming_y20	1	Nominal clear state; total-nutrient-variation = 1% per 10 days; random-seed =137	[“perturbationday” [3051 100 4051]]	Environmental change starting after “perturbationday”
NUTADDvar_y40	2	Nominal clear state; initial year = 0	“total-nutrient-variation” = 10,20,40,60,70 μg/L per 100 days	Nutrient load starting in the 7th sim year
NUTADD10_vDEPTH_y70	10	Nominal clear state; total-nutrient-variation = 10% per 100 days; random-seed =137	ini-water-depth [0.2 0.2 5]	Environmental change starting after 10 years
NUTADD1_vDEPTH_y70	10	Nominal clear state; total-nutrient-variation = 1% per 10 days; random-seed =137	“ini-water-depth” [0.2 0.2 5]	Environmental change starting after 10 years
NUTADD0.1_vDEPTH_y70	1	Nominal clear state; total-nutrient-variation = 0.1% per day; random-seed =137	“ini-water-depth” [1.6 0.2 3.4]	Environmental change starting after 10 years
NUTADD20_vDEPTH_y71	1	Nominal clear state; total-nutrient-variation = 20% per 200 days; random-seed =137	“ini-water-depth” [1.6 0.2 3.4]	Environmental change starting after 10 years

TBComprehens_v5_y274	1	Nominal clear state; initial year = 1895	temperaure-variation = 0.05℃ per year; average reclamation area = 4.5 per year; total-nutrient-variation = 4.164% per 100 day	Reclamation and nutrient loading starting from 1906; Temperature change starting from 1981
TBRecNutADD_once_y164	1	Turbid stable state generated by NutADD_once_y30	None	50 planktivorous and 10 herbivorous fishes were added around Day 27000 when a turbid stable state was formed
TBRecNut_once_y80	1	Turbid stable state generated from a eutrophication scenario with random seed -275272531	None	total-nutrient-variation = -10% per 100 days after Year 41
TBRecComprehens_v4_y41	1	Nominal turbid state	[“piscivores-adding” [0 1 5]] [“macrophyte-start-amount” [5 5 20]] [“total-nutrient-variation” [-20 5 0]] [“algae-control” [-20 5 0]]	

The length of the duration of the experiment was essentially determined by the purpose of the experiment. Based on knowledge of the model behaviour (obtained by running the steady-state model and observing changes in the system dynamics), a period of 0-10 years was set as the period of adaptation and stabilisation of the system components, during which no changes in the environment were made to facilitate the development of a steady state. To check for changes in the system state driven by the environment that may occur over a ten year period, the total experiment length was set at 20 years, with the first ten years being the steady state period and the second ten years being the change observation period. To obtain more realistic simulation models, such as comprehensive environmental changes in which the researcher seeks to observe the erosion of system resilience by slow driving forces over a longer period of time, it is possible to observe a time length of 50-100 years and stop the experiment after the new steady state has emerged and stabilised. This flexible time scale setting helps to simulate changes in ecosystem response under conditions of varying rates of environmental change, and this is also dictated by the nonlinear nature of emergent phenomena in complex systems.

Table Apx 3: The initial settings of turbid-water states (on Day 25000 in Experiment #NutADD_once_y30) for the follow-up experiment TBRecNutADD_once_y164

Variable	**Value**	**Variable**	**Value**
System-composition	“algae + macrophytes + zoopk “		
ini-water-temperature	20	planktivore-reproduce-rate	20
ini-water-depth	2	herbivore-reproduce-rate	20
initial-nutrient	91.624	piscivore-reproduce-rate	10
phytoplankton-start-amount	118	zoopk-hunt-rate	40
zooplankton-start-amount	34	pf-hunt-rate	10
macrophyte-start-amount	1008	hf-hunt-rate	40
planktivore-fish-start-amount	0	pisci-hunt-rate	20
herbivore-fish-start-amount	0	max-pxcor	30
piscivore-start-amount	0	max-pycor	30
phytoplankton-reproduce-rate	100	macrophyte-reproduce-rate	35
zooplankton-reproduce-rate	50		

Table Apx 4: The initial settings of turbid-water states for the follow-up experiment (generated from the eutrophication scenario with random seed - 275272531)

Variable	**Value**	**Variable**	**Value**
System-composition	“algae + planktivorous fish “		
ini-water-temperature	23	planktivore-reproduce-rate	20
ini-water-depth	2	herbivore-reproduce-rate	20
initial-nutrient	92	piscivore-reproduce-rate	10
phytoplankton-start-amount	500	zoopk-hunt-rate	40
zooplankton-start-amount	0	pf-hunt-rate	10
macrophyte-start-amount	0	hf-hunt-rate	40

planktivore-fish-start-amount	1800	pisci-hunt-rate	20
herbivore-fish-start-amount	0	max-pxcor	30
piscivore-start-amount	0	max-pycor	30
phytoplankton-reproduce-rate	100	macrophyte-reproduce-rate	35
zooplankton-reproduce-rate	50		

The experiment was designed to validate part of the field observations and predict possible scenarios if the drivers remain as they were. Three main groups divided by main drivers were conducted with no interference, nutrient-driven interference, and fish-driven interference respectively. In terms of the patterns of interference, pulse-like and press-like approaches to applying the were are considered.

The external forcing is hypothesized as being applied unidirectionally on the biological communities. The nutrient pollution in the ecosystem simulates two types: slow non-point pollution from farmland fertilizers through soil penetration and diluted sewage, and fast point pollution from aquacultural fertilizer added in water. For planktivorous fish, a certain number of new fish were added into the system gradually or as a single event. The changes in external conditions were implemented in the System Dynamics Modeler in NetLogo, which allows developers to manipulate variables through simple system dynamic models. The variables in experiments are seen as “stocks” and the changing rate is defined in the equations.

Comprehensive simulation adds to the nutrient and temperature changes the actual driving forces of the MLYB lake ecosystem. These forces were caused by the reduction of the lake area and the release of large quantities of planktivorous fish and small quantities of herbivorous fish, which altered the environmental change conditions. This change scenario can be simulated after the 27th year by selecting “TBComprehens” in the “driving-scenario” variables in the model interface.